Informing Mechanism through Application: Chemical Mimicry and Comparative Decay Studies of Brown Rot Fungi

A DISSERTATION
SUBMITTED TO THE FACULTY OF
UNIVERSITY OF MINNESOTA
BY

Justin Kaffenberger

IN PARTIAL FULFILLMENT OF THE REQUIREMENTS
FOR THE DEGREE OF
DOCTOR OF PHILOSOPHY

Advisor: Dr. Jonathan Schilling

December 2015

ACKNOWLEDGEMENTS

I am eternally obliged to my advisor, Dr. Jonathan Schilling, for his undying personal support and brilliant academic guidance. It's not every mycologist who would take in a chemical engineer. He always puts his students first and has provided me with countless opportunities and experiences. How many people can say they've driven the Dalton Highway? My time at the University of Minnesota came with many major life changes and Jonathan was supportive throughout. I can't thank him enough.

I would also like to thank my friends and colleagues in BBE and the Schilling lab past and present, including Dr. Shona Duncan, Mr. Feng Jin Liew, Dr. Zewei Song, Mr. Jason Oliver, Ms. Amy Fox, Mr. Gerry Presley, Dr. Jon Menke, and Dr. Jewei Zhang, who made the lab a thoroughly enjoyable work environment. I'm fortunate to have worked with each and every one of them. Coming to U of M with close to no practical knowledge of biology and even less knowledge about fungi specifically, I'm extremely grateful to have had such incredibly intelligent colleagues who were eager to share their ideas and insights.

A special thanks to Ms. Audrie Ayres, Ms. Heather Connelly, Mr. Nick Greatens, Ms. Emily Mickelson, and Mr. Quinn O'Leary for their long hours of sample grinding and glassware washing. It wasn't always glamorous, but their work greatly facilitated this research. They all have bright futures ahead of them.

I deeply value the support and time of my committee members: Dr. Ulrike Tschirner, Dr. Robert Blanchette, and Dr. Ping Wang. Their open doors, frank

discussions, and valuable feedback have bettered this dissertation and my graduate experience.

My gratitude also goes out to Dr. Ben Held and Mr. Nik Prevanost for their assistance with preparation of samples used in Chapter 4 and Ms. Lucy Li who graciously spent her summer with me assembling the final set of reaction equations used in the modeling study of Chapter 6. I would also like to recognize my friend and former colleague, Dr. Craig Chmielewski, for his invaluable mentorship and insistence that I pursue this degree.

I wouldn't be who I am today without my parents and grandparents, who not only provided me with a loving and supportive childhood, but taught me the importance of education and the value of hard work along the way.

Last, but certainly not least, I would like to thank my family for their constant love and support. The incredible patience and sacrifice of my wife, Lina, made this dissertation possible. She let me completely uproot our lives in pursuit of my dream, put up with my long nights and weekends in the lab, and managed to pick up my resulting domestic slack. All throughout, she's been my rock, even when I've wavered. Mariam has brought deeper meaning to my life and will always be my constant inspiration.

Funding for this research was provided by the University of Minnesota Initiative for Renewable Energy and the Environment (IREE) Early Career award (RC-00008–11) and seed grant (RS-0010-12), as well as generous support from the Buckman Foundation through a departmental (BBE) fellowship and the University of Minnesota doctoral dissertation fellowship.

DEDICATION

For Lina and Mariam. I love you both more than words can express.

ABSTRACT

Biodegradation of wood by fungi offers an example of how lignocellulose can be efficiently converted from a recalcitrant mixture of complex biopolymers into readily metabolized sugars. Representing a diverse group, brown rot fungi utilize a unique, yet incompletely understood cellulolytic decay process, believed to involve the generation of hydroxyl radicals by Fenton chemistry, which rapidly depolymerize cellulose. Thermodynamically driven in the absence of enymzatic catalysis, this process can be chemically mimicked, allowing for accelerated bioconversion as fungal growth and colonization rates often bottleneck biological pretreatment times. Furthemore, brown rot fungi are able to circumvent lignin, leaving behind a potentially value-added byproduct in the form of an oxidized lignin-rich residue.

This dissertation expands our understanding of brown rot decay through a set of studies with differing approaches. First, decay residues were compared across phylogenetic groupings of brown rot fungi to explore decay variability. As substrate can dictate decay rates, three distinct and representative substrate types were used. Noting significant differences in the *Antrodia* clade on corn stover, a separate study was conducted to explore the relationship between membership in this clade and the extent of decay they can cause in *Poales* grasses. Next, a survey of wood-degrading fungi was conducted to assess their ability to improve saccharification yield, the differences in variability across decay types, and to determine the relationship between chemical changes within the substrate and yield improvement. Lastly, hydroquinone-driven Fenton oxidation was both chemically mimicked and theoretically modeled to discern the

efficacy of this mechanism in improving cellulose accessibility, its compatibility with cellulases, and the potential role that other redox active chemical species might have in the brown rot mechanism. Saccharification potential in relation to chemical and compositional changes in various substrates was used as a metric in most studies, allowing for consideration of the applied biotechnological benefit of brown rot, while furthering our fundamental understanding of this remarkable decay mechanism.

The progression of substrate chemical component losses on a mass loss basis was found to be consistently identical among all known clades of brown rot fungi in all relevant studies. This contrasted with white rot decay, which displayed notably greater variation among tested species in how decay progressed. Despite this consistency in how brown rot decay progressed, there were notable differences between clades in their ability to initiate decay. Where a Gloeophyllum-clade representative was capable of degradation rates similar to those observed on wood substrates, *Antrodia* clade brown-rotters were found to have a limited ability to degrade *Poales* grasses. Meta-analysis indicated that this finding was consistent with previous studies. Lastly, the direct use of the Fenton reaction resulted in chemical composition changes that were consistent with brown rot. Despite this, improvement in saccharification yield was difficult to realize because of the reactivity of hydroxyl radical with the desired monosaccharide product. This suggests that if the mechanism for brown is dependent on Fenton chemistry, the manner in which hydroxyl radicals are produced by this reaction must be highly controlled.

TABLE OF CONTENTS

LIST OF TABLES

LIST OF FIGURES

Chapter 1

Introduction

1.1 Problem Statement

While energy demands continue to grow, total fossil fuel production is expected to peak by 2030 (Li, 2007). Models suggest that reduced availability of energy resources and building global pollution could lead to catastrophic collapse in global industrial output and food per capita, resulting in a drop in human population (Meadows et al., 1972; Turner, 2008). US national security assessments of both climate change and peak oil scenarios corroborate these risks (Schwartz & Randall, 2003; Hirsch et al., 2005), stressing the urgent need to develop energy alternatives.

As part of efforts to begin US energy supply diversification, Congress passed the energy independence and security act in 2007, which was subsequently expanded in 2009. This law mandates the blending of 9 billion gallons of renewable fuels into the national fuel supply and sets a target blend volume of 36 billion gallons by 2022. To meet this mandate, corn-based ethanol production has rised dramatically, along with the percentage of US corn crop yield devoted to it.

At a current production rate of 14 billion gallons annually, corn-based ethanol comprises the overwhelming majority of current US biofuel production (US EIA, 2013), but this fuel source comes with several drawbacks. Studies suggest significant associated environmental impacts including increased eutrophication (Donner & Kucharik, 2008), reduced water availability due to increased demand for crop irrigation (Dominguez-Faus

et al., 2009), and increased particulate emissions (Hill et al. 2009). Corn-based ethanol has also caused increased food prices through diversion of crop land. In the US, from 2006 to 2007, the area used to plant corn rose 23%, displacing soybean crops. The resulting drop in soybean production contributed to a 75% rise in soybean prices (Mitchell, 2008). Apart from direct land displacement, other factors that can contribute to rising food commodity prices such as drought and petroleum price are further exacerbated by demand for corn-based ethanol (Tokgoz et al., 2008).

Transitioning to cellulosic biofuels ameliorates many of these issues. Climate change and health costs associated with corn-based ethanol are estimated to be as much as double those of gasoline, but these costs for cellulosic ethanol are less than half those of gasoline (Hill et al., 2009). Nutrient leaching, drought susceptibility, and biodiversity reduction associated with corn production can be overcome with cellulosic energy crop cultivation (Börjesson, 1999). Cellulosic biofuels also have a greater potential in terms of the amount of petroleum they could displace. In 2011, the U.S. Department of Energy issued an update to the "billion ton study" affirming the results of a 2005 study that concluded that the U.S. could have a sustainable supply of 1.1 to 1.6 billion tons of biomass by 2030, enough to replace 30 percent of the nation's current petroleum consumption (Perlack & Stokes, 2011).

Transition to cellulosic biofuels, however, is currently beset by technical and financial obstacles. Due in some part to high capital and operating costs and poor yields, cellulosic bio-fuels remain economically uncompetitive with gasoline, limiting development of commercial-scale operation (Wyman, 2007). The economic barriers to

cellulosic ethanol are related to the intensive processing required to convert cellulosic biomass. While starch conversion to glucose is relatively straightforward, physical limitations inhibit lignocellulosic conversion. The structural and ultra-structural heterogeneity of biomass, the presence of lignin, and the crystallinity of cellulose all impart mass transport limitations on chemical reactants and enzymes, constraining the achievable hydrolysis rate and extent of conversion (Himmel et al., 2007).

Due to these features of lignocellulosic biomass, its conversion to simple sugars requires pretreatment (Wyman, 2007). Pretreating lignocellulosic biomass enables higher saccharification yields by improving enzyme accessibility during subsequent hydrolysis (Jeoh et al., 2007). Enzyme accessibility to cellulose can be improved through hemicellulose removal (Irwin et al., 2003), delignification (Cowling and Kirk, 1976), removal of ester-ether bridges between heteroxylans and lignin (Lam et al., 2003), increased pore size (Grethlein et al., 1984), decreased cellulose degree of polymerization (Puri, 1984), and increased substrate surface area (Thompson, 1992).

Innumerable pretreatments, comprising a combination of physical, thermal, and chemical processes, have been proposed (Mosier et al., 2005; Kumar et al., 2009; Alvira et al., 2010; Chiaramonti et al, 2012). Most of these pretreatments require harsh operating conditions, demanding corrosion resistant equipment capable of handling high temperature and pressure. A techno-economic assessment of various pretreatment technologies performed by Eggeman & Elander (2005) compared dilute acid, ammonia fiber explosion (AFEX), ammonia recycle percolation, lime, steam, and hot water. They

concluded that dilute acid pretreatment was the most cost effective, but all process designs were projected to be capital intensive.

According to the US Department of Energy's biomass multi-year program plan (2011), with 2010 state of technology to convert corn stover into cellulosic ethanol using a dilute acid pretreatment, enzymatic hydrolysis, and co-fermentation, pretreatment accounts for 23% of cellulosic ethanol cost ($0.64 of $2.77 minimum selling price), second only to feedstock in cost contribution. Two-thirds of this pretreatment cost was tied to capital cost. The DOE targeted pretreatment cost reductions of 50% by the end of 2012, with an expected 83% reduction in pretreatment capital cost. Given its need for specialized equipment, it is unlikely these cost reductions will be realized with dilute acid pretreatment and cost-competitive cellulosic biofuel will most likely require a different approach.

In the pursuit of alternatives, there has been growing interest in the natural lignocellulosic degradation mechanisms of wood-degrading fungi. The Department of Energy's Joint Genome Institute program has recently launched the Fungal Genomics Program to ramp up sequencing and annotation of fungal genomes in part to explore their potential bioenergy applications (Grigoriev et al., 2011). To date, more than 140 fungal genomes have been sequence, assembled, annotated, and published.

During decay, these fungi impart many of the same chemical and physical changes on wood that are associated with pretreatment. The nature of these changes is largely determined by the type of decay a fungal species produces. The three main types of decay are white rot, brown rot, and soft rot. White rot decay is always associated with

lignin removal, either simultaneously with holocellulose, or selectively preceding holocellulose removal. In contrast, brown rot fungi rapidly depolymerize and remove holocellulose, but leave behind a residue that is composed mostly of oxidized lignin (Cowling, 1961). While most research has centered on white rot fungi for their ability to selectively remove lignin, the ability of brown rot fungi to circumvent lignin while thoroughly removing biomass polysaccharides would allow for co-generation of potentially valuable by-products in a biorefinery setting (Doherty et al., 2011).

There are several other features of brown rot that make it an interesting model for study: 1.) While lignin is often a barrier to bioconversion, some brown rot fungi may require lignin to be present to effectively degrade cellulose (Highley, 1977; Nilsson, 1974). 2.) Excepting the *Boletales*, brown rot fungi lack glycoside hydrolases (GH) GH6 and GH7 cellobiohydrolases (Floudas et al., 2012). Understanding how these fungi are able to completely metabolize holocellulose with a reduced set of cellulases could lead to novel approaches to bioconversion. 3.) Brown rot fungi carry out polysaccharide de-polymerization and assimilation under ambient conditions, demonstrating that harsh operating conditions are not necessary for bioconversion. Eliminating these conditions would be a big step forward in reducing cellulosic biofuel capital costs and their financial feasibility. 4.) Brown rot fungi appear to co-localize seemingly conflicting enzymatic and oxidative reactions (Schilling et al., 2013). Understanding this process could lead to consolidation of pretreatment and saccharification steps in bioconversion processes and potential application in other industries. 5.) Aside from its potential applications to bioconversion, the brown rot biochemical mechanism is vital to carbon cycling in boreal

forest communities (Gilbertson and Ryvarden, 1987) and is a major cause of structural lumber damage (Zabel and Morrell, 1992), making advances in this area applicable to such fields as wood preservation, biogeochemistry, and ecology.

Direct biological pretreatment would confer the benefits outlined above, but the use of a biological agent would come with several drawbacks. Wood-decaying fungi require a carbon source, in the form of cellulose and hemi-cellulose, to survive. This means a portion of the theoretical maximum saccharification yield must be sacrificed in a biological pretreatment. Furthermore, the growth of wood-degrading fungi is slow. While dilute acid pretreatment can be performed in a matter of hours, wood-degrading fungi can take weeks. To have the same throughput as dilute acid, a processing plant using a direct biological pretreatment would require substantially more space to allow for this difference in processing time.

The limitations of direct biological pretreatment can be overcome by mimicking the biological mechanism chemically. In the case of brown rot, the mechanism behind the "pretreatment" stage of decay is theorized to be largely non-enzymatic and the proposed components of this mechanism are commercially available. Along with the benefits associated with direct biological pretreatment, the use of a chemical mimic for pretreatment would offer several additional benefits: 1.) Reaction conditions are not tied to the survival of a biological agent so conditions that would improve the rate of reaction, but would compromise the viability of the fungus, can be considered. 2.) With a chemical mimic, the benefits of the biological agent are realized without sacrificing

saccharification yield. 3.) A chemical mimic simplifies and standardizes the reaction system, allowing for greater process control and easier downstream processing.

1.2 Objectives

Given its potential for bioconversion, as well as its standing importance to timber decay and natural carbon cycling, this dissertation expands on our current understanding of the brown rot decay mechanism through a set of experiments designed to address the following objectives.

Objective 1: Determine clade-specific differences in the brown rot mechanism through analysis of decay progression. Chapter 3 provides a comparison between clades of brown rot to assess variation in decay mechanism across phylogenetic clades. Progression of chemical component losses in a hardwood, softwood, and grass were used as an indicator of underlying variability in lignocellulolytic machinery.

Objective 2: Determine the efficacy of brown rot and white rot fungi for direct biological pretreatment. Addressed in chapter 4 through broad comparison decay progression and saccharification potential imparted by wood-degrading fungi on aspen, this objective provides an overview of pretreatment potential, while also providing an overview of variation in the substrate compositional changes resulting from wood-degrading fungi.

Objective 3: Determine the decay potential of *Antrodia* clade brown rot fungi on *Poales* grasses. Born from observations in previous studies like those in Chapter 3 which indicated that *Postia placenta* does not readily degrade corn stover, this objective

explores the regularity of poor grass degradation across the *Antrodia* clade of brown rot fungi.

Objective 4: Determine the efficacy of brown rot relevant means of hydroxyl radical generation as a chemical pretreatment on wood. Fenton's reagent, the currently proposed brown rot mechanism of hydroquinone-mediated hydroxyl radical formation, and other potential chemical mechanisms derived from a kinetic computer model were used to pretreat wood as described in Chapter 6. The composition of the resulting biomass was characterized and saccharification potential was tested.

Chapter 2

Literature Review

2.1 Plant Biomass

Heterogeneities in plant biomass exist on macro-, micro-, and ultra-structural scales. Each plant tissue has a unique cellular make up and each cell type has its own characteristic chemical composition. Even within a single species, growing conditions and plant age can greatly alter biomass composition (Waring et al., 1985). This underscores the need for a versatile pretreatment capable of handling this variability.

Cell walls, which account for the vast majority of dried plant biomass are composed of middle lamella, a primary cell wall, and a secondary cell wall that is composed of three layers, S1, S2, and S3 (**Figure 2.1**). In turn, each layer of the cell wall has a distinct chemical composition comprised of three main polymers: the polyphenolic lignin and the two polysaccharides cellulose and hemi-cellulose (Sjöström, 1993). Cellulose is a straight chain β-linked 1-4 glucan that, through hydrogen bonding, can coalesce to form 2- 5 nm thick crystalline microfibrils, which can further bundle to form fibrils (Sjöström, 1993). These cellulose fibrils are surrounded by hemi-cellulose and lignin (**Figure 2.2.2**).

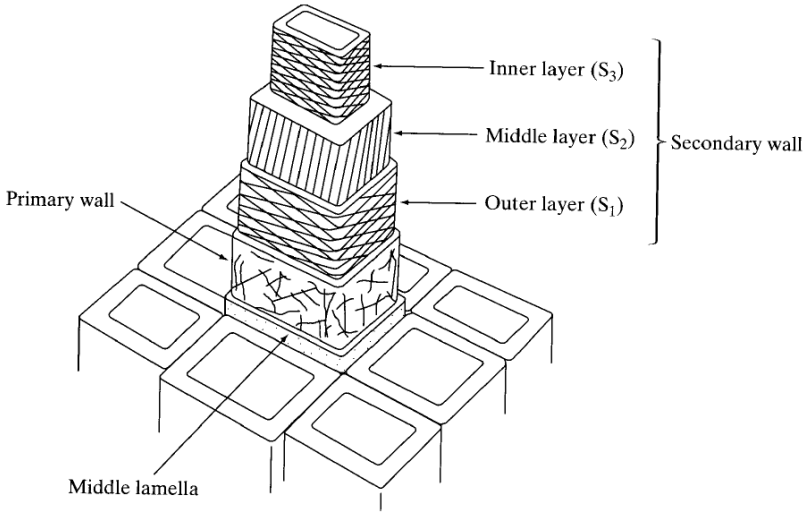

Figure 2.1 Structure of the plant cell wall (Dinwoodie, 1989)

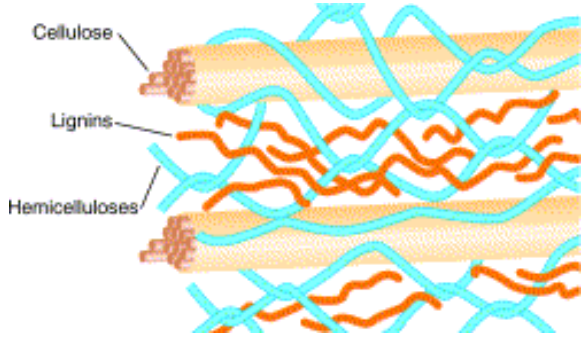

Figure 2.2 Spatial organization of cellulose fiber (yellow) in relation to lignin (orange), and hemicellulose (blue) (Boudet et al., 2003)

Hemi-cellulose is composed of various saccharide and sugar acid monomers. Hemi-cellulose chains can also contain side-chain ester bonds in the form of acetyl groups and coumarate and ferulate bridges (Grabber et al., 2008). The arrangement of these hemi-cellulose components varies with differing monomer composition, linkage

positions, degree of polymerization, and extent of branching. Examples of typical hemicelluloses can be found in **Figure 2.3**.

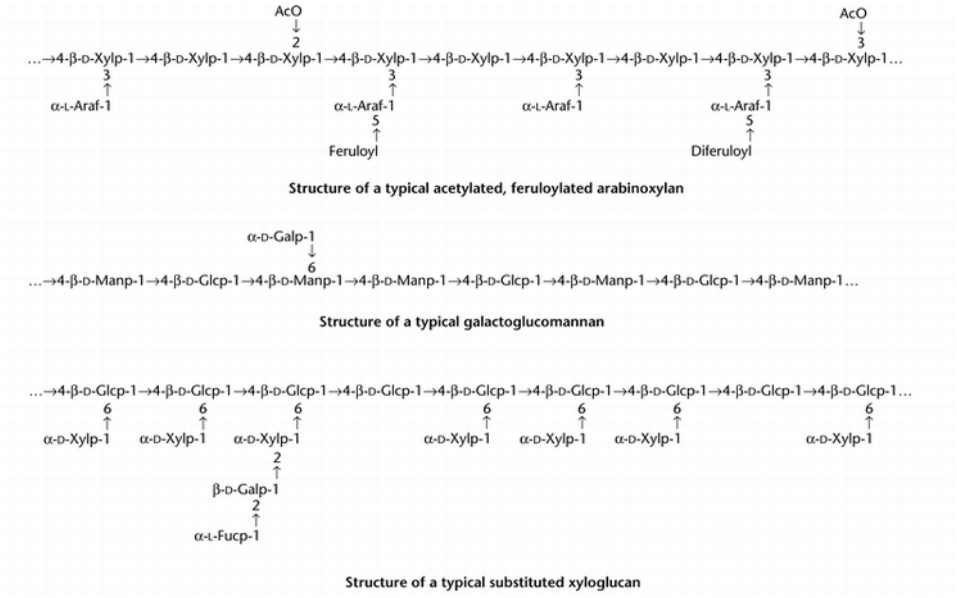

Figure 2.3 Structure of some hemicelluloses (Morrisson, 2001)

In contrast to the hydrophilic polysaccharides, lignin is comprised of three hydrophobic phenylpropanoid monomers: p-coumaryl alcohol, coniferyl alcohol, and sinapyl alcohol, which correspond to hydroxyphenyl (H), guaiacyl (G), and syringyl (S) units in lignin (Sjöström, 1993). These monomers are believed to be polymerized through radical coupling during biosynthesis to form various covalent bonds between monomers, with β-O-4 linkages being the most common (Boerjan et al., 2003). A typical softwood lignin is shown in **Figure 2.4**.

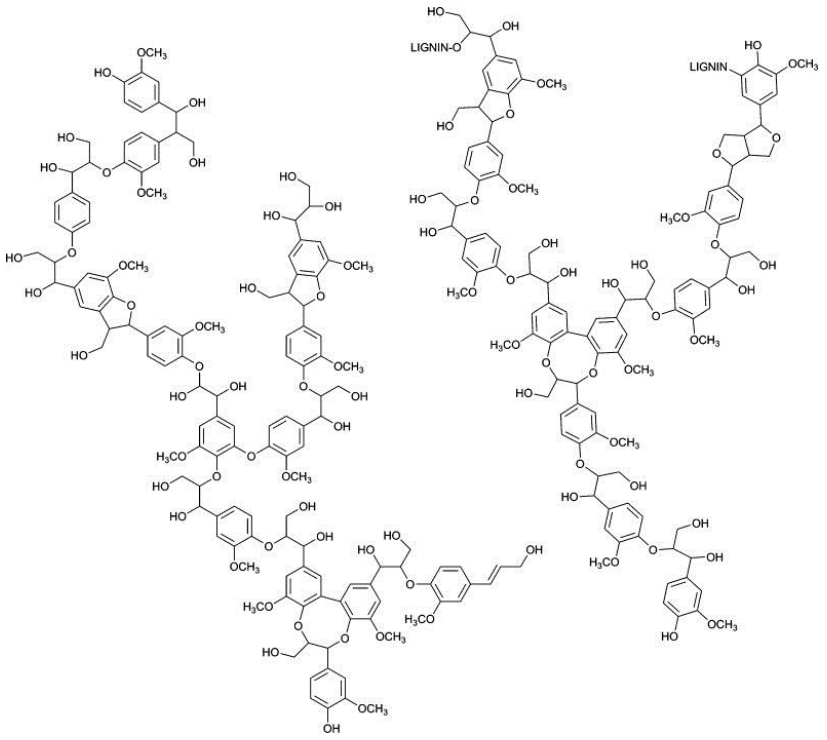

Figure 2.4 Representative structure of lignin (Crestini et al., 2010)

There are four main types of plant biomass: hardwood, softwood, herbaceous and grass (*Poaceae*), which possess their own unique compositional features. Softwoods typically contain between 45-50% cellulose, which is comparable to hardwoods (45-55%), but slightly more than grasses (25-40%) (Malherbe and Cloete, 2002). Softwood hemicellulose is predominantly galactoglucomannan, but also contains some arabinoglucuronoxylan (Schädel et al., 2010). Softwoods are also distinguished by lignin that is composed primarily of G units (Mansfield et al., 2012). Hardwood hemi-cellulose is predominately composed of glucuronoxylans and glucoxylans (Pettersen, 1984). Unlike softwoods, mannan is a minor component of hardwood hemi-cellulose. Hardwood lignin contains a greater amount of S-type lignin as compared to softwoods.

Cinnamyl alcohol and p-hydroxybenzoate moieties are also components of hardwood lignin (Mansfield et al., 2012). Herbaceous plants have a lignin composition that is comparable to hardwoods, with the exception that they have a greater amount of H subunits with respect to G and S, do not contain p-hydroxybenzoate groups (Mansfield et al., 2012), and tend to have a lower S/G ratio. Like hardwoods, the hemi-celluloses of herbaceous plants are dominated by xylans. Herbaceous material also tends to contain more protein, starch, ash, and pectin than woody biomass (Hames, 2009).

While similar to herbaceous plants, grasses have several unique compositional features. Understanding these unique aspects is of particular importance for bioconversion as many agricultural residues such as wheat straw and corn stover, as well as proposed biomass crops like miscanthus and switchgrass, are *Poales* grasses. In terms of hemicellulose, grass cell walls uniquely contain glucuronoarabinioglucans (GAX), which are xylans with α-linked arabinan and β-linked glucuronic acid side chains (Vogel, 2008). GAX arabinan side chains can also terminate in feruloyl moieties. Mixed-linkage glucans (MLGs) are also a significant component of grass hemicelluloses. MLGs are unbranched β-linked glucans that contain both C1-C4 and C1-C3 linkages (Vogel, 2008). Grass lignin is characterized as a mixture of G and S like hardwoods, but also contains more H than woody plants (Sjöström, 1993). Grass lignin also tends to contain a significant amount of free coumaric and ferulic acid, as well as the corresponding diesters (Vogel, 2008). The silica content of grasses also tends to be particularly high, even when compared with most herbaceous plants (Hodson et al., 2005).

2.2 Biomass Characterization

Various methodological techniques have been employed to characterize and quantify constituents of plant biomass. These methods are well established and have been adopted by the American Society for Testing and Materials (ASTM). The National Renewable Energy Laboratory (NREL) also has a set of protocols for biomass characterization, most of which was adopted from methods developed in the pulp and paper industry (TAPPI standards) and the animal feed industry (Hames, 2009). These methods consist of sample preparation, removal of non-structural components via solvent extraction, ash measurement, hydrolysis and analysis of the resulting insoluble and soluble fractions (Sluiter et al., 2010). With feedstock types containing different components, the overall analysis can be tailored by the inclusion of additional methods with the overall goal of accounting for at least 95% of biomass components. For example, grasses may additionally require methods to measure ferulate (Jung & Shalita-Jones, 1990), protein (Hames et al., 2005), and uronic acid and acetyl content (Sluiter et al., 2008) to achieve mass closure.

Biomass hydrolysis consists of a two-stage acid treatment, which results in soluble and insoluble fractions. Referred to as Klason lignin, the insoluble fraction may also contain ash and protein, which must be accounted for to avoid double-counting. The hydrolysate contains structural sugars (glucose, xylose, galactose, arabinose, and mannose), acetic acid, and uronic acids all of which are quanitified via high performance liquid chromatography (HPLC). Acid-soluble lignin is also present in the hydrolysate

and is quantified by UV spectroscopy and reported with the Klason lignin (Sluiter et al., 2008).

There are several potential interferences associated with these methods, most involving the acid hydrolysis step (Sluiter et al., 2010). Many extractives in biomass can condense and precipitate during acid hydrolysis. This can result in overestimation of the lignin present. Ash and protein can also contribute to the mass of the insoluble acid hydrolysis fraction, as well as the mass of extractives. To avoid counting these fractions multiple times, their quantity in the original material, extract-free samples, and the insoluble fraction after hydrolysis must be determined. Klason lignin can also be overestimated if the particle size of the biomass used is too large, as acid hydrolysis will be incomplete, leaving behind acid insoluble cellulose oligomers. In measuring acid-soluble lignin, non-lignin constituents of the hydrolysate such as furfural and HMF also absorb in the UV range and can lead to overestimation of the soluble fraction of lignin. Failure to remove free sucrose from biomass will result in overestimation of structural glucan. Biomass that has been ground too fine degrades more rapidly into byproducts, resulting in underestimation of structural sugars. High ash or moisture content can also interfere with hydrolysis by neutralizing or diluting the acid, resulting in incomplete hydrolysis, and lower structural sugar underestimation.

Due to the need to conduct multiple methods and its heavy reliance on wet chemistry techniques, biomass characterization can be time consuming. High throughput techniques are under development to alleviate this issue. NIR spectroscopy has been of particular interest, as bulk samples can be rapidly analyzed non-destructively, reducing

sample preparation and analysis time (Sanderson et al., 1996; Hames, et al., 2003; Foston & Ragauskas, 2012). This method still requires high quality wet chemistry against which to calibrate NIR spectra and form a multivariate model, but once established this model can accurately and rapidly characterize biomass (Wolfrum & Sluiter, 2009).

Due to its role in biomass recalcitrance, much effort has been placed in the characterization of lignin. While acid hydrolysis provides the total lignin and acid-soluble fraction masses, it does not provide detail about the characteristics of the lignin, such as the G:H:S ratio and bond connectivity. Both liquid state (Yelle et al., 2008a; Mansfield, 2012) and solid state (Baldock et al., 1997) NMR techniques have been used to provide this detail. Alternately, lignin has been characterized via tetramethyl ammonium hydroxide (TMAH) thermochemolysis coupled with GC-MS (Clifford et al., 1995; Filley et al., 1999). Traditionally, lignin characterization has involved a number of degradative techniques, the most popular being flash pyrolysis coupled with GC-MS (Sarkanen & Ludwig, 1971).

2.3 Wood-Degrading Fungi

The elements of plant biomass are naturally cycled by decomposers. A diverse range of bacteria and fungi carry out this decomposition, often in consortium. Wood-degrading fungi are particularly adept at degrading lignin-containing recalcitrant biomass and can do so in the absence of other organisms.

Wood-degrading basidiomycetes produce three main rot types: white rot, soft rot, and brown rot. These rot types are characterized by the localization of rot occurring

within the cell wall and have associated progressions of component removal. White rot fungi either simultaneously remove all three cell wall structural polymers starting from the S3 layer or selectively remove lignin, particularly from the lignin-rich middle lamella prior to holocellulose (Ander &Eriksson, 1977; Eriksson et al., 1990).

The ability of white rot fungi to delignify biomass has been linked to their production of ligninolytic enzymes such as peroxidases (Floudas et al, 2012). Lignolytic peroxidases produced by white rot fungi include lignin peroxidases, manganese peroxidases, and versatile peroxidases (Wong, 2009). Laccases may also play a part in oxidizing phenolic compounds (Baldrian, 2006).

Largely lacking lignolytic enzymes, brown rot fungi comprise only 7% of North American homobasidiomycetes by name, but are both morphologically and phylogenetically diverse. Though 70% of North American brown rot fungi are in the *Polyporaceae* family, they can also be found in the *Coniophoraceae*, *Corticiaceae*, *Paxillaceae*, *Sparassidaceae*, *Stereaceae*, and *Tricholomataceae* (Hibbett and Donoghue, 2001). Furthermore, Hibbett and Donoghue (2001) found using phylogenetic analyses that brown rot fungi have arisen at least six times from ancestral white rot species, likely in coupled with ligninolytic enzyme loss (Floudas et al., 2012).

2.4 The Brown rot Decay Mechanism and the Fenton Reaction

It is believed that brown rot fungi take a unique approach to lignocellulose degradation. They cause rapid cellulose depolymerization throughout the S2 layer prior to pore size enlargement. With the maximum pore size of sound wood being ~20 Å

(Flournoy et al., 1991) and the smallest degradative enzymes having a molecular weight of more than 40 kDa, Cowling and Brown (1969) noted that the causative agent of brown rot decay must be smaller than any known cellulase.

It was subsequently noted by Halliwell (1965) that brown rotted wood chemically resembled that treated with Fenton's reagent: hydrogen peroxide and ferrous iron. Shown in equation 1, the Fenton reaction involves an oxidation-reduction reaction between ferrous iron and hydrogen peroxide to produce hydroxyl radical (Haber and Weiss, 1932), which can then proceed to non-specifically oxidize lignin, cellulose, and hemi-cellulose.

$$Fe^{2+} + H_2O_2 \rightarrow Fe^{3+} + OH^- + OH^{\bullet} \qquad (1)$$

Halliwell (1965) noted that the small size of the Fenton reactants makes it possible for them to penetrate sound cell walls and cause the extensive damage observed within the secondary cell wall. It was later shown by Koenigs that brown rot fungi produce hydrogen peroxide (1974a), enough iron is present in wood, and that treatment of wood with Fenton resembles brown rot residue (1974b), making Halliwell's theory conceivable.

Since Koenig's validation of the potential role of Fenton chemistry in brown rot decay, numerous theories have been proposed to explain how these fungi produce hydrogen peroxide and reduce iron. It was initially theorized that the high concentrations of oxalic acid secreted by brown rot fungi lead to the formation of ferric oxalate, which could decompose to form reduced iron, CO_2, and a carbon dioxide anion radical

(Schmidt, 1981), but it was later shown that in the absence of light, this reaction does not occur (Hyde and Wood, 1997). While investigating the role of Fenton's reagent in degradation, it was also proposed that the release of organic acids alone may hydrolyze cellulose (Shimada et al., 1991). Though acid hydrolysis may be a factor in degradation of the more labile hemicellulose, its role in cellulose degradation has been dismissed due to the extensive lignin and carbohydrate oxidation observed in brown rot residues (Kirk et al., 1991; Cohen et al., 2002).

Hyde and Wood proposed that cellobiose dehydrogenase (CDH) may reduce iron (1997), but not all brown rot fungi possess CDH and furthermore, the reaction of CDH with iron oxalate is exceedingly slow, even at low pH (Goodell et al., 1997). Around this time, it was discovered that brown rot fungi release benzenediols into the cell lumen (Goodell et al., 1997; Kerem et al., 1999). These extracellular metabolites are central to current theory regarding the brown rot mechanism. Benzenediols can reduce iron and autoxidize to form hydrogen peroxide, providing both Fenton reactants. It was subsequently shown that the quantity of benzenediols released generated enough hydroxyl radical to cause significant cellulose depolymerization (Suzuki et al., 2006).

A schematic of the brown rot mechanism as currently understood is provided in **Figure 2.5**. While the localization and timing of the release of the components of this reaction system is incompletely understood, their average quantities have been measured.

2.4.1 Oxalic Acid

Brown rot fungi release and accumulate oxalic acid in concentrations of up to 48 mM (Akamatsu et al., 1994). Oxalic acid concentration is closely regulated by the

fungus (Schilling & Jellison 2005; Hastrup et al., 2012a). Along with other organic acids, oxalate acidifies the wood cell lumen to a pH as low as 1.5 (Green et al., 1991). Acidification promotes solvation of ferric iron oxides and hydroxides. The lowering of the pH of the lumen may also be a protection mechanism. The Fenton reaction and the proposed steps that lead to Fenton reactants are highly dependent on pH. At low pH, hydroxyl radical formation is limited (Varela and Tien, 2003), reducing the risk of self-inflicted oxidative damage. Oxalic acid is also an excellent chelator that readily binds with ferric iron, a property that may improve iron availability. It has also been proposed that oxalic acid may undergo esterification with hydroxyl groups in cellulose, increasing cellulose hydrophilicity and decreasing cellulose crystallinity (Hunt et al., 2004). In this way, oxalic acid may also increase cell wall pore size and improve enzyme access to cellulose.

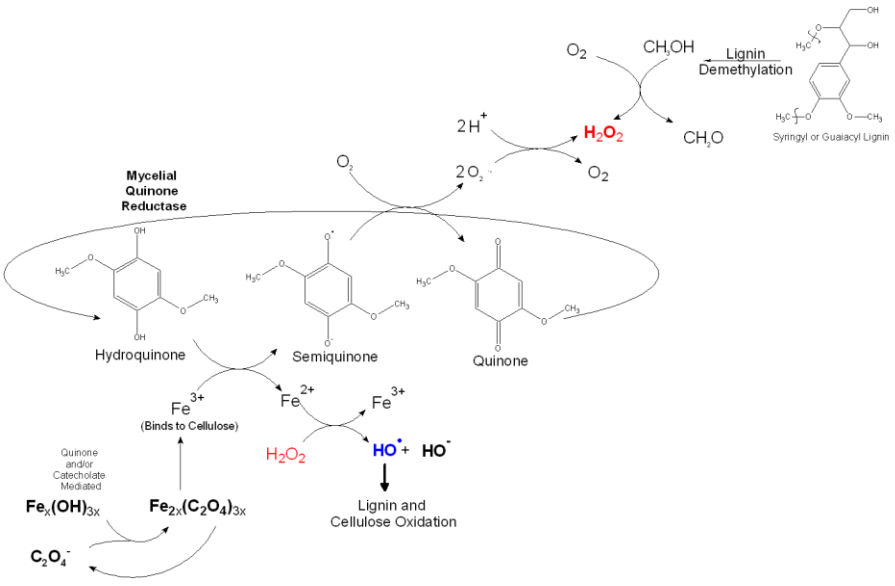

Figure 2.5 Proposed hydroquinone-mediated brown rot mecchanism. Modified from Goodell et al. (1997) and Daniel et al. (2007).

Though not previously proposed, oxalate may also play a role in hydrogen peroxide formation. It has been shown that under dark, acidic, aerobic conditions, manganese (II) oxalate is oxidized to form hydrogen peroxide (Kolthoff et al., 1972).

2.4.2 Iron and other transition metals

Iron concentrations in wood are often between 0-2 μM (Jellison et al., 1993) and most iron present in wood is found as insoluble ferric oxides and hydroxides (Jellison et al., 1997). Like most microbes, fungi improve the bioavailability of iron through iron binding compounds known as siderophores (Fekete et al., 1989). Qian (2008) has demonstrated that oxalic acid plays an important role in sequestering iron. Ferric iron can form up to three ligand complexes with oxalate and catecholates (Elhabiri et al., 2007). While these complexes can still participate in redox reactions, the presence of ligands can greatly alter their reaction rates. Iron and other transition metals readily bind to cellulose (Xu & Goodell, 2001), with oxidation state and the presence of ligands determining the absorption equilibrium. Because of the short reaction radius of hydroxyl radicals, this property may direct hydroxyl radical attack to the desired oxidation target.

Aside from iron, other transition metals, including copper and manganese, can participate in hydroxyl radical redox chemistry. Though copper is not often found in significant concentrations in wood, manganese is often present in concentrations exceeding those of iron (Connolly & Jellison, 1997). The role of manganese in the brown rot mechanism is interesting for several additional reasons. While the presence of iron has been shown to interfere with cellulase function, manganese does not (Tejirian & Xu, 2010). Unlike ferric oxalate, manganese oxalate can form hydrogen peroxide in the

absence of light (Koltoff et al., 1972). Formation of Mn(II) has been observed in brown rot systems (Illman et al., 1989), indicating that manganese is playing some role. It is also worth noting that manganese is accumulated by white rot fungi (Blanchette, 1984) and plays a key role in the functionality of many ligninolytic peroxidases (Bonnarme & Jeffries, 1990).

2.4.3 Benzendiols

One feature that separates brown rot from white rot fungi is that brown rot fungi biosynthesize and release benzenediols (Suzuki et al., 2006). Only one white rot fungus, *Bjerkandera fumosa*, has been associated with dimethyl benzoquinone (DMBQ), the oxidized hydroquinone (Bu'Lock, 1955). Furthermore, these metabolites appear to be ubiquitous across brown rot clades, having been found in *Serpula lacrymans* (Korripally et al., 2013), *Gloeophyllum trabeum* (Goodell et al., 1997; Suzuki et al., 2006), *Postia placenta* (Wei et al., 2010), and *Wolfiporia cocos* (Machuca et al., 2001). Chemical structures of phenolic compounds released by *G. trabeum* can be found in **Figure 2.6**.

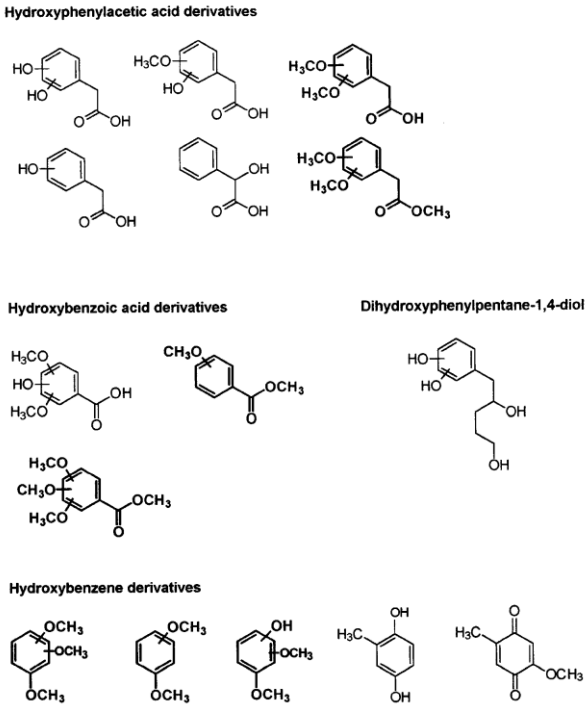

Figure 2.6 Identified phenolic compounds isolated from *G. trabeum* (Goodell et al., 1997)

Many benzenediols, including 2,5-dimethyl-1,4-hydroquinone (DMHQ), can reduce iron via a 1-electron transfer. The resulting semiquinone is readily autoxidized to generate superoxide, which goes on to form hydrogen peroxide. Though not previously proposed with respect to the brown rot mechanism, many of the semiquinones resulting from 1-electron oxidation of oxygen can directly oxidize H_2O_2 to form hydroxyl radical. Though considerably slower, this would eliminate the need for transition metals to be present to carry out Fenton chemistry. This reaction is thermodynamically favorable when the semiquinone/quinone redox potential is between -330 and 460 mV (Prousek, 2007). With a reduction potential of -67 (Wardman, 1989) metal-independent hydroxyl radical formation would be favorable with DMHQ.

2.4.4 Proteins

Alcohol oxidase may also play a role in Fenton chemistry. Daniel et al. (2007) isolated an extracellular alcohol oxidase from *G. trabeum*. This enzyme was shown to preferentially oxidize methanol to form formaldehyde and H_2O_2. The formaldehyde can be oxidized further by the same enzyme to produce another molar equivalent of H_2O_2. It was proposed that the methanol resulting from lignin demethylation could be used to generate H_2O_2 for Fenton chemistry in this manner. This enzyme, however, showed poor activity at low pH. The enzyme's association with the hyphal sheath and the theory that the pH of the cell lumen around the hyphae is low calls into question the importance of this enzyme. The authors proposed that the pH gradient in the lumen around the hyphae is much more complex than the gradient proposed by Hyde and Wood, with calcium ions contributing to the neutralization of oxalic acid in the sheath, a fact supported by the often observed appearance of calcium oxalate crystals in the hyphal sheath (Green et al., 1991).

Though less often discussed, it has also been shown that several brown rot fungi release small glycopeptides with high iron affinity. These proteins are small enough to penetrate a sound cell wall (12 kDa) and can carry out single electron reduction of iron (Enoki et al., 2003). These proteins are present in the *P. placenta* genome and are upregulated when the fungus is grown in the presence of wood (Martinez et al., 2009). The proposed mechanism for the action of these glycopeptides is shown in **Figure 2.7**.

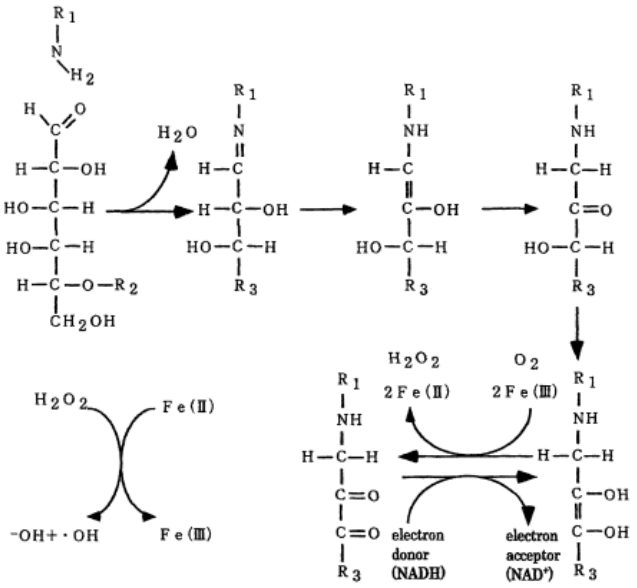

Figure 2.7 Proposed glycopeptide-mediated hydroxyl radical generation (Enoki et al., 1997).

2.5 Alternative Means of Biological Hydroxyl Radical Generation

While focus has been placed on Fenton's reagent, as the source of hydroxyl radicals in brown rot, there are a multitude of analogous chemical routes with other metals and oxidants that lead to hydroxyl radical formation (Wardman and Candeias, 1996) and many of these alternate "Fenton-like" pathways are available to brown rot fungi.

Along with hydrogen peroxide, Fenton (1894) showed that hypohalous acid (HOCl) was also an effective oxidant. In fact, it was later shown that HOCl reacts seven times faster than H_2O_2 with superoxide radical via reaction (2) (Long and Bielski, 1980). Reaction (3) with ferrous iron can also result in hydroxyl radical formation (Prousek, 2007).

$$O_2^{\bullet-} + HOCl \rightarrow O_2 + OH^{\bullet} + Cl^- \quad (2)$$

$$Fe^{2+} + HOCl \rightarrow Fe^{3+} + OH^{\bullet} + Cl^- \quad (3)$$

Although chlorinated organics are generally considered to be anthropogenic, at least 68 genera of basidiomycetes biosynthesize (and degrade) chlorinated organic metabolites in appreciable quantities (DeJong and Field, 1997). Brown rot genera including *Serpula, Coniophora, Gloeophyllum, Poria,* and *Fomitopsis* are among those that produce chlorinated organics (DeJong and Field, 1997). The formation of these compounds is believed to be the result of reaction with HOCl, formed from chloroperoxidase-catalyzed oxidation of chlorine ion with hydrogen peroxide. All of the genomes of brown rot fungi sequenced to date encode haloperoxidases. Chlorinated organics have been associated with fungi that degrade organic matter, suggesting that HOCl may play a role in degradation mechanisms of a variety of decay fungi.

2.6 Hydroxyl radical chemistry

Once formed, the hydroxyl radical is a strong oxidant, reacting non-selectively at diffusion-limited rates with most compounds. Due to its reactivity, the hydroxyl radical has a half-life of about one nanosecond, giving it an angstrom-scale reaction radius. Because of this, the site of hydroxyl radical reaction must also be the site of its formation.

Given its indiscriminant reactivity, it remains unclear how the fungus protects itself and its extracellular enzyme system from hydroxyl radical oxidation, though it has

been proposed that the fungus is able to localize hydroxyl radical generation by controlling pH, utilizing reactant adsorption equilibria (*e.g.*, the iron binding affinity of cellulose), applying the porosity of the cell wall as a physical barrier, and timing enzyme release.

With lignin, hydroxyl radicals cause oxidation of the aromatic ring, demethylation of methoxy groups, phenolic coupling, and C_α- C_β side chain cleavage (**Figure 2.8**). These same effects on lignin have been observed as a result of brown rot decay. Hydroxyl radicals can also react with cellulose and hemicellulose in a number of ways (**Figure 2.9**). These reactions result in a variety of products, including glucose, oligosaccharides, and more extensively oxidized products. Glucose can further react with hydroxyl radical, forming gluconic acid, formaldehyde, and formic acid (Von Sonntag, 1980). These byproducts have been observed in brown rot residues (Hammel et al., 2002), providing further evidence for oxidation during brown rot decay.

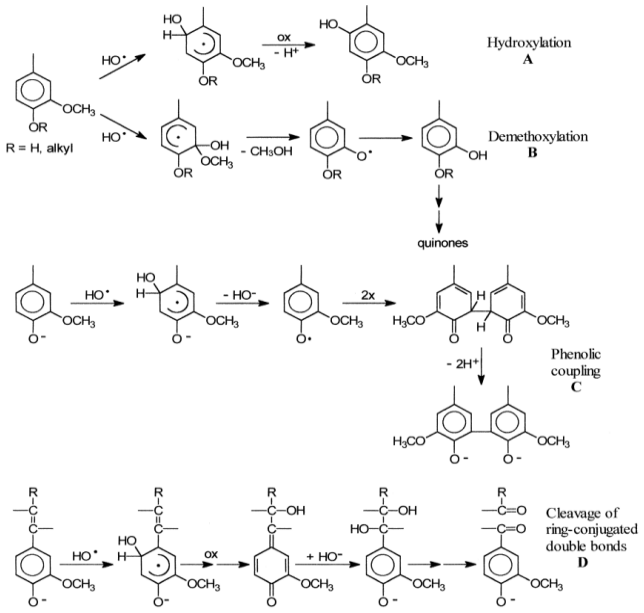

Figure 2.8 Hydroxyl radical reactions with lignin (Lanzalunga and Bietti, 2000).

In comparing Fenton's reagent with brown rot, there are clear differences in the accumulation of soluble byproducts. Halliwell (1965) observed little accumulation of soluble material when cotton was treated with Fenton's reagent. This is in contrast with observations of brown rot residues, which show a significant accumulation of free sugars (Kaffenberger et al., unpublished (See chapter 4)). The discrepancy in Halliwell's results with what is observed in brown rot suggests that brown rot fungi closely regulate hydroxyl radical generation to prevent over oxidation. Since the hydroquinones produced mediate the Fenton reaction, regulation of hydroquinone synthesis or the redox cycling of the quinone product is critical. Alternately, hydroxyl radical generation might be localized only on the insoluble substrate fraction, possibly through pH control or iron sequestration.

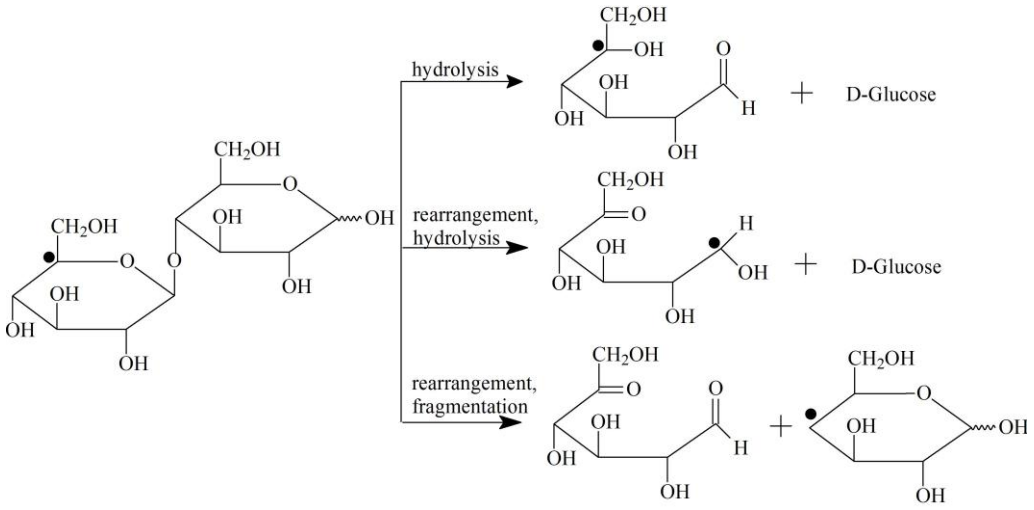

Figure 2.9 Sample of reactions that can occur with cellobiose after hydrogen abstraction by hydroxyl radical (Von Sonntag, 1980).

Apart from its role in brown rot decay, Fenton chemistry is relevant to a wide array of fields including water and atmospheric chemistry and biogeochemical and soil science. It is also believed to be a major contributing factor in cellular aging and is thus important in medicine and physiology as related to biochemical damage cause by reactive oxygen species (ROS). Fenton's reagent has also been employed for a wide range of applications including soil and wastewater remediation, organic synthesis, and polymerization initiation (Wardman & Candeias, 1996).

2.7 Compositional Characterization of Brown rot Decay

Many of the same methods used to characterize sound plant biomass have been used to analyze decay residues. The change in the composition of wood resulting from the progression of brown rot decay was first conducted by Cowling (1961) on sweetgum

sapwood with *Poria monticola* (= *Postia placenta*) and was compared with decay by the white rot fungus *Polyporus versicolor*, a.k.a. *Trametes versicolor*. Using the two-stage acid hydrolysis previously described, Cowling fractionated the decay residues. The insoluble fraction was deemed Klason lignin, while the total mass of the structural sugars in the hydrolysate was assumed to make up the difference. The five structural sugars were resolved by paper chromatography and were quantified spectrophotometrically based on reducing power. Cowling also determined the composition using another method that consisted of pre-extraction with ethanol/benzene, ethanol, and hot water, followed by the composition by holocellulose preparation from the extractive-free biomass. This involved removal of lignin by sequential chlorination and monoethanolamine extractions. Using these methods, Cowling found that brown rot caused rapid early loss of hemicellulose, steady loss of cellulose, and retention of most lignin. Over time, this finding has been generalized to represent all brown rot decay (Eriksson et al., 1990; Yelle et al., 2011; Arantes et al., 2012).

Through no fault of the author's, this compositional analysis suffers from some shortcomings. First, extractives were not removed from the wood prior to acid hydrolysis. As explained earlier, extractives can condense and precipitate with the Klason lignin. For this reason, it is likely Cowling's estimation of lignin content is high, particularly in degraded samples where extractives content tends to rise (Kaffenberger & Schilling, 2013, 2014). In fact, when Cowling (1961) used a method in which the biomass was pre-extracted there was a steady decline in lignin content over the course of decay. Due to the limitations of the methods selected, his compositional analysis was

reported as percentages of the determined quantities, disregarding all non-polymeric biomass constituents. Though this approach will result in a fair representation of the ratio of polymeric components, it results in their overall overestimation. Without accounting for the non-polymeric materials, it remains unclear how these materials contribute to the total weight loss over the course of decay. Since percentages were appropriately corrected to the original wood mass, changes in the weights of these non-polymeric components would further lead to over or under estimation of the polymeric constituents, depending on their flux over the course of decay.

Subsequent studies have had mixed results with respect to lignin loss by brown rot fungi. Kirk and Highley (1973) treated western hemlock, engelmann spruce, sitka spruce, and southern pine with *Poria monticola* (= *Postia placenta*), *Lenzites trabea* (= *Gloeophyllum trabeum*), and *Lentinus lepideus* (= *Neolentinus lepideus*) and found that neither the wood species nor fungus appeared to influence the pattern of decay, with little observed lignin loss. In a follow up study performed by Highley (1987), two *Coniophoraceae* fungi, *P. placenta*, and *G. trabeum* were used to degrade pine and maple blocks in soil jar microcosms and on agar plates. In this study, it was found that lignin losses as high as 22% were observed after 58% weight loss. As in the previous study, it was concluded that wood species, nutrient medium, and fungal species did not influence the pattern of decay. Neither of these studies used extractive-free material for compositional analysis. In other compositional studies, extractive-free material was not used (Winandy and Morrell, 1993) and methodologies for characterization were not

clearly defined (Yelle et al., 2011), while others extrapolated based on data from low weight loss samples (Monrroy et al., 2011).

Several studies do indeed show significant lignin loss with brown rot decay. Using fungi from the *Dacrymycetales* clade, Siefert (1983) demonstrated significant loss of lignin, with upwards of 31% lost after a weight loss of 37%. The likely reason for this observed lignin loss is that unlike previous studies, Seifert utilized a benzene/ethanol pre-extraction prior to Klason lignin analysis. Yelle et al. (2011) saw lignin losses of 32% after 70% weight loss by *Postia placenta* on aspen and Schilling et al. (2012) observed lignin losses of up to 45% after 34% weight loss in aspen, further supporting that at least a portion of lignin is lost during brown rot decay.

A number of other methods have been used to characterize brown rot decay residues. Microscopy has been used to compare the ultra-structural changes induced by brown rot with those caused by other rot types (Highley et al., 1983; Daniel, 1994; Anagnost, 1998). This method has demonstrated that the S3 layer of the cell wall remains intact during decay (Green and Highley, 1997a) and that large molecular weight molecules are incapable of penetrating the cell wall (Blanchette et al., 1997).

FTIR (Pandey & Pitman, 2003; Fackler et al., 2010) and NIR (Kelley et al., 2002; Fackler et al., 2007; Stirling et al., 2007) have also been employed to analyze brown rotted cell walls, wood residues, and lignin, showing that the changes observed in brown rotted biomass are consistent with the oxidation products expected from Fenton oxidation. IR methods are non-destructive and when used in concert with microscopy, can be used obtain spatial information of decay, information that is lost in traditional wet

chemistry techniques. NMR and GC-MS have also been used to characterize brown rot residues, in particular lignin. These studies have been used to show that extensive lignin demethylation (Filley et al., 2002) and alkyl chain cleavage (Yelle et al., 2008b) occurs during brown rot, consistent with the reactions expected with hydroxyl radical and corroborating observed lignin losses.

2.8 Chemical Mimicry of Brown rot

If the brown rot decay mechanism involves chemically-driven Fenton oxidation, there is potential to mimic brown rot decay *in vitro*. Indeed, chemical mimicry was the first method used to recognize the link between Fenton chemistry and brown rot decay (Halliwell, 1965; Koenigs, 1974b).

Jain & Vigneshwaran (2011) used Fenton's reagent (0.25-1.25 mM Fe^{2+} and 0.5-2.5% H_2O_2) to pretreat cotton cellulose to determine its effects on apparent enzyme activity. It was found that 0.5 mM Fe^{2+} and 2% H_2O_2 slightly enhanced cellulase activity on cotton cellulose, but microcrystalline cellulose was found to be recalcitrant to this pretreatment. Ratto et al. (1997) came to similar results, observing that microcrystalline cellulose (Avicel) treated with ferrous iron (0.5 mM) and 1% H_2O_2 did not result in greater yields of reducing sugar when enzymatically hydrolyzed. For comparison, spruce wood treated in the same manner resulted in a 2-fold increase in reducing sugar yield over the control (32.5% vs. 17.1%, respectively).

Xie et al. (2010) used 2,3-DHBA, an iron-chelating phenolic compound, and hydroquinone, a non-chelating phenolic to show that both increased the rate of hydrogen

peroxide consumption, but strength loss representative of depolymerization of Scots pine actually decreased with increasing phenolic concentration, contradicting the proposed mechanism. This was attributed to diversion of hydroxyl radical formation away cellulose and radical scavenging by the phenolics. In contrast, Arantes & Milagres (2006) found that the catecholate phenolic dihydroxy phenyl acetic acid accelerated Fenton-driven degradation of hemicellulosic and cellulosic substrates.

Arantes et al. (2009) used a chelator-mediated fenton reaction (CMFR) to demonstrate that its effect on lignin was similar to that observed with the Fenton reaction, causing extensive demethylation and oxidative modifications. The main difference apart from the presence of DHBA between the Fenton and CMFR reactions used was the use of ferric and ferrous iron for each reaction respectively. While this study demonstrated the ability of DHBA to reduce iron, it did not demonstrate that hydrogen peroxide can be formed *in situ* as theorized.

While combinations of ferric iron and DMHQ have been shown to lead to lipid peroxidation (Varela & Tien, 2003) and polyethylene glycol (Kerem et al., 1999), this system has not been used to depolymerize a plant substrate without supplementation with hydrogen peroxide. Assuming that there is an adequate concentration of iron in wood and hydroquinone autoxidizes to form hydrogen peroxide, then the addition of hydroquinone alone should be sufficient to carry out Fenton oxidation.

Only one study has considered the role of manganese in chemical mimic of brown rot. Fenton-driven depolymerization of amorphous cellulose with manganese in lieu of iron was investigated by Hastrup et al. (2012). It was observed that depolymerization

properties comparable to those seen with iron were attained with manganese. This study also considered the effect of oxalic acid alone which caused significant depolymerization at a concentration of 10 mM. It was also generally found that higher pH conditions resulted in greater loss in DP, in agreement with Varela & Tien (2003).

2.9 Direct Biological Pretreatment

Various decay fungi and bacteria have been considered for direct biological pretreatment for bioconversion, including white rot fungi (Hatakka, 1983; Lee et al., 2007; Vaidya & Singh, 2012; Yu et al., 2009; Zhang et al., 2007; Salvachùa et al., 2011), brown rot fungi (Tewalt and Schilling, 2010; Ray et al., 2010; Monrroy et al., 2011; Vaidya & Singh, 2012; Gao, 2012), and cellulose-hydrolyzing strains of bacteria (Kurakake et al., 2007).

The ability of white rot fungi to selectively break down lignin has made them desirable for many applications. Apart from biological pretreatment for bioconversion, white rot fungi have been considered for bioremediation (Reddy, 1995), sewage treatment (Wesenberg et al., 2003), bio-pulping (Blanchette et al., 1988), and the conversion of lignocellulose into more digestible animal feed (Hatakka, 1989; Tian et al., 2012). Because some white rot fungi can selectively degrade lignin and lignin content correlates with saccharification yield, they are an excellent fit for biomass conversion. The best reported saccharification yield achieved with white rot pretreatment has been 69% with *Poria subvermispora* (=*Ceriporiopsis subvermispora*) on wheat straw

(Salvachùa et al., 2011). In general, reported white rot treatments have resulted in a 3-6 fold improvement in saccharification yield over untreated controls.

Brown rot fungi have been less commonly considered for direct biological pretreatment. Ray et al. (2010) exposed *Pinus sylvestris* to the brown rot fungus *Coniophora puteana* for up to 25 days. The resulting residues were enzymatically hydrolyzed using commercial cellulases and the resulting hydrolysate sugars were quantified by HPLC. 15 days of exposure gave the best results, improving glucose release by roughly four-fold (32% versus 8% for the control). A follow-up study was performed using *Pinus radiata* chips that were exposed to one of two brown rot fungi (*Coniophora puteana* or *Postia placenta*), a white rot fungus (*Trametes versicolor*), a soft rot fungus (*Chaetomium globosum*), or one of two molds (*Trichoderma viride* and a *Mucor* sp.) as pretreatment agents for up to 35 days. Both brown rot species showed the best glucose release (15 – 20%) after 20-25 days. None of the other tested species showed improved glucose release. The discrepancy in maximum yield for *C. puteana* between the two experimental studies was attributed to the difference in substrate species. Based on an assumed glucan percentage in the starting biomass of 44-47%, they report an overall glucose yield in excess of 70%, approaching the 80% level targeted for commercialization.

2.10 Pretreatment Consolidation

Investigation of the consolidation of a chemical pretreatment process with enzymatic hydrolysis has not been previously reported to the author's knowledge.

Process consolidation has been seen as a viable means of reducing biofuel production cost. Saccharification and fermentation have been consolidated through simultaneous saccharification and fermentation (SSF), simultaneous saccharification and co-fermentation (SSCF), and consolidated bio-processing (CBP). Each of these processes builds off of the other to reduce processing steps. SSF combines cellulase hydrolysis and hexose fermentation, SSCF includes pentose fermentation with SSF, and CBP includes cellulase production in SSCF (Olofsson et al., 2008). CBP requires organisms that produce glycoside hydrolases and can ferment both C5 and C6 sugars. Examples of organisms include *Ruminococcus albus* and *Clostridium thermocellum*.

Despite the issue of capital costs in cellulosic biofuel production, consolidation of pretreatment with hydrolysis has not been a major focus of research. One of the few studies to suggest pretreatment and hydrolysis was proposed by Li et al. (2008). In this work, various lignocellulosic materials were dissolved in several ionic liquids. Once in solution, cellulose and hemicellulose fractions were hydrolyzed with hydrochloric acid (7% by weight of biomass) at 100°C. Total reducing sugar yields using this process were as high as 66%, 74%, 81% and 68% for corn stalk, rice straw, pine wood, and bagasse, respectively. While pretreatment and hydrolysis are combined, there are several downsides to this process, namely the further reaction of sugars to form inhibitory compounds and reduce overall yield and the expense of ionic liquids.

Others have suggested developing cellulolytic microorganisms that can tolerate ionic liquids. Khudyakov et al. (2012) isolated a strain of *Enterobacter lignolyticus* that can grow in the presence of 0.5 M concentration of the ionic liquid 1-ethyl-3-

methylimidazolium chloride. This approach may ultimately lead to a microorganism that can perform CBP in an ionic liquid, bypassing pretreatment altogether. As with Li et al., however, the required use of expensive ionic liquids for process consolidation limits its potential for cost improvement.

Chapter 3

Comparing lignocellulose physiochemistry after decomposition by brown rot fungi with distinct evolutionary origins

3.1 Introduction

Wood-degrading fungi are vital participants in terrestrial ecosystem carbon cycling through direct carbon mineralization and improved carbon accessibility for secondary degraders (Harmon et al., 1986; Osono, 2007). These fungi can be segregated by the functional rot types they cause in wood, a consequence that depends on how they access carbohydrates embedded in lignin (Eriksson et al., 1990). The two traditionally prescribed rot types are white rot, during which lignin is removed enzymatically to gain access to cellulose, and brown rot, which releases sugars more selectively. This capacity to cause brown rot was an adaptation in multiple, taxonomically distinct white rot lineages (Hibbett and Donoghue, 2001), thus the brown rot classifier denotes the properties of decay in plant tissues rather than phylogeny. Although it is clear that rot type produces unique physical and chemical signatures in wood residues (Filley et al., 2002; Song et al., 2012) and can influence the microbial communities that develop in resulting soils (Waid, 1999), it is unclear how uniform this process is among the diverse lineages of brown rot fungi.

Our underlying knowledge of how fungi cause brown rot in wood has largely been informed by studying deeply the mechanisms of relatively few model fungi. Brown rot is believed to involve oxidation of all lignocellulose components through Fenton-type

chemistry, where reduced iron is oxidized by hydrogen peroxide to yield hydroxyl radicals (Goodell et al., 1997; Hyde and Wood, 1997; Kerem et al., 1999). This initial non-selective oxidation causes early and significant strength loss in wood (Winandy and Morrell, 1993), and the high incidence of brown rot in building materials has led both to a prevalence of pest fungi as models and to a focus on early stage wood metabolism. As a case in point, it has been corroborated among pest fungi from different brown rot clades, *Gloeophyllum trabeum* (Kerem et al., 1999), *Postia placenta* (Wei et al., 2010), and *Serpula lacrymans* (Korripally et al., 2013), that each releases a stoichiometrically significant quantity of hydroquinones that likely contribute at least in part to the formation of the Fenton reactants. This depth of inquiry using model fungi is essential given the complexity of studying the mechanism, regardless of the historical logic of model selection. It is, however, useful to know how robust these biological mechanisms are among the varied brown rot lineages, given that brown rot fungi are collectively prescribed an ecological and a biotechnological function as a single rot type.

Facilitated by modern molecular tools, recent –omics data show significant variability in genomic and secretomic diversity among brown rot fungal lineages and suggest the possibility of multiple routes to a similar consequence in wood. The convergent evolution of brown rot lineages has seen extensive gene losses in several decay-related gene families, including white rot associated lignin-degrading class II peroxidases (PODs) and carbohydrate active enzymes (CAZymes) that target crystalline cellulose, e.g. cellobiohydrolases (Floudas et al., 2012). Recently, it has also been associated with an expansion in reducing polyketide synthases (RPKSs) (Riley et al.,

2014). Though the origins of brown rot coincide with gene losses, the lignocellulolytic machinery of the brown rot decay mode is diverse (Riley et al., 2014). An example of this is the presence of cellobiohydrolase (GH6) and cellulose-binding modules (CBM1) in *S. lacrymans* (Bolete clade) (Eastwood et al., 2011). These cellulolytic agents are in common with white rot ancestral genomes but absent from the *P. placenta* genome (Antrodia clade) (Martinez et al., 2009) and the genomes of other brown rot clade representatives (Floudas et al., 2012). In contrast, Wei and colleagues (2010) showed that *P. placenta* codes two putative laccase enzymes that are often associated with white rot fungi, shown in this case to promote 2,5- dimethoxyhydroquinone oxidation for faster hydrogen peroxide generation. As another example and a complement to evidence for clade-specific diversity, the tolerance of copper-based wood preservatives among brown rot fungi also varies (Green and Clausen, 2003), likely related to distinct pathways for carbon metabolism and varying secretion of copper-binding oxalate as a product (Munir et al., 2001; Schilling and Jellison, 2005).

Brown rot, if characterized by wood modifications rather than fungal taxonomy, has not been studied with detail in multi-clade comparisons and rarely on substrates other than conifer wood. Brown rot fungi are commonly associated with conifer wood, but this relationship is far from absolute in forests, with some found almost exclusively on angiosperm wood (e.g. *Piptoporus betulinus* on birch) (Gilbertson and Ryvarden, 1986). Component deconstruction trends generated on brown rotted conifer substrates have also been correlated with strength loss to infer the relative roles of hemicellulose component loss versus cellulose depolymerization (Curling et al., 2002). These patterns are not

typically studied on angiosperm wood but have twice shown, in coarse bulk analyses, a concomitant loss of carbohydrate fractions rather than initial hemicellulose removal (Cowling, 1961 – sweet gum; Schilling et al., 2012 – aspen). Concerning fungal taxonomic diversity, Kaffenberger and Schilling (2013) demonstrated empirically and with a meta-analysis that *G. trabeum* (Gloeophyllum clade) could effectively decompose a grass substrate, corn stalk, but that several members of the Antrodia clade including *P. placenta* could not. This substrate-induced variability among brown rot fungi, combined with known metabolic diversity among clades, suggests that wood disassembly (i.e., the order of sugar release) may proceed differently among brown rot clades toward producing similar lignin-rich residues.

The goal of this study was to discern whether brown rot fungal clades are monolithic in the order and effects of lignocellulose component removal. To achieve this, three distinct plant tissue types were inoculated by one of seven species of brown rot fungi, each representing a distinct brown rot clade. The genomes of five of the representative species have been sequenced and annotated [*S. lacrymans* (Eastwood et al., 2011), *Fomitopsis pinicola*, *W. cocos*, *G. trabeum* and *Dacryopinax* sp. (Floudas et al., 2012)], and the genome of *Fistulina hepatica* is designated for sequencing and annotation as part of the Joint Genome Institute (JGI) 1000 fungal genomes project (JGI, 2013). Residues were harvested and characterized at seven points along a time series in order to track the progress of decomposition. Characterization included mass loss and residue chemical composition, as well as an accessibility measure after incubation with a

cellulase preparation. Results were approached descriptively as well as correlatively, allowing comparative analyses of physiochemistry at comparable decay stages.

3.2 Experimental procedures

3.2.1 Cultures

Isolates were acquired from either American Type Culture Collection (ATCC, Manassas, VA, USA) or the USDA Forest Products Laboratory (FPL, Madison, WI, USA) and included *Wolfiporia cocos* (FPL, FP-97438-Sp), *Fistulina hepatica* (FPL, FP-24077-T), *Ossicaulis lignatilis* (FPL, DAOM-187956), *S. lacrymans* (ATCC, 32750), *F. pinicola* (FPL, FP105877R) and *G. trabeum* (ATCC, 11539). *Dacryopinax* sp. (DJM-731) was provided by Dr Robert A. Blanchette (Forest Mycology Collection, University of Minnesota). Strains of *G. trabeum* and *Dacryopinax* sp. were identical to those used for genome sequencing (Floudas et al., 2012). Isolates selected included a representative from each of the seven known taxonomic brown rot clades (Hibbett and Donoghue, 2001). Each isolate was maintained on 2% (w/v) malt extract agar for 2 weeks prior to addition to microcosms.

3.2.2 Microcosms

Soil-block microcosms were prepared following the guidelines of ASTM standard D1413 (ASTM, 2007). Equal parts by volume of vermiculite, fertilizer-free potting soil, and peat moss were wetted and thoroughly mixed. Wetted soil mix (250 g) was added to canning jars (473 ml capacity) along with two birch feeder strips (40 × 10 × 2 mm) placed in parallel on top of the soil mixture. Feeder strips were included to ensure rapid

initial colonization and adequate nutrient availability for optimal growth. Jars were autoclave sterilized twice for 1 h (121°C, 103 kPa) with a 48 h interval. For each jar, one colonized agar plug (7 mm diameter) was placed at each end of the two feeder strips. All inoculated jars, excluding *S. lacrymans*, were incubated at 25°C and 70% relative humidity for 2 weeks. *Serpula lacrymans* was incubated at its lower optimal growth temperature of 20°C (Maurice et al., 2011) and 65% relative humidity for 2 weeks.

3.2.3 Substrates and harvest

Angiosperm (hardwood) and coniferous gymnosperm (softwood) woods were used as substrates, along with a grass. Pine (*Pinus radiata*) and aspen (*Populus tremuloides*) were used as representative softwood and hardwood types respectively. Sapwood blocks (19 cubic millimeters) of each were cut from single pieces of untreated lumber. As the representative grass, corn (*Zea mays*) stalk internodes were prepared as previously described (Kaffenberger and Schilling, 2013). Prior to use, prepared blocks and internodes were dried at 100°C for 48 h to determine initial mass. Aspen blocks (n = 252) weighed 2.77 g on average [95% confidence interval (CI; 2.76, 2.78)], pine blocks (n = 252) weighed 2.59 g [95% CI (2.58, 2.60)], and corn internodes (n = 252) weighed 2.04 g [95% CI (1.98, 2.11)]. All blocks and internodes were sterilized at 121°C (103 kPa) for 1 h prior to addition to soil-block microcosms. Though autoclaving can alter substrate chemical structure, namely through the loss of side-chain hemicellulosic carbohydrates, the alternative, gamma irradiation produces comparably detrimental structural effects (Curling and Winandy, 2008). The effects of autoclaving were

controlled for by the inclusion of both autoclaved controls and unsterilized material in composition and accessibility testing.

Six blocks or internodes of a given substrate type were placed in each microcosm. Including controls (no fungal inoculation), there were 756 total samples in 126 jars, with one sample being a single block or internode. After 2, 3, 4, 6, 8 and 16 weeks, one randomly selected sample was aseptically removed from each microcosm. Half of each sample was dried in a convection oven at 100°C for 48 h to determine moisture content. A portion of the remaining half was dried at room temperature over anhydrous calcium sulfate desiccant and retained for enzymatic hydrolysis. Oven-dried samples with like treatments (n = 6) were pooled, ground to 40 mesh in a Wiley mill and characterized.

3.2.4 Chemical characterization

Compositional analyses included ash, ethanol-soluble extractives, lignin and structural sugar content of the ground treated substrates and time zero, unsterilized controls. Analytical procedures followed much of the National Renewable Energy summative mass closure approach (Sluiter and Sluiter, 2010) but did not include water-soluble extractives, protein or organic acid measurements. All procedures were performed in triplicate and mean results were reported. Sugar concentrations were measured by high performance liquid chromatography (HPLC) using an HPX-87P Aminex column (Bio-Rad Laboratories Inc., Hercules, CA, USA) and an in-line de-ashing guard column (Bio-Rad). Mobile phase consisted of 85°C HPLC-grade water at a flow rate of 0.4 ml min^{-1}. Sugars measured were compared with standard calibration curves and included glucose as well as hemicellulosic components xylose, galactose,

arabinose and mannose. Acid-soluble lignin was determined with a UV-Vis spectrometer (PerkinElmer, Waltham, MA, USA) at a wavelength of 320 nm for corn stalk samples and 240 nm for aspen and pine. Extinction coefficients of 30, 25 and 12 l g^{-1} cm^{-1} were used for corn stalk, aspen and pine samples, respectively, as recommended by Sluiter and colleagues (2008).

3.2.5 Enzyme accessibility

Enzymatic hydrolysis of embedded residual carbohydrates (saccharification) was conducted to complement physiochemical characterization as a biologically relevant 'accessibility' character, in accordance with Selig and colleagues (2008). Samples were saccharified for 5 days with Celluclast 1.5L (cellulase mixture) (Sigma, Saint Louis, MO, USA) at a concentration of 60 filter paper units per g of biomass and with Novozyme 188 (cellobiase) at 64 pNPGU g^{-1} (Novozymes, Bagsvaerd, Denmark). Tetracycline and cycloheximide (Sigma) were added as antimicrobial agents. Cellulase activities were determined according to Adney and Baker (1996). Sugar concentration in the hydrolysate was measured by HPLC as described for structural sugar analysis. Sugar yield, corrected for mass loss and using standard hydration factors, was calculated using the following equation, where m refers to mass and C_i refers to a given carbohydrate:

$$\text{Yield (\%)} = [1 - \text{wt loss (\%)}] \text{ X } m_{Ci} \text{ released} / [m_{\text{hydrolysed}} \text{ X } C_{i \text{ initial}} (\%)].$$

3.2.6 Statistics

Statistical analyses were used to compare the sequence of wood chemical constituent removal among the evolutionarily distinct fungal isolates (e.g. side-chain hemicellulose fractions) and their effects on accessibility. First, a regression model was

selected. For each substrate, the mass loss corrected percentage of component loss was plotted versus the weighted average mass loss. Data for each set were fit to linear, exponential, cubic, power, growth and sigmoidal regression models. Setting α level at 0.05, models with random scatter residual plots were compared pairwise for significant difference in their residual sum of squares (SS) using an *F*-test, as outlined by Motulsky and Ransnas (1987). The simplest model that was not significantly different from the model with the lowest SS was selected for further analysis. Nash–Sutcliffe model efficiency coefficient (E), root mean square error, mean absolute error and index of agreement (d) were calculated as previously reported (Nash and Sutcliffe, 1970; Willmott, 1982) and were determined as goodness-of-fit indicators.

Once the appropriate regression model was established, data sets were split into subsets per fungal species. Fits of each treatment subset were made using the appropriate model. *F*-test comparisons between the individual and pooled fits were used to determine if there were significant differences among treatments. *F* value was calculated as described by Motulsky and Ransnas (1987). After determining whether treatment subsets significantly differed in the progression of loss of a given component (fungal species dependence), the comparison was made across substrates for each component using the same *F* test (substrate species dependence), with *P* values greater than 0.05 suggesting no significant difference in the progression of component loss between the two pairwise-compared substrates.

Additionally, general regression analysis was performed using component concentrations as predictors of glucan yield from saccharification. To reduce collinearity,

all data were standardized by mean subtraction and division by the standard deviation. The concentrations of individual components were compared with glucan yield to determine the presence of non-linear relationships. The glucan yield for most components was best described linearly, but a quadratic fit was best for ash, glucan, xylan and the remaining unaccounted fraction. Given this relationship, the square of these components was included in the general regression. Regression analysis was performed iteratively until the *P* values of all predictive variables were < 0.05. The analysis was independently performed on each substrate individually and on the combined data set of all three substrates. To account for differences across substrates in initial component concentration, analyses were performed with absolute percentages. Once significant variables were established with the standardized data, the regression was also performed with the unstandardized data of these variables for ease of coefficient interpretation. Predicted glucan yields calculated from the resulting regression equation were then plotted against the corresponding experimental glucan yields to determine regression model explanation of glucan yield variance.

3.3 Results

3.3.1 Mass loss

The rate of mass loss varied over the course of decay in 5 of the 7 clades with significant mass loss, with lag, log and deceleration phases in wood (**Figure 3.1**). The decay phases of corn stover were less pronounced, with no clear lag phase and a steady rate of mass loss. At week 16, corn stalk mass loss averaged 31.6%, while woody substrate mass loss averaged 55.8% and 52.2% for aspen and pine, respectively. The rate

and extent of mass loss per wood block or stalk section varied with substrate and fungal species. *W. cocos*, *S. lacrymans* and *O. lignatilis* caused the most mass loss on woody substrates. *F. pinicola* caused the greatest corn stalk mass loss, but only after a considerable lag phase that was not present with the other species. *F. hepatica* and *Dacryopinax* sp. did not cause significant mass loss, leaving 5 clades represented for further analyses.

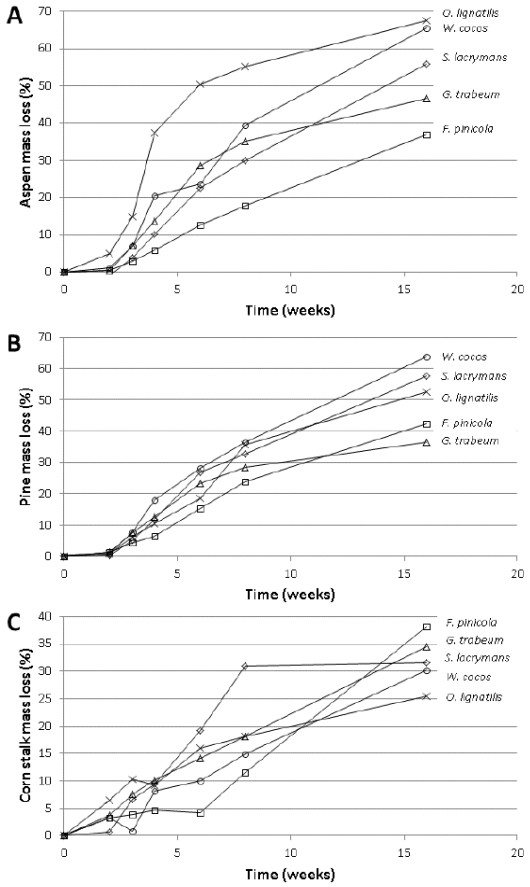

Figure 3.1 Mean mass loss of treated blocks or internodes. SE for all mass loss data are provided in Tables S3.1 - S3.3. **A**, aspen; **B**, pine; **C**, corn stalk.

3.3.2 Composition and component loss

Initial compositions of pine, aspen and corn stalk (**Table 3.1**) were comparable to previously reported values (Ladisch et al., 1983). Pine contained substantially more

mannan and lignin and less xylan than the angiosperms, and the ash and extractives contents were greater in corn stover than in the woody substrates, likely due to high levels of silica and non-structural sugars, respectively. Comparison of the composition of unsterilized time zero samples and autoclaved week two control samples showed some initial hemicellulose losses due to steam sterilization (Supplemental Tables S3.1–S3.3).

Table 3.1 Mean component weight percentage (wt% ± SE) of non-degraded substrates. [a]Corn stalk ash and extractives include silica and non-structural sugars, respectively. A, aspen; P, pine; CS, corn stalk.

Component	A	P	CS
Ash	0.21	0.59	5.25[a]
	(0.03)	(0.07)	(0.04)
Ext	3.01	2.38	13.38[a]
	(0.28)	(0.33)	(1.23)
Lig	20.44	27.05	15.22
	(0.18)	(0.54)	(0.13)
Glu	44.16	45.03	35.29
	(1.14)	(0.30)	(0.23)
Xyl	15.82	3.50	20.27
	(0.20)	(0.05)	(0.16)
Gal	0.50	2.82	0.00
	(0.02)	(0.07)	(0.00)
Ara	0.44	1.37	5.91
	(0.03)	(0.01)	(0.31)
Man	2.77	12.82	0.60
	(0.18)	(0.19)	(0.08)
Uronic acid	3.05	1.14	1.46
	(0.00)	(0.10)	(0.05)
Acetate	4.18	1.37	4.43
	(0.01)	(0.10)	(0.05)
Total	94.58	98.07	101.81
	(1.49)	(0.41)	(1.31)

Detailed component analysis data for aspen, pine and corn stalk over the time course of decay by each test fungus are provided in Tables S3.1, S3.2 and S3.3, respectively. Component loss is also presented as a function of total mass loss in **Figure**

3.2. Total mass loss, rather than time, was used as the independent variable to enable comparison between fungi that caused decay at differing rates. Among all fungal isolates tested, removal of plant cellulose (as glucan) progressed linearly with mass loss. Hemicellulose saccharides, particularly mannan and arabinan, were rapidly lost during incipient decay. Extractives content in the woody substrates increased nearly three-fold, while corn stalk extractives declined. Lignin loss was minor in pine, but up to 40% lignin removal was observed in aspen and corn stover. Loss progression for a given substrate component was similar for all five of the fungi that affected mass loss (

Figure 3.2).

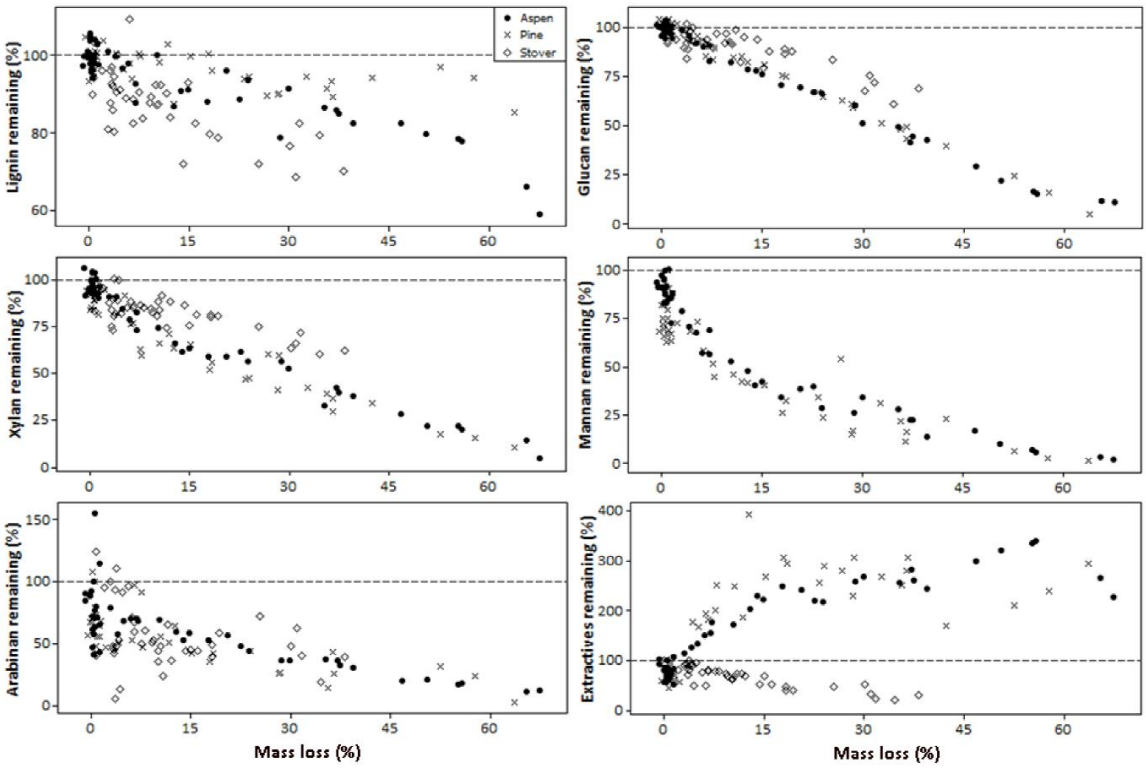

Figure 3.2 Change in lignocellulose chemical components with mass loss. Component content is expressed as a mass loss corrected percentage of original content. Each point represents an individual treatment: a combination of fungal isolate & decay time. Error bars are excluded for clarity of visualization, though detailed composition data for each isolate, including SE, are provided in Tables S3.1 – S3.3.

The model best describing mass loss-dependent removal differed among chemical components. An exponential model was found to be most representative of lignin and mannan, while power and cubic models described the change in extractives and xylan content, respectively. Linear fits best described glucan, galactan and arabinan loss. Using 0.5 as a cut-off for goodness of fit indicators d and E, most models reasonably fit the component loss data with exceptions involving minor hemicellulose components, i.e. galactan and arabinan loss in aspen and arabinan and mannan loss in corn stover (**Table 3.2**).

Table 3.2 Model parameter values and goodness of fit statistics for model equations describing substrate component loss. RMSE, root mean square error; MAE, mean absolute error; *d*, index of agreement; *E*, Nash-Sutcliffe model efficiency coefficient; **L**, linear (y = A*x + B); **E**, exponential (y = A*exp(B*x)); **C**, cubic (y = A*x3+B*x2+C*x+D); **P**, power (y = A*xB)

	Comp.	Ext	Lig	Glu	Xyl	Gal	Ara	Man
	Model	P	E	L	C	L	L	E
Aspen	A	3.54	1.00	-1.44	-3.36	-2.36	-1.10	0.90
	B	0.29	-0.51	0.99	4.23	1.66	0.77	-4.43
	C	NA	NA	NA	-2.67	NA	NA	NA
	D	NA	NA	NA	0.98	NA	NA	NA
	RMSE	0.26	0.04	0.03	0.05	0.81	0.12	0.06
	MAE	0.25	0.03	0.03	0.04	0.59	0.13	0.05
	d	0.98	0.95	1.00	0.99	0.59	0.76	0.99
	E	0.85	0.82	0.99	0.98	0.21	0.41	0.97
Pine	A	3.58	0.99	-1.47	-4.56	-1.35	-1.01	0.77
	B	0.26	-0.18	1.01	5.18	0.72	0.69	-4.12
	C	NA	NA	NA	-2.80	NA	NA	NA
	D	NA	NA	NA	0.93	NA	NA	NA
	RMSE	0.52	0.04	0.02	0.06	0.16	0.16	0.09
	MAE	0.71	0.03	0.02	0.05	0.13	0.12	0.07
	d	0.61	0.75	1.00	0.99	0.90	0.85	0.97
	E	0.24	0.40	0.99	0.94	0.69	0.57	0.88
Corn stover	A	0.41	0.95	-0.78	-0.58	NA	-0.72	0.16
	B	-0.19	-0.75	0.98	-0.94	NA	0.63	2.42
	C	NA	NA	NA	-0.32	NA	NA	NA
	D	NA	NA	NA	0.89	NA	NA	NA

RMSE	0.14	0.06	0.05	0.06	NA	0.25	0.27
MAE	0.12	0.04	0.04	0.18	NA	0.04	0.20
d	0.82	0.82	0.91	0.87	NA	0.36	0.29
E	0.54	0.51	0.72	0.62	NA	0.08	0.04

All the fungi tested removed substrate components in the same progression, but this pattern differed depending on substrate type. *F*-test comparison of the pooled data set with the subset data for each individual fungus resulted in the *P* values provided in **Table 3.3**. A *P* value < 0.05 indicated that the data subsets were not well fit by a single curve, while a $P > 0.05$ indicates that a single curve is representative of all data subsets. For all substrate components, *P* values were > 0.05, which is a standalone result that underscores the lack of distinction in component removal among these clade representative fungi. After establishing that pooling component loss of all species for a given substrate was appropriate, a similar comparison was made between the pooled data sets of each substrate. *P* values for comparison of aspen and pine were > 0.05, suggesting no statistical difference in the progression of change in extractives, glucan, and arabinan content.

Table 3.3 *P* values for comparison of model fit between treatments and substrates. $P > 0.05$ indicates no significant difference among treatments in progression of rate of loss of the given component. A, aspen; P, pine; CS, corn stalk.

	by treatment			between substrates		
Component	A	P	CS	A+P	A+CS	P+CS
Ext	0.111	0.352	0.138	0.338	0.000	0.000
Lig	0.816	0.390	0.530	0.000	0.000	0.000
Glu	0.159	1.000	0.508	0.103	0.000	0.000
Xyl	0.343	0.292	0.838	0.014	0.000	0.000
Gal	0.175	0.312	ND	0.000	ND	ND
Ara	0.890	0.244	0.908	0.101	0.083	0.705
Man	0.228	0.053	0.631	0.000	0.000	0.000

3.3.3 Saccharification accessibility

Woody substrate accessibility, measured as glucan saccharification yields, generally improved to a point over the course of brown rot decay, while corn stover glucan accessibility declined (**Figure 3.3**). Aspen controls had the lowest glucan yield of the three substrates (11.4%) but generally gave the best overall yield and yield improvement after exposure to brown rot. Aspen exposed to *G. trabeum* for 6 weeks gave the best glucan yield, 44.7%, a 3.9-fold improvement over the control. In pine, 4 week exposure to *G. trabeum* gave the best glucan yield at 33.8%, a 2.3-fold improvement over the control. Initial glucan yields from corn stover were the highest of the three substrates (29.3%), but exposure to brown rot led to glucan yield losses, likely related to non-structural sugar contents included in the extractives analyses. *Dacryopinax* sp. and *F. hepatica*, which did not cause significant mass loss, also failed to improve yield in comparison with substrate controls.

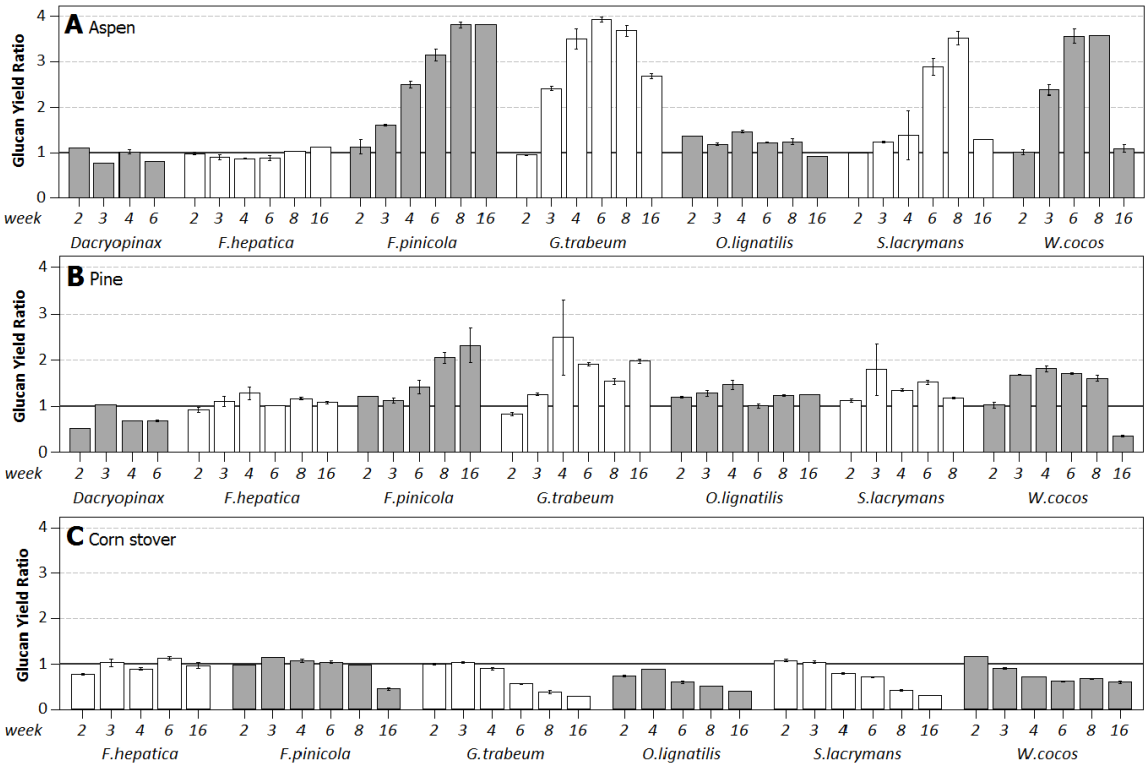

Figure 3.3 Mean ratio of glucan yield (± SE) of pretreated substrates versus the control value. A, aspen (control yield = 11.4%); B, pine (control yield = 13.6%); C, corn stalk (control yield = 29.3%).

As observed for component loss patterns, glucan yields followed a universal mass loss-dependent progression for all fungi. When plotted relative to mass loss, not time (**Figure 3.4**), cubic, quadratic and exponential equations best described the aspen, pine and corn stover glucan yield curves, respectively. With aspen, change in glucan yield for *O. lignatilis* and *S. lacrymans* were significantly different ($P < 0.05$), but the glucan yield curve of all other tested fungi were statistically the same ($P = 0.26$). On pine, all fungi followed the same glucan yield curve ($P = 0.38$), as they did on corn stover ($P = 0.11$). With aspen and pine, maximum glucan yield was observed at a mass loss of 21.4% and 21.1%, respectively.

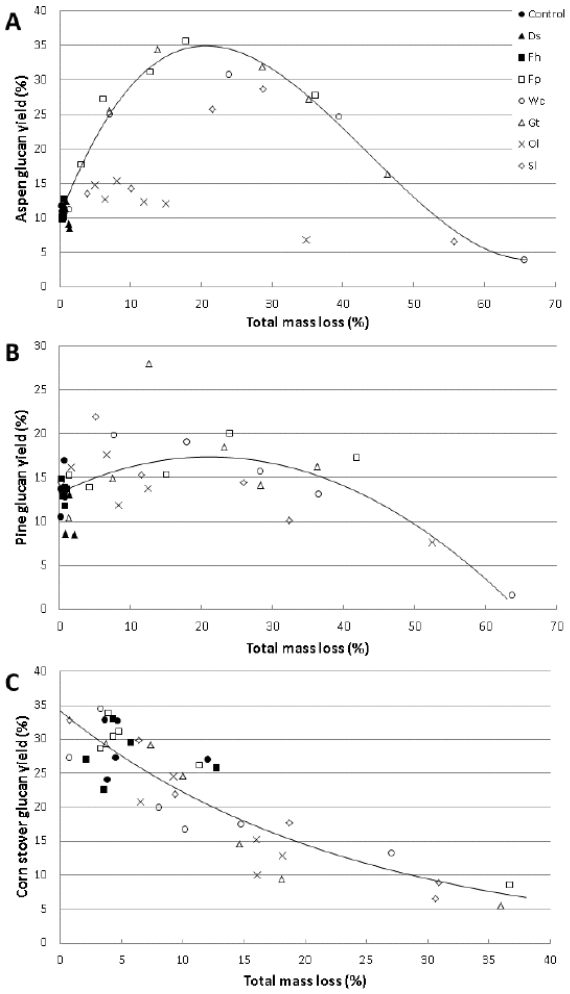

Figure 3.4 Glucan yield based on original glucan content as related to total mass loss for aspen (A), pine (B), and corn stover (C)

3.3.4 Composition effect on accessibility

The type and number of chemical components that were significant to glucan yield outcomes varied with substrate (**Table 3.4**). Glucan and extractives concentrations significantly contributed to glucan yield variability in all three substrates, as well as in the combined results. In addition, lignin, xylan and galactan content were also significant in the combined data. There was a slight increase in average glucan yield with rising absolute lignin concentration. Reduced hemicellulose content, namely galactan and

mannan also resulted in increased glucan yield. Given their non-linear association, glucan yield went through maxima with xylan and glucan concentration. When combined, the biomass components accounted for 60.1% of the variance (R^2) in glucan yield (**Figure 3.5**). Separately,biomass composition accounted for 87.6%, 58.9% and 85.7% of the variance in glucan yield of aspen, pine and corn stover, respectively, suggesting some correlation between composition and glucan accessibility.

Table 3.4 Regression coefficients for glucan yield models derived from standardized experimental data from all three substrates, as well as the data of each individual substrate. Corresponding coefficients for unstandardized data are provided in parentheses. All explanatory variables shown were tested. NS, not significant ($P > 0.05$). The main effect variable of squared terms was kept in the model regardless of its significance, provided that the squared term was significant. A, aspen; P, pine; CS, corn stalk.

	A	P	CS	Combined
Y-int	0.28 (-1.84)	0.20 (-0.29)	0.22 (0.00)	0.31 (-1.12)
Ash	-0.05 (-0.088)	NS	NS	NS
Ext	0.25 (0.041)	0.05 (0.014)	0.07 (0.015)	0.10 (0.013)
Lig	NS	NS	NS	0.08 (0.0097)
Glu	0.07 (0.078)	0.001 (0.019)	-0.02 (0.24)	0.09 (0.03)
Xyl	NS	NS	0.03 (-0.49)	0.03 (0.04)
Gal	NS	NS	NS	-0.03 (-0.033)
Man	NS	NS	-0.03 (-0.17)	NS
unaccounted	-0.0028 (-0.0085)	NS	NS	NS
Glu^2	-0.10 (-0.00081)	-0.02 (-0.00021)	-0.02 (-0.0033)	-0.02 (-0.00024)
Xyl^2	NS	NS	0.02 (0.014)	-0.08 (-0.0017)
$unaccounted^2$	0.03 (0.00097)	NS	NS	NS

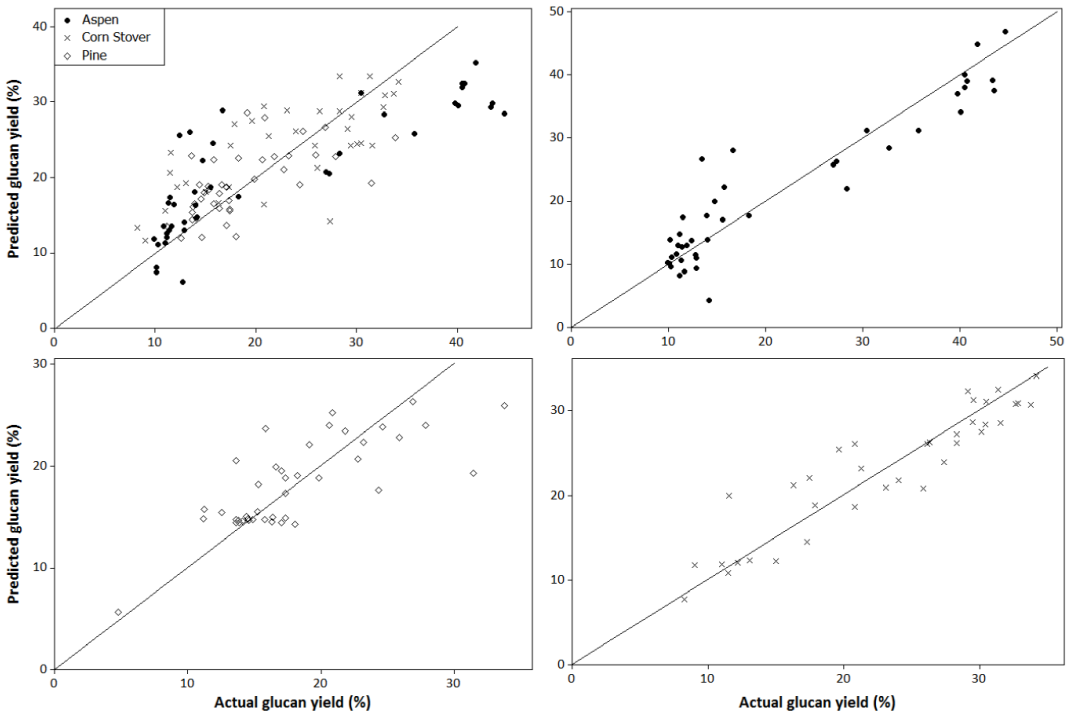

Figure 3.5 Comparison of experimental glucan yield and glucan yield values calculated using the regression equations determined from the composition analysis of aspen, pine, and corn stover separately, and the combined data of all three substrates.

3.4 Discussion

When brown rot fungi deconstructed pine in this study, we observed rapid hemicellulose loss, steady cellulose removal and the retention of most lignin, all classic brown rot patterns (Cowling, 1961; Kirk and Highley, 1973). In the angiosperm substrates, however, we saw deviation from this pattern with lignin loss exceeding 40% in late stage decay and with lignin removal in corn stover outpacing lignin loss in woody substrates in early stages. Considerable losses in lignin during brown rot have been previously reported (Seifert, 1983; Adaskaveg et al., 1991; Schilling et al., 2012), and there is significant evidence that brown rot is associated with extensive lignin demethylation and oxidation, including cleavage of arylglycerol-β-aryl ether, the most

common lignin bond type (Kirk and Adler, 1970; Yelle et al., 2008, 2011). Products of lignin oxidation like benzoic acids, benzaldehydes and phenylglycerols (Yelle et al., 2011) are likely removed during ethanol extraction, a step that was not included in early chronological studies of brown rot component loss (Cowling, 1961). These by-products can co-precipitate with acid-insoluble lignin during acid treatment, inflating the apparent lignin content of the sample in an irreproducible manner (Dean, 1997; Marles et al., 2008; Sluiter et al., 2008). Although brown rot fungi are typically associated with conifers, brown rot-angiosperm associations are common, with *Laetiporus sulphureus* on oak and *P. betulinus* on birch as examples. As the commonly held belief is that brown rot causes negligible lignin loss, our observations suggest that lignin-bound carbon mobilization may be underestimated, especially in angiosperms. Substrate-driven variation in lignin removal rate is likely driven by differences in lignin structure. Several brown rot species preferentially attack syringyl over guaiacyl phenols in birch wood (Hedges et al., 1988). Given the extent of aromatic demethylation caused by brown rot, the higher S:G ratio and methoxyl content in angiosperms (Baucher et al., 1998) likely contributed to the greater lignin losses we observed. In addition to the relatively high S:G ratio associated with angiosperms, Poales grasses are also known to contain an abundance of p-coumarates and ferulates that cross-link lignin and hemicelluloses (Grabber et al., 1995). As esters, these bonds are likely more labile than the ether and carbon-carbon linkages that predominate in most lignin structures and may be a factor in the rapid early lignin losses observed in corn stover.

Substrate driven differences in polysaccharide losses were less pronounced than in lignin losses but also showed a pattern of relevance to brown rot fungi colonizing conifer wood. The relative rate of mannan, xylan and glucan losses observed were in agreement with previously determined rates of polysaccharide losses in softwoods and hardwoods (Kirk and Highley, 1973; Highley, 1987). As in these previous studies, differences were particularly pronounced during incipient decay, suggesting the early, preferential removal of hemicellulose typically associated with brown rot. This observation may be skewed, however, by hemicellulosic losses incurred during autoclave sterilization. Although xylan and mannan loss curves were nearly identical in aspen and pine, respectively, model fit analysis indicated a significant difference between the two data sets. In both hardwoods and softwoods, mannose and xylose are predominantly β 1–4 linked into the polymeric backbones of glucomannans and glucuronoxylans, respectively (Sjöstrom, 1993). Yet despite the similarity in bond type within hemicellulose, loss of mannan tended to outpace xylan loss. It is plausible that glucomannans are more accessible to brown rot fungi than xylans in these wood types, potentially making glucomannan-rich conifer wood an easier substrate to dominate when competing with other organisms for wood, though again we cannot rule out some hemicellulose degradation during steam sterilization as a potential artifact.

Enzyme accessibility in substrates paralleled component loss curves and complemented patterns observed in other studies (Schilling et al., 2009, 2012; Vaidya and Singh, 2012), including similar lack of improvement in corn stover (Gao et al., 2012). Schilling and colleagues (2012) noted a two-fold improvement in cellulose-to-

glucose conversion in milled corn stover degraded by *P. placenta* for 1 week and a 1.5-fold improvement with *G. trabeum* after 8 weeks, though yields could not be corrected for mass loss. Similar poor improvements in glucan yield have also been observed in another *Poales* grass substrate, wheat straw (Salvachúa et al., 2011). Contrasting the lack of cellulose accessibility improvement, we observed declining glucan contents, implying that brown rot fungi removed cellulose. As in previous studies (Öhgren et al., 2007), improved cellulose accessibility was associated with reduced hemicellulose content, but contrary to some findings (Chen and Dixon, 2007), accessibility was also associated with higher absolute lignin content. This implies caution should be taken when using crude insoluble lignin content alone to predict digestibility and warrants more detailed structural analyses of post-decay lignin, as in Yelle and colleagues (2008, 2011).

Microcosm environments, including exogenous soil and feeder strips, may have contributed variable growth rates and decay capacities in our study. First, we saw some isolates fail to decay wood. The low decay by *F. hepatica* was not surprising given an association with *Quercus* and *Castanea* spp. wood, previous difficulty producing decay on oak (Schwarze et al., 2000), and generally low vigor outside of oak tree heartwood (Cartwright, 1937; Owens et al., 1994). The inability of *Dacryopinax* sp. was less clear, given previous success in soil-block tests (Worrall et al., 1997) and agar plates (Floudas et al., 2012). Second, we saw one isolate perform differently than in agar microcosms when degrading stover. Our previous studies indicated inefficient degradation of *Poales* grasses by *P. placenta* and its relatives in water-agar microcosms, including *F. pinicola* (Kaffenberger and Schilling, 2013). In this study in soil-block microcosms, *F. pinicola*

caused significant mass loss on stover after a long lag phase. The presence or absence of wood constituents can influence the ability of brown rot fungi to degrade pure cellulose (Highley, 1975; 1977), and it is well known that fungal hyphae extending beyond the wood matrix can influence decay rates within via import/export dynamics (e.g. Schilling, 2010). Despite these differences, our set up produced typical mass losses at 16 weeks for well-studied isolates *G. trabeum, W. cocos* and *S. lacrymans*. Using these standard isolates as a benchmark, the most aggressive isolate in our trial was *O. lignatilis*, a fungus that to our knowledge has not been tested in a time series such as this before.

Of greatest interest, all of our distinct clade representatives carried out a substrate-specific but statistically identical progression of component loss. With the ancestral white rot fungi from which brown rot have evolved likely exhibiting distinctly different decay modes (Ruiz-Duenas et al., 2013), it would not be unreasonable to assume diversity in brown rot mechanisms and corresponding differences in physiochemical outcomes. Though the convergent evolution of brown rot largely coincides with extensive gene losses, particularly in PODs and CAZymes active on crystalline cellulose (Floudas et al., 2012), diversity in this decay mode exists across the remaining relevant lignocellulolytic genes (Riley et al., 2014). Combined with this heterogeneity, our findings suggest the possibility of multiple routes to the same outcome, although they cannot rule out the presence of a single mechanism that underpins all brown rot decay. Drawing conclusions bears a familiar caveat of resolution in chemical analyses, but in our case with weight% characterization, mass closure is nearly 100% for all substrates and offers useful insight into the temporal process of brown rot. In conjunction with studies that have shown

significant reduction and loss of carbohydrate-active and lignin-degrading enzymes in brown rot fungi (Floudas et al., 2012), this finding is in line with the evolutionary convergence of a less specific non-enzymatic oxidation strategy as the main mechanism of brown rot decay. In terms of implications on forest carbon cycling, the consistency across phylogenetic clades in component loss and cellulose accessibility suggests that brown rot fungi may play similar functional roles when defining 'function' as residue chemistry or carbon release.

3.5 Supplemental Data

Table S3.1 Mean mass loss (± SE) and compositions (mean ± SE) of aspen decay residues

Treatment	Weeks	Mass Loss (%)	Component (%)								
			Ash	Ext	Lig	Glu	Xyl	Gal	Ara	Man	Total
Control	0	-	0.21 (0.03)	3.01 (0.28)	20.44 (0.18)	44.16 (1.14)	15.82 (0.20)	0.50 (0.02)	0.44 (0.03)	2.77 (0.18)	94.58 (1.49)
	2	0.30 (0.16)	0.34 (0.03)	3.20 (0.01)	19.87 (0.97)	53.30 (0.42)	20.84 (0.23)	0.14 (0.01)	1.32 (0.39)	4.14 (0.21)	103.15 (2.32)
	3	0.14 (0.20)	0.34 (0.00)	2.67 (0.08)	19.43 (0.47)	51.81 (0.24)	19.90 (0.51)	0.17 (0.04)	0.95 (0.14)	3.72 (0.04)	98.99 (1.55)
	4	0.11 (0.10)	0.40 (0.06)	2.74 (0.03)	20.76 (1.35)	52.29 (1.80)	19.24 (1.13)	0.17 (0.09)	1.22 (0.01)	3.91 (0.28)	100.73 (4.79)
	6	-0.14 (0.22)	0.47 (0.02)	2.56 (0.09)	20.00 (0.17)	53.34 (0.21)	19.79 (0.14)	0.28 (0.00)	1.16 (0.01)	4.02 (0.02)	101.62 (0.71)
	8	0.27 (0.29)	0.30 (0.02)	2.45 (0.15)	21.01 (1.07)	51.77 (0.11)	20.62 (2.06)	0.38 (0.00)	0.81 (0.61)	3.44 (1.20)	100.77 (5.25)
	16	-0.89 (0.44)	0.32 (0.03)	2.93 (0.22)	19.08 (0.44)	53.22 (1.27)	21.78 (0.06)	0.26 (0.09)	1.18 (0.48)	3.83 (0.31)	102.60 (2.93)
F. hepatica	2	0.57 (0.35)	0.52 (0.05)	1.98 (0.46)	18.76 (0.36)	52.06 (0.70)	19.22 (0.17)	0.42 (0.07)	2.05 (0.95)	3.80 (0.00)	98.81 (2.80)
	3	0.23 (0.29)	0.32 (0.04)	1.82 (0.18)	20.61 (0.53)	51.68 (0.58)	20.71 (0.45)	0.00 (0)	0.00 (0)	3.94 (0.04)	99.09 (1.84)
	4	0.30 (0.42)	0.30 (0.05)	2.25 (0.11)	19.13 (0.47)	54.44 (0.52)	20.47 (0.52)	0.12 (0.06)	0.62 (0.05)	3.62 (0.16)	100.95 (1.97)
	6	0.44 (0.53)	0.27 (0.02)	2.30 (0.04)	19.07 (0.07)	55.08 (1.02)	21.66 (0.60)	0.15 (0.04)	0.76 (0.21)	3.65 (0.10)	102.94 (2.14)
	8	-0.23 (0.64)	0.33 (0.01)	1.82 (0.13)	19.66 (0.16)	50.49 (0.56)	19.31 (1.27)	0.00 (0)	0.00 (0)	3.76 (0)	95.37 (5.18)

	16	0.47 (0.41)	0.41 (0.02)	2.42 (0.32)	19.60 (0.32)	50.19 (0.28)	21.74 (0.40)	0.13 (0.03)	0.55 (0.06)	3.46 (0.04)	98.50 (1.51)
F. pinicola	2	0.52 (0.15)	0.40 (0.08)	2.24 (0.44)	19.10 (0.39)	54.49 (0.09)	20.04 (0.31)	0.15 (0.12)	0.84 (0.51)	3.80 (0.21)	101.06 (2.18)
	3	2.85 (0.46)	0.23 (0.06)	3.79 (0.10)	20.58 (0.26)	53.85 (0.42)	19.46 (0.23)	0.26 (0.02)	1.07 (0.03)	3.36 (0.01)	102.60 (1.17)
	4	5.95 (0.69)	0.41 (0.03)	5.10 (0.58)	20.66 (0.13)	50.93 (0.54)	17.35 (0.47)	0.14 (0.06)	0.98 (0.23)	2.51 (0.59)	98.07 (2.66)
	6	12.68 (0.89)	0.46 (0.05)	7.49 (0.29)	19.68 (1.59)	47.59 (0.27)	15.72 (0.17)	0.17 (0.01)	0.90 (0.02)	2.26 (0.03)	94.27 (2.47)
	8	17.68 (1.02)	0.49 (0.07)	9.68 (0.41)	21.22 (1.10)	45.32 (0.15)	14.94 (0.10)	0.18 (0.02)	0.85 (0.03)	1.74 (0.09)	94.42 (2.02)
	16	36.03 (2.76)	1.06 (0.03)	14.10 (0.20)	26.65 (0.21)	34.18 (0.21)	13.79 (0.03)	0.00 (0)	0.76 (0)	1.47 (0.54)	92.00 (1.24)
W. cocos	2	1.26 (0.14)	0.24 (0.01)	3.51 (0.05)	20.61 (1.19)	51.99 (0)	19.01 (0)	0.28 (0.07)	0.87 (0.57)	3.04 (0.15)	99.55 (2.07)
	3	7.01 (0.59)	0.47 (0.02)	6.06 (0.02)	18.68 (0.34)	47.39 (0.09)	16.29 (0.39)	0.54 (0.33)	0.97 (0.03)	2.51 (0.02)	92.91 (1.27)
	4	20.37 (1.57)	0.54 (0.05)	9.70 (0.15)	23.92 (0.24)	46.07 (0.88)	15.47 (0.88)	0.18 (0.03)	0.94 (0.54)	2.00 (0.33)	98.82 (3.14)
	6	23.76 (1.16)	0.47 (0.00)	9.15 (0.83)	24.34 (0.14)	46.33 (0.13)	15.42 (0.13)	0.00 (0)	0.76 (0)	1.55 (1.06)	98.03 (2.32)
	8	39.35 (1.14)	0.97 (0.01)	12.89 (0.13)	26.95 (0.46)	37.15 (0.13)	13.02 (0.05)	0.10 (0.01)	0.67 (0.02)	0.98 (0.02)	92.72 (0.86)
	16	65.46 (0.72)	1.95 (0.04)	24.59 (1.47)	38.02 (0.27)	18.01 (1.64)	8.82 (0.90)	0.00 (0)	0.44 (0.26)	0.45 (0.45)	92.27 (5.05)
G. trabeum	2	0.57 (0.16)	0.26 (0.03)	2.47 (0.14)	19.44 (0.07)	54.30 (0.15)	19.88 (0.09)	0.30 (0.01)	1.02 (0.24)	3.46 (0.35)	101.12 (1.11)
	3	6.93 (0.95)	0.10 (0.00)	5.33 (0.20)	19.74 (0.19)	51.91 (0.28)	18.39 (0.10)	0.22 (0.03)	1.00 (0.04)	3.07 (0.12)	99.76 (1.01)
	4	13.77 (0.92)	0.27 (0.07)	8.53 (0.08)	20.87 (0.19)	47.90 (0.70)	14.83 (0.31)	0.12 (0.01)	0.80 (0.04)	1.95 (0.06)	95.27 (1.49)
	6	28.58 (1.15)	0.54 (0.03)	11.62 (0.12)	21.91 (0.21)	44.88 (0.21)	16.35 (0.16)	0.71 (0.02)	0.67 (0.04)	1.54 (0.33)	98.22 (1.15)
	8	35.16 (0.93)	0.74 (0.03)	12.65 (0.76)	26.42 (0.63)	40.43 (0.22)	10.64 (0.53)	0.21 (0.03)	0.76 (0.53)	1.81 (0.09)	93.67 (2.86)
	16	46.24 (2.32)	1.90 (0.03)	17.87 (0.56)	30.37 (0.47)	28.92 (0.09)	10.89 (0.21)	0.00 (0)	0.50 (0)	1.32 (0.91)	91.78 (2.30)
S. lacrymans	2	-0.78 (0.59)	0.87 (0.01)	3.23 (0.51)	19.61 (0.08)	52.90 (0.57)	18.88 (0.24)	0.35 (0.01)	1.11 (0.02)	3.72 (0.08)	100.66 (1.55)
	3	3.87 (0.90)	0.98 (0.00)	4.24 (0.08)	20.57 (0.44)	52.66 (0.22)	19.69 (0.26)	0.45 (0.04)	0.80 (0.15)	3.05 (0.12)	102.45 (1.35)
	4	10.04 (2.46)	0.94 (0.01)	6.13 (0.14)	22.06 (0.74)	48.66 (0.30)	17.09 (0.67)	0.25 (0.00)	1.02 (0.05)	2.43 (0.26)	98.57 (2.22)
	6	21.49 (4.80)	1.43 (0.17)	9.02 (0.44)	22.40 (0.41)	45.33 (1.08)	16.28 (0.57)	0.00 (0)	0.80 (0)	2.11 (0.66)	97.36 (3.35)

	8	28.68 (4.68)	1.27 (0.02)	12.06 (1.53)	25.45 (0.05)	38.20 (0.60)	15.34 (0.38)	0.00 (0)	0.68 (0)	2.01 (0.85)	95.00 (3.46)
	16	55.73 (0.67)	1.47 (0.04)	24.56 (3.82)	34.81 (0.59)	17.98 (0.33)	9.58 (0.62)	0.22 (0.12)	0.55 (0.12)	0.57 (0.20)	89.75 (5.87)
O. lignatilis	2	4.93 (2.72)	0.39 (0.04)	3.90 (0.28)	20.34 (0.51)	50.93 (0.33)	18.03 (0.18)	0.49 (0.08)	0.80 (0.07)	2.73 (0.17)	97.6 (0.85)
	3	14.86 (12.36)	0.61 (0.02)	6.68 (0.11)	21.25 (0.38)	46.79 (0.31)	15.24 (0.33)	0.25 (0.05)	0.76 (0.16)	1.91 (0.07)	93.48 (0.61)
	4	37.38	1.10 (0.05)	10.13 (0.19)	27.20 (0.52)	37.23 (0.80)	13.05 (0.67)	0.22 (0.02)	0.57 (0.05)	1.41 (0.29)	90.91 (1.22)
	6	50.52	1.64 (0.05)	15.24 (0.31)	31.87 (0.44)	23.22 (0.49)	9.08 (0.30)	0.01 (0.01)	0.48 (0.20)	0.79 (0.37)	82.32 (3.87)
	8	55.25	1.62 (0.03)	17.24 (0.52)	34.48 (0.59)	19.02 (0.30)	9.97 (0.74)	0.27 (0.04)	0.42 (0.16)	0.63 (0.38)	83.64 (3.20)
	16	67.47	2.52 (0.04)	15.38 (1.10)	35.20 (0.39)	17.85 (0.64)	3.16 (0.38)	0.00 (0.00)	0.44 (0.08)	0.25 (0.41)	74.79 (5.26)

Table S3.2 Mean mass loss (± SE) and compositions (mean ± SE) of pine decay residues

Treatment	Weeks	Mass loss (%)	Component (%)								
			Ash	Ext	Lig	Glu	Xyl	Gal	Ara	Man	Total
Control	0	-	0.59 (0.07)	2.38 (0.33)	27.05 (0.54)	45.03 (0.30)	3.50 (0.05)	2.82 (0.07)	1.37 (0.01)	12.82 (0.19)	98.07 (0.41)
	2	-0.16 (0.11)	0.26 (0.02)	1.68 (0.05)	27.14 (0.03)	50.77 (0.14)	5.70 (0.07)	1.79 (0.06)	1.23 (0.01)	13.59 (0.10)	102.17 (0.48)
	3	0.06 (0.22)	0.40 (0.05)	2.00 (0.01)	27.05 (0.09)	49.66 (0.10)	5.11 (0.01)	3.01 (0.10)	1.28 (0.11)	12.48 (0.02)	101.00 (0.47)
	4	0.14 (0.07)	0.36 (0.05)	1.48 (0.03)	27.10 (0.52)	50.71 (0.08)	5.91 (0.05)	2.40 (0.14)	1.25 (0.36)	11.58 (1.05)	100.79 (2.28)
	6	0.58 (0.25)	0.08 (0.01)	1.20 (0.12)	26.59 (0.26)	49.92 (0.20)	5.12 (0.60)	2.27 (0.38)	1.84 (0.03)	14.27 (0.73)	101.29 (2.34)
	8	0.69 (0.32)	0.19 (0.03)	1.20 (0.07)	25.85 (0.38)	50.78 (0.19)	6.12 (0.32)	2.62 (0.40)	0.00 (0.00)	14.30 (1.80)	101.06 (3.17)
	16	0.65 (0.40)	0.27 (0.02)	0.93 (0.38)	25.91 (0.75)	49.74 (0.04)	5.68 (0.28)	3.04 (0.42)	0.00 (0.00)	16.67 (0.28)	102.24 (2.18)
F. hepatica	2	0.70 (0.12)	0.21 (0.05)	1.65 (0.41)	27.33 (0.03)	48.73 (0.31)	5.83 (0.34)	3.71 (0.49)	0.00 (0.00)	13.25 (1.21)	100.72 (2.85)
	3	0.67 (0.16)	0.17 (0.03)	1.81 (0.00)	26.11 (0.15)	52.74 (0.28)	5.44 (0.02)	2.00 (0.03)	0.00 (0.00)	12.15 (0.28)	100.42 (0.79)
	4	-0.02 (0.49)	0.23 (0.04)	1.74 (0.09)	25.38 (0.48)	51.77 (0.43)	5.67 (0.04)	2.44 (0.06)	0.00 (0.00)	11.95 (0.11)	99.17 (1.24)
	6	0.53 (0.29)	0.22 (0.04)	1.53 (0.03)	27.30 (0.19)	51.45 (0.35)	5.42 (0.18)	3.13 (0.28)	1.46 (0.43)	10.51 (1.00)	101.02 (2.50)

	8	0.17 (0.18)	0.24 (0.01)	1.46 (0.05)	28.60 (0.35)	51.03 (0.00)	5.19 (0.44)	2.62 (0.28)	1.99 (0.37)	10.90 (0.00)	102.01 (1.49)
	16	0.92 (0.43)	0.19 (0.01)	1.49 (0.22)	27.40 (0.20)	51.46 (0.67)	5.87 (0.07)	4.15 (0.22)	0.00 (0.00)	11.57 (0.45)	102.13 (1.84)
F. pinicola	2	1.25 (0.33)	0.22 (0.03)	1.58 (0.06)	27.73 (0.57)	50.56 (0.02)	5.65 (0.09)	2.22 (0.38)	1.20 (0.01)	11.22 (0.27)	100.38 (1.42)
	3	4.13 (0.80)	0.11 (0.06)	3.69 (0.40)	28.45 (0.01)	49.31 (0.02)	5.23 (0.03)	2.61 (0.10)	0.98 (0.03)	11.79 (0.20)	102.19 (0.85)
	4	6.43 (0.84)	0.12 (0.08)	3.90 (0.10)	27.32 (0.19)	46.31 (0.13)	4.98 (0.05)	2.38 (0.11)	1.90 (0.35)	10.16 (0.08)	97.07 (1.09)
	6	15.04 (0.81)	0.26 (0.03)	6.32 (0.36)	31.94 (0.35)	48.27 (0.22)	4.68 (0.09)	0.98 (0.02)	0.92 (0.08)	7.92 (0.09)	101.29 (1.23)
	8	23.86 (1.14)	0.35 (0.03)	7.62 (0.59)	33.80 (0.14)	43.00 (0.14)	3.82 (0.05)	1.82 (0.01)	1.06 (0.20)	5.15 (0.28)	96.61 (1.44)
	16	41.78 (2.61)	1.07 (0.05)	5.88 (0.81)	43.95 (0.55)	34.65 (0.59)	3.54 (0.26)	2.08 (0.59)	0.00 (0.00)	6.70 (0.92)	97.88 (3.76)
W. cocos	2	0.79 (0.11)	0.05 (0.04)	1.67 (1.00)	27.54 (0.34)	53.21 (0.84)	5.79 (0.14)	3.14 (0.16)	1.35 (0.35)	11.13 (0.71)	103.89 (3.58)
	3	7.65 (1.18)	0.33 (0.04)	5.45 (0.01)	29.37 (0.58)	49.38 (0.18)	3.92 (0.09)	1.79 (0.18)	0.94 (0.11)	8.09 (0.24)	99.28 (1.43)
	4	17.85 (1.13)	0.14 (0.04)	7.47 (0.16)	33.18 (0.26)	46.53 (1.28)	3.83 (0.39)	1.48 (0.20)	0.80 (0.03)	5.28 (0.28)	98.72 (2.64)
	6	28.24 (0.58)	0.55 (0.03)	6.45 (0.50)	34.06 (1.28)	42.92 (0.08)	3.49 (0.28)	1.12 (0.11)	0.67 (0.04)	3.51 (0.21)	92.77 (2.52)
	8	36.35 (0.40)	0.67 (0.02)	8.82 (0.19)	39.88 (0.58)	34.57 (0.19)	3.49 (0.05)	0.87 (0.03)	1.24 (0.05)	3.06 (0.02)	92.60 (1.14)
	16	63.61 (0.66)	2.20 (0.17)	16.25 (0.00)	63.64 (0.61)	6.83 (0.01)	1.74 (0.39)	0.17 (0.09)	0.17 (0.17)	0.68 (0.24)	91.69 (1.68)
G. trabeum	2	1.34 (0.26)	0.17 (0.02)	1.48 (0.33)	27.40 (0.35)	50.55 (0.02)	5.02 (0.42)	2.98 (0.35)	1.04 (0.35)	10.68 (0.90)	99.31 (2.75)
	3	7.53 (0.90)	0.08 (0.01)	4.37 (0.01)	29.53 (0.32)	45.79 (0.00)	4.13 (0.54)	3.05 (0.66)	1.81 (0.31)	9.27 (0.31)	98.03 (2.16)
	4	12.63 (0.75)	0.17 (0.05)	9.02 (0.56)	27.21 (0.50)	47.71 (0.17)	4.41 (0.07)	1.32 (0.14)	1.35 (0.07)	7.89 (0.11)	99.10 (1.67)
	6	23.20 (1.32)	0.44 (0.05)	6.70 (0.50)	33.24 (0.03)	44.16 (0.04)	3.70 (0.20)	1.45 (0.08)	0.00 (0.00)	7.46 (1.04)	97.15 (1.95)
	8	28.34 (1.28)	0.66 (0.03)	8.61 (0.00)	34.19 (0.31)	41.87 (0.47)	5.04 (0.07)	1.36 (0.04)	0.68 (0.34)	4.01 (0.36)	96.43 (1.61)
	16	36.34 (2.58)	1.08 (0.07)	9.71 (0.91)	38.12 (0.35)	39.25 (0.91)	2.82 (0.23)	0.68 (0.15)	0.74 (0.41)	4.32 (0.37)	96.72 (3.40)
S. lacrymans	2	0.18 (0.57)	0.23 (0.03)	2.07 (0.18)	26.92 (0.05)	51.30 (0.00)	5.59 (0.33)	1.97 (0.09)	1.29 (0.07)	13.60 (0.20)	102.98 (0.95)
	3	5.10 (0.96)	0.57 (0.01)	3.53 (0.15)	27.62 (0.36)	51.04 (0.37)	5.86 (0.28)	2.84 (0.00)	0.00 (0.00)	12.85 (0.00)	104.33 (1.17)
	4	11.51 (2.46)	0.56 (0.02)	4.23 (0.00)	31.63 (0.24)	48.81 (0.17)	4.88 (0.05)	2.16 (0.21)	1.05 (0.09)	7.98 (0.07)	101.31 (0.85)

	6	25.93 (4.12)	0.79 (0.03)	7.61 (0.35)	32.90 (0.67)	42.83 (0.06)	4.96 (0.12)	2.53 (0.10)	0.00 (0.00)	12.18 (0.35)	103.81 (1.69)
	8	32.40 (3.73)	0.93 (0.00)	7.98 (0.09)	38.00 (0.38)	38.46 (0.71)	3.84 (0.38)	1.90 (0.51)	0.00 (0.00)	7.72 (0.06)	98.84 (2.13)
	16	57.71 (1.62)	0.86 (0.09)	11.39 (0.58)	60.49 (0.34)	18.56 (4.84)	2.30 (0.42)	0.49 (0.24)	1.03 (0.63)	1.26 (0.12)	96.39 (7.26)
O. lignatilis	2	0.70 (0.23)	0.15 (0.03)	1.19 (0.34)	26.39 (0.23)	50.16 (0.22)	5.13 (0.23)	1.87 (0.26)	0.45 (0.13)	10.43 (0.57)	95.76 (0.82)
	3	6.16 (3.84)	0.16 (0.03)	2.93 (0.10)	27.78 (0.25)	48.14 (0.16)	4.55 (0.16)	1.81 (0.18)	0.53 (0.09)	8.61 (0.17)	94.51 (0.44)
	4	10.50 (7.22)	0.16 (0.05)	3.95 (0.16)	29.22 (0.36)	47.59 (0.38)	4.15 (0.11)	1.35 (0.14)	0.59 (0.15)	7.13 (0.28)	94.14 (0.66)
	6	18.35 (13.64)	0.21 (0.03)	5.11 (0.31)	31.35 (0.46)	45.92 (0.16)	3.85 (0.24)	0.89 (0.16)	0.48 (0.10)	5.56 (0.57)	93.37 (0.87)
	8	35.56	0.59 (0.02)	5.56 (0.17)	37.73 (0.36)	37.35 (0.28)	3.41 (0.22)	1.10 (0.21)	0.20 (0.16)	4.77 (0.42)	90.72 (0.73)
	16	52.52	0.72 (0.07)	6.33 (0.48)	54.45 (0.47)	25.83 (1.17)	2.11 (0.28)	0.00 (0.00)	0.62 (0.20)	1.86 (0.40)	91.91 (1.48)

Table S3.3 Mean mass loss (± SE) and compositions (mean ± SE) of corn stalk decay residues

			Component (%)								
Treatment	Weeks	Mass Loss (%)	Ash	Ext	Lig	Glu	Xyl	Gal	Ara	Man	Total
Control	0	-	5.25 (0.04)	13.38 (1.23)	15.22 (0.13)	35.29 (0.23)	20.27 (0.16)	0.00 (0.00)	5.91 (0.31)	0.60 (0.08)	101.81 (1.31)
	2	4.48 (0.94)	3.38 (0.10)	12.93 (0.61)	21.34 (0.04)	38.63 (0.67)	21.03 (0.49)	0.00 (0.00)	0.52 (0.47)	0.45 (0.45)	98.27 (2.83)
	3	3.58 (0.73)	2.24 (0.10)	25.31 (2.03)	18.19 (0.86)	32.09 (1.45)	16.83 (0.87)	0.00 (0.00)	3.56 (0.80)	0.00 (0.00)	98.23 (6.10)
	4	3.79 (1.20)	2.77 (0.04)	18.28 (0.10)	20.54 (0.32)	37.83 (0.60)	18.71 (0.24)	0.00 (0.00)	1.62 (0.13)	0.15 (0.07)	99.91 (1.50)
	6	-0.67 (1.42)	2.37 (0.03)	23.79 (2.50)	18.21 (0.09)	35.25 (0.18)	18.59 (0.11)	0.00 (0.00)	1.50 (0.06)	0.12 (0.01)	99.83 (2.98)
	8	4.57 (2.27)	2.35 (0.08)	23.59 (0.11)	17.32 (0.23)	38.17 (0.19)	18.44 (0.27)	0.00 (0.00)	3.85 (1.03)	0.00 (0.00)	103.73 (1.92)
	16	11.99 (1.25)	2.43 (0.09)	19.16 (0.91)	19.48 (0.16)	39.66 (0.65)	20.10 (0.66)	0.10 (0.10)	1.55 (0.19)	0.10 (0.10)	102.58 (2.85)
F. hepatica	2	3.50 (0.51)	ND	ND	ND	ND	ND	ND	ND	ND	ND
	3	5.72 (1.27)	ND	ND	ND	ND	ND	ND	ND	ND	ND
	4	2.08 (0.72)	ND	ND	ND	ND	ND	ND	ND	ND	ND

	6	4.25 (1.04)	ND	ND	ND	ND	ND	ND	ND	ND	ND
	8	6.86 (1.59)	ND	ND	ND	ND	ND	ND	ND	ND	ND
	16	12.67 (1.80)	ND	ND	ND	ND	ND	ND	ND	ND	ND
F. pinicola	2	3.25 (0.55)	2.41 (0.08)	23.40 (0.15)	20.28 (0.18)	36.77 (0.26)	17.41 (0.65)	0.20 (0.20)	1.77 (0.16)	0.26 (0.26)	102.50 (1.94)
	3	3.86 (0.79)	2.61 (0.03)	23.44 (2.84)	20.07 (0.14)	34.10 (0.11)	17.05 (0.80)	0.00 (0.00)	4.24 (0.64)	0.00 (0.00)	101.52 (4.56)
	4	4.71 (0.89)	2.02 (0.08)	24.31 (0.01)	19.51 (0.15)	35.71 (0.19)	17.27 (0.08)	0.00 (0.00)	3.52 (1.06)	0.00 (0.00)	102.34 (1.56)
	6	4.22 (1.66)	2.07 (0.08)	23.17 (0.91)	19.26 (0.38)	37.76 (0.13)	18.65 (0.79)	0.00 (0.00)	2.03 (0.06)	0.02 (0.02)	102.95 (2.37)
	8	11.28 (1.95)	1.99 (0.07)	20.77 (0.78)	20.74 (0.35)	34.05 (0.19)	16.79 (0.08)	0.00 (0.00)	2.72 (0.20)	0.00 (0.00)	97.06 (1.67)
	16	36.65 (3.02)	2.90 (0.06)	12.28 (0.75)	22.56 (0.63)	39.99 (0.11)	19.71 (0.66)	0.24 (0.12)	2.30 (0.43)	0.25 (0.16)	100.24 (2.92)
W. cocos	2	3.25 (0.48)	1.86 (0.07)	23.82 (0.05)	18.50 (0.18)	34.17 (0.55)	15.51 (0.57)	0.00 (0.00)	1.83 (0.11)	0.16 (0.12)	95.85 (1.65)
	3	0.69 (0.47)	2.94 (0.09)	19.94 (2.58)	21.27 (0.07)	34.50 (0.22)	16.81 (0.13)	0.00 (0.00)	4.59 (0.72)	0.00 (0.00)	100.05 (3.81)
	4	7.99 (1.50)	1.93 (0.13)	21.01 (0.22)	18.59 (0.21)	38.90 (0.31)	18.52 (0.17)	0.00 (0.00)	2.44 (0.92)	0.00 (0.00)	101.39 (1.95)
	6	10.11 (1.39)	2.28 (0.11)	17.69 (1.07)	20.95 (0.29)	37.84 (0.51)	18.06 (0.31)	0.06 (0.04)	1.45 (0.09)	0.17 (0.02)	98.50 (2.44)
	8	14.71 (2.04)	2.08 (0.05)	20.07 (0.39)	22.20 (0.08)	34.15 (0.00)	17.75 (0.66)	0.00 (0.00)	1.95 (0.69)	0.01 (0.01)	98.21 (1.89)
	16	27.00 (4.38)	3.12 (0.06)	17.81 (1.57)	21.44 (0.80)	34.01 (1.40)	17.45 (0.95)	0.00 (0.00)	2.45 (0.27)	0.00 (0.00)	96.28 (5.04)
G. trabeum	2	3.72 (0.97)	3.61 (0.12)	22.99 (1.58)	17.03 (0.12)	36.14 (0.00)	18.83 (0.65)	0.00 (0.00)	1.85 (0.10)	0.04 (0.02)	100.50 (2.59)
	3	7.37 (1.53)	2.87 (0.13)	20.65 (3.77)	19.91 (1.36)	35.56 (0.00)	18.72 (0.14)	0.38 (0.18)	2.01 (0.25)	0.10 (0.10)	100.19 (5.93)
	4	9.99 (1.26)	3.09 (0.04)	17.18 (2.09)	19.73 (0.17)	37.66 (0.17)	19.64 (0.07)	0.00 (0.00)	1.83 (0.21)	0.09 (0.09)	99.21 (2.84)
	6	14.61 (3.51)	4.32 (0.07)	14.85 (0.16)	17.20 (0.19)	40.60 (0.30)	20.39 (0.25)	0.09 (0.09)	1.91 (0.13)	0.16 (0.16)	99.51 (1.36)
	8	18.09 (6.84)	4.96 (0.10)	12.13 (0.67)	19.82 (0.08)	39.89 (0.13)	20.01 (0.07)	0.22 (0.12)	1.78 (0.10)	0.40 (0.02)	99.21 (1.28)
	16	35.98 (5.10)	5.80 (0.08)	8.30 (1.28)	25.26 (0.43)	34.93 (0.48)	18.99 (0.32)	0.00 (0.00)	1.11 (0.56)	0.25 (0.25)	94.64 (3.41)
S. lacrymans	2	0.74 (1.63)	1.42 (0.04)	21.44 (0.03)	19.35 (0.12)	34.22 (0.41)	18.80 (0.27)	0.00 (0.00)	1.51 (0.09)	0.09 (0.05)	96.82 (1.01)
	3	6.41 (2.60)	1.28 (0.03)	20.61 (1.93)	17.99 (0.39)	35.67 (0.60)	18.45 (0.46)	0.00 (0.00)	2.66 (0.29)	0.00 (0.00)	96.65 (3.70)

	4	9.39 (1.37)	1.43 (0.03)	18.58 (0.79)	20.12 (0.11)	39.38 (0.25)	18.23 (0.14)	0.03 (0.03)	2.15 (0.36)	0.00 (0.00)	99.92 (1.70)
	6	18.71 (3.66)	1.65 (0.02)	12.21 (2.63)	19.75 (0.25)	39.84 (0.61)	19.95 (0.46)	0.00 (0.00)	2.67 (0.38)	0.00 (0.00)	96.07 (4.35)
	8	30.93 (1.92)	2.00 (0.02)	11.63 (2.20)	20.29 (0.14)	40.16 (0.38)	19.14 (0.34)	0.00 (0.00)	3.36 (0.26)	0.00 (0.00)	96.59 (3.33)
	16	30.65 (2.77)	2.01 (0.09)	8.75 (1.35)	24.22 (0.18)	38.13 (0.65)	20.84 (0.28)	0.00 (0.00)	2.15 (0.04)	0.73 (0.04)	96.85 (2.62)
O. lignatilis	2	6.56 (0.70)	1.71 (0.08)	18.17 (0.48)	18.13 (0.13)	36.44 (0.38)	17.03 (0.52)	0.00 (0.00)	1.41 (0.19)	0.02 (0.18)	92.91 (0.86)
	3	10.38 (1.87)	1.87 (0.07)	16.18 (2.63)	18.65 (0.56)	37.04 (0.48)	17.49 (0.48)	0.00 (0.00)	1.19 (0.54)	0.00 (0.02)	92.42 (2.83)
	4	9.22 (3.09)	1.73 (0.06)	16.92 (0.64)	18.51 (0.19)	36.92 (0.30)	17.35 (0.14)	0.00 (0.00)	1.26 (0.54)	0.02 (0.03)	92.71 (0.92)
	6	15.96 (2.57)	2.70 (0.06)	12.74 (1.45)	18.79 (0.24)	37.83 (0.35)	18.04 (0.38)	0.00 (0.00)	1.16 (0.15)	0.00 (0.04)	91.28 (1.57)
	8	18.13 (3.19)	2.70 (0.06)	12.16 (0.83)	18.59 (0.18)	38.52 (0.18)	18.26 (0.28)	0.00 (0.00)	1.34 (0.45)	0.05 (0.01)	91.63 (1.02)
	16	25.37 (1.44)	1.11 (0.07)	13.26 (1.17)	18.48 (0.44)	40.69 (0.66)	18.77 (0.57)	0.00 (0.00)	2.14 (0.30)	0.03 (0.01)	94.5 (1.56)

Chapter 4

Screening of wood-degrading fungi for their potential in the biological pretreatment of lignocellulose for saccharification improvement

4.1 Introduction

Conversion of lignocellulosic biomass to fermentable sugars requires pretreatment to improve cellulose accessibility and to achieve sufficient sugar yields (Wyman, 2007). Traditional pretreatments, such as dilute acid and ammonia fiber explosion (AFEX), require chemical recovery to be cost effective and involve harsh reaction conditions that necessitate corrosion-resistant processing equipment capable of pressurization (Kumar et al., 2009).

Biological pretreatment, and more specifically, pretreatment with wood-degrading fungi, offers an alternative to thermochemical processing. Fungal pretreatment requires relatively low capital cost requirements, while improving yields without generating fermentation inhibitors. Biological pretreatment, however, does come with its own drawbacks, as it typically requires a prolonged treatment timeframe (days as compared with minutes for most thermochemical technologies) and some yield loss to sustenance of the biological agent (Sun and Cheng, 2002).

Despite these issues, surveying wood-degrading fungi as potential agents for biological pretreatment can provide insight into alternate routes for lignocellulosic conversion. Recent fungal genomics studies have indicated that wood-degrading fungi greatly differ in the type and number of enzymes at their disposal for lignocellulose

degradation (Eastwood et al., 2011; Floudas et al., 2012; Riley et al., 2014). This variety suggests a broader spectrum of decay potential and a wider array of decay mechanisms than those offered with the traditional white rot/brown rot dichotomy (Riley et al. 2014). It has been known for some time that white rot fungi can exhibit at least two decay modes: selective lignin degradation and simultaneous degradation of all wood structural bio-polymers (Blanchette, 1980; 1984). Even individual species are capable of exhibiting either selective or simultaneous decay depending on substrate and environmental conditions (Otjen et al., 1987). In contrast, brown rot fungi do not appear to show this degree of mechanistic diversity, despite its polyphyletic nature, exhibiting a consistent decay pattern across genetic clades (Kaffenberger and Schilling, 2014).

This study aimed to survey a wide range of wood-degrading fungi for their ability to improve bioconversion yield by relating these yields to physiochemical changes brought on by different decay types. We also considered the variability in conversion and chemical changes among decay types to determine if our results supported the broader "spectrum of decay" proposed by Riley et al. (2014). Additionally, we set out to determine if these changes and resulting bioconversion improvements were translatable across substrate types by degrading a representative hardwood, softwood, and grass with the fungi that demonstrated the greatest conversion improvements on aspen.

4.2 Material and Methods

4.2.1 Substrates and Fungal Cultures

Most fungi used in this study were field isolates collected across North and South America, though several strains were obtained from culture collections (**Table 4.1**).

Isolates included 15 brown rot species, 22 white rot species, and 3 species of unknown decay type (**Table 4.1**). All isolates are publically available through the Forest Mycology Culture Collection (University of Minnesota). Strain identity was determined or verified by amplification and sequencing of the ITS1 and ITS4 regions of isolated genomic DNA and sequence matching with Genbank BLASTn database as previously described (Arenz et al., 2006). Isolates were maintained on 2% (w/v) potato dextrose agar (PDA) plates.

All southern yellow pine (SYP, *Pinus* sp.) and aspen (*Populus tremuloides*) substrates used were prepared from single pieces of untreated lumber. Corn (*Zea mays*) substrates were prepared from stalks collected from University of Minnesota field plots (St. Paul, MN). After harvest, stalks were dried at 65°C for 4 days and the leaves and cobs were removed. The remaining stems were stored indoors under ambient conditions until needed. Substrates for this study were prepared from the bottom three internodes to obtain desired sample dimensions. Internodes were cut into 50 mm long sections. The outer rind of these sections was removed and samples were cut into pieces with final dimensions of 5x10x50 mm.

4.2.2 Substrate Characterization and Preparation

Aspen, SYP sapwood, and corn (*Zea mays*) stem internode pith (CS) were characterized as described by Sluiter and Sluiter (2010), with the exceptions that only the ethanol soluble extractives of corn stover were measured and protein content was not determined. Additionally, the composition of aspen substrates from the initial screening of 40 fungal isolates was determined following the same procedure. Prior to characterization, untreated substrates were soaked for 10 minutes in water under vacuum

and oven-dried at 100°C for 48 hours as described above. This ensured that the material used for compositional analysis was handled in the same manner as the material used for fungal pretreatment. Substrates were ground to a 40 mesh powder with a Wiley Mill before characterization. All characterization tests were replicated four times.

4.2.3 Pretreatment

Aspen used for initial compositional characterization was cut into 19 mm^3 blocks. Blocks were exposed to one of the 40 tested fungi for 2 or 4 weeks following the ASTM soil block test (ASTM, 1994). Controls were placed in sterile soil jars for 2 or 4 weeks. Equal parts by volume of peat moss, potting soil, and vermiculite were wetted with distilled water and thoroughly mixed. 250 g of this mixture were lightly packed in 473 mL glass jars. Birch feeder strips (40 x 10 x 2 mm) were water-soaked under vacuum for 10 minutes and placed in parallel on top of the soil in each jar. Two fungal plugs were sterilely placed on the ends of each feeder strip and allowed to grow for two weeks before substrate addition. All treatments were duplicated. Initial and final oven-dried masses were recorded after drying at 100°C for 48 hours.

4.2.4 Enzymatic Hydrolysis

After grinding to 40 mesh and homogenization with a Wiley mill, a portion of each treated aspen block was enzymatically hydrolyzed following Selig et al. (2008). After oven-drying at 100°C for 24 hours, 100 ± 0.1 mg of powder from each sample was weighed into 4 dram vials. A set of two vials was weighed for each ground block. 5 ml of 0.1 M citrate buffer (citric acid (Sigma Aldrich) and sodium hydroxide (JT Baker)), 40 µl of 10 kg/m^3 tetracycline (Sigma-Aldrich) in 70% ethanol (Decon Laboratories), 30 µl

of 10 kg/m^3 cyclohexamide (Sigma Aldrich) in distilled water were added to all vials. 60 "filter paper units" (FPU)/g biomass of Celluclast and 64 pNPGU/g biomass of Novozyme 188 (Sigma Aldrich) were used in one of each set of vials. Enzyme activities were determined in accordance with NREL laboratory analytical procedure TP-510-42628 (Adney and Baker 1996). The volume contained in all vials was brought to 10 ml with distilled water. The other vial in each set was used as a reagent blank and distilled water was used to compensate for cellulose solution volume. An enzyme blank was also included, with water used to compensate for the volume of biomass, assuming a biomass density of 1 g-ml^{-1}. All vials were shaken at 100 RPM at 50°C for 5 days, after which 1.5 ml aliquots were removed and filtered through 0.2 μm filters in to 2 ml vials in preparation for high performance liquid chromatography (HPLC).

4.2.5 Sugar Analysis

HPLC (Agilent Technologies 1200 series) was used to determine the quantity of carbohydrates in the resulting enzymatic hydrolysate, as well as the hydrolysate resulting from acid hydrolysis performed for compositional characterization. Carbohydrates were separated using an Aminex HPX-87P analytical column (Bio-rad) and two in-line guard columns: Micro-guard Carbo-P and Micro-guard De-ashing (Bio-Rad). Mobile phase was degassed HPLC grade deionized water (Sigma Aldrich) at an operating flow rate of 0.4 ml/min. Operating column temperature was at 85°C, injection volume was 20 μL, and refractive index was used for detection. Standard response calibration curves were developed with reagent grade glucose, arabinose (Sigma Aldrich), galactose, xylose, and mannose (Acros Organics).

4.2.6 Yield Calculation

Calibration curves were used to determine the concentration of individual carbohydrates. The concentrations were used to determine the total mass present in the hydrolysate by multiplying by the total volume (10 ml). The mass of each monomer was converted to its equivalent mass for the corresponding polymer by multiplying by 0.9 for 6 carbon sugars and 0.88 for 5 carbon sugars to account for the addition of water during hydrolysis.

Yields were then calculated based on original carbohydrate content using the mass loss, the mg of released polymeric sugar ($m_{C_1\ released}$), the mass used for enzymatic hydrolysis ($m_{hydrolyzed}$), and the initial percentage of a given polymer found in untreated aspen as follows ($\%\ C_{1\,initial}$):

$$Yield\ (\%) = \frac{(1 - \%\ wt\ loss) * m_{C_1\ released}}{m_{hydrolyzed} * \%\ C_{1\,initial}}$$

4.2.7 Chemical Characterization

The chemical constituents of sound and decayed aspen were determined as outlined in Sluiter and Sluiter (2009), though extractive analysis was not performed due to the number of samples collected. Components measured included glucan, largely representative of cellulose, as well as the hemicellulosic structural carbohydrates (xylan, galactan, arabinan, and mannan). Carbohydrates were quantified by HPLC as described in section 2.5. Additionally, acid-insoluble (Klason) and acid-soluble lignin were measured. Acid-soluble lignin was quantified by UV-Vis spectrometer at a wavelength of 240 nm and with an extinction coefficient of 30, as recommended by Sluiter et al. (2008).

The solubility of decay residues in 0.2 M sodium hydroxide was also determined as described by Shortle (2010). The solubility of degraded woody biomass in dilute alkali (DAS) offers a quick method of determining likely decay type and was used as a metric of decay type for samples degraded by unknown species based on previous work (Schilling et al., 2015).

4.2.8 Statistical Analysis

Statistical significance of mass loss was determined by comparing week 2 and week 4 samples with corresponding controls using Dunnett's multiple comparison test ($\alpha = 0.05$). Significance of differences in the progression of chemical component losses between white rot and brown rot was determined by first selecting a model fit for the loss of the chemical component as a function of total mass loss for both groups. Total mass loss was used as the independent variable in lieu of exposure time to control for variability among species in growth rate. Comparisons between the residual sum of squares (SS) from each group and the SS resulting from analysis when all data were pooled were made using *F* tests as described by Motulsky and Ransnas (1987). For all components, a linear model fit was deemed sufficient, as additional terms were not significant. This same model fitting approach was used for glucose and xylose yields of enzymatically hydrolyzed samples.

For DAS, a modified Michaelis-Menten equation offered the best model fit. This equation is described as follows, where DAS_{sound} is the DAS of undecayed controls, m_{loss} is the mass loss of the sample, and θ_1 and θ_2 are coefficients:

$$DAS = DAS_{sound} + \frac{\theta_1 * m_{loss}}{\theta_2 + m_{loss}}$$

Both decay type groups were separately fit to this equation by minimizing the residual sum of squares by varying θ_1 and θ_2. The same DAS_{sound} constant was used for both groups. After establishing the best fit equation for each group, comparison of variance about model fits for each decay type was made using Levene's test. Likewise, Levene's test was used to compare decay types for variance differences among the fit residuals for chemical component and sugar yield analyses.

A generalized linear regression model was used to assess the significance of the role of decay type in the release of free sugar over the course of aspen degradation by the 40 tested isolates. Xylose and glucose yields were tested as response variables. Mass loss, decay type, and their interaction term were factors included in the model. A generalized linear regression model was also used to determine the aspen chemical components that were most predictive of enzyme digestibility, using glucose yield after enzymatic hydrolysis as the response variable. Total lignin, glucan, xylan, arabinan, and mannan content (wt %) were included factors in all initial models, but a factor was eliminated from the final model if it was not significant ($P > 0.05$). For this reason, regression models were independently developed for white rot and brown rot data.

4.2.9 Follow-up Testing

Follow-up pretreatments included two treatment sets. In the first, aspen blocks were treated from between 8 and 30 days in 2 day increments with *S. galactinum* (TAB-197), the isolate with the highest saccharification yield in the initial screening. Four replicates were harvested at each time point. Aspen wafers at time-zero (n=6) and after 30 days in sterilized soil block microcosms (n=6) were used as controls. The second

treatment set involved soil block decay studies of corn stalk pith, aspen, and southern yellow pine (*Pinus* sp.) exposed to either a strain of three tested *Scytinostroma* sp., *Phlebia brevispora*, *Gloeophyllum trabeum,* or *Corticiales* sp. for 2, 3, or 4 weeks. These follow up tests used the same soil jar setup as the initial screening, but used wood wafers (5x19x19 mm) instead of cubes. Additionally, when added to the soil jars, substrates were sandwiched between the two inoculated feeder strips to maximize contact with the top and the bottom of the substrate. This was done to promote acceleration of the rate of fungal colonization in the hope of decreasing treatment and turnaround time. Each time and treatment combination was repeated in triplicate. Controls for each substrate were placed in sterile soil jars and removed after 2, 3, or 4 weeks (n=3). Enzyme hydrolysis, sugar analysis, and yield calculations were performed on these samples as described above.

4.3 Results and Discussion

4.3.1 Mass Loss

Of the 40 isolates tested in initial screening with aspen wood, 25 caused a mean mass loss in excess of 5% after 4 weeks (**Table 4.1**). The brown rot fungus *N. lepideus* caused the greatest mass loss (30.48%), while *G. lucidum* caused the greatest mass loss among white rot isolates (23.17%). Seven isolates (2 BR and 5 WR) caused statistically greater mass loss than controls ($P < 0.05$) after 2 weeks and an additional 11 isolates (5 BR, 6 WR) caused significant mass loss after 4 weeks. Eleven isolates, including those of unclear or unknown decay type (*J. argillacea* and the two *Sistotrema* sp.), produced mean mass losses less than 2% after 4 weeks.

Table 4.1 GenBank accession numbers of indicated fungal isolates and mean (standard error) mass loss of aspen blocks after 2 and 4 weeks in initial soil block microcosm screening. ATCC=American Type Culture Collection (Manassas, VA, USA), FPL = USDA Forest Products Laboratory Culture Collection (Madison, WI, USA). All other isolates are available through the University of Minnesota Forest Mycology Collection (St. Paul, MN, USA). Mass losses for 2 wk and 4 wk controls were 0.15% (0.06%) and 0.03% (0.08%), respectively.

Fungus by decay type	Source	U of MN isolate code	GenBank Accession #	Mass loss (%)	
				2 wk	4 wk
Brown rot					
Antrodia alpina	NA	202A	KC514838	0.48 (0.06)	7.10 (0.97)
Antrodia carbonica	FPL	753 FPL	KC514806	0.42 (0.20)	1.04 (0.15)
Basidiomycete sp.	Chile	ChBrnRt1	KC514808	3.63 (1.38)	17.55 (7.64)[b]
Basidiomycete sp.	Chile	Ten. #91	KC514814	3.04 (2.15)	12.33 (2.95)[b]
Basidiomycete sp.	Chile	Ach. #46	KC514825	2.44 (0.40)	16.57 (4.42)[b]
Basidiomycete sp.	USA	PC2-2	KC514831	0.06 (0.05)	0.13 (0.09)
Fistulina hepatica	USA	FP-103444-T	KC514826	0.12 (0.11)	0.24 (0.04)
Fomitopsis cajanderi	USA	33A	KC514811	0.56 (0.14)	0.50 (0.31)
Fomitopsis cajanderi	USA (MN)	TAB 83	KC514827	6.78 (4.17)[b]	22.01 (0.01)[b]
Gloeophyllum sepiarium	USA	206A	KC514817	6.11 (0.06)[b]	15.61 (6.05)[b]
Neolentinus lepideus	USA	751	KC514815	2.30 (1.64)	30.48 (0.02)[b]
Oligoporus balsaminus	USA	212A	KC514830	0.43 (0.29)	7.28 (0.14)
Phaeolus schweinitzii	USA	209	KC514818	1.62 (0.30)	14.31 (0.35)[b]
Pyrofomes demidoffii	USA (AZ)	PJ-1	KC514835	0.33 (0.00)	1.17 (0.01)
White rot					
Agaricomycetes sp.	USA (MN)	BY1	KC514809	1.88 (0.50)	4.60 (1.55)
Ceriporiopsis subvermispora[a]	USA	105725 FPL	KC514810	0.80 (0.53)	9.48 (4.55)[b]
Corticiales sp.	NA	Tyro292	KC514840	1.56 (0.41)	5.62 (1.04)
Dichomitus squalens[a]	USA	4C	KC514837	2.08 (0.33)	21.32 (3.85)[b]
Ganoderma lucidum	USA (MN)	GL-MN1	KC514839	9.13 (1.92)[b]	23.17 (2.94)[b]
Ganoderma	USA (MN)	HoneyL1	KC514812	8.97	21.29

resinaceum				(0.24)[b]	(0.83)[b]
Ganoderma tsugae[a]	USA (WI)	WI-7C	KC514828	1.34 (0.16)	10.64 (3.35)[b]
Hymenochaete corrugata	USA (MN)	H-2 MN	KC514813	2.67 (1.15)	14.44 (0.06)[b]
Inonotus dryophilus[a]	USA (MN)	ID1	KC589014	0.18 (0.05)	3.74 (0.46)
Irpex lacteus	USA (MN)	34A	KC514829	9.97 (0.17)[b]	19.58 (0.32)[b]
Peniophorella pertenuis	Chile	Ten. #74	KC514832	0.06 (0.11)	0.10 (0.08)
Perenniporia subacida[a]	USA	11A	KC514821	4.63 (0.25)[b]	9.37 (0.01)[b]
Phellinus arctostaphyli	USA (AZ)	PM-1	KC589015	0.38 (0.04)	2.48 (0.47)
Phellinus pini[a]	USA (MN)	TAB 19	KC514836	0.37 (0.01)	1.67 (0.38)
Phlebia brevispora	NA	64C	KC514833	0.93 (0.21)	8.00 (0.96)
Phlebia chrysocreas	Chile	604	KC514834	4.38 (0.43)[b]	9.58 (4.08)[b]
Phlebia sp.	Chile	Park #82	KC514819	-0.20 (0.05)	5.00 (0.96)
Phlebia tremellosa	FPL	PRL 2845	KC514820	0.64 (0.50)	8.17 (5.14)[b]
Scytinostroma sp.[a,b]	USA (NH)	B360	KC514822	-0.08 (0.10)	6.68 (1.52)
Stereum hirsutum	Chile	Cale. #67	KC514824	1.31 (0.17)	7.53 (0.88)
Stereum hirsutum	Chile	Brown 67	-	2.31 (0.45)	12.34 (2.93)[b]
Trametes betulina	USA	611A	KC514816	0.83 (0.08)	3.52 (0.26)
Xylariaceae sp.	NA	303B	KC514841	0.44 (0.06)	1.12 (0.28)
Unknown decay type					
Jaapia argillacea	Antarctica (Deception Island)	Di44-5	KC514904	0.49 (0.52)	1.79 (0.40)
Sistotrema brinkmannii	Chile	Quin. 25A	KC514823	0.24 (0.12)	0.39 (0.24)
Basidiomycete sp.	Canada	WBR-1	KC514807	0.11 (0.05)	0.07 (0.06)

[a] known to selectively degrade lignin [b] indicates significantly greater mass loss than corresponding control (Dunnett's multiple comparison, family error rate = 0.05). [c] Two additional *Scytinostroma* sp. were used in follow up testing with U of MN isolate codes of B361 and 3262.

4.3.2 Progression of component loss

The mass closure of sound aspen was near complete with 94.59% of total mass accounted for (**Table 4.2**). Aspen chemical composition was comparable to previously described values (Rowell, 1984; Wang et al., 2012; Saddler and Mackie, 1990). Typical of hardwoods, hemicelluloses were predominantly composed of xylan, and a relatively small portion of mannan was present as compared with pine. Uronic acids and acetyl groups were abundant as compared with pine, while quantities of ash and extractives were less than corn stover for both wood types.

Table 4.2 Initial composition of tested substrates expressed as % of dried mass (standard error)

Component	SYP[a]	Aspen	Corn stalk[b]
Ash	0.22 (0.01)	0.20 (0.03)	5.25 (0.04)
Extractives	3.35 (0.57)	3.01 (0.28)	13.38 (1.23)
Lignin	26.38 (0.62)	20.44 (0.18)	15.22 (0.13)
Glucan	45.56 (0.31)	44.16 (1.14)	35.29 (0.23)
Xylan	7.19 (0.29)	15.82 (0.20)	20.27 (0.16)
Galactan	1.24 (0.03)	0.50 (0.02)	0.00 (0.00)
Arabinan	1.28 (0.01)	0.44 (0.03)	5.91 (0.31)
Mannan	10.63 (0.05)	2.77 (0.18)	0.60 (0.08)
Uronic acid	1.08 (0.10)	3.05 (0.00)	1.46 (0.05)
Acetyl	1.53 (0.10)	4.18 (0.01)	4.43 (0.05)
Total	98.46 (0.95)	94.59 (1.49)	101.80 (1.31)

[a]SYP = Southern Yellow Pine. [b]Corn (*Zea Mays*) stalk pith.

Progression of component losses in aspen generally followed patterns characteristic of decay type (**Figure 4.1**). T-tests showed that lignin mass was lost by white rot species at a significantly faster rate (11.8 X) than brown rot ($t(65) = 4.44$, $P < 0.0001$). Collectively, white rot species caused comparable loss rates for all components (**Figure 4.2**). However, white rot species known to selectively degrade lignin (n = 7) caused lignin loss at a rate that was more than twice that of the other tested white rot

fungi (**Table 4.4**). Selective lignin degraders also appeared to cause a slower rate of xylan loss than the other white rot fungi ($P = 0.053$), though these data were poorly fit by the model equation ($R^2 = 0.021$).

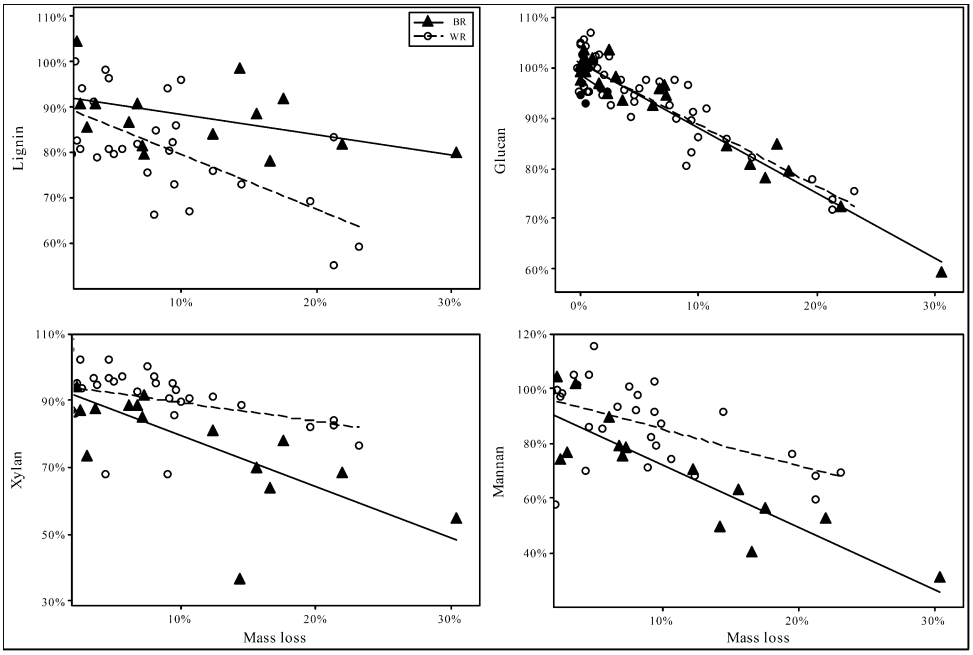

Figure 4.1 Percentage of chemical component remaining in aspen as a function of mass loss after decomposition by fungi with functionally different nutritional modes (BR - brown rot type; WR – white rot). Results from 37 fungal isolates are shown (15 BR, 22 WR). Remaining percentage is based on the amount of component present in sound aspen. Trend fits are linear.

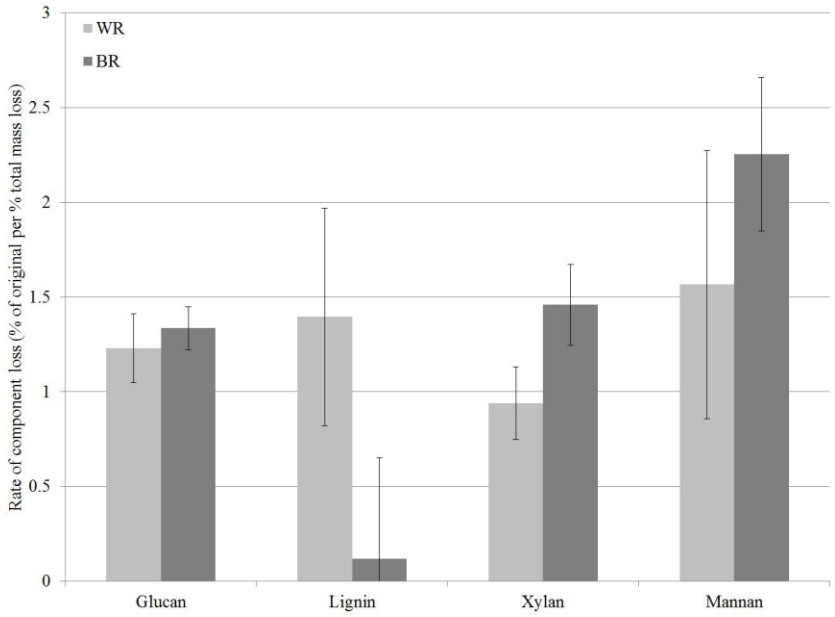

Figure 4.2 Comparison of the rate of aspen component loss relative to the rate of total mass loss for white rot and brown rot decay types. A value greater than 1 indicates faster loss relative to other components. Error bars represent standard error.

As often observed, brown rot hemicellulose losses tended to outpace white rot (Cowling 1961; Kirk and Highley, 1973). Xylan and mannan loss rates were 55% and 44% greater than white rot, though only the difference in the rate of xylan loss was statistically significant (**Table 4.3**). The low initial concentration of arabinan resulted in high variance in arabinan loss rates. Galactan was not present in an appreciable amount.

Table 4.3 Linear (Y = M*X + B) model fit coefficients, standard error (S), and the coefficient of determination (R2) for the % of component remaining in aspen wood as a function of mass loss after degradation by tested brown rot and white rot fungi. Results of two sample t-tests comparing the effect of brown rot and white rot on the rate of loss and Levene's test for equal variances about the model fits between the two decay types are also included.

		Glucan	Xylan	Mannan	Lignin
Brown rot	*M*	-1.335	-1.459	-2.253	-0.118
	B	1.009	0.987	0.965	0.877
	S	0.023	0.032	0.061	0.07
	R^2	0.97	0.953	0.922	0.258
White rot	*M*	-1.228	-0.938	-1.565	-1.395
	B	1.009	1.016	1.02	0.945

	S	0.038	0.03	0.111	0.09
	R^2	0.805	0.813	0.449	0.497
T-test	*T*	0.5	2.65	1.17	-4.44
	P	0.619	0.01	0.244	0
	DF	69	58	67	65
Levene's test	*F*	6.84	0.24	0.25	1.46
	P	0.011	0.625	0.62	0.231

Table 4.4 Linear (Y = M*X + B) model fit coefficients, standard error (S), and the coefficient of determination (R2) for the % of component remaining in aspen wood as a function of mass loss after degradation by known selective white rot species and all other tested white rot fungi. Additionally, the results of two sample t-tests comparing the effect of selective and other white rot species on rate of loss for each component are provided.

		Glucan	Xylan	Mannan	Lignin
Selective white rot	*M*	-1.116	-0.115	-1.285	-1.976
	B	0.994	0.906	0.97	0.94
	S	0.038	0.051	0.148	0.093
	R^2	0.77	0.021	0.224	0.636
Other white rot	*M*	-1.273	-0.867	-1.334	-0.93
	B	1.016	0.987	0.992	0.906
	S	0.04	0.097	0.135	0.084
	R^2	0.809	0.248	0.286	0.333
T-test	*T*	-0.76	2.01	-0.06	2.13
	P	0.457	0.053	0.951	0.046
	DF	23	31	20	20

The rate of glucan loss was statistically identical in both decay types, but the variance about the linear fit for white rot was significantly greater than that for brown rot based on Levene's test, with $P = 0.0011$ (**Table 4.3**). Based on standard error, variance about model fits for other components also tended to be greater in white rot, but the difference as compared with brown rot were not statistically significant.

4.3.3 Dilute Alkali Solubility

The DAS of brown rotted wood tends to rise substantially as compared with the DAS of sound wood, while white rotted wood exhibits only modest increases in DAS (Cowling 1961; Shortle 2010). The % DAS at which brown rot can be distinguished from white rot varies with substrate species and mass loss, but as a general rule, a DAS in excess of 40% is indicative of brown rot decay in wood (Schilling et al. 2015). DAS values in our study held true to this rule, as only brown rotted aspen exceeded a DAS value of 40% (**Figure 4.3**). Additionally, values for parameters θ_1 and θ_2 obtained by the fit of both decay types to the modified Michaelis-Menten equation were compared (**Figure 4.3**). When added to the initial DAS value (DAS of sound wood), θ_1 represents the asymptotic maximum DAS, while θ_2 represents the mass loss at which the DAS is at half of this maximum asymptote. Brown rot exhibited a significantly greater ($P = 0.018$) theoretical maximum DAS ($\theta_1 = 0.54$, versus 0.06 for white rot) and reached half of this maximum value at a greater mass loss ($\theta_1 = 0.16$, versus 0.02 for white rot), though this was not significant, statistically ($P = 0.242$). Variance about the model fit of the white rot DAS was higher than that of brown rot (standard deviation of 0.089 versus 0.071), but was also not statistically significant (*Levene's test* = 1.61, $P = 0.209$).

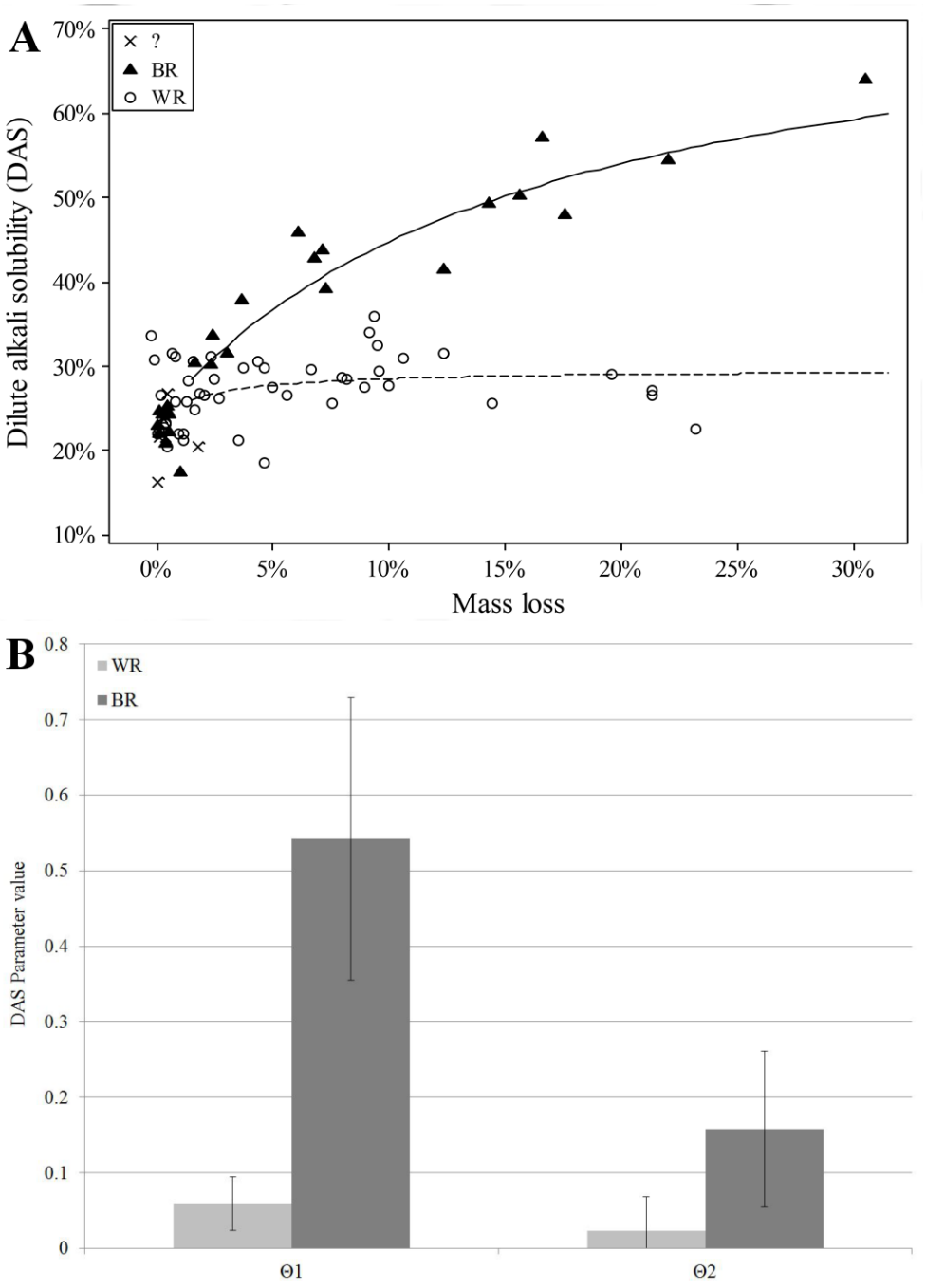

Figure 4.3 A: Change in DAS with mass loss. **B:** Comparison of the model coefficients for white rot and brown rot resulting from the fit of DAS values to the equation: $Y = Y0 + (\theta1*X)/ (\theta2+X)$. Resulting model fits are depicted in Figure 3A. The maximum DAS approached is described by θ_1 and the mass loss at which half of this maximum is achieved is described by θ_2. Error bars represent standard error.

Due to the distinctive signatures left by brown rot on DAS, this value could be used to corroborate decay classification when a specific species cannot be clearly established by genetic sequencing and BLAST query alone. For example, the best BLAST ID matches of known species for *Basidiomycete* sp. (KC514825) were several *Laetiporus* sp., a genus of brown rot fungi, at 93%. This would suggest that the unknown *Basidiomycete* sp. might also be a brown rot, but with an ID match < 95%, the match with *Laetiporus* sp. is not deemed significant. A DAS value of 57% at 17% mass loss for KC514825 bolsters the likelihood that this species does indeed employ a brown rot mode of decay.

Unfortunately, this approach is less straightforward with samples exhibiting little mass loss. For example, fungal species tested for which the decay type has not been firmly established (*Jaapia* sp. and *Sistotrema* sp.) could not be discerned by DAS due to the low mass loss in these samples. However, if it is assumed that the relationship between DAS and mass loss in aspen is comparable to that in birch, we can solve for the probability that either of these species produces brown rot by plugging the DAS and mass loss values of these samples into the logit equation for birch provided in Schilling et al. (2015). This estimates the probability that *Jaapia* sp. and *Sistotrema* sp. have a brown rot decay mode at 40.6% and 21.4%, respectively.

4.3.4 Carbohydrate Analysis

4.3.4.1 Monosaccharide Presence after Decay

Degradation by many of the tested fungal species resulted in the generation of monomeric sugars beyond those present in sound aspen (**Table 4.5**, Supplemental Table

S4.1). Glucose and xylose yields resulting solely from fungal degradation were as high as 2.15% and 1.17%, respectively.

Table 4.5 Yield of glucose and xylose after treatment with the indicated fungus for 2 or 4 weeks. Yields are expressed as a percentage of the xylan or glucan content of untreated aspen.

			Xylose		Glucose	
			2 weeks	4 weeks	2 weeks	4 weeks
Species	Accession #	Decay type				
Control	-	-	0.06%	0.09%	0.09%	0.03%
Corticiales sp.	KC514840	W	0.11%	2.11%[a]	0.23%	1.17%[a]
Basidiomycete sp.	KC514808	B	0.19%	1.85%[a]	0.15%	1.01%[a]
Basidiomycete sp.	KC514825	B	0.10%	0.52%	0.10%	0.71%[a]
P. schweinitzii	KC514818	B	0.00%	1.81%[a]	0.00%	0.69%[a]
N. lepideus	KC514815	B	0.00%	1.10%	0.17%	0.66%
F. cajanderi	KC514827	B	0.18%	0.50%	0.13%	0.59%
Basidiomycete sp.	KC514814	B	0.10%	0.89%	0.12%	0.53%
G. sepiarium	KC514817	B	0.36%	0.43%	0.25%	0.50%
G. resinaceum	KC514812	W	0.08%	0.42%	0.21%	0.33%
P. tremellosa	KC514820	W	0.00%	0.77%	0.00%	0.25%
A. alpina	KC514838	B	0.00%	0.21%	0.03%	0.20%
J. argillacea	KC514904	?	0.00%	0.75%	0.00%	0.19%
D. squalens	KC514837	W	0.05%	0.22%	0.15%	0.16%
H. corrugata	KC514813	W	0.00%	0.12%	0.10%	0.15%
Agaricomycetes sp.	KC514809	W	1.57%	0.59%	0.41%	0.13%
S. hirsutum	KC514824	W	0.17%	0.86%	0.07%	0.12%
I. lacteus	KC514829	W	0.85%	0.00%	0.17%	0.10%
P. chrysocreas	KC514834	W	0.25%	0.00%	0.20%	0.08%
Phlebia sp.	KC514819	W	0.00%	0.21%	0.03%	0.07%
O. balsaminus	KC514830	B	0.01%	0.22%	0.01%	0.07%
Basidiomycete sp.	KC514807	?	0.00%	0.00%	0.24%	0.05%
P. subacida	KC514821	W	0.00%	0.20%	0.00%	0.04%
C. subvermispora	KC514810	W	0.00%	0.21%	0.00%	0.03%
Basidiomycete sp.	KC514831	B?	2.15%[a]	0.00%	0.52%	0.00%
P. arctostaphyli	KC589015	W	1.15%	0.00%	0.26%	0.00%
F. hepatica	KC514826	B	0.90%	0.00%	0.23%	0.00%
P. pertenuis	KC514832	W	0.99%	0.00%	0.19%	0.00%
I. dryophilus	KC589014	W	0.02%	0.00%	0.16%	0.00%
Scytinostroma sp.	KC514822	W	0.00%	0.00%	0.15%	0.00%
P. pini	KC514836	W	0.00%	0.00%	0.12%	0.00%
T. betulina	KC514816	W	0.00%	0.00%	0.11%	0.00%
P. demidoffii	KC514835	W	0.00%	0.00%	0.07%	0.00%
Xylariaceae sp.	KC514841	W	0.01%	0.00%	0.04%	0.00%
S. hirsutum	KC514824	W	0.09%	0.06%	0.03%	0.00%
G. lucidum	KC514839	W	0.02%	0.00%	0.03%	0.00%
G. tsugae	KC514828	W	0.04%	0.00%	0.01%	0.00%
P. brevispora	KC514833	W	0.00%	0.00%	0.01%	0.00%

A. carbonica	KC514806	B	0.00%	0.00%	0.00%	0.00%
F. cajanderi	KC514811	B	0.00%	0.00%	0.00%	0.00%
S. brinkmanii	KC514823	?	0.00%	0.00%	0.00%	0.00%

[a] indicates significantly greater mass loss than corresponding control (Dunnett's multiple comparison, family error rate = 0.05)

General linear regression indicated that neither the main effect of decay type nor the interaction term between decay type and mass loss were significant factors in modeling xylose yield ($P = 0.926$ and $P = 0.053$, respectively). For glucose yield, however, the interaction term between mass loss and decay type was highly significant ($P < 0.001$), though the main effect of decay type was not significant ($P = 0.547$). The significance of this interaction term was driven by the large difference in glucose yield between brown rotted samples that exhibited more than 10% mass loss and those that did not exceed 10% mass loss. This mass loss distinction had no effect on the glucose yield of white rot (**Figure 4.4**). While regression analysis narrowly did not show a significant interaction term for decay type and mass loss, this same effect of mass loss was observed with xylose yield (**Figure 4.4**). As with glucose, xylose yield for brown rot was substantially higher than that of white rot when mass loss exceeded 10%.

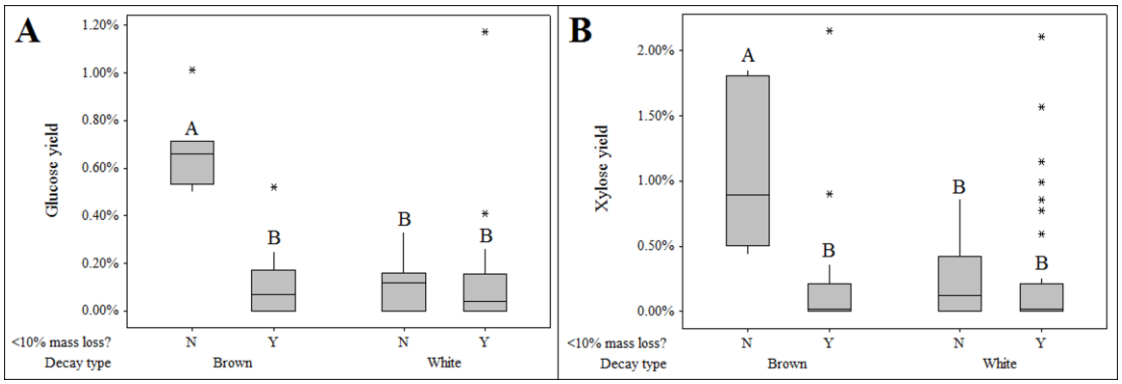

Figure 4.4 Box plots of glucose (**A**) and xylose (**B**) yield based on original glucan and xylan content, respectively, following pretreatment but preceding enzymatic hydrolysis, with respect to decay type and extent of decay (> 10%). Plots within the same graph sharing the same letter are not significantly different based on Tukey's post-hoc comparisons.

The observation of higher free monosaccharide in brown rotted wood contradicts prior work of Jurgensen et al. (1989), who noted differences in soluble sugar concentrations for brown rot and white rot in logs native to six conifer forests. With an uncontrolled environment and unknown decay progression and community composition, it is highly likely that observed concentrations were the result of generation and consumption of soluble sugars by various microorganisms and not limited to just fungi of a specific decay type. Our findings, however, are generally in agreement with Cowling (1961), who found that brown rotted sweetgum tended to have a greater concentration of "available reducing substances" in its hot water extractives, which would include water-soluble saccharides, than white rotted sweetgum in all stages of decay.

Traditionally, lignin content is the distinguishing chemical characteristic driven by fungal decay type that influences wood and soil community assembly and function (Zeikus, 1981; Cornwell et al., 2008; Talbot et al., 2015). Differing monosaccharide yields at higher mass losses suggest an additional means by which fungal decay type can

affect community composition, as the concentration and type of free sugars present in an environment can alter an ecological community. This has been observed in community structure dynamics of varied environments, including the microbiomes of the human digestive tract (Sonnenberg et al., 2010), soils (Luo et al. 2008; Chen et al. 2008), and forest litter (Scheu and Schaefer 1998). Alterations in community compositions can alter functional outcomes and further effect higher order community structure and environmental conditions on various scales. For example, changes in community composition can influence community level metabolic rates and the release rate of atmospheric carbon.

4.3.4.2 Susceptibility to Enzymatic Hydrolysis

Fungal degradation by both decay types resulted in improved enzymatic hydrolysis yields of xylose and glucose (**Table 4.6**). As yields were calculated based on the polysaccharide content of untreated aspen and not the content of the pretreated (post-decay) aspen, significant improvements were seen beyond losses incurred by fungal carbon metabolism.

Table 4.6 Glucose and xylose yields after enzymatic saccharification of aspen wood pretreated with the indicated fungus for 2 or 4 weeks, expressed as a percentage of the provided control yield (i.e. yield after enzymatic hydrolysis of undecayed aspen). Yields are based on carbohydrate content of sound aspen.

			Xylose		Glucose	
			2 weeks	4 weeks	2 weeks	4 weeks
		Control Yield	12.30%	15.04%	12.60%	16.11%
Species	Accession #	Decay type				
Scytinostroma sp.	KC514822	W	100.8%	237.5%[a]	104.0%	349.2%[a]
P. brevispora	KC514833	W	152.8%	230.7%	168.3%	289.3%[a]
S. hirsutum	KC514824	W	142.3%	213.5%	185.7%[a]	270.5%[a]
G. tsugae	KC514828	W	139.0%	192.3%[a]	181.7%	260.6%[a]
Corticiales sp.	KC514840	W	213.8%	228.7%[a]	228.6%[a]	251.3%[a]
D. squalens	KC514837	W	139.0%	248.4%	167.5%	217.7%[a]
S. hirsutum	KC514824	W	215.4%	178.7%[a]	259.5%[a]	206.5%[a]

P. subacida	KC514821	W	158.5%	171.8%	169.8%	204.4%[a]
Basidiomycete sp.	KC514825	B?	109.8%	163.3%	125.4%	199.2%[a]
I. dryophilus	KC589014	W	103.3%	176.7%	96.8%	193.4%
Phlebia sp.	KC514819	W	143.1%	182.7%[a]	146.0%	192.1%
P. tremellosa	KC514820	W	150.4%	191.8%[a]	150.0%	188.8%
P. chrysocreas	KC514834	W	49.6%	159.7%	166.7%	185.0%
C. subvermispora	KC514810	W	158.5%	185.6%[a]	158.7%	183.4%
Basidiomycete sp.	KC514808	B	167.5%	168.0%	161.1%	178.0%
P. arctostaphyli	KC589015	W	101.6%	157.7%	104.8%	177.6%
H. corrugata	KC514813	W	167.5%	177.1%	182.5%	176.1%
N. lepideus	KC514815	B	124.4%	187.3%[a]	114.3%	176.0%
G. lucidum	KC514839	W	134.1%	139.7%	148.4%	172.6%
F. cajanderi	KC514827	B	177.2%	171.3%	161.1%	170.3%
O. balsaminus	KC514830	B	74.0%	154.7%	71.4%	168.4%
P. schweinitzii	KC514818	B	136.6%	169.3%	127.0%	167.1%
A. alpina	KC514838	B	109.8%	143.3%	106.3%	160.6%
G. sepiarium	KC514817	B	196.7%	137.3%	195.2%[a]	149.4%
P. demidoffii	KC514835	W	93.5%	113.3%	95.2%	134.5%
Basidiomycete sp.	KC514814	B	162.6%	129.3%	157.9%	132.9%
P. pini	KC514836	W	92.7%	112.9%	88.9%	131.3%
I. lacteus	KC514829	W	621.1%[a]	111.7%	123.8%	129.7%
P. pertenuis	KC514832	W	70.7%	92.9%	92.9%	116.0%
T. betulina	KC514816	W	119.5%	105.3%	115.1%	108.9%
G. resinaceum	KC514812	W	134.1%	87.2%	136.5%	93.5%
A. carbonica	KC514806	B	85.4%	90.7%	97.6%	93.0%
S. brinkmanii	KC514823	?	94.3%	82.1%	100.0%	93.0%
Agaricomycetes sp.	KC514809	W	172.4%	87.9%	181.0%	85.2%
Basidiomycete sp.	KC514807	?	46.3%	80.0%	48.4%	80.8%
F. hepatica	KC514826	B	48.8%	69.3%	123.8%	80.0%
Xylariaceae sp.	KC514841	W	112.2%	79.3%	121.4%	79.7%
Basidiomycete sp.	KC514831	B	78.9%	78.7%	79.4%	77.2%
J. argillacea	KC514904	?	124.4%	84.7%	118.3%	76.0%
F. cajanderi	KC514811	B	113.8%	82.7%	115.1%	74.9%

[a] Significantly ($P < 0.05$) greater yield than enzymatically hydrolyzed sound aspen.

Though improved yields were seen with both decay types, white rot produced the ten highest glucan yields, two of which were realized after two weeks of exposure (*Corticiales sp.* and *S. hirsutum*). *G. sepiarium* and one likely brown rot (*Basidiomycete* sp., KC514825) were the only brown rot species to generate significant improvement in glucose yield over the control. Only one of the nine isolates that caused significant improvement in xylose yield was a brown rot fungus (*N. lepideus*). *Scytinostroma sp.*

brought the highest glucose yield at 56.3%, 3.5 times the control (**Table 4.6**). This approaches the 70% glucose-to-cellulose conversion observed by Ray et al. (2010) after pretreatment of Scots pine with the brown-rotting fungus *C. puteana* for 20 days. Though higher yields have been observed on other substrates, to our knowledge, our results are the highest reported hardwood glucan yield resulting from biological pretreatment alone.

Improvements in susceptibility to enzymatic hydrolysis were governed by losses in chemical components that were distinctly different in white rot and brown rot. Results of regression analysis indicate that cellulose accessibility was inversely proportional to lignin concentration with white rotted aspen, while all other chemical components were not significant predictors of glucose yield (**Table 4.7**). This is not surprising, as lignin is often highly correlated with saccharification potential (Mandels et al., 1974; Studer et al., 2011) and the persistence of plant litter and forest detritus (Meentemeyer, 1978; Freschet et al., 2012). Interestingly, lignin content was not a significant predictor of cellulose accessibility in brown rotted aspen. Instead, glucose yield was inversely proportional to hemicellulose content (xylan and arabinan). Hemicellulose content also commonly correlates with saccharification potential (Leu and Xu, 2013). This would suggest that brown rot and white rot differ in the decay properties one would target for optimizing saccharification. Namely, brown rot fungi that most rapidly remove arabinan and xylan and white rot fungi that most rapidly remove lignin are ideal. Furthermore, hemicellulose losses by white rot and lignin losses by brown rot are not indicative of saccharification potential. The lower peak glucose yield of brown rot relative to white rot was also

captured in the constants of the regression models (**Table 4.7**), with the absence of relevant components yielding maximum glucose yields of 47% and 69% for brown rotted and white rotted aspen, respectively.

Table 4.7 Unbiased coefficients for regression explanatory variables describing the response factor: glucose yield after enzymatic hydrolysis. Both models were highly significant ($P < 0.001$). Content percentages are mass loss corrected. Additionally, the standard error of estimates and adjusted R^2 are provided as indicators of goodness of model fit. NS: not significant ($P > 0.05$). DF: degrees of freedom.

Variable	White Rot	Brown Rot
Constant	0.69	0.47
Lignin (%)	-1.90	NS
Xylan (%)	NS	-1.70
Arabinan (%)	NS	-14.37
Standard Error	0.082	0.038
R^2 (adjusted)	35.31	68.21
DF	46	25

Ultimately, this suggests a difference in the mode by which white rot and brown rot improve accessibility to cellulose in a way that is analogous to differences seen in lignin-targeting (e.g. AFEX) and hemicellulose-targeting (e.g. dilute acid) thermochemical pretreatment methods. Given this, we might expect to see that pretreatment methods that target lignin removal might outperform those that target hemicellulose removal.

Susceptibility to enzymatic hydrolysis changed with mass loss in discernable and distinct patterns for each decay type. Over the course of time considered, glucose yields of brown rotted samples tended to increase with increasing mass loss to an asymptotic value, while white rotted samples tended to peak around 8% mass loss before declining (**Figure 4.5**). These patterns lead to differences in the best equation fit for yield with respect to mass loss for the two decay types, with a cubic fit (maximum-exhibiting) and a

modified Michaelis-Menten fit (concave) being most representative for white rot and brown rot, respectively. Likewise, xylose yields exhibited a comparable pattern, with brown rot being best described by Y = A+B*ln(mass loss) (concave) and white rot was best described using a quadratic equation (maximum-exhibiting). Comparison of residual variance about model fits suggested that white rot varied significantly more than brown rot with respect to glucose (*Levene's Test* = 13.24, *P* = 0.001) and xylose (*Levene's Test* = 11.90, *P* = 0.001) yields. This high variance among white rot species, both in sugar yields and in the progression of losses in substrate chemical components corroborates the proposal of Riley et al. (2014) that a brown rot/white rot dichotomy does not adequately describe the diversity of lignocellulosic decay mechanisms. However, it suggests that this mechanistic diversity exists largely among white rot fungi and is less pronounced, if at all present, among brown rot fungi. This is in agreement with our previous findings that all clades of brown rot exhibit the same progression of decay (Kaffenberger and Schilling, 2014).

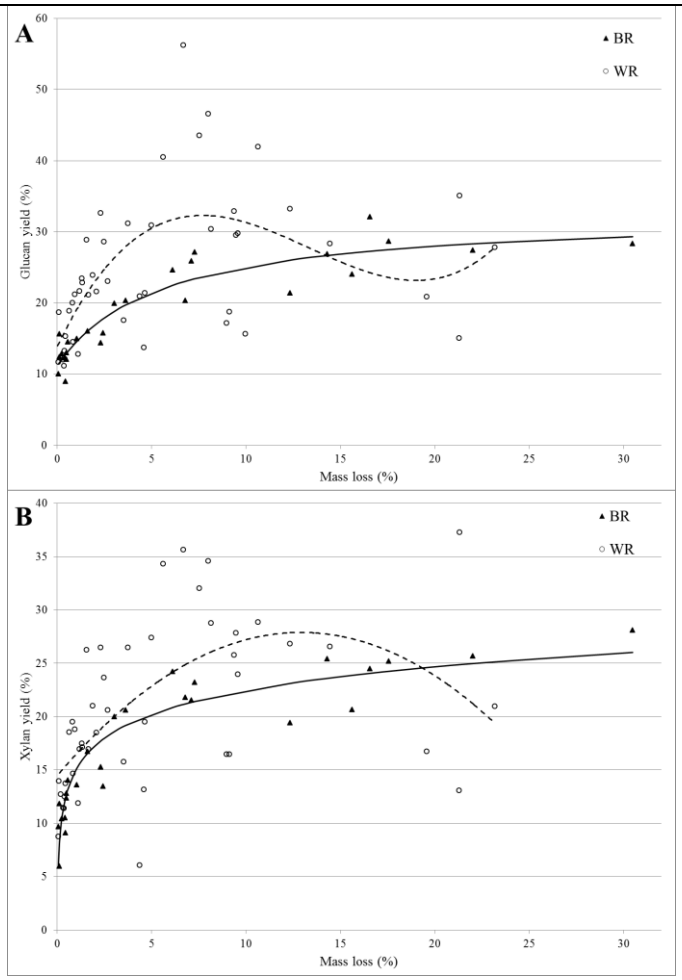

Figure 4.5 Glucose (A) and xylose (B) yields, with respect to mass loss and decay type. White rot and brown rot data for glucose are fit to a cubic equation ($Y = A*X^3 + B* X^2 + C*X + D$) and a modified Michaelis-Menten equation ($Y = Y_0 + (\theta_1*X)/ (\theta_2+X)$), respectively. Xylose data for white rot and brown rot are fit to a quadratic equation ($Y = A* X^2 + B*X + C$) and $Y=A+B*\ln(X)$, respectively.

4.3.5 Refined time series and substrate effects

4.3.5.1 *Scytinostroma* sp. on aspen

As 2 and 4 week time points were arbitrarily selected for the initial screening, the isolate yielding the highest glucose content in the initial screening, *Scytinostroma* sp., was selected for a follow-up soil block decay study using a more refined time series. The changes made in the experimental design of the soil block test (substrate size and

inoculum application) accelerated the rate of degradation, as desired. While 6.7% mass loss was caused by *Scytinostroma* sp. after 28 days in the initial screening, this extent of mass loss was realized in only 17 days in the follow-up study (**Figure 4.6**). This also reduced the time required to reach optimum enzymatic hydrolysis glucose yield, which was reached after 14 days, as compared to 28 in the original screening. Control glucose yields, however, were significantly lower than control yields observed in the initial screening (4.3% versus 12.6%) and maximum glucose yield for treated aspen was only 19.4% (**Figure 4.6**).

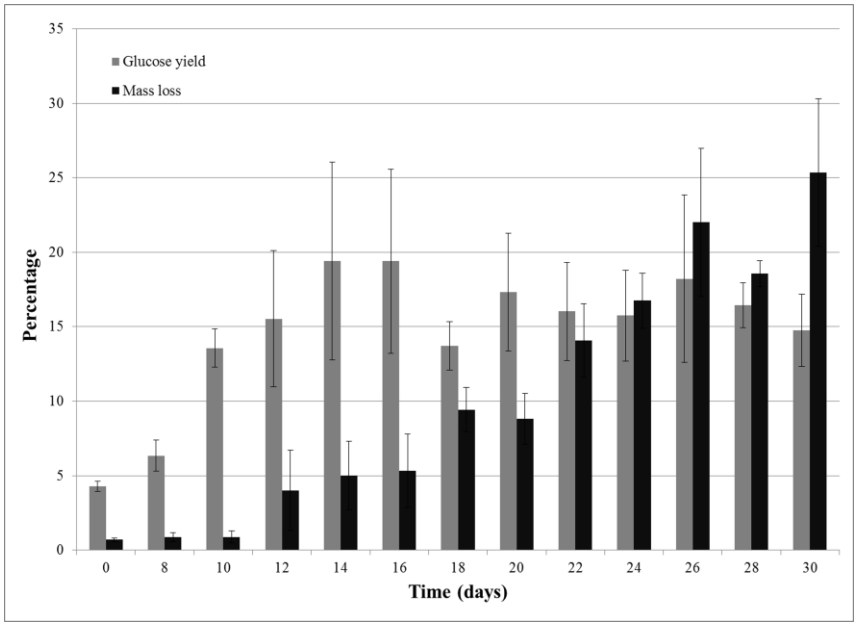

Figure 4.6 Glucose yield and mass loss of aspen degraded by Scytinostroma sp. (B360). Error bars represent standard deviation.

The reason for the discrepancy in glucose yield between the two studies is unclear. Though the same piece of aspen sapwood was used to make both blocks and wafers, it may be that the smaller substrate size made the wafers more susceptible to hornification during drying, leading to reduced cell wall accessibility. With wafers, the

sample mass was 26% that of the blocks used in the initial screening. Furthermore, the aspect ratio of the wafers was also greater. These changes would allow for the entirety of the wafer to reach oven temperature at a faster rate. Faster heating rates have been shown to cause more extensive hornification (Brancato and Banerjee, 2010), reducing enzyme accessibility and thus glucose yield. Despite exhibiting lower yields, peak post-enzyme hydrolysis yields were still 4.5 times enzymatically hydrolyzed controls.

4.3.5.2 Substrate studies

Mass losses among tested substrates (aspen, SYP, and CS) varied (**Figure 4.7**). On aspen, *P. brevisporum* and *Corticiales* sp. exhibited no significant mass loss after 28 days, while the three strains of *Scytinostroma* sp. induced a mean mass loss of 17.7% and *G. trabeum* caused 42.2% mass loss. In comparison, *P. brevisporum*, *Corticiales* sp., and *Scytinostroma* sp. (B360) caused 8.0%, 5.6%, and 6.7% mass loss, respectively, after 28 days in the initial screening. All fungal isolates were slower to degrade pine than the other substrates. *G. trabeum* exhibited the greatest pine mass loss (26.5% on average). *Scytinostroma* sp. isolates B361 and B360 produced mass losses significantly ($P < 0.05$) greater than the control, at 7.2% and 4.6%, respectively. *P. brevisporum*, *Corticiales* sp., and the 3262 isolate of *Scytinostroma* sp. exhibited no significant mass loss after 28 days. Corn stalk controls saw a mean mass loss of 10.5% after 28 days. As initial extractives content was 13.4% of the dried mass, control mass losses were likely due to water-soluble extractive leaching. *G. trabeum* and the three *Scytinostroma sp*. isolates (B361, 3262, and TAB-197) exhibited significantly higher mass loss than the controls at 52.2%,

27.9%, 23.8%, and 18.9%, respectively. As with the other two substrates, *P. brevisporum* and *Corticiales* sp. induced no more mass loss than the controls.

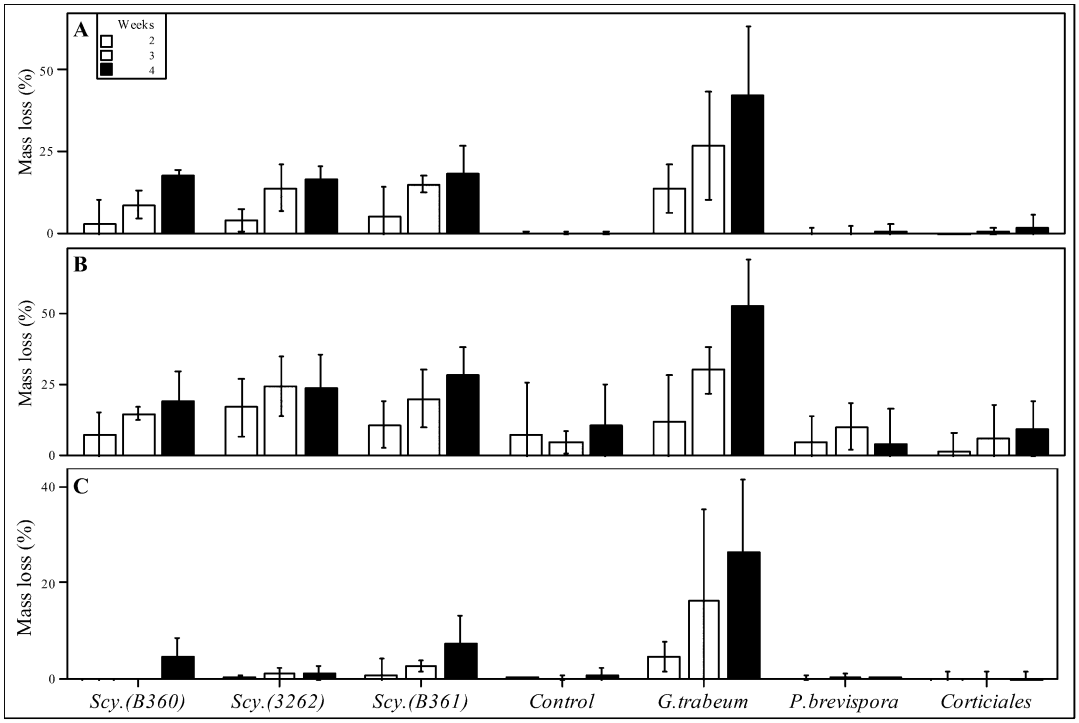

Figure 4.7 Mass loss of aspen (A), corn stover (B), and pine (C) following exposure to indicated fungal isolate for 2, 3, or 4 weeks. Error bars represent 95% confidence interval.

Substrate type impacted glucose yield and fungal pretreatment efficacy (**Figure 4.8**). Overall, corn stalk provided the highest glucose yields, followed by aspen. Aspen, however, showed the greatest improvement with pretreatment. Fungal inoculation of corn stalk produced no significant improvement in glucose yield over the control and often led to reduced yields. This may be in part due to the higher initial concentrations of free glucose and soluble oligosaccharides that were present in corn stalk, as indicated by sugar analysis of non-hydrolyzed samples (Supplemental Table S4.4). The presence of soluble sugars can competitively and non-competitively inhibit cellulase activity

(Holtzapple et al., 1990; Qing et al., 2010). Glucose, in particular, has been shown to act as a regulatory inhibitor of cellulase transcription in the model species *Trichoderma reesei* (Ilmén et al., 1997).

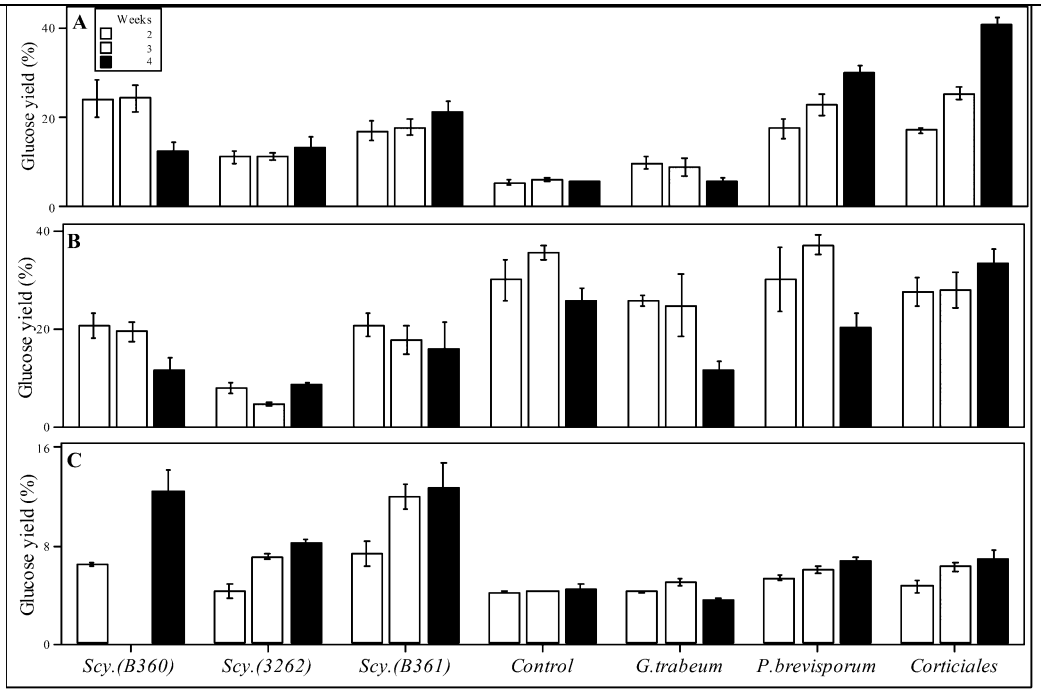

Figure 4.8 Glucose yield of aspen (A), corn stover (B), and pine (C) following exposure to indicated fungal isolate for 2, 3, or 4 weeks and enzymatic hydrolysis with a commercial enzyme. Error bars represent standard error.

Previous studies have demonstrated improvements in sugar yields with biological pretreatment of corn stover. Xu et al. (2010) saw a peak holocellulose conversion ratio of 66.4% after 25 days of pretreatment with *I. lacteus*. Wan and Li (2010) observed glucose yields of 66.6% after pretreatment of corn stover with *C. subvermispora* for 35 days. Sun et al. (2011) observed glucose yields as high as 73.99% (based on pretreated material) with 42 days of pretreamtent with *Trametes hirsutum*, a significant improvement over

control yields. In these studies, however, it is unclear how much free sugar was present in non-degraded corn stover. This may be an important factor in pretreatment efficacy.

Pine controls exhibited an average glucan yield of 4.3%. Treatment with *Scytinostroma* sp. provided the most benefit, with yields increasing to 12.7% after 4 weeks of exposure with the B360 and B361 isolates: three times the control yield. Isolate 3262 was less effective, but showed the same improving trend as the other two isolates. Despite exhibiting no significant mass loss, *P. brevisporum* and *Corticiales* sp. also improved pine glucose yields (**Figure 4.5**), but to a lesser extent than *Scytinostroma* sp., with yields of 6.8% and 6.9% respectively after 4 weeks exposure. Surprisingly, *G. trabeum* treated pine showed little improvement over controls, with a peak yield of 5.0%. Previous studies have shown improvement in pine glucan conversion rates after treatment with *G. trabeum* (Monrroy et al., 2011), with up to a two-fold improvement in yield over controls (Schilling et al., 2009). Given the rapid rate of mass loss seen with *G. trabeum*, the optimal harvest time for peak glucan yield may have been missed.

Aspen controls exhibited an average yield of 5.6%. *G. trabeum* showed the most improvement at week 2 (1.7 times the control yield) and declining yields thereafter, indicating that the optimum mass loss may have been overshot. As with pine, *P. brevisporum* and *Corticiales* sp. exhibited substantial improvements in yield (5.3 and 7.3 times the control, respectively), despite no discernible mass loss. Comparatively, yields for *P. brevisporum* and *Corticiales* sp. after 4 weeks of decay were 46.6% and 40.5% respectively in the original screening. It is unclear why such substantial improvement in glucan yield was observed for these two species with such little apparent mass loss.

4.4 Conclusions

Among the 40 fungal isolates tested as biological pretreatment agents in this study, white rot fungi outperformed brown rot in terms of improvement in lignocellulosic conversion yields. In particular, *Scytinostroma* sp., a lignin-selective white rot, showed the greatest yield improvement on aspen, with a 3.5-fold improvement over untreated controls. White rot fungi also showed significantly higher variability than brown rot fungi, in terms of both progression of change in substrate chemical composition and carbohydrate yields. This is in agreement with the "spectrum of fungal decay" proposed by Riley et al. (2014) among white rot species.

Beyond bioconversion and in contrast to previously reported field studies, our work also demonstrated a higher level of free monosaccharide content in aspen following brown rot decay than white rot. Differences in soluble sugar availability with decay type may be an additional factor, beyond lignin, which influences ecological community-level dynamics in white and brown rot decay residues.

4.5 Supplemental Data

Table S4.1 Yields of carbohydrate monomers after treatment of aspen with indicated fungus for 2 or 4 weeks. No arabinose was detected in any 4 week samples.

			Glu (%)		Xyl (%)		Gal (%)		Ara (%)	Man (%)	
		Wks	2	4	2	4	2	4	2	2	4
Species	Access. #	Type									
Control	-	-	0.09	0.03	0.06	0.09	0.00	17.23	0.24	0.29	261.1
J. argillacea	KC514904	?	0.00	0.19	0.00	0.75	21.10	0.00	0.00	272.1[a]	242.9
Basidiomycete sp.	KC514825	B	0.10	0.71[a]	0.10	0.52	0.00	14.32	0.72	0.00	219.5[a]
A. carbonica	KC514806	B	0.00	0.00	0.00	0.00	38.31	0.00	0.00	262.6[a]	253.0
Basidiomycete sp.	KC514807	?	0.24	0.05	0.00	0.00	0.00	0.00	0.99	105.4	253.1
Basidiomycete sp.	KC514808	B	0.15	1.01[a]	0.19	1.85[a]	19.78	0.00	0.00	130.7	213.5[a]
F. cajanderi	KC514811	B	0.00	0.00	0.00	0.00	18.35	0.00	0.00	132.0	245.3
Basidiomycete sp.	KC514814	B	0.12	0.53	0.10	0.89	0.00	0.00	0.43	101.4	208.6[a]
N. lepideus	KC514815	B	0.17	0.66	0.00	1.10	16.97	4.47	0.00	133.1	176.2[a]
T. betulina	KC514816	W	0.11	0.00	0.00	0.00	15.03	0.00	5.73	188.5	236.3

G. sepiarium	KC514817	B	0.25	0.50	0.36	0.43	34.59	0.00	0.00	266.8[a]	211.4[a]
P. schweinitzii	KC514818	B	0.00	0.69[a]	0.00	1.81[a]	11.29	14.63	0.00	262.4[a]	223.9[a]
S. hirsutum	KC514824	W	0.07	0.12	0.17	0.86	0.00	0.00	0.60	122.8	223.0[a]
F. hepatica	KC514826	B	0.23	0.00	0.90	0.00	0.00	16.89	3.99	52.76	264.8
F. cajanderi	KC514827	B	0.13	0.59	0.18	0.50	0.00	26.36	0.75	46.90	209.3[a]
O. balsaminus	KC514830	B	0.01	0.07	0.01	0.22	0.00	39.12	0.00	0.00	246.5
Basidiomycete sp.	KC514831	B	0.52	0.00	2.15[a]	0.00	0.00	31.95	12.56	0.00	274.6
P. demidoffii	KC514835	W	0.07	0.00	0.00	0.00	16.78	34.31	0.00	1.53	268.3
A. alpina	KC514838	B	0.03	0.20	0.00	0.21	0.00	38.48	0.50	53.35	238.8
Corticiales sp.	KC514840	W	0.23	1.17[a]	0.11	2.11[a]	0.00	16.12	0.00	52.86	253.8
Agaricomycetes sp.	KC514809	W	0.41	0.13	1.57	0.59	20.96	0.00	0.00	191.4	238.4
C. subvermispora	KC514810	W	0.00	0.03	0.00	0.21	0.00	0.00	0.00	135.9	225.1[a]
G. resinaceum	KC514812	W	0.21	0.33	0.08	0.42	0.00	8.06	0.00	125.8	198.2[a]
H. corrugata	KC514813	W	0.10	0.15	0.00	0.12	20.45	0.00	2.62	176.2	219.9[a]
Phlebia sp.	KC514819	W	0.03	0.07	0.00	0.21	20.22	13.31	1.49	194.6	243.2
P. tremellosa	KC514820	W	0.00	0.25	0.00	0.77	39.56	7.71	0.00	260.7[a]	229.1[a]
P. subacida	KC514821	W	0.00	0.04	0.00	0.20	40.30[a]	12.34	0.00	258.8[a]	224.3[a]
Scytinostroma sp.	KC514822	W	0.15	0.00	0.00	0.00	20.29	20.83	0.00	191.3	240.0
S. brinkmanii	KC514823	?	0.00	0.00	0.00	0.00	0.00	0.00	4.71	107.7	249.8
G. tsugae	KC514828	W	0.01	0.00	0.04	0.00	0.00	33.97	0.45	0.00	241.8
I. dryophilus	KC589014	W	0.16	0.00	0.02	0.00	0.00	36.79	0.51	0.00	253.2
I. lacteus	KC514829	W	0.17	0.10	0.85	0.00	0.00	34.84	47.99[a]	88.69	206.2[a]
P. pertenuis	KC514832	W	0.19	0.00	0.99	0.00	0.00	33.28	2.53	54.01	267.6
P. brevispora	KC514833	W	0.01	0.00	0.00	0.00	0.00	36.45	0.00	54.53	254.5
P. chrysocreas	KC514834	W	0.20	0.08	0.25	0.00	0.00	11.94	15.88	0.00	236.0
P. arctostaphyli	KC589015	W	0.26	0.00	1.15	0.00	0.00	34.63	0.00	47.48	264.5
P. pini	KC514836	W	0.12	0.00	0.00	0.00	0.00	35.57	5.76	46.66	270.1
D. squalens	KC514837	W	0.15	0.16	0.05	0.22	0.00	29.67	0.00	51.07	223.7[a]
G. lucidum	KC514839	W	0.03	0.00	0.02	0.00	0.00	31.77	0.00	0.00	202.1[a]
S. hirsutum	KC514824	W	0.03	0.00	0.09	0.06	19.76	20.66	0.00	175.6	231.4
Xylariaceae sp.	KC514841	W	0.04	0.00	0.01	0.00	0.00	17.39	1.30	0.00	262.1

[a] indicates significantly greater mass loss than corresponding control (Dunnett's multiple comparison, family error rate = 0.05)

Table S4.2 Yields of carbohydrate after enzymatic hydrolysis of aspen treated with indicated fungus for 2 or 4 weeks.

			Glucose (%)		Xylose (%)		Galactose (%)		Arabinose (%)		Mannose (%)	
		Wks	2	4	2	4	2	4	2	4	2	4
Species	Access. #	Type										
Control	-	-	12.6	16.1	12.3	15.0	10.9	47.8	13.7	0.0	-84.1	38.3
J. argillacea	KC514904	?	14.9	12.2	15.3	12.7	17.0	75.6	0.0	5.8[a]	34.1	22.6
Basidiomycete sp.	KC514825	B	15.8	32.1[a]	13.5	24.5	0.0	51.4	-1.3	0.0	-49.2	30.2
A. carbonica	KC514806	B	12.3	15.0	10.5	13.6	47.4	69.6	0.0	0.0	18.3	29.1
Basidiomycete sp.	KC514807	?	6.1	13.0	5.7	12.0	1.5	73.1	-3.8	0.0	-94.0	33.7
Basidiomycete sp.	KC514808	B	20.3	28.7	20.6	25.2	8.6	71.0	13.1	0.0	-25.5	22.2
F. cajanderi	KC514811	B	14.5	12.1	14.0	12.4	19.2	68.2	1.6	0.0	-26.2	31.5
Basidiomycete sp.	KC514814	B	19.9	21.4	20.0	19.4	15.5	67.8	0.7	9.0[a]	-39.6	21.0

N. lepideus	KC514815	B	14.4	28.4	15.3	28.1[a]	13.6	53.6	9.1	0.0	-28.9	12.8
T. betulina	KC514816	W	14.5	17.6	14.7	15.8	9.9	63.1	7.5	0.0	-25.1	26.1
G. sepiarium	KC514817	B	24.6[a]	24.1	24.2	20.6	19.4	65.9	0.0	0.0	28.6	12.8
P. schweinitzii	KC514818	B	16.0	26.9	16.8	25.4	16.9	69.0	0.0	0.0	21.9	35.4
S. hirsutum	KC514824	W	32.7[a]	33.3[a]	26.5	26.8[a]	52.0	71.8	17.3	0.0	-7.9	38.0
F. hepatica	KC514826	B	15.6	12.9	6.0	10.4	12.7	46.7	11.4	0.0	-98.1	28.8
F. cajanderi	KC514827	B	20.3	27.4	21.8	25.7	36.2	43.7	32.6	0.0	-78.5	13.5
O. balsaminus	KC514830	B	9.0	27.1	9.1	23.2	10.1	68.5	2.2	0.0	-98.3	29.7
Basidiomycete sp.	KC514831	B	10.0	12.4	9.7	11.8	3.1	46.9	9.7	0.0	-102.7	29.2
P. demidoffii	KC514835	W	12.0	21.7	11.5	17.0	0.0	19.8	15.3	0.0	-75.5	37.1
A. alpina	KC514838	B	13.4	25.9	13.5	21.5	0.0	24.0	14.3	0.0	-49.1	23.7
Corticiales sp.	KC514840	W	28.8[a]	40.5[a]	26.3	34.3[a]	5.6	44.8	11.4	0.0	-70.2	49.7
Agaricomycetes sp.	KC514809	W	22.8	13.73	21.2	13.18	7.5	71.61	14.6	0.0	-20.4	16.1
C. subvermispora	KC514810	W	20.0	29.54	19.5	27.84[a]	25.4	68.46	9.6	0.0	-23.5	41.4
G. resinaceum	KC514812	W	17.2	15.07	16.5	13.08	25.4	72.55	25.4	0.0	-27.0	26.3
H. corrugata	KC514813	W	23.0	28.37	20.6	26.57	19.6	67.65	-1.9	0.0	29.1	47.9
Phlebia sp.	KC514819	W	18.4	30.95	17.6	27.41[a]	7.5	56.71	6.7	0.0	-26.3	48.3
P. tremellosa	KC514820	W	18.9	30.42	18.5	28.77[a]	15.0	74.80	0.0	0.0	14.2	62.4
P. subacida	KC514821	W	21.4	32.93[a]	19.5	25.77	12.5	49.55	0.0	0.0	26.6	45.7
Scytinostroma sp.	KC514822	W	13.1	56.26[a]	12.4	35.62[a]	34.1	73.67	3.8	0.0	-32.6	75.4[a]
S. brinkmanii	KC514823	?	12.6	14.99	11.6	12.31	1.4	70.23	13.3	0.0	-90.1	21.2
G. tsugae	KC514828	W	22.9	41.98[a]	17.1	28.85[a]	10.3	40.49	26.8	0.0	-33.6	38.2
I. dryophilus	KC589014	W	12.2	31.16	12.7	26.50	2.5	44.23	18.4	0.0	-89.3	47.3
I. lacteus	KC514829	W	15.6	20.90	76.4[a]	16.75	14.0	13.60	10.9	0.0	-84.0	21.5
P. pertenuis	KC514832	W	11.7	18.69	8.7	13.94	0.0	16.16	15.1	0.0	-97.4	38.3
P. brevispora	KC514833	W	21.2	46.61[a]	18.8	34.60	9.6	39.42	37.9	0.0	-86.6	43.0
P. chrysocreas	KC514834	W	21.0	29.80	6.1	23.95	0.0	35.70	658.4[a]	0.0	-80.6	34.2
P. arctostaphyli	KC589015	W	13.2	28.61	12.5	23.66	12.3	41.88	28.8	0.0	-90.5	36.1
P. pini	KC514836	W	11.2	21.15	11.4	16.94	4.8	39.88	11.6	0.0	-95.5	34.2
D. squalens	KC514837	W	21.1	35.07[a]	17.1	37.26	11.2	14.51	29.5	0.0	-32.4	29.2
G. lucidum	KC514839	W	18.7	27.81	16.5	20.95	24.0	40.60	14.2	0.0	-75.7	34.3
S. hirsutum	KC514824	W	23.4[a]	43.58[a]	17.5	32.02	13.4	38.22	5.6	0.0	-32.4	42.6
Xylariaceae sp.	KC514841	W	15.3	12.84	13.8	11.90	0.3	42.47	11.2	0.0	-86.6	24.7

[a] indicates significantly greater mass loss than corresponding control (Dunnett's multiple comparison, family error rate = 0.05)

Table S4.3 Mean monosaccharide yields (standard error) after enzymatic hydrolysis of follow-up study samples. Yields are based on original content.

		Aspen						Corn Stalk						Pine					
	Weeks	Mass loss (%)	Glucose (%)	Xylose (%)	Galactose (%)	Arabinose (%)	Mannose (%)	Mass loss (%)	Glucose (%)	Xylose (%)	Galactose (%)	Arabinose (%)	Mannose (%)	Mass loss (%)	Glucose (%)	Xylose (%)	Galactose (%)	Arabinose (%)	Mannose (%)
Control	2	0.26	5.31	4.64	0.00	11.24	7.20	7.36	29.99	12.84	0.00	8.37	30.32	0.32	4.13	3.73	7.39	6.15	2.74
		(0.08)	(0.59)	(0.47)	(0.00)	(2.21)	(0.88)	(4.28)	(4.18)	(0.62)	(0.00)	(0.31)	(17.00)	(0.03)	(0.06)	(0.25)	(0.41)	(0.54)	(0.15)
	3	0.01	6.11	5.17	5.44	0.00	13.70	4.61	35.48	14.03	0.00	15.14	30.34	0.12	4.27	4.02	11.17	6.67	2.72
		(0.04)	(0.46)	(0.40)	(5.44)	(0.00)	(6.28)	(0.93)	(1.44)	(0.81)	(0.00)	(1.12)	(27.17)	(0.14)	(0.05)	(0.11)	(1.12)	(0.08)	(0.21)
	4	0.14	5.54	4.98	15.42	0.00	41.80	10.48	25.93	12.32	0.00	8.17	36.96	0.60	4.41	4.37	9.01	2.31	3.30
		(0.11)	(0.13)	(0.17)	(2.93)	(0.00)	(4.07)	(3.32)	(2.49)	(2.24)	(0.00)	(1.63)	(7.98)	(0.41)	(0.39)	(0.27)	(0.87)	(1.16)	(0.73)
Scytinostroma sp. (B360)	2	2.74	24.08	18.65	0.00	6.86	16.82	6.95	20.76	8.87	0.00	4.35	83.87	-1.05	6.47	9.67	10.95	5.11	3.57
		(1.73)	(4.17)	(3.26)	(0.00)	(6.86)	(2.53)	(1.95)	(2.62)	(1.93)	(0.00)	(0.49)	(26.11)	(0.36)	(0.19)	(0.66)	(0.87)	(0.35)	(0.37)
	3	8.81	24.33	18.36	4.98	0.00	15.95	14.70	19.43	6.34	0.00	3.10	25.81	ND	ND	ND	ND	ND	ND
		(1.03)	(3.06)	(1.59)	(4.98)	(0.00)	(2.47)	(0.52)	(2.08)	(0.88)	(0.00)	(0.53)	(16.83)	ND	ND	ND	ND	ND	ND
	4	17.87	12.24	10.15	17.92	0.00	14.63	18.93	11.63	6.79	0.00	2.53	22.84	4.56	12.50	11.32	8.94	0.00	7.41
		(0.41)	(2.30)	(1.85)	(2.76)	(0.00)	(3.67)	(2.38)	(2.34)	(1.11)	(0.00)	(0.19)	(6.68)	(0.89)	(1.70)	(1.27)	(0.30)	(0.00)	(0.70)
Scytinostroma sp. (3262)	2	4.01	11.06	9.58	0.00	2.67	10.38	16.82	8.02	4.56	0.00	2.93	62.36	0.52	4.24	4.33	5.94	3.65	2.47
		(0.83)	(1.43)	(1.06)	(0.00)	(2.67)	(1.31)	(2.33)	(1.04)	(0.39)	(0.00)	(0.49)	(36.41)	(0.07)	(0.58)	(0.01)	(0.62)	(0.21)	(0.21)
	3	13.80	11.09	9.64	9.14	0.00	9.27	24.28	4.64	3.65	0.00	2.05	4.04	1.23	7.09	7.29	7.62	4.91	4.26
		(1.67)	(0.84)	(0.55)	(4.60)	(0.00)	(0.44)	(2.41)	(0.40)	(0.90)	(0.00)	(0.53)	(0.72)	(0.28)	(0.25)	(0.33)	(0.76)	(0.37)	(0.31)
	4	16.85	13.21	10.99	15.61	0.00	8.75	23.75	8.57	6.67	0.00	3.81	25.65	1.16	8.18	8.69	9.08	0.00	5.75
		(0.93)	(2.21)	(1.67)	(1.27)	(0.00)	(1.97)	(2.77)	(0.33)	(1.01)	(0.00)	(0.59)	(7.37)	(0.38)	(0.35)	(0.22)	(0.64)	(0.00)	(1.16)
Scytinostroma sp. (B361)	2	5.39	16.93	13.67	0.00	0.00	12.61	10.77	20.74	7.27	0.00	4.55	52.04	0.62	7.30	8.19	8.87	4.99	3.12
		(2.03)	(2.11)	(1.35)	(0.00)	(0.00)	(0.75)	(1.95)	(2.38)	(1.34)	(0.00)	(1.62)	(28.05)	(0.86)	(1.04)	(0.99)	(1.17)	(0.73)	(0.62)
	3	15.06	17.79	14.59	4.03	0.00	12.04	19.91	17.80	10.82	0.00	4.28	7.95	2.78	12.00	11.63	8.07	4.28	5.80
		(0.57)	(1.84)	(1.45)	(4.03)	(0.00)	(0.76)	(2.31)	(2.94)	(2.39)	(0.00)	(0.78)	(4.46)	(0.29)	(1.00)	(1.24)	(0.20)	(0.38)	(0.32)
	4	18.53	21.23	17.38	15.71	0.00	12.83	27.91	16.03	8.87	0.00	2.80	8.65	7.21	12.75	10.99	8.18	0.00	7.60
		(1.91)	(2.34)	(1.91)	(1.93)	(0.00)	(1.87)	(2.39)	(5.23)	(1.31)	(0.00)	(0.65)	(2.33)	(1.34)	(2.14)	(1.52)	(0.75)	(0.00)	(1.71)
Corticiales sp.	2	-0.81	17.11	15.51	0.00	0.00	13.79	1.18	27.56	13.27	0.00	7.79	51.13	-0.68	4.63	6.77	9.26	5.52	3.30
		(0.20)	(0.55)	(0.51)	(0.00)	(0.00)	(0.97)	(1.54)	(2.84)	(0.73)	(0.00)	(0.51)	(25.69)	(0.49)	(0.56)	(1.24)	(1.22)	(0.32)	(0.56)
	3	0.50	25.26	22.67	4.80	3.59	16.79	6.08	27.85	14.16	0.00	7.04	4.47	0.00	6.29	7.20	9.16	6.87	4.11
		(0.22)	(1.44)	(1.12)	(4.80)	(3.59)	(0.34)	(2.73)	(3.64)	(1.57)	(0.00)	(0.59)	(2.41)	(0.35)	(0.36)	(0.70)	(0.64)	(0.32)	(0.21)
	4	1.83	40.90	35.73	15.74	0.00	24.98	9.14	33.29	17.01	0.00	5.72	4.36	-0.32	6.88	9.19	8.20	1.06	5.44
		(0.89)	(1.36)	(0.61)	(7.93)	(0.00)	(2.55)	(2.33)	(2.98)	(1.05)	(0.00)	(0.94)	(2.20)	(0.47)	(0.73)	(1.48)	(1.27)	(1.06)	(0.99)
P. brevispora	2	0.01	17.51	14.56	0.00	0.00	15.57	4.31	30.16	11.42	0.00	7.08	85.92	0.05	5.35	5.65	7.18	5.11	2.80
		(0.41)	(2.21)	(1.76)	(0.00)	(0.00)	(1.33)	(2.26)	(6.48)	(2.15)	(0.00)	(0.68)	(21.61)	(0.14)	(0.18)	(0.10)	(0.47)	(0.41)	(0.27)
	3	0.25	22.84	18.85	3.53	0.00	15.83	9.92	37.11	12.60	0.00	6.65	7.74	0.37	6.04	5.88	6.83	5.27	4.30
		(0.48)	(2.45)	(2.30)	(3.53)	(0.00)	(1.28)	(1.91)	(1.92)	(0.89)	(0.00)	(0.13)	(1.31)	(0.23)	(0.34)	(0.49)	(0.51)	(0.64)	(0.04)
	4	0.58	29.95	24.44	8.88	0.00	25.42	4.00	20.22	10.66	0.00	5.78	6.42	0.35	6.82	6.56	6.92	0.00	4.41
		(0.57)	(1.51)	(1.21)	(8.88)	(0.00)	(2.37)	(2.81)	(3.12)	(0.96)	(0.00)	(1.87)	(3.79)	(0.05)	(0.26)	(0.28)	(0.29)	(0.00)	(0.35)
G. trabeum	2	13.83	9.68	11.12	12.15	0.00	6.09	12.07	25.76	13.94	0.00	8.39	79.77	4.63	4.24	7.80	11.30	3.59	4.16
		(1.72)	(1.35)	(1.21)	(1.28)	(0.00)	(0.93)	(3.82)	(1.25)	(1.27)	(0.00)	(3.39)	(34.42)	(0.76)	(0.06)	(0.08)	(1.31)	(0.19)	(0.91)
	3	26.97	8.87	11.46	6.34	0.00	4.91	30.07	24.85	12.30	0.00	3.80	19.02	16.08	4.98	7.44	9.81	3.93	4.00
		(3.86)	(1.89)	(1.60)	(2.71)	(0.00)	(0.42)	(1.92)	(6.41)	(2.34)	(0.00)	(0.75)	(9.85)	(4.44)	(0.24)	(1.17)	(2.35)	(0.57)	(0.34)
	4	42.21	5.67	7.98	16.34	0.00	13.06	52.16	11.65	6.01	0.00	1.57	13.30	26.46	3.57	5.45	8.50	0.76	3.67
		(5.03)	(0.69)	(0.53)	(1.49)	(0.00)	(6.58)	(3.83)	(1.82)	(0.65)	(0.00)	(0.21)	(4.21)	(3.43)	(0.10)	(0.17)	(0.66)	(0.76)	(0.27)

Table S4.4 Mean monosaccharide yields (standard error) after the indicated follow-up study treatment, but without enzymatic hydrolysis. Yields are based on original content.

	Weeks	Aspen							Corn Stalk							Pine						
		Mass loss (%)	Glucose (%)	Xylose (%)	Galactose (%)	Arabinose (%)	Mannose (%)	Cellobiose (%)	Mass loss (%)	Glucose (%)	Xylose (%)	Galactose (%)	Arabinose (%)	Mannose (%)	Cellobiose (%)	Mass loss (%)	Glucose (%)	Xylose (%)	Galactose (%)	Arabinose (%)	Mannose (%)	Cellobiose (%)
Control	2	0.26	0.00	0.00	4.38	0.00	8.34	0.01	7.36	0.66	0.00	0.00	0.00	121.65	2.46	0.32	0.00	0.00	0.00	0.00	0.00	0.01
		(0.08)	(0.00)	(0.00)	(4.38)	(0.00)	(4.17)	(0.01)	(4.28)	(0.28)	(0.00)	(0.00)	(0.00)	(5.43)	(1.23)	(0.03)	(0.00)	(0.00)	(0.00)	(0.00)	(0.00)	(0.01)
	3	0.01	0.01	0.02	3.55	0.00	15.06	0.06	4.61	0.50	0.03	0.00	0.00	165.26	2.53	0.12	0.00	0.00	0.00	0.00	6.55	0.04
		(0.04)	(0.01)	(0.02)	(2.62)	(0.00)	(6.93)	(0.01)	(0.93)	(0.09)	(0.03)	(0.00)	(0.00)	(22.49)	(0.30)	(0.14)	(0.00)	(0.00)	(0.00)	(0.00)	(3.08)	(0.02)
	4	0.14	0.01	0.02	5.44	0.84	9.05	0.35	10.48	0.57	0.10	0.00	0.00	94.29	2.89	0.60	0.00	0.00	0.00	0.00	5.45	0.06
		(0.11)	(0.01)	(0.02)	(0.40)	(0.84)	(4.54)	(0.26)	(3.32)	(0.18)	(0.09)	(0.00)	(0.00)	(9.30)	(1.57)	(0.41)	(0.00)	(0.00)	(0.00)	(0.00)	(3.06)	(0.01)
Scytinostroma sp. (B360)	2	2.74	0.11	0.15	0.00	0.00	11.48	0.46	6.95	0.34	0.17	0.00	0.36	69.24	1.90	-1.05	0.07	0.93	0.00	0.00	2.74	0.26
		(1.73)	(0.05)	(0.08)	(0.00)	(0.00)	(1.80)	(0.07)	(1.95)	(0.10)	(0.03)	(0.00)	(0.16)	(26.34)	(0.76)	(0.36)	(0.03)	(0.32)	(0.00)	(0.00)	(1.11)	(0.03)
	3	8.81	0.60	0.96	1.97	0.50	20.08	0.74	14.70	0.33	0.02	0.00	0.00	123.35	3.07	ND	ND	ND	ND	ND	ND	ND
		(1.03)	(0.19)	(0.30)	(1.97)	(0.50)	(3.80)	(0.02)	(0.52)	(0.08)	(0.02)	(0.00)	(0.00)	(29.71)	(0.60)	ND	ND	ND	ND	ND	ND	ND
	4	17.87	0.25	0.07	3.93	0.00	16.32	0.56	18.93	0.23	0.12	0.00	0.07	30.35	1.24	4.56	0.09	0.00	1.20	0.00	7.39	0.25
		(0.41)	(0.06)	(0.07)	(2.00)	(0.00)	(3.21)	(0.02)	(2.38)	(0.02)	(0.02)	(0.00)	(0.07)	(14.50)	(0.19)	(0.89)	(0.02)	(0.00)	(1.20)	(0.00)	(2.32)	(0.05)
Scytinostroma sp. (3262)	2	4.01	0.19	0.31	0.81	0.00	11.81	0.46	16.82	0.20	0.06	0.00	0.49	110.58	0.77	0.52	0.00	0.00	0.27	0.21	3.31	0.02
		(0.83)	(0.03)	(0.07)	(0.81)	(0.00)	(2.81)	(0.10)	(2.33)	(0.03)	(0.03)	(0.00)	(0.11)	(12.09)	(0.09)	(0.07)	(0.00)	(0.00)	(0.27)	(0.21)	(1.99)	(0.02)
	3	13.80	0.14	0.27	3.07	0.00	11.83	0.76	24.28	0.25	0.10	0.00	0.31	61.68	0.92	1.49	0.00	0.00	0.53	0.00	6.38	0.16
		(1.67)	(0.05)	(0.18)	(0.26)	(0.00)	(5.61)	(0.23)	(2.41)	(0.17)	(0.02)	(0.00)	(0.07)	(35.74)	(0.35)	(0.17)	(0.00)	(0.00)	(0.53)	(0.00)	(1.29)	(0.03)
	4	16.85	0.31	0.34	2.38	0.00	14.01	0.69	23.75	0.26	0.14	0.00	0.27	50.32	1.19	1.16	0.01	0.00	0.00	0.00	5.38	0.16
		(0.93)	(0.10)	(0.03)	(1.25)	(0.00)	(2.30)	(0.05)	(2.77)	(0.04)	(0.07)	(0.00)	(0.27)	(23.96)	(0.08)	(0.38)	(0.01)	(0.00)	(0.00)	(0.00)	(3.41)	(0.02)
Scytinostroma sp. (B361)	2	5.39	0.18	0.31	1.70	0.00	14.61	0.64	10.77	0.19	0.03	0.00	0.16	26.65	1.84	0.62	0.00	0.30	0.00	0.34	2.45	0.28
		(2.03)	(0.04)	(0.08)	(0.86)	(0.00)	(5.00)	(0.16)	(1.95)	(0.09)	(0.03)	(0.00)	(0.16)	(7.94)	(1.04)	(0.86)	(0.00)	(0.30)	(0.00)	(0.34)	(1.68)	(0.04)
	3	15.06	0.17	0.23	2.72	0.00	12.20	0.64	19.91	0.71	0.19	0.00	0.32	57.21	2.10	2.78	0.02	0.00	0.00	0.62	5.72	0.22
		(0.57)	(0.04)	(0.12)	(0.71)	(0.00)	(5.59)	(0.05)	(2.31)	(0.57)	(0.08)	(0.00)	(0.11)	(30.88)	(0.85)	(0.29)	(0.02)	(0.00)	(0.00)	(0.62)	(2.04)	(0.03)
	4	18.53	0.22	0.36	5.43	0.00	13.60	0.71	26.18	0.23	0.06	0.00	0.00	44.07	0.91	7.21	0.05	0.00	0.00	0.00	9.02	0.33
		(1.91)	(0.07)	(0.14)	(2.36)	(0.00)	(1.98)	(0.10)	(2.86)	(0.03)	(0.06)	(0.00)	(0.00)	(6.44)	(0.03)	(1.34)	(0.02)	(0.00)	(0.00)	(0.00)	(0.22)	(0.01)
Corticiales sp.	2	-0.81	0.09	0.21	0.58	0.00	8.42	0.13	1.18	0.73	0.05	0.00	0.63	84.98	0.89	-0.68	0.01	0.33	0.00	0.00	3.58	0.07
		(0.20)	(0.04)	(0.11)	(0.58)	(0.00)	(4.06)	(0.02)	(1.54)	(0.23)	(0.05)	(0.00)	(0.11)	(21.65)	(0.07)	(0.49)	(0.01)	(0.23)	(0.00)	(0.00)	(1.80)	(0.03)
	3	0.50	0.30	0.28	4.41	0.00	16.96	0.19	6.08	0.69	0.03	0.00	0.32	127.91	2.09	0.00	0.05	0.11	0.00	1.55	6.46	0.09
		(0.22)	(0.08)	(0.14)	(0.55)	(0.00)	(2.33)	(0.02)	(2.73)	(0.30)	(0.03)	(0.00)	(0.16)	(9.08)	(0.88)	(0.35)	(0.03)	(0.11)	(0.00)	(0.79)	(1.40)	(0.01)
	4	1.19	0.13	1.11	6.69	0.00	20.35	0.22	9.14	0.57	0.04	0.00	0.08	107.49	0.83	-0.32	0.02	0.29	0.00	0.00	3.96	0.08
		(1.07)	(0.06)	(0.23)	(3.97)	(0.00)	(2.02)	(0.00)	(2.33)	(0.22)	(0.04)	(0.00)	(0.08)	(13.07)	(0.20)	(0.47)	(0.02)	(0.29)	(0.00)	(0.00)	(3.23)	(0.01)
P. brevispora	2	0.01	0.00	0.00	0.00	0.00	6.94	0.15	4.31	0.62	0.00	0.00	0.16	98.08	4.63	0.05	0.00	0.10	0.00	0.00	1.01	0.03
		(0.41)	(0.00)	(0.00)	(0.00)	(0.00)	(4.91)	(0.02)	(2.26)	(0.27)	(0.00)	(0.00)	(0.09)	(19.41)	(1.99)	(0.14)	(0.00)	(0.10)	(0.00)	(0.00)	(1.01)	(0.01)
	3	0.25	0.06	0.04	3.33	0.00	12.95	0.30	9.92	0.59	0.01	0.00	0.19	100.04	2.33	0.37	0.00	0.00	0.00	0.00	11.81	0.10
		(0.48)	(0.03)	(0.04)	(1.68)	(0.00)	(1.90)	(0.05)	(1.91)	(0.12)	(0.01)	(0.00)	(0.19)	(23.88)	(0.83)	(0.23)	(0.00)	(0.00)	(0.00)	(0.00)	(0.64)	(0.01)
	4	0.58	0.10	0.03	3.84	2.33	14.31	0.24	4.00	0.27	0.10	0.00	0.40	48.88	0.74	0.35	0.00	0.00	1.62	0.00	5.43	0.12
		(0.57)	(0.02)	(0.03)	(2.11)	(2.33)	(5.50)	(0.01)	(2.81)	(0.05)	(0.10)	(0.00)	(0.25)	(11.19)	(0.14)	(0.05)	(0.00)	(0.00)	(1.62)	(0.00)	(3.40)	(0.01)
G. trabeum	2	13.83	0.17	0.35	2.35	0.00	10.60	0.27	12.07	0.27	0.27	0.00	0.83	1.05	0.39	4.63	0.00	0.00	0.00	3.33	1.94	0.05
		(1.72)	(0.03)	(0.10)	(2.35)	(0.00)	(2.18)	(0.03)	(3.82)	(0.14)	(0.13)	(0.00)	(0.42)	(1.05)	(0.11)	(0.76)	(0.00)	(0.00)	(0.00)	(3.33)	(1.57)	(0.03)
	3	26.97	0.22	0.17	0.74	0.00	8.90	0.50	30.07	0.41	0.23	0.00	0.38	83.39	0.60	16.08	0.09	0.00	0.00	0.34	6.69	0.35
		(3.86)	(0.05)	(0.06)	(0.74)	(0.00)	(3.67)	(0.05)	(1.92)	(0.05)	(0.04)	(0.00)	(0.09)	(29.42)	(0.04)	(4.44)	(0.06)	(0.00)	(0.00)	(0.34)	(0.74)	(0.16)
	4	42.21	0.28	0.20	3.00	0.00	11.76	0.48	52.16	0.51	0.24	0.00	0.00	103.51	0.84	26.46	0.78	0.00	0.43	0.52	5.55	0.26
		(5.03)	(0.09)	(0.03)	(2.01)	(0.00)	(2.64)	(0.10)	(3.83)	(0.30)	(0.13)	(0.00)	(0.00)	(34.93)	(0.20)	(3.43)	(0.63)	(0.00)	(0.43)	(0.52)	(1.90)	(0.01)

Chapter 5

Using a grass substrate to compare decay among two clades of brown rot fungi

5.1 Introduction

Though more often studied for their role in carbon cycling (Gilbertson and Ryvarden 1988) and as a major cause of structural lumber damage (Zabel and Morrell 1992), wood-degrading fungi metabolize lignocellulose and are thus natural models of bioconversion. Like chemical pretreatment, wood-degrading fungi alter the structure of lignocellulose to improve access to cell wall polysaccharides. While white rot is often studied in bioconversion for its ability to selectively remove lignin (Hatakka, 1983), understanding the brown rot mechanism would offer unique opportunities from a bioconversion perspective. Brown rot fungi preferentially remove hemicellulose and cellulose from lignocellulose substrates, leaving behind a lignin-rich residue (Cowling, 1961). The ability to access cell wall polysaccharides in the presence of lignin provides an example of how lignin, a component of lignocellulose that is associated with recalcitrance, can be circumvented.

Recognizing this characteristic of brown rot, a number of more recent studies have considered these fungi for biological pretreatment (Tewalt and Schilling 2010; Ray et al. 2010; Monrroy et al. 2011; Vaidya and Singh 2012; Gao et al. 2012) and have generally shown a 3-5 fold improvement in saccharification yield with pretreatment. Ray et al. (2010) have claimed a cellulose-to-glucose yield of nearly 70% by treating *Pinus*

sylvestris blocks with *Coniophora puteana* for 20 days, showing that brown rot pretreatment can approach the target of 80% deemed relevant for commercial use (Saha and Woodward 1997).

Current theory holds that brown rot fungi induce early stage decay through Fenton oxidation (Goodell et al. 1997; Kerem et al. 1999; Eastwood et al. 2011). As proposed, this reaction involves iron reduction and in situ hydrogen peroxide production via extracellular catechol and hydroquinone metabolites. This proposed mechanism can potentially be mimicked, optimized, and accelerated in the absence of the organism, eliminating sugar losses associated with direct biological pretreatment and making feedstock turnover rates commercially viable.

Postia placenta and *Gloeophyllum trabeum* are two brown rot fungi that have been considered for biological pretreatment. They are often studied due to their role in the decay of in-service lumber and history as research models, and the genomes of both species have been sequenced and annotated (Martinez et al. 2009; Floudas et al. 2012). While both produce brown rot, these fungi reside in separate phylogenetic clades, with *P. placenta* in the *Antrodia* clade and *G. trabeum* in the *Gloeophyllum* clade (Hibbett and Donoghue 2001). In total, there are at least seven clades of brown rot fungi, all of which independently evolved from white rot ancestors (Hibbett and Donoghue 2001).

In a recent study by Schilling et al. (2012) that considered the impact of brown rot-induced compositional changes on saccharification potential, it was suggested that these two brown rot fungi differ in their ability to degrade milled corn stover, a major cellulosic biofuel feedstock. Exposure to *P. placenta* resulted in only minor arabinan loss

over the course of 16 weeks, while *G. trabeum* caused substantial loss of all polysaccharide monomers. However, weight loss was not quantified given the difficulty of separating hyphal mass from milled substrate mass, and the linear carbohydrate losses induced by *G. trabeum* on this grass species, as opposed to wood, meant a simultaneous loss of components could not be ruled out for *P. placenta*. Although there are examples (Han et al., 2012) where *P. placenta* has been used in tandem with *G. trabeum* to degrade a grass species, these trials have been to test durability of pellets or composite boards, using a single *P. placenta* isolate and focusing measurements on durability and strength. This study was designed to determine the ability for *P. placenta* and others in its *Antrodia* clade to degrade corn stalk as a representative *Poales* grass. The goal was to determine grass decay potential as a trait among this group, relative to *G. trabeum* from the *Gloeophyllum* clade. In addition to weight loss measures made possible by using the solid stover component (stalk), chemical composition analyses were used to determine if observed weight loss differences correlate with differences in the progression of component loss.

5.2 Material and Methods

5.2.1 Substrate preparation

Corn stalks were collected from a University of Minnesota research field (St. Paul, MN) in August of 2011. Corn stalk was selected as the representative grass as agricultural residues like corn stover would represent a large portion of lignocellulosic feedstock in a bio-based economy (US DOE et. al 2011). The seed from which these stalks were grown was collected from commercial farms across Minnesota to represent

the state crop. The stalks were dried at 65°C for 4 days before removing the cobs and leaves. The internodes from the remaining stems were cut to a length of 43 mm. Stalk nodes were discarded and the remaining pieces were stored indoors at ambient conditions (25°C).

Aspen blocks were used as a positive control. Although brown rot is most often associated with softwoods, aspen was selected as it has a lignin and hemicellulose composition that is more comparable to corn stalk (Sarker et al., 2009). 19 mm^3 blocks were cut from a single untreated board. Prior to use, aspen blocks and corn stalk pieces were weighed after drying at 100°C for 48 hours. Blocks (n = 16) weighed 2.76 g on average (95% CI [2.74, 2.79]) and stalk pieces (n = 76) averaged 1.07 g (95% CI [1.06, 1.09]). Prior to sterile introduction into culture dishes, all substrates were autoclaved at 121°C and 110 kPa for 1 h.

5.2.2 Cultures

Isolates were acquired from American Type Culture Collection (ATCC, Manassas, VA, USA) or the USDA Forest Products Laboratory (FPL, Madison, WI, USA), both publicly-accessible culture collections. Isolates used included *Postia balsamea* (FPL, L-15445-Sp), *Postia caesia* (FPL, L-14308-T), *Postia fragilis* (FPL, FP-71321-T), *Postia guttulata* (FPL, L-8050-Sp), *Postia stiptica* (FPL, L-3378-R), *Postia undosa* (FPL, UBA-2024-T), *P. placenta* (FPL, MAD-698), *G. trabeum* (ATCC, 11539), and *Fomitopsis pinicola* (FPL, FP-105877-R). *G. trabeum* was included as previous work indicated that it extensively degrades corn stover in a similar microcosm setup (Schilling et al., 2012). *P. stiptica* and *P. undosa* exhibited limited growth on both

substrates and were excluded from further analysis. The species selected are typically found on dead conifer trees, but have occasionally been found on deciduous species. Exceptions are *P. balsamea*, which is most often found on living conifers and *G. trabeum*, which is commonly found on deciduous trees. *P. placenta* and *G. trabeum* are also commonly cause decay in structural timbers (Gilbertson and Ryvarden, 1988). Each isolate was freshly grown on 2% malt extract agar (MEA) plates for two weeks to ensure actively growing hyphae were used for treatment plate inoculation. Treatment plates were prepared as described in the standard durability test EN-113 (1996). Each treatment plate contained 20 ml of water agar and was inoculated with one centrally placed 7 mm diameter agar plug taken from the MEA medium. A sterilized 7 mm X 7 mm mesh high density polyethylene screen (Amerimax Home Products, Lancaster, PA, USA) cut to fit the entirety of the plate was added to keep the substrate from direct agar contact.

5.2.3 Treatment

Each sterilized substrate was placed in its own treatment plate and incubated at 25°C and 70% RH. After 12 weeks, all substrates were harvested and oven-dried at 100°C for 48 hours prior to measuring post-treatment weight. Comparison of weight loss in corn stalk samples with both the aspen controls and the untreated corn stalk controls were made with two sample t-test comparisons using the statistics program Minitab (v. 16.2.3, Minitab Inc., State College, PA, USA). Due to the relatively large weight loss in the corn stalk controls, comparisons between weight loss in treated corn stalk and aspen were made relative to the control. For aspen, it was assumed that no weight loss occurred

on untreated samples. This assumption was made based on the previous observation that untreated aspen weight loss on an agar plate set-up is negligible (Schilling and Norcutt 2010). Excepting untreated controls (n=4), seven replicates were used for all corn stalk treatment sets. Knowing that *P. placenta* and *G. trabeum* are effective degraders of aspen (Schilling et al. 2012), only one replicate was used for all aspen treatments, except the *P. placenta* treatment (n=7), as an indicator of fungal isolate viability under plate conditions.

5.2.4 Characterization

The chemical composition of the treated substrates, including ash, ethanol extractives, lignin, glucan, xylan, galactan, arabinan, and mannan content, was determined in duplicate in accordance with the National Renewable Energy Laboratory (NREL) summative mass closure procedure (Sluiter and Sluiter 2010). Samples with like treatments were pooled and ground to 40 mesh. Untreated aspen and corn stalk were similarly ground and characterized.

Ash content was determined as described by Sluiter et al. (2005). Due to the sensitivity of the crucibles to moisture absorption, final ash mass was determined from the difference in the crucible weight before and after removing the ash from it, rather than determining and subtracting the oven dry mass of the crucible. Reported values are the average of duplicate measurements.

Extractives content was determined as described by Sluiter et al. (2008a). The solvent used was 95% ethanol and extraction time was 16 hours. In lieu of a vacuum oven, flasks were dried before and after extraction at 100°C for 24 hours in a convection

oven. Water extractives were not measured. Extractives content is reported as the average of duplicate measurements.

Lignin content and structural sugar concentrations were determined as described by Sluiter et al. (2008b), with the exception that the sugar recovery standard solution was split so that only half was autoclaved. The portion that was not autoclaved was prepared for high performance liquid chromatography (HPLC) like the autoclaved samples. Rather than calculating the sugar recovery correction factor based on the prepared sugar concentration, it was calculated based on the ratio in the sugar peak area of the autoclaved and un-autoclaved sugar recovery standard solution. In determining the concentration of acid-soluble lignin, light absorption was measured at 320 nm for corn stalk samples and 240 nm for aspen. Extinction coefficients of 30 and 25 were used for corn stalk and aspen samples, respectively.

The percent dilute alkali solubility (DAS) of initial and treated corn stalk and aspen samples was determined on ethanol extractive-free samples as previously described by Shortle et al. (2010). It has been observed that brown rot increases the DAS of wood due to carbohydrate depolymerization (Cowling 1961). Thus, this method was employed to give insight into the extent of carbohydrate depolymerization induced by brown rot regardless of observed weight loss.

5.2.5 Meta-analysis

A meta-analysis using synthesized data compiled from various previous studies was added as a complement to the empirical testing. No past studies have been geared to test inefficiency in *Antrodia*-clade fungi on grass substrates, but there are studies that

have 1) compared *Antrodia*-clade isolates, particularly *P. placenta*, against *G. trabeum*, using paired microcosms with woody substrates (Eslyn and Highley 1976; Highley 1978; Worrall et al. 1997; DeGroot et al. 1998; Clausen et al. 2000; Kelley et al. 2002; Kamdem et al. 2002; Schilling et al. 2012) or 2) included some form of *Poales*-based substrate with an *Antrodia*-clade fungus for a distinct but unrelated reason (Martin and Dale 1980; Antai and Crawford 1982; Arora 1995; Troya et al. 2009; Suprapti 2010; Salvachúa et al. 2011; Schmidt et al. 2011; Han et al. 2012; Schilling et al. 2012). Using these two criteria, a total of 17 different studies were compared, accounting for substrate quality (eg, solid-state powders versus whole blocks), conditions (agar versus soil-block microcosms), and duration, and using rate of weight loss (oven-dried basis) as the standard for comparison to eliminate the bias of duration. Because the only *Antrodia*-clade fungus in studies meeting these criteria was *P. placenta*, and because so few studies compare *G. trabeum* with *P. placenta* on grass substrates directly, weight loss averages among substrates and across studies was compared rather than averaging per-study differences.

5.3 Results

5.3.1 Weight Loss

Untreated corn stalk controls exhibited an average weight loss of 13.8% (**Table 5.1**) with color in the plate media suggesting that extractives leaching occurred. In comparison with the control, corn stalk exposed to *P. placenta* ($P = 0.22$), *P. balsamea* ($P = 0.11$), and *P. fragilis* ($P = 0.55$) did not show significant mass loss. However, corn stalk exposed to *F. pinicola* ($P < 0.01$), *P. caesia* ($P = 0.03$), and *P. guttulata* ($P = 0.02$)

showed significantly greater loss than the control with values of 23.7%, 21.6%, and 26.8%, respectively. Total corn stalk weight loss when cultured with the *Antrodia*-clade fungi was significantly less ($P < 0.01$) than that with *G. trabeum* (58.3%). In relation to aspen, all *Antrodia*-clade fungi induced comparably lower corn stalk weight loss (**Figure 5.1**), suggesting that there was no significant difference ($P = 0.28$) in corn stalk assimilation ability among the tested members of this clade.

Table 5.1 Weight loss (SE), composition, and dilute alkali solubility of corn stalk samples. Composition results are expressed as percentage of initial.

	Mass loss	Adjusted % weight							DAS
Treatment	(%)	Ash	Ext	Lig	Glu	Xyl	Gal	Ara	(%)
	0.0	3.4	30.9	14.9	30.3	15.1	0.1	2.3	
Initial	(0.0)	(0.0)	(0.8)	(0.3)	(0.6)	(0.4)	(0.0)	(0.1)	56.4
		% of initial							
	58.2								
G. trabeum	(5.2)	ND	ND	ND	ND	ND	ND	ND	61.6
	26.8	96.5	21.1	100.7	82.1	80.9	0.0	33.1	
P. guttulata	(4.1)	(1.3)	(3.2)	(1.8)	(1.4)	(0.9)	(0.0)	(6.2)	57.2
	23.7	136.9	32.0	104.2	94.2	90.9	0.0	69.3	
F. pinicola	(1.6)	(1.3)	(1.7)	(2.2)	(3.1)	(2.0)	(0.0)	(8.6)	55.4
	21.6	111.9	25.1	105.5	93.5	91.6	0.0	43.7	
P. caesia	(2.6)	(1.0)	(0.2)	(3.5)	(1.8)	(3.0)	(0.0)	(7.1)	53.7
	20.0	111.8	24.3	132.4	90.8	67.5	0.0	44.6	
P. placenta	(4.4)	(6.1)	(1.5)	(0.1)	(1.3)	(0.4)	(0.0)	(5.2)	50.2
	19.2	97.6	26.6	103.5	93.6	92.3	0.0	55.9	
P. balsamea	(2.9)	(0.6)	(0.5)	(2.8)	(3.0)	(0.6)	(0.0)	(6.5)	53.5
	16.0	109.2	34.5	135.5	89.8	62.8	0.0	43.1	
P. fragilis	(3.3)	(9.4)	(2.0)	(2.1)	(0.6)	(0.1)	(0.0)	(3.0)	56.8
	13.8	117.6	31.4	135.6	97.7	100.7	0.0	95.7	
Control[a]	(1.3)	(9.3)	(2.5)	(0.7)	(0.1)	(1.2)	(0.0)	(6.7)	60.2

[a] kept in inoculum free agar plates for 12 weeks

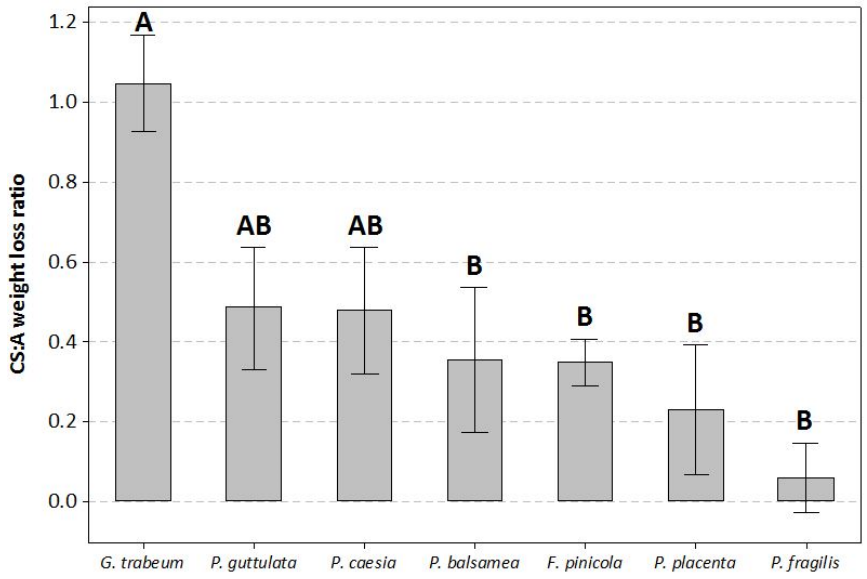

Figure 5.1 Ratio of corn stalk to aspen weight loss for all fungal treatments. Corn stalk weight loss was adjusted to account for weight loss observed in the negative control due to leaching. Values marked with the same letter are not significantly different (Tukey's HSD, $\alpha = 0.05$). Error bars represent 1 standard error (SE), n = 7

Aspen weight loss caused by the *Antrodia* fungi ranged from 15.8% to 37.5% (**Table 5.2**). In comparison, *G. trabeum*-induced aspen weight loss was 42.5%, only slightly more than the greatest *Antrodia* clade-induced weight loss. After adjusting for extractive loss, all *Antrodia*-clade fungi induced significantly ($P < 0.05$) greater weight loss on aspen than corn stalk. *G. trabeum* caused comparable weight loss in both substrates. While the mean ratio of corn stalk to aspen weight loss was 1.05 for *G. trabeum*, this ratio was less than 0.5 for all *Antrodia*-clade fungi (**Figure 5.1**). The mean weight loss ratio for *G. trabeum* was significantly higher ($P < 0.05$) than four of the six *Antrodia*-clade fungi, including *P. placenta*. Furthermore, the corn stalk:aspen weight loss ratio of the *Antrodia*-clade fungi tended to decrease with increasing aspen weight loss.

It was noted that heavily degraded corn stalk, i.e. those degraded by *G. trabeum*, exhibited heterogeneous decay. While the corn stalk pith was mostly removed, the rind remained largely intact. Heavy corn stalk degradation also resulted in the separation of the pith from the rind.

5.3.2 Composition

Initial substrate compositions were typical of their respective biomass type, with corn stalk containing higher ash, extractive, and arabinan content and aspen containing more mannan (**Table 5.1** and **Table 5.2**). Decayed corn stalk compositions demonstrated that most of the weight loss associated with treatment was due to the loss of extractives, reducing the assumed weight-loss contributions due to carbohydrate or lignin loss. This is in contrast with aspen, which exhibited an increase in extractives content as decay progressed (**Table 5.2**).

Table 5.2 Mass loss, composition (SE) and dilute alkali solubility of aspen samples. Composition results are expressed as percentage of initial content.

		Adjusted Mass (%)								
Treatment	Mass loss (%)	Ash	Ext	Lig	Glu	Xyl	Gal	Ara	Man	% DAS
Initial	0.0	0.2 (0.0)	3.0 (0.5)	20.4 (0.1)	44.2 (1.3)	15.8 (0.3)	0.5 (0.0)	0.4 (0.0)	2.8 (0.1)	18.6
		% of initial								
G. trabeum	42.5	30.3 (2.1)	246.9 (6.2)	60.0 (0.4)	28.9 (2.7)	29.1 (1.0)	0.0 (0.0)	79.1 (2.4)	0.0 (0.0)	70.0
P. fragilis	37.5	63.9 (4.2)	194.8 (3.9)	67.7 (5.8)	28.3 (0.5)	35.9 (0.8)	10.8 (5.7)	0.0 (0.0)	11.2 (1.8)	70.0
F. pinicola	28.5	159.4 (24.9)	339.8 (7.5)	73.5 (6.5)	63.0 (4.1)	43.3 (1.4)	2.1 (0.8)	44 .0 (6.8)	8.9 (1.7)	59.7
P. guttulata	26.8	34.8 (1.0)	128.6 (1.8)	89.8 (0.4)	62.8 (3.9)	44.9 (5.7)	0.0 (0.0)	0.0 (0.0)	13.1 (3.8)	66.4
P. placenta	25.1	36.5 (0.0)	154.2 (5.0)	91.6 (0.5)	72.3 (0.3)	69.1 (1.1)	2.1 (2.6)	0.0 (0.0)	27.6 (1.5)	50.2

P. caesia	16.4	77.2 (1.2)	100.0 (6.0)	96.8 (0.4)	86.4 (3.1)	58.9 (0.7)	0.0 (0.0)	29.5 (3.5)	34.2 (4.2)	58.9
P. balsamea	15.8	320 (4.5)	168.6 (3.7)	89.8 (5.6)	87.5 (3.0)	59.1 (0.1)	2.3 (2.6)	71.7 (4.5)	34.4 (2.6)	59.1

For each substrate, compositional changes with weight loss followed the same trend for all tested fungi (**Figure 5.2** and **Figure 5.3**). After accounting for the rapid initial weight loss associated with extractives leaching, corn stalk component loss was linear with weight loss with R^2 values of 0.78, 0.77, 0.64, and 0.44 for arabinan, xylan, glucan, and lignin, respectively. In aspen, glucan and lignin loss followed a sigmoidal trend with weight loss while xylan and mannan loss was exponential (Fig. 3). Linear functions, however, reasonably represented the trends in aspen component loss with R^2 values ranging from 0.73 to 0.86 and were used for comparing component loss rates. Since all *Antrodia*-clade fungi followed the same trend, these results were grouped when compared with *G. trabeum*.

Decayed corn stalk samples exhibited little change in lignin content over the course of decay (**Figure 5.2**). In contrast, brown rot of aspen resulted in upwards of 40% lignin loss (**Figure 5.3**). Extensive lignin loss occurred with both *Antrodia*-clade fungi and *G. trabeum* treated aspen. No difference in the progression of component loss between fungal clades was observed (**Figure 5.4**). Without sufficient material for compositional analysis from *G. trabeum* decay, this comparison could not be made with corn stalk.

Between aspen and corn stalk, there were similarities and differences in the rate of component loss (**Figure 5.5**). Loss of hemicellulose components was generally faster than cellulose loss, which in turn was lost faster than lignin. The rate of arabinan loss in

corn stalk was comparable to the rate of mannan loss in aspen, but glucan and xylan losses were greater in aspen than in corn stalk.

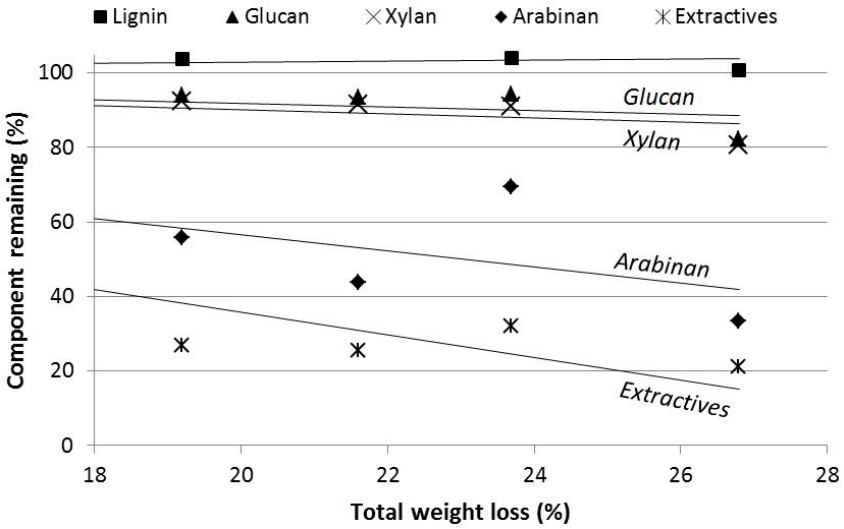

Figure 5.2 Corn stalk component remaining with brown rot induced weight loss. The amount of component remaining is expressed as a percentage of the initial content. Data are fit to a linear trend. All treatments but *G. trabeum* are included.

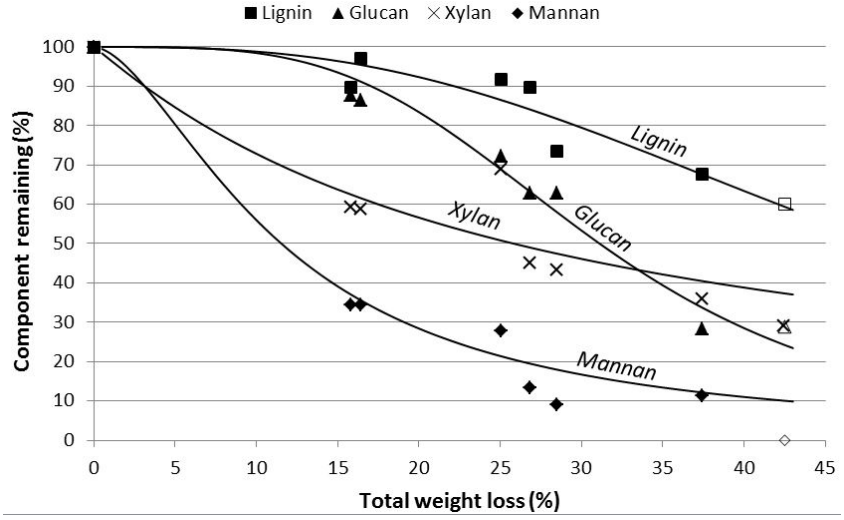

Figure 5.3 Aspen component remaining with brown rot-induced weight loss. The amount of component remaining is expressed as a percentage of the initial content. Data were fit to a loglogistic trend. Filled data points represent Antrodia-clade fungi, while unfilled represent *G. trabeum.*

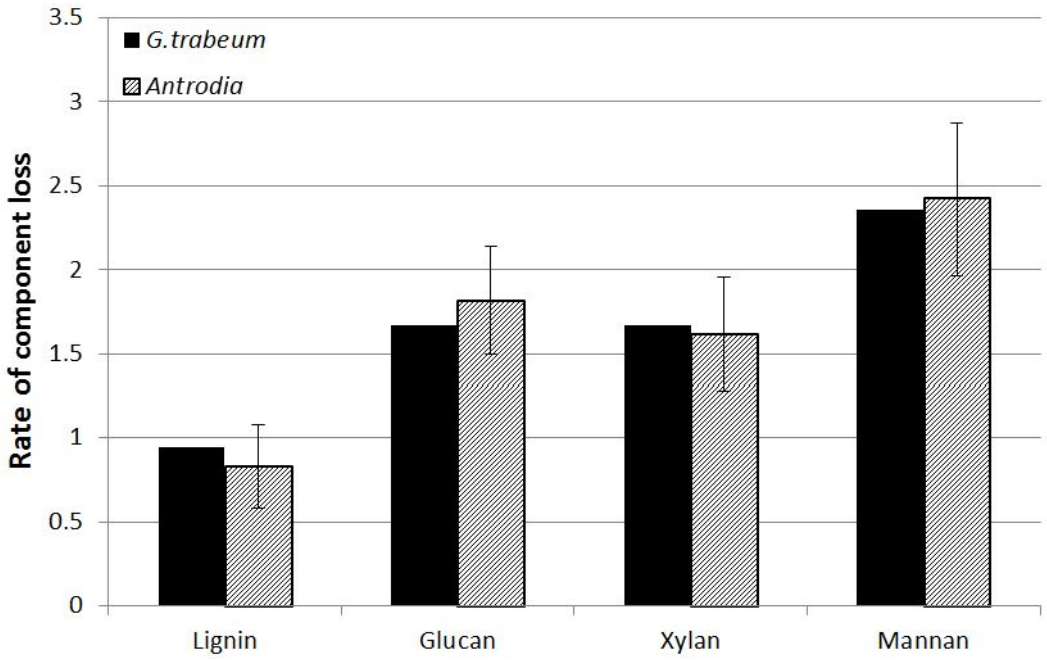

Figure 5.4 Mass loss-dependent rate of aspen component loss induced by *G. trabeum* and *Antrodia* fungi. Rate of component loss is defined as the % of initial component lost divided by the total % weight loss. Error bars represent SE, n = 7.

The extract-free DAS of aspen generally increased with weight loss, going from the initial 18.6% to 70.0% at 37.5% weight loss (**Table 5.2**). Untreated extract-free corn stalk had a comparatively high initial DAS (56.4%) that did not greatly change with weight loss, increasing to 61.6% with extensive weight loss. Aspen DAS correlated strongly with xylan ($R^2 = 0.90$) and mannan ($R^2 = 0.80$) concentrations and, to a lesser extent, with lignin content ($R^2 = 0.65$). Due to the relatively high time-zero DAS value for corn stalk, there was insufficient resolution in the DAS to relate it to polysaccharide depolymerization.

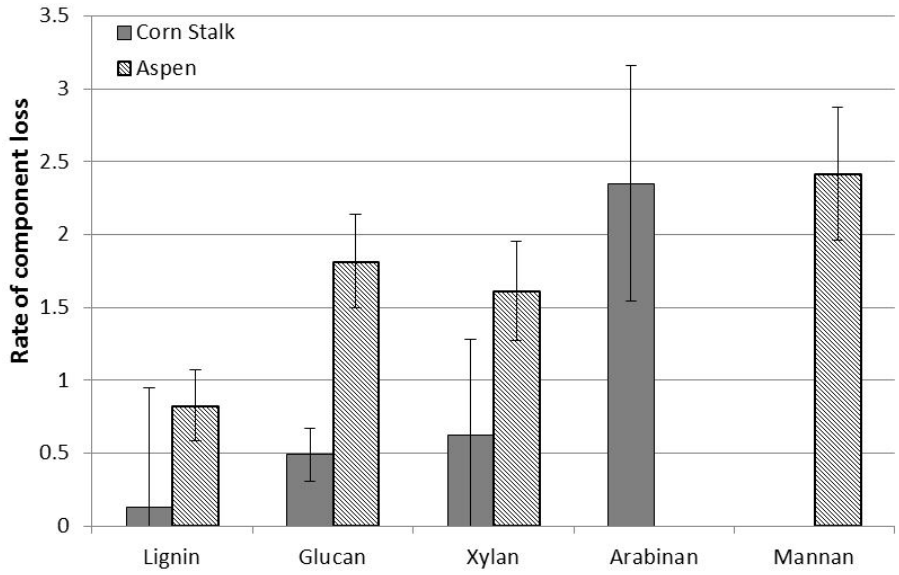

Figure 5.5 Mass loss-dependent rate of aspen and corn stalk component loss induced by *Antrodia*-clade fungi. Rate of component loss is defined as the % of initial component lost divided by the total % weight loss. Error bars represent SE, n = 7.

5.3.3 Meta-analysis

Table 5.3 and **Figure 5.6** summarize and compare the weight loss results of 17 studies that used *G. trabeum* or *P. placenta* to treat hardwoods, softwoods, or *Poales* grasses including corn stover, turf grasses, quackgrass, wheat straw, bamboo, and reed. Comparison of the weight loss rates across substrate type suggests that *G. trabeum* and *P. placenta* induce comparable weight loss in both softwoods ($P = 0.41$) and hardwoods ($P = 0.93$). These meta-data assert that *G. trabeum* caused significantly ($P < 0.01$) less weight loss on grass substrates than on wood. This differs from our empirical results and suggests a caveat when using stover as representative of all grasses, but may also reflect the lack of direct comparative data. Meta-data comparisons between the fungi, however, affirm that *P. placenta* has caused significantly ($P < 0.01$) less weight loss than *G. trabeum* on grass substrates used in these various study configurations.

Table 5.3 Literature review of weight loss caused by *G. trabeum* and *P. placenta* on various substrates

	Substrate	Substrate dimensions	Conditions[e]	Mass loss		Reference
				P. placenta	*G. trabeum*	
Softwoods	*Picea sp.*	19 mm^3	S, 16 wks	36.5	53.6	Schilling et al. (2012)
	Pinus sp.	0.94 X 2.54^2 cm	A, 12 wks	30	23	Eslyn and Highley (1976)
	Pinus sp.	19 mm^3	S, 12 wks	52.18	42.46	Clausen et al. (2000)
	Pinus contorta	9 X 25^2 mm	S, 12 wks	62	68	Highley (1978)
	Pinus ponderosa	9 X 25^2 mm	S, 12 wks	60	60	Highley (1978)
	Pinus resinosa	9 X 25^2 mm	S, 12 wks	57	69	Highley (1978)
	Pinus sp.	9 X 25^2 mm	S, 12 wks	51	55	Highley (1978)
	Pinus monticola	9 X 25^2 mm	S, 12 wks	63	68	Highley (1978)
	Pinus resinosa	10 mm^3	S, 12 wks	51.7	60.3	DeGroot et al. (1998)
	Pinus contorta	10 mm^3	S, 12 wks	43.6	50.7	DeGroot et al. (1998)
	Pseudotsuga menziesii	10 mm^3	S, 12 wks	50.1	50.7	DeGroot et al. (1998)
	Tsuga heterophylla	10 mm^3	S, 12 wks	40.5	34.9	DeGroot et al. (1998)
	Pinus sp.	20 X 10 X 5 mm	S, 12 wks	55.8	59.8	Worrall et al. (1997)
	Picea rubens	26 X 26 X 13 mm	S, 32 wks	54.6	70.7	Kelley et al. (2002)
	Pinus sp.	19 mm^3	S, 12 wks	54	57	Kamdem et al. (2002)
	Pinus sp.	19 mm^3	A, 8 wks	55	47	Kamdem et al. (2002)
	Average			**51.1**	**54.4**	
Woody dicots	*Populus sp.*	19 mm^3	S, 16 wks	34.2	57.9	Schilling et al. (2012)
	Populus balsamifera	9 X 25^2 mm	S, 12 wks	62	62	Highley (1978)
	Liquidambar sp.	9 X 25^2 mm	S, 12 wks	67	42	Highley (1978)
	Betula alleghaniensis	20 X 10 X 5 mm	S, 12 wks	68.8	57.5	Worrall et al. (1997)
	Populus sp.	10 mm^3	S, 12 wks	41.1	73.9	DeGroot et al. (1998)
	Liquidambar sp.	10 mm^3	S, 12 wks	43.8	42.5	DeGroot et al. (1998)
	Quercus rubra	10 mm^3	S, 12 wks	33.7	42.1	DeGroot et al. (1998)
	Liriodendron tulipifera	10 mm^3	S, 12 wks	55.1	38.5	DeGroot et al. (1998)
	Acer saccharum	10 mm^3	S, 12 wks	42.1	53.6	DeGroot et al. (1998)
	Acer rubrum	10 mm^3	S, 12 wks	45.9	37.2	DeGroot et al. (1998)
	Populus balsamifera	0.94 X 2.54^2 cm	A, 12 wks	49	30	Eslyn and Highley (1976)
	Average			**49.3**	**48.8**	

***Poales* grasses**	*Cynodon dactylon*	1 g oven-dried pellets	S, 90 days	18.8[b]	34.4[b]	Martin and Dale (1980)
	Stenotaphrum secundatum	1 g oven-dried pellets	S, 90 days	4.9[b]	26.5[b]	Martin and Dale (1980)
	Zoysia sp.	1 g oven-dried pellets	S, 90 days	-	36.8[b]	Martin and Dale (1980)
	Zea mays stover	1 g of 40 mesh powder	S, 16 wks	none[a]	extensive[a]	Schilling et al. (2012)
	Elymus repens	500 mg	SS, 12 wks	12.1	-	Antai and Crawford (1982)
	Triticum sp. straw	2 g of 0.5 - 2 cm fibers	SS, 30 days	1.5	-	Arora (1995)
	Triticum sp. straw	2 g chopped (< 1 cm)	SS, 21 days	3[c]	-	Salvachúa et al. (2011)
	Triticum sp. straw board	25 X 16 X 3 mm	S, 12 wks (*G.trabeum*) A,12 wks (*P. placenta*)	6.2	56.3	Han et al. (2012)
	Bambusa vulgaris board	0.95 X 2.5 cm^2	S, 12 wks	-	20.46	Stangerlin et al. (2011)
	Bambusa vulgaris	5 X 2.5 X 0.5-3.5 cm	A, 12 wks	3.8[d]	-	Suprapti (2010)
	Dendrocalamus asper	5 X 2.5 X 0.5-3.5 cm	A, 12 wks	5.2 [d]	-	Suprapti (2010)
	Gigantochloa apus	5 X 2.5 X 0.5-3.5 cm	A, 12 wks	7.0 [d]	-	Suprapti (2010)
	G. atroviolacea	5 X 2.5 X 0.5-3.5 cm	A, 12 wks	5.1 [d]	-	Suprapti (2010)
	G. pseudoarundinacea	5 X 2.5 X 0.5-3.5 cm	A, 12 wks	9.0 [d]	-	Suprapti (2010)
	Bambusa maculata	3 X 1 cm^2	A, 52 wks	-	1.9	Schmidt et al. (2011)
	G. atroviolacea	3 X 1 cm^2	A, 52 wks	-	5.7	Schmidt et al. (2011)
	Phyllostachys pubescens	3 X 1 cm^2	A, 52 wks	-	5.3	Schmidt et al. (2011)
	Melocanna bambusoides	5 X 2 cm^2	A, 52 wks	6.8	-	Schmidt et al. (2011)
	Phragmites communis	5 X 2.5 X 1.5 cm bundle	S, 16 wks	1.41	14.45	Troya et al. (2009)
	Average			**6.5**	**22.4**	

[a] Extent of weight loss is inferred based on characterization since the use of powder did not allow for weight loss measurements. [b] Control weight loss subtracted from total weight loss. [c] Calculated from loss in chemical components. [d] Average of tests on top, middle, and bottom portions. [e] S = soil, SS = solid-state, A = agar

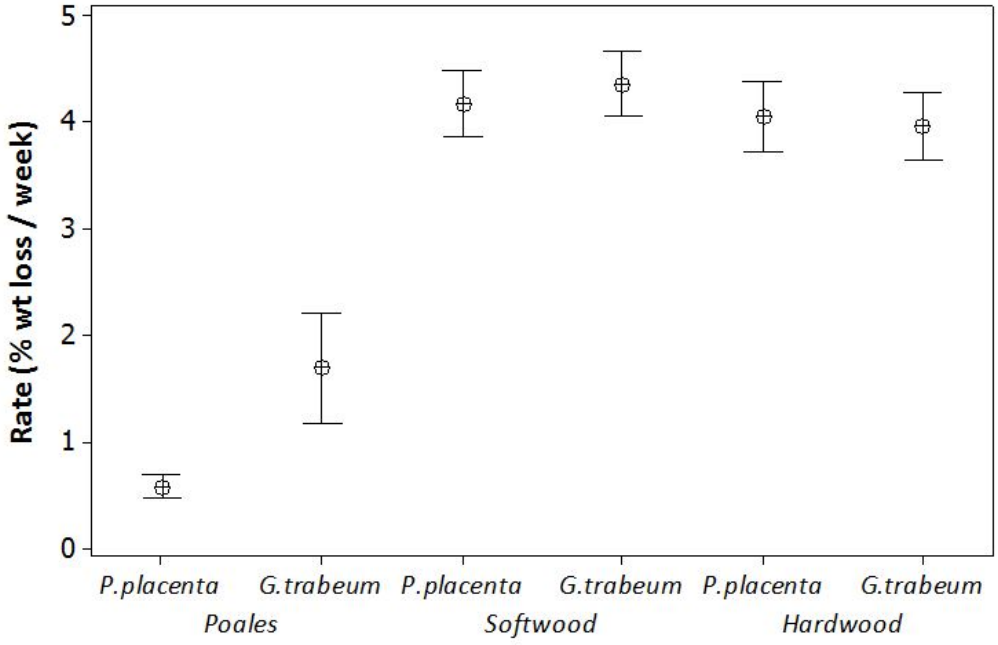

Figure 5.6 Summary of literature weight loss rates calculated from the data listed in table 3. Error bars represent SE. n = 16 for both fungi on softwood. n = 11 for both fungi on hardwood. n = 13 and n = 9 respectively for P. placenta and *G. trabeum* on *Poales*

5.4 Discussion

Supporting chemical data from previous observations on solid-state cultures (Schilling et al. 2012), *P. placenta* struggled to assimilate corn stalk, along with others in the *Antrodia* fungal clade not previously tested. Chemical composition analysis confirmed that most of the weight loss in corn stalk degraded by the *Antrodia*-clade fungi was due to the loss of extractives, generally higher in grasses than in woody biomass (Torget et al. 1990). Although filling of corn stalk void space with hyphal biomass could be assumed to lead to less apparent weight loss in corn stalk, the low degree of compositional change in corn stalk beyond extractives loss makes this unlikely. Brown

rot decomposition is characterized by selective removal of carbohydrates and subsequent increase in lignin composition (wt%), and in this case, lignin increases were insignificant. It is also unlikely that either growth rate or extractives toxicity explain this disparity in decay capacities. The ratio of corn stalk:aspen weight loss corroborates a difference in corn stalk assimilation between *G. trabeum* and the *Antrodia*-clade fungi as something other than growth rate disparity. As aspen was progressively decomposed, this ratio progressively decreased. This is consistent with Troya et al. (2009) who exposed a different monocot species (reed) to *G. trabeum* and *P. placenta* for 16 weeks and saw ratios of reed weight loss to pine control of 0.07 for *P. placenta* and 0.34 for *G. trabeum*. The time series study of Antai and Crawford (1982) with *P. placenta* on extractive-free quackgrass further suggests that growth rate is not a factor. Over the course of 12 weeks, weight loss was logarithmic with time with the lag phase beginning at only 11% weight loss (Antai and Crawford 1982). In terms of extractives, corn stalk extractives consist primarily of monomeric and oligomeric sugars, alditols, and aliphatic acids (Chen et al. 2007) not likely having toxic qualities. Furthermore, the Antai and Crawford (1982) study, in which *P. placenta* was grown on extractive-free grass, showed comparably little weight loss.

Among mechanistic explanations for this observation on grasses, the enzymatic portion of the secretome among *Antrodia*-clade fungi may be inadequate to efficiently degrade stover. Comparison of carbohydrate-active enzyme (CAZyme) genes present in the two sequenced fungi along with CAZyme genes present in the known *Poales*-degrading fungus *Volvariella volvacea* (Chen et al. 2013) could provide insight into

which enzymes are important in corn stover decay. For instance, both *G. trabeum* and *V. volvacea* have genes for GH10 endoxylanases with a CBM1 cellulose binding module. While *P. placenta* also has genes for GH10 endoxylanase, CBM1 is not present (Floudas et al. 2012; Chen et al. 2013). CAZyme gene expression studies have been carried out with *P. placenta* on sugar agar (Chen et al. 2013; Martinez et al. 2009; Vanden Wymelenberg et al. 2011), cellulose (Martinez et al. 2009), and pine and aspen (Vanden Wymelenberg et al. 2011), but grass substrates have been absent from these studies. Our findings suggest that grass substrate gene expression studies may be worth investigating, along with other tests that harness the unique chemical attributes of grasses.

Brown rot fungi are also theorized to employ a non-enzymatic Fenton-based mechanism (Arantes et al. 2012), and variation in how Fenton oxidation is carried out may also be a factor. This could be manifested by features of corn stalk such as its lignin composition and silica content. The lignin content of secondary cell walls of grasses and woody dicot angiosperms is comparable (~20%) and both are composed primarily of guaiacyl and syringyl monolignol monomers, but grass lignin also contains a substantial portion of hydroxylphenyl units (4-15% of lignin) resulting in reduced lignin methoxyl group content (Vogel 2008). Both *G. trabeum* and *P. placenta* cause extensive demethylation in spruce (Filley et al. 2001) and aspen (Schilling et al. 2012), and *G. trabeum* is known to produce an extracellular alcohol oxidase, which can convert methanol, produced as a result of this demethylation, into hydrogen peroxide (Daniel et al. 2007). The resulting hydrogen peroxide can participate in the Fenton chemistry theorized to induce brown rot decay (Koenigs 1974). *P. placenta* expresses a protein

similar to the *G. trabeum* methanol oxidase and is also likely able to produce hydrogen peroxide in this manner (Martinez et al. 2009). Since lignin demethylation is a result of Fenton oxidation, hydrogen peroxide production by alcohol oxidase is likely a secondary pathway. This is further supported by the observation of significant hydrogen peroxide generation by *P. placenta* in the absence of lignin (Ritschkoff and Viikari 1991). Yet with the observed differences in corn stalk degradation, *P. placenta* may rely on high methoxy group content for efficient degradation, though it is unclear why this would not also inhibit corn stalk degradation by *G. trabeum*.

In regards to silica, the relevance in stover could relate to iron (Fe) and manganese (Mn), two transition metals at similar concentrations in stover and aspen that can partake in Haber-Weiss reactions (Hoskinson et al. 2007; Fengel and Wegener 1984). Plants with high silica concentrations resist Mn and Fe toxicity by blocking the generation of reactive oxygen species (ROS) (Ma 2004), the same ROS employed in decay by brown rot fungi. The presence of high concentrations of silica in stover (1.5-2% of total mass in this case) may interfere with ROS oxidation by binding to the surface of the cell wall, altering the cell wall cation binding capacity (Liang et al. 2007) and potentially also limiting cation availability. If high silica content is the cause of poor assimilation by *P. placenta*, it would suggest that *G. trabeum* has a means of mobilizing these cations or utilizes a metal-free hydroxyl radical generation mechanism that *P. placenta* lacks.

Differences in the hemicellulose composition of corn stalk, relative to wood, could also play a role and was correlated with polysaccharide loss in this study. Dicot

angiosperms like aspen have primary walls that are rich (~20-25%) in xyloglucans, while in grasses they are mostly composed of xylans (20-40% of total mass), in particular glucuronoarabinoxylans (GAX) (Vogel 2008). Xylose monomers reside in the β-linked backbone of GAX, but are α-linked side chains in xyloglucan (Fry 1989). This difference in linkage and position makes aspen xylan more prone to hydrolysis than corn stalk xylan, in agreement with observed loss rates (Fig. 5). Much like xylan in xyloglucans, arabinan is mostly an α-linked side chain in both substrates. Mannans and glucomannans account for 5-10% of the mass of dicot angiosperm primary walls (Vogel 2008). Given that mannose is located in the backbone of these hemi-celluloses, it would be expected that it would be less vulnerable to hydrolysis than as a side chain. However, the rate of mannan loss in aspen was as fast as arabinan in corn stalk, indicating that mannans and glucomannans are readily accessible and rapidly depolymerized by brown rot fungi. Rapid initial glucan loss in aspen further supports early glucomannan degradation. Mixed linkage glucans (MLG) in corn stalk may also contribute to the discrepancy in initial glucan loss between corn stalk and aspen. MLGs are unbranched chains of β-1-4 linked glucan that are interrupted by single β-1-3 linkages (Buckeridge et al. 2004). Varying linkage points may make MLGs more difficult to enzymatically hydrolyze, resulting in slower glucan loss. Given these differences and the effect of hemicellulose on cellulose accessibility (Irwin et al. 2003), *P. placenta* may lack enzyme functionality to hydrolyze corn stalk hemicelluloses required for efficient assimilation.

In conclusion, we have shown that the first brown rot fungus to be sequenced, *P. placenta*, does not efficiently degrade one of the most viable 'next generation' feedstock

options, corn stover. This inefficiency was shared among all tested *Antrodia*-clade fungi, yet *G. trabeum* readily assimilated stover. This inherent difference in ability to degrade corn stover suggests the possibility of clade-specific differences in the decay mechanisms of brown rot fungi. The similarity in the compositional changes induced by *G. trabeum* and *Antrodia*-clade fungi insinuates that these differences may represent multiple means to the same outcome. It was also shown that the progression of component loss agreed with known differences in hemicellulose structure and the expected susceptibility of these components to hydrolysis. The existence of distinct modes of brown rot decay would present an opportunity for the discovery and potential application of novel biochemical pathways, and it emphasizes distinctions among important agents in the carbon cycle, traditionally grouped based on residue characters.

Chapter 6

Mimicry and modeling studies

6.1 Introduction

Due to their ability to mineralize lignin, white rot fungi have most commonly been studied for their biotechnological potential in animal feed digestibility (e.g., Hatakka, 1989; Tian et al., 2012), biopulping (e.g., Blanchette et al, 1988), and bioremediation (e.g., Reddy, 1995). White rot fungi rely on an enzymatic approach to oxidize and remove lignin to improve cellulose accessibility. Though white rot fungi are defined by their ability to degrade lignin, the mechanism by which they carry out this task can vary (Riley et al., 2014), with particular fungi using one or more of a range of lignin-degrading enzymes that include lignin and manganese peroxidases, laccases, etc.

Contrasting with their white rot counterparts, brown rot fungi oxidatively modify lignin (Yelle et al., 2008b), but only a minor portion is fully mineralized to carbon dioxide. Despite increasingly higher concentration of lignin in degradation residues, brown rot fungi are able to achieve near complete conversion of polysaccharides within the lignocellulosic substrate. As the removal of lignin is often viewed as a desirable, if not necessary, step in bioconversion technologies, the brown rot mechanism offers an interesting alternative viewpoint.

Brown rot fungi have a reduced set of cellulolytic enzymes relative to white rot that is supplemented with a non-enzymatic means of oxidizing lignocellulose. This non-enzymatic portion of the brown rot decay mechanism is believed to involve the

generation of hydroxyl radicals via Fenton chemistry. More specifically, hydroxyl radicals are thought to be generated by hydroquinones (Goodell et al., 1997; Kerem et al., 1999; Arantes, 2009), which are produced intracellularly through phenylalanine metabolism (Wymelenberg et al., 2010) and transported into the extracellular space. Additionally, brown rot fungi are known to release organic acids (e.g. oxalic acid), which improve ferric iron availability directly as chelators and by reducing pH. Hydroquinones can act as a reducing agent through a single electron transfer with available ferric iron, leading to the accumulation of ferrous iron. The semi-quinone product can then auto-oxidize to its quinone derivative, while generating a superoxide radical. The superoxide radical is in equilibrium with hydrogen peroxide, which can oxidize ferrous iron to generate anionic hydroxide and a hydroxyl radical.

Hydroxyl radicals are one of the most potent aqueous-phase oxidizing agents and are capable of reacting indiscriminately with a wide range of chemical species. For this reason, hydroxyl radicals have a half-life of approximately one nanosecond and an effective reaction radius of 0.22 nm (Buxton et al., 1988). This suggests an intimate spatial relationship is necessary between the reactants that generate hydroxyl radicals and the species that are ultimately oxidized by these radicals. Underscoring the reactivity of hydroxyl radicals, numerous studies have implicated their damaging effects on biological systems through oxidation and cleavage of DNA, proteins and membrane lipids (Halliwell and Gutteridge, 1989). This same oxidative potential has led to the use of hydroxyl radicals in water treatment (Glaze et al., 1987) and environmental remediation (Watts et al., 1990) applications where oxidation of potentially toxic and highly

recalcitrant chemical species is a desirable outcome. Their short lifespan and *in situ* generation make hydroxyl radicals attractive for these applications from a safety perspective, as no toxic remnants from the reagent itself are left behind. Due to its importance in medicine and environmental remediation, hydroxyl radical chemistry has been studied extensively. Among studies conducted on hydroxyl radicals has been kinetic modeling of the Fenton reaction (De Laat and Gallard, 1999; Kang et al., 2002; Deusterberg and Waite, 2006).

To investigate the feasibility of the proposed non-enzymatic system, a theoretical kinetic model was developed that expanded upon a previously developed Fenton kinetic model (Deusterberg and Waite, 2007) to include the role of hydroquinone in the redox chemistry of brown rot and to investigate the effects of other chemical species at concentrations representative of what is naturally present in wood. Additionally, *in vitro* experiments were conducted to examine the effect of the Fenton reaction on cellulose accessibility and changes in lignocellulose biochemistry.

6.2 Material and Methods

6.2.1 *In Silico* Kinetic Modeling

Theoretical kinetic studies were performed using the Microsoft Excel-based software program Kintecus (Ianni, 2006). This program outputs the change in concentration of defined chemical species given an inputed list of kinetic and equilibrium reactions, the associated rate constants, and the intial concentrations of all chemical species represented. Reaction equations are used to define a system of second-order ordinary differential equations that are numerically integrated using a Runge-Kutta-Cash-

Karp method (Ianni, 2006) over a predefined time interval and step size. Kintecus can also be used to generate thermodynamic models, though this feature was not used in this study since we assumed constant temperature, volume, and pressure.

A list of the chemical reactions assembled for this model are provided in Supplemental Table S6.1. These reactions were aggregated by first determining which chemical species were included in Duesterberg and Waite (2007). Next, chemical species that are relevant to brown rot decay, including oxalic acid and 2,5-dimethoxy, 1,4-hydroquinone (DMHQ) were added at their experimentally measured concentrations (Suzuki et al., 2006). Relevant cationic species, as described by Jellison et al. (1997), were also included at expected concentrations. Potential reactions between these chemical species and additional chemical products were identified using the National Institute of Standards and Technology solution kinetics database (Manion et al., 2013). Reactions in which new resulting products could participate as reactants were included. This process was repeated until no new chemical species were identified.

Beyond constant temperature, pressure, and volume, several other additional assumptions were made in this model. There were no points of inlet or outlet flow from the reactor (i.e. all reactions were occurring within a closed system. Perfect mixing was assumed, eliminating mass transfer limitations. Additionally, it was assumed that reactor volume remained constant (i.e. no change in density), water concentration remained constant (55.5 M), and pH was held constant at relevant values and assumed not to affect rate constants.

All chemical species with non-zero initial concentrations, their intial concentrations, and the source of these values are listed in **Table 6.1**. These initial conentrations were used with the understanding that these values are experimentally measured estimates that would need to be determined on a case-by-case basis, as they can vary greatly among plant species.

Table 6.1 Concentrations of chemical species typically present in brown-rotted wood. These values were used as kinetic model initial concentrations.

Chemical Species	Conc. (M)	Source
Mn^{+2}	1.46E-04	Jellison et al., 1997
K^{+}	9.17E-03	Jellison et al., 1997
Cu^{+2}	1.63E-05	Jellison et al., 1997
Zn^{+2}	5.71E-06	Jellison et al., 1997
Cr^{+3}	3.99E-07	Jellison et al., 1997
Cl^{-}	8.59E-04	Fakankun & Loto, 1990
SO_4^{-2}	4.17E-03	Fakankun & Loto, 1990
SO_3^{-2}	2.45E-03	Fakankun & Loto. 1990
PO_4^{-3}	3.13E-04	Fakankun & Loto. 1990
Fe^{+3}	1.13E-05	Suzuki et al., 2006
$C_2O_4^{-2}$	5.20E-04	Suzuki et al., 2006
DMHQ	2.07E-05	Suzuki et al., 2006
O_2	2.47E-04	CRC Handbook, 2008
CO_2	3.29E-02	CRC Handbook, 2008

The resulting model was used to systematically analyze the effect of each chemical species on hydroxyl radical generation. To do this, all hydroxyl radical consuming reactions were removed from the model. While deviating from reality, this allowed for hydroxyl radical accumulation, which could be quantified based on rate and the final concentration after equilibrium is reached. Effect of chemical species on these

values was determined by varying a chemical species' initial concentration while holding the initial concentration of all other chemical species at their typical values.

6.2.2 *In Vitro* Experiments

6.2.2.1 Feedstock Characterization

Untreated aspen (*Populus tremuloides*) and spruce (*Picea sp.*) lumber were purchased from a local hardware store and a portion of each was milled to 40 mesh powder with a Wiley mill. Each powder was fully characterized in accordance with the summative mass closure analytical procedure published by the National Renewable Energy Laboratory (NREL) (Sluiter and Sluiter 2010). This analysis provides the percentage of ash, extractives, acid soluble and insoluble lignin, glucan, xylan, galactan, arabinan, mannan, uronic acid, and acetyl contained in the oven-dried wood.

6.2.2.2 Pretreatments

6.2.2.2.1 Fenton Mimic

Two grams of 40 mesh aspen or spruce powder were constantly stirred at 30°C in 200 mL of solution (9.9 kg/m^3) in the presence or absence of 0.5 mM ferrous sulfate 7-hydrate (Mallinckrodt Chemicals) and 1% hydrogen peroxide (Macron Chemicals). Treatment of aspen powder using high solids loading (155.4 kg/m^3) through reduction of total reaction volume to 12.72 mL with 0.05 mM of ferrous sulfate and 15% or 30% hydrogen peroxide were also performed. After stirring for 24 hours, the remaining solids were removed by centrifugation (2000 X *g* for 10 minutes). Manganese oxide powder was added to the decanted hydrolysate to catalytically decompose residual hydrogen peroxide. The hydrolysate was then gravity filtered to remove the remaining manganese oxide solid. The pH of the hydrolysate was measured and the acid concentration was

adjusted to 4% with 72% sulfuric acid. The acidified hydrolysate was then heated to 121°C for one hour along with sugar recovery standards, in agreement with Sluiter et al. (2006). The solids from the pretreatment slurry were washed (5 X 30 mL) with distilled water that was removed by centrifugation and decantation. The final mass of the air-dried weight solids was measured and the moisture content of this sample was determined for the final oven-dried weight mass of the sample after pretreatment. A portion of the washed solids was set aside for compositional analysis following the same methodology used for the initial feedstock.

6.2.2.2.2 Effect of Reducing Agent and Full Factorial Investigation

The effect of each chemical component of the brown rot oxidative pretreatment mechanism was determined through a full factorial study (2^4+1). The two levels in the factorial design were the absence of the chemical and the presence at a concentration derived from past studies (Ratto et. al. 1997; Varela & Tien 2003). Factors included iron(III) (467 μM), 2,5-dimethoxy hydroquinone (DMHQ) (48.3 μM), hydrogen peroxide (3%), and the reducing agent sodium dithionite (0.82 mM) . DMHQ was prepared from 2,5-Dimethoxy-1,4-benzoquinone (TCI America) following the synthesis described by Foti et al. (2008).

In comparison with ferrous iron, ferric iron has been shown to absorb strongly to cellulose (Xu and Goodell 2001). Given the short radius of reactivity for hydroxyl radical, the reactants responsible for hydroxyl radical generation and the species that ultimately reacts with hydroxyl radical must be in close proximity. Binding iron to the cellulose target may improve the efficiency of Fenton oxidation. For this reason, runs

that included ferric iron were performed using a separate binding step. This ensured that only adsorbed iron was present in the reaction system and directed formation of hydroxyl radicals to ferric adsorption sites in the wood, limiting hydroxyl radical formation in the surrounding solution. Ferric ammonium sulfate dodecahydrate (1.917 g) was dissolved in 2L of distilled water. Milled spruce (134.45 g ODW, 40 mesh) was added to the solution and was allowed to stir overnight at room temperature. Initial pH of the mixture was 4.43. The mixture was allowed to settle and the liquid supernatant was decanted off. The remaining solids were washed 4 X 1.5 L with distilled water and retained for further processing. A 6 g sample was reserved for NREL summative mass closure analysis.

All pretreatment runs were conducted at room temperature (23°C). The solution volume of all pretreatment mixtures was 950 mL and was comprised of 50mM acetate buffer at a pH of 4.2. For runs including hydrogen peroxide, the volume of acetate buffer added was the difference between the volume of hydrogen peroxide solution added and the target volume of 950mL. 15 g of ODW biomass was used for all runs. The order and timing of addition of all reactants was consistent. After addition of the biomass to the buffer solution and 10 minutes of stirring, hydrogen peroxide was added. After 30 minutes, DMHQ was added. Six hours after DMHQ addition, sodium dithionite was added before an additional 20 hours of stirring. Time of addition for a given chemical over the 20.7 hour course of the reaction was kept constant regardless of the exclusion of any chemicals in a given run.

After 20 hours, the solid and liquid fractions were separated via centrifuge. 100mL of the liquid fraction were retained for solids content and sugar composition

analysis. The remaining solids were washed with distilled water (5 X 500 mL). A 6g sample of each pretreatment run was retained for NREL summative mass closure analysis (ash content, solids content, extractives, klason lignin, and structural sugars). The remaining solids were used for enzymatic hydrolysis.

6.2.2.2.3 Pretreatment Consolidation with Saccharification

Spruce powder (0.5 g ODW, 40 mesh) was added to a 20 mL scintillation vial, along with 15 mL of the standard citric acid buffer (50 mM, pH: 4.8) used for enzymatic hydrolysis (Selig et al., 2008). Fenton's reagent was added in one of five levels, immediately followed by Celluclast (60 "filter paper units" (FPU)/g biomass) and Novozymes 188 (64 pNPGU/g biomass). A filter paper unit is defined as the amount of enzyme required to release 2 mg of reducing sugar equivalents from filter paper in 1 h at 50°C and a pH of 4.8. This mixture was shaken for 5 days at 23°C at 100 RPM before analyzing the supernatant for monosaccharide content.

6.2.2.2.4 Effect of Manganese

Air-dried 40 mesh aspen (2 g) was treated in a total reaction volume of 300 ml. Pretreatment variables included pH (2 or 4.8), ferric ion concentration (0, 1, or 10 mM), manganese (II) cation concentration (0, 1, or 10 mM), and oxalic acid concentration (0, 10, or 100 mM). pH was adjusted with sulfuric acid and sodium hydroxide. After mixing for 24 hours in the dark, the reaction mixture was centrifuged and the liquid fraction was decanted. The remaining solid fraction was washed with distilled water (5 X 30 mL) and allowed to air dry before enzymatic hydrolysis and carbohydrate analysis.

6.2.2.2.5 Effect of DMHQ and Fe alone

Since all previous trials included direct addition of hydrogen peroxide, we set out to determine if DMHQ alone could cause cellulose cleavage, as indicated by reducing sugar concentration as measured by DNS assay (Miller, 1959). Avicel (0.1 g) was placed in 15 mL citrate buffer (50 mM) in 20 mL scintillation vials. The mixture was treated with either ferric ammonium sulfate or ferric ammonium oxalate (0.5 mM), in the presence or absence of DMHQ (10 mM), at pH of 3, 4, or 5 for a total of 12 test conditions. Additionally, all tests were performed in the absence of avicel to account for potential interferences of Fe^{3+} or DMHQ in the DNS assay. DMHQ was prepared from DMBQ as previously described (Foti et al., 2008) and dosed in saturated ethanol. Vials were capped and vortex homogenized. The mixtures were gently shaken (50 RPM) for 18 hours before performing DNS assay on the thoroughly homogenized cellulose/hydrolysate mixture.

6.2.2.3 Enzymatic Hydrolysis

Enzymatic hydrolysis was carried out in accordance with Selig et. al. (2008). 100 mg (air-dried weight) of washed, pretreated solids were weighed into 20 mL scintillation vials at the same time that moisture content was determined so that the oven-dried weight added could be later calculated. The solids were suspended in 10 mL of solution consisting of 5 mL of 0.1 mM citrate buffer (pH = 4.8), 40 µL of tetracycline, 30 µL of cyclohexamide, 60 FPU/g biomass of Celluclast and 64 pNPGU/g biomass of Novozyme 188 (Sigma Aldrich) with the difference made up with distilled water. Celluclast and Novozyme 188 activities were measured as described by Adney and Baker (2006). Sealed samples were constantly shaken (100 RPM) at 50°C for 5 days.

6.2.2.4 Sugar Analysis

Sugar content of the hydrolysate from the pretreatment slurry and the hydrolysate after enzymatic hydrolysis were independently determined by HPLC (Agilent Technologies 1200 series). Carbohydrate separation was performed using an Aminex HPX-87P analytical column (Bio-rad) and a 2 column microguard de-ashing guard column (Bio-Rad) for the pretreatment sample and a microguard carbo-P guard column for the enzymatic hydrolysate. Mobile phase was degassed HPLC grade deionized water (Sigma Aldrich) at an operating flow rate of 0.4 ml/min. Operating column temperature was 85°C, injection volume was 20 μL, and refractive index was used for detection. Standard response calibration curves were developed with reagent grade glucose, arabinose (Sigma Aldrich), galactose, xylose, and mannose (Acros Organics).

In some cases, sugar concentrations were determined via assay with 3,5-dinitrosalicylic acid as described by Miller (1959). Absorption values were determined at a wavelength of 575 nm. Glucose standards were used to generate a calibration curve that was used to convert spectrophotometric absorption values into glucose equivalents (kg/m^3).

Yields were calculated based on original mass using the mass loss, the mass of released polymeric sugar (mg) ($m_{(C1\ released)}$), the mass used for enzymatic hydrolysis ($m_{hydrolyzed}$), and the initial percentage of a given polymer found in untreated aspen as follows (% $C_{(initial)}$):

$$\text{Yield (\%)} = ((1-\%\ \text{mass loss}) * m_{(C1\ released)}) / (m_{hydrolyzed} * \%\ C_{(initial)})$$

6.3 Results and Discussion

6.3.1 Kinetic Model

In most runs, $C_2O_4^-$ and Fe^{3+} equilibrated with respective counterspecies within the first 20 picoseconds of reaction. In the first three seconds, all DMHQ is oxidized to DMBQ. When termination reactions for hydroxyl radical were excluded from the model, the time required for hydroxyl radical concentration to reach equilibrium varied with ferric iron, oxalate, DMHQ, and pH (**Figure 6.1**). The presence of iron was required for hydroxyl radical generation, but too much iron acted as a hinderance. This was similar to experimental observations by Xu and Goodell (2001), who treated cellulose with Fenton's reagent and noted that the cellulose degree of polymerization went through a minimum value with Fe (III) concentration. Optimum iron concentration in this study was dependent on hydrogen peroxide concentration, but was around 200 μM and 600 μM for 10 mM and 80 mM of initial hydrogen peroxide at a pH of 4, respectively. This was lower than the 1130 μM optimum that we observed at pH of 3, but the trend was consistent.

Contradicting experimental observations (Varela and Tien, 2003), the kinetic model indicated an increase in hydroxyl radical concentration with decreasing pH. This discrepancy is most likely due to the use of un-representative rate constants, given the pH-dependency of many key redox reactions. While this makes it difficult to look at the effect of pH on hydroxyl radical generation and will affect the model's accuracy in predicting true hydroxyl radical generation rates and concentrations, general trend comparisons made at constant pH should be similar to experimental results.

In addition to the effect of ferric iron, variations in oxalate and DMHQ concentrations also showed trends that agreed with reported experimental values. Varela

and Tien (2003), showed that lipid peroxidation, as a product of hydroxyl radical reaction, increased to a maximum at an oxalate concentration of 50 μM before declining rapidly with increased oxalate. A similar trend is observed in the kinetic model, as the final hydroxyl radical concentration declines when the concentration of oxalate exceeds ~100 μM (Schilling, 2010). As oxalate concentration affects pH, the differences in the display of the maximum value between the kinetic model and the experimental data may be driven by pH. This may imply that secretion of oxalic acid by brown rot fungi may also play a protective role, among the other functions to which it has been ascribed (Schmidt et al., 1981; Green et al., 1991; Shimada et al., 1997; Munir et al., 2001). Apart from reducing the rate of hydroxyl radical generation near hyphae by lowering the pH in the adjacent liquid media, it appears that higher concentrations of oxalate alone diminish hydroxyl radical generation, since this same effect is observed even when pH is held constant. By combining the inhibitory effects of both pH and oxalic acid, the fungus may be able to greatly limit self-inflicted oxidative damage to its hyphae.

Not surprisingly, given its role in hydrogen peroxide generation and iron reduction, increased DMHQ concentration was positively correlated with hydroxyl radical generation. At around 20 mM, however, the pace of the effect of increased DMHQ levels on hydroxyl radical generation declined. This was due to a shift in the limiting reagent from DMHQ to O_2, as no external source of O_2 was assumed to replenish what was initially present.

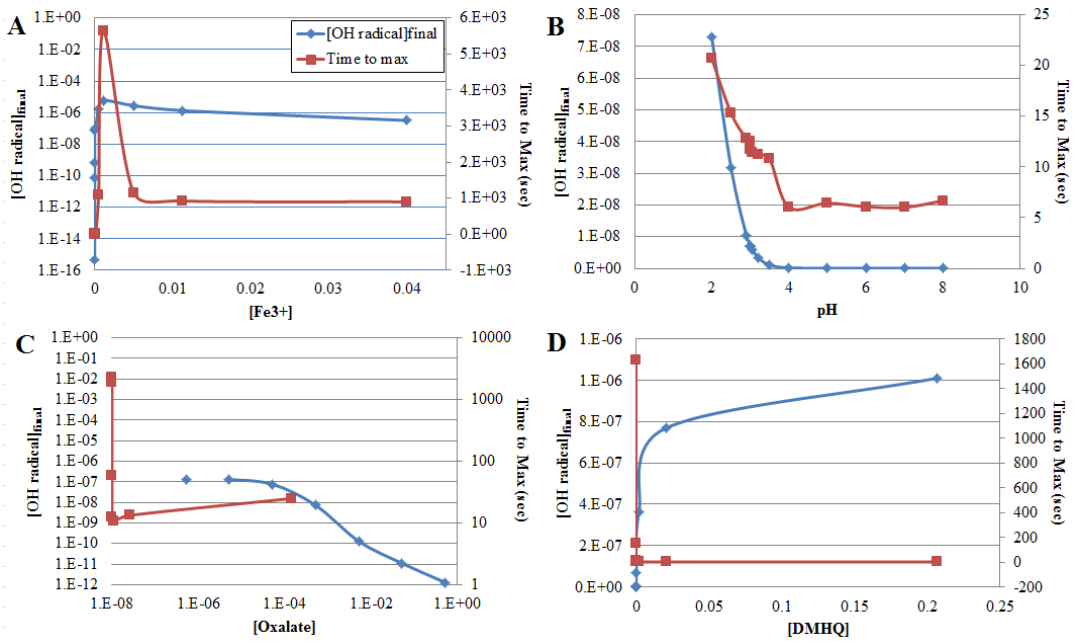

Figure 6.1 Change in maximum hydroxyl radical concentration and time to hydroxyl radical equilibrium with change in concentration of ferric iron (**A**), pH (**B**), oxalate (**C**), and DMHQ (**D**). Concentrations are expressed in mol/L. For each only the concentration of the indicated species was changed and all other intial concentrations were held constant.

Manganese and other transition metals had no discernible effect on the the rate or extent of hydroxyl radical generation. This was somewhat unexpected, as manganese-catalyzed Fenton reactions are known to occur when present in the (IV) transition state (Sarasa et al., 2005). Furthermore, a recent study indicated that treatment of cellulose with manganese (II) and hydrogen peroxide can cause a loss in degree of polymerization of cellulose comparable to that seen with ferric iron and hydrogen peroxide (Hastrup et al., 2011). It is possible that not all relevant reactions related to manganese are included, particularly those involved with the interactions between manganese and DMHQ and manganese and hydrogen peroxide. However, these results are corroborated by the experimental results outlined in section 6.3.5.

6.3.2 Fenton Mimic

Previous studies (Rättö et al., 1997; Jain and Vigneshwaran, 2012; Jung et al., 2015) have suggested that the use of Fenton's reagent as a pretreatment can result in improved saccharification yields. Expanding on these studies, we tested the effect of 1% hydrogen peroxide and 0.5 mM on the composition and saccharification yield of aspen and spuce. 15% and 30% hydrogen peroxide were also tested. Fenton-pretreated aspen saw mass losses in excess of those observed in the control (**Table 6.2**). Mass losses comparable to Fenton were observed when treated with 1% hydrogen peroxide. This suggests that iron supplementation is not required. Mass loss in spruce did not seem to be dependent on pretreatment, as the highest observed mass loss (9%) was in the control sample.

Table 6.2 Mass losses in aspen and spruce following various pretreatments.

		Aspen	Spruce
H2O2 (%)	FeSO4 (mM)	Weight Loss (%)	Weight Loss (%)
1	0.5	14.71%	8.90%
1	0	13.54%	5.39%
0	0.5	8.78%	4.98%
0	0	7.82%	9.00%
15	0.05	11.21%	ND
30	0.05	17.86%	ND

The composition of pretreated spruce also remained largely unchanged (**Table 6.3** and **Table 6.4**). In combination with the lack of mass loss, this suggests that Fenton pretreatment in the concentrations used were ineffective. This was unexpected, as mass

losses in Rättö et al. (1997) using the same set up, but different wood, were in excess of 24%, resulting mostly from hemicellulose losses.

Table 6.3 Composition of pretreated spruce (40 mesh). $[Fe^{2+}]$ = 0.5 mM, $[H_2O_2]$ = 1%.

Sample	Total Lignin	Soluble Lignin	Glucan	Xylan	Galactan	Arabinan	Mannan
Reference	27.8%	0.2%	45.6%	5.1%	1.4%	1.0%	9.9%
just Fe	28.4%	0.3%	44.3%	5.0%	1.3%	1.0%	9.7%
just H_2O_2	26.9%	0.3%	44.1%	4.9%	1.2%	1.5%	10.4%
Both	29.1%	0.6%	47.5%	4.9%	1.1%	1.3%	11.0%

Table 6.4 Pretreated spruce composition expressed as percentage of concentration in untreated spruce wood. $[Fe^{2+}]$ = 0.5 mM, $[H_2O_2]$ = 1%.

Sample	Total Yield	Total Lignin	Soluble Lignin	Glucan	Xylan	Galactan	Arabinan	Mannan
just Fe	104.4%	106.6%	144.5%	101.3%	103.5%	95.4%	102.5%	102.3%
just H_2O_2	104.0%	100.5%	188.3%	100.4%	101.0%	85.3%	151.8%	108.5%
Both	100.1%	105.0%	297.6%	104.3%	96.9%	78.4%	125.1%	111.0%

Similar consistencies in composition before and after pretreatment were also observed in aspen (**Table 6.5** and **Table 6.6**). A substantial change in composition, primarily in lignin loss, was only after treatment with 30% hydrogen peroxide and 0.05 mM ferric iron. Again, this suggests that these reaction conditions did not effect change in the substrate structure.

Table 6.5 Composition of pretreated aspen (40 mesh). [Fe^{2+}] = 0.5 mM, [H_2O_2] = 1%, except where indicated otherwise.

Sample	Total Lignin	Soluble Lignin	Glucan	Xylan	Galactan	Arabinan	Mannan
Reference	21.7%	0.4%	48.5%	16.1%	0.2%	0.6%	2.4%
just Fe	20.6%	0.5%	49.7%	16.5%	0.2%	0.9%	2.6%
just H_2O_2	22.7%	0.4%	53.3%	18.0%	0.1%	1.1%	2.9%
Both	20.8%	0.4%	48.0%	16.2%	0.2%	1.4%	1.7%
15% H_2O_2/0.05 mM Fe	20.6%	0.3%	49.0%	16.4%	0.1%	0.7%	2.4%
30% H_2O_2/0.05 mM Fe	14.7%	0.8%	50.2%	15.9%	0.3%	0.3%	1.9%

Table 6.6 Pretreated spruce composition expressed as percentage of concentration in untreated aspen wood. [Fe^{2+}] = 0.5 mM, [H_2O_2] = 1%, except where indicated otherwise.

Sample	Total Yield	Total Lignin	Soluble Lignin	Glucan	Xylan	Galactan	Arabinan	Mannan
just Fe	99.0%	93.9%	134.4%	101.3%	101.3%	104.5%	136.0%	109.3%
just H_2O_2	93.8%	98.1%	95.0%	103.0%	104.9%	46.8%	161.1%	115.9%
Both	92.5%	88.7%	95.3%	91.5%	93.1%	107.2%	202.4%	64.9%
15% H_2O_2 / 0.05 mM Fe	96.3%	91.3%	82.4%	97.2%	97.7%	67.1%	105.1%	97.1%
30% H_2O_2 / 0.05 mM Fe	127.9%	86.8%	243.9%	132.3%	126.0%	160.6%	51.3%	99.8%

The lack of change in substrate composition was also manifested in the enzymatic saccharification yields of the pretreated substrates. No significant changes in monosaccharide yields were observed in spruce (**Table 6.7**). Only 30% H_2O_2 and 0.05 mM Fe^{2+} treatment showed substantial change in monosaccharide yield in aspen (**Table 6.8**). Though not realistic in comparison with hydrogen peroxide levels measured in natural wood decay and a significantly higher concentration than that used in other Fenton pretreatment, glucose yields were doubled with this treatment. This was likely due to the loss of lignin associated with the pretreatment, though this mode of action on the substrate is more similar to white rot than brown rot.

Table 6.7 Sugar yields following enzymatic hydrolysis calculated based on untreated and pretreated spruce wood.

	Yield (% of initial)					Yield (% of pretreatment including pretreatment hydrolysate)				
Pretreatment	Glucan	Xylan	Galactan	Arabinan	Mannan	Glucan	Xylan	Galactan	Arabinan	Mannan
Reference	9.4%	7.6%	5.1%	3.1%	40.2%	8.8%	7.7%	5.9%	5.1%	27.5%
just Fe	9.9%	9.4%	16.9%	4.5%	44.8%	9.3%	9.6%	12.9%	6.2%	30.8%
just H_2O_2	9.6%	7.6%	4.3%	1.6%	38.5%	8.7%	7.5%	4.2%	3.4%	27.0%
Both	9.7%	6.4%	5.5%	2.4%	44.9%	9.2%	6.3%	4.0%	4.0%	32.2%

Table 6.8 Sugar yields following enzymatic hydrolysis calculated based on untreated and pretreated aspen wood.

	Yield (% of initial)					Yield (% of pretreatment including pretreatment hydrolysate)				
Pretreatment	Glucan	Xylan	Galactan	Arabinan	Mannan	Glucan	Xylan	Galactan	Arabinan	Mannan
Reference	15.3%	11.2%	27.8%	8.4%	228.3%	15.7%	11.3%	12.4%	14.8%	205.9%
just Fe	15.9%	12.9%	14.9%	4.2%	172.9%	16.4%	12.7%	8.2%	10.9%	172.0%
just H_2O_2	14.2%	11.5%	129.5%	2.7%	121.4%	14.4%	11.4%	29.7%	5.4%	117.0%
Both	16.0%	12.9%	6.3%	3.9%	253.4%	14.6%	11.3%	8.7%	12.2%	139.1%
15% H_2O_2 / 0.05 mM Fe	17.1%	13.1%	29.5%	6.1%	231.5%	16.9%	12.7%	9.4%	12.7%	201.8%
30% H_2O_2 / 0.05 mM Fe	31.7%	30.4%	102.6%	53.2%	299.9%	41.7%	37.9%	64.5%	60.4%	263.5%

6.3.3 Effect of Reducing Agent

Material balance diagrams, as recommended by Zhang et al. (2009), for all pretreatment sets, including substrate component concentrations of initial, pretreated and enzymatically saccharified material are provided in Supplemental Table S6.2. Generally, pretreatment did not lead to substantial improvement in yields of sugar in the hydrolysate following enzymatic saccharification (**Figure 6.2**). When glucose yields are calculated based on the difference in the glucan content of the untreated sound material and the glucan content of the pretreated and saccharified material, the glucose yields are substantially greater. This was especially true in pretreatments that included DMHQ, as well as those that included additional ferric iron. When all four components were included, the greatest glucan loss was observed (47%).

The discrepancy between the sugar concentrations present in the hydrolysate following saccharification and the glucan losses observed over the course of pretreatment and saccharification suggests incomplete mass balance of glucan. This is likely due to the consumption of glucose in subsequent reactions, most likely continued oxidation of glucose to reaction products including D-glucono-1,5-lactone, its hydrolysis product D-gluconic acid, and 2-deoxy-D-glucono-1,5-lactone (Von Sonntag, 1980). If brown rot fungi do indeed conduct Fenton chemistry during decay, given the effect of this chemistry on glucose yield, it seems there must be a mechanism to prevent over oxidation of produced monosacharrides. Alternatively, fungi may use the byproducts of radical oxidation of these sugars as a major carbon source through certain metabolic pathways (e.g.Entner-Doudoroff). Indeed, gluconic acid and other sugar acid byproducts of radical oxidation of cellulose have been found in cellulose degraded by *Postia placenta*, as well as in Fenton treated cellulose, which are not present in cellulose treated with hydrochloric acid or periodic acid and bromine (Kirk et al., 1991).

Sodium dithionite is a reducing agent that is used in the synthesis of DMHQ from DMBQ. The late addition of sodium dithionite was meant to simulate the regeneration of DMHQ that may be performed intracellularly by quinone reductase during brown rot decay (Jensen et al., 2002). Although sodium dithionite is a less specific reducing agent than quinone reductase, its presence tended to accelerate glucan loss, particularly when also in the presence of iron and DMHQ. Its presence with hydrogen peroxide or hydrogen peroxide and DMHQ without iron had the opposite effect, with even lower glucan losses than the control.

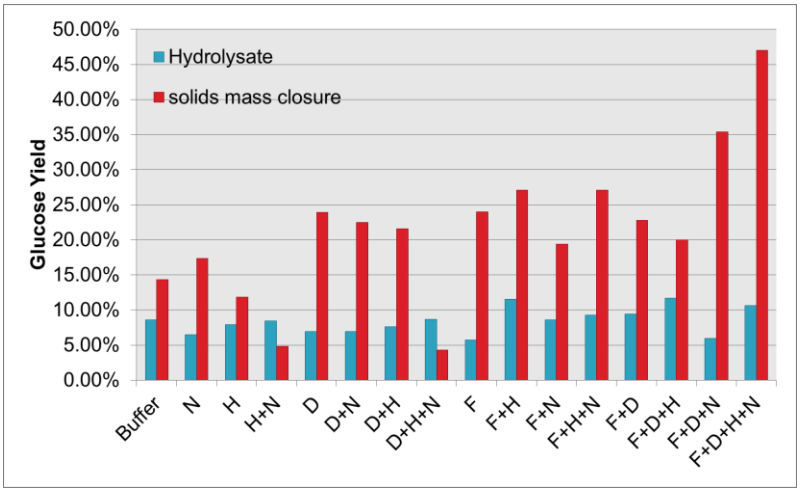

Figure 6.2 Glucose yield from enzymatically hydrolyzed spruce as calculated from glucose concentration measured in the enzymatic hydrolysate (blue) and as the difference in glucan content in untreated spruce and the glucan content after pretreatment and enzymatic hydrolysis (red). Indicated pretreatment components included N = sodium dithionite (0.12 mM), H = hydrogen peroxide (1%), D = DMHQ (6.5 µM), F = ferric ammonium sulfate (0.62 mM). All pretreatments were performed in an acetate buffer (4.2 pH, 50 mM).

6.3.4 Pretreatment Consolidation

Control glucose yields were relatively low (9%) but consistent with previous results with spruce. Addition of low concentrations of Fenton's reagent during saccharification had no effect on glucose yield, but reduced yields were observed as concentrations were increased (**Figure 6.3**). In addition to the potential for oxidative damage to cellulases in a combined process, it is known that iron cations can interfere with cellulase functionality (Tejirian and Xu, 2010). The addition of iron before or after the addition of enzymes did not have a significant effect on the glucose yield, but samples with later addition did tend to have slightly higher values than those where iron was added before the cellulases.

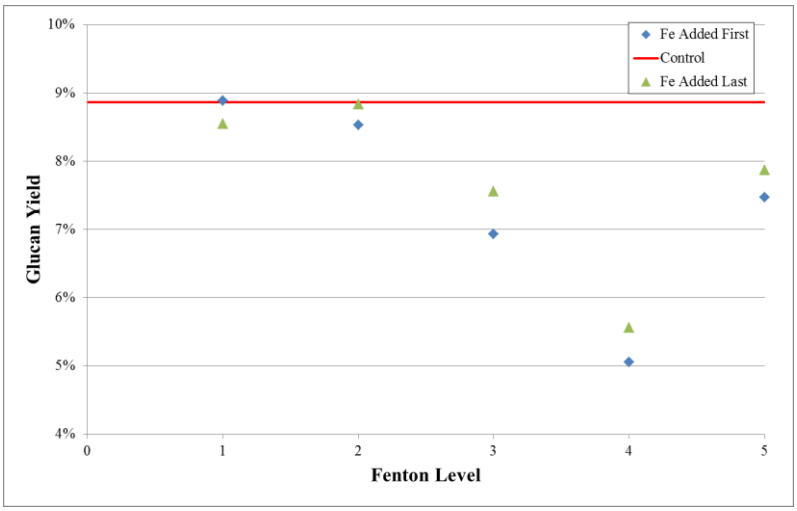

Figure 6.3 Change in glucan yield with increasing concentration of Fenton's reagent (pH = 4.8).

6.3.5 Effect of Manganese

Kolthoff et al. (1972) demonstrated that hydrogen peroxide can be generated from oxalic acid when in the presence of manganese (III) oxalate and manganese (II). This experiment was designed to explore this as a potential chemical route to hydrogen peroxide generation for Fenton chemistry during brown rot.

Glucan yields ranged from 22.1% to 11.7% with controls at pH 2 and 4.8 exhibiting yields of 19.8% and 16.9% respectively. Main effect plots show that oxalate and manganese concentrations had no effect on glucan yield. Increasing iron concentration and increasing pH negatively affected yield, but only slightly. Overall, there was no significant improvement in glucan yield with any of the treatments performed. **Figure 6.4** summarizes the glucan yields as a function of iron concentration at both pH values at the extremes in oxalate and manganese (II) concentrations.

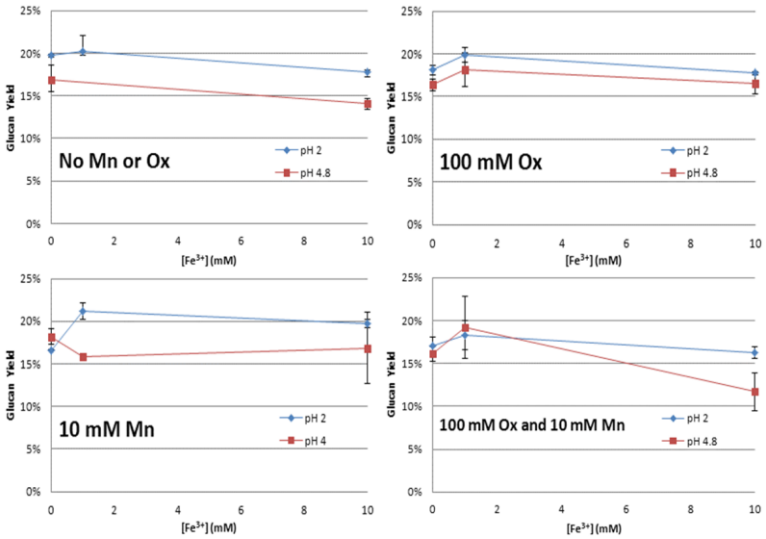

Figure 6.4 Glucan yield with varying ferric cation concentration at pH = 2 and 4.8 in the absence of oxalate or manganese(II) (upper left), the presence of 100 mM oxalate (upper right), the presence of 10 mM manganese(II) (lower left), or the presence of 10 mM manganese(II) and 100 mM oxalate (lower right). Error bars represent standard error (n = 3).

Xylan yields ranged from 25.5% to 9.3% with controls at pH 2 and 4.8 exhibiting yields of 16.0% and 13.2% respectively. Main effect plots show that pH was the only variable that significantly effected xylan yield. **Figure 6.5** summarizes xylan yields as a function of iron concentration at both pH values at the extremes in oxalate and manganese(II) concentrations.

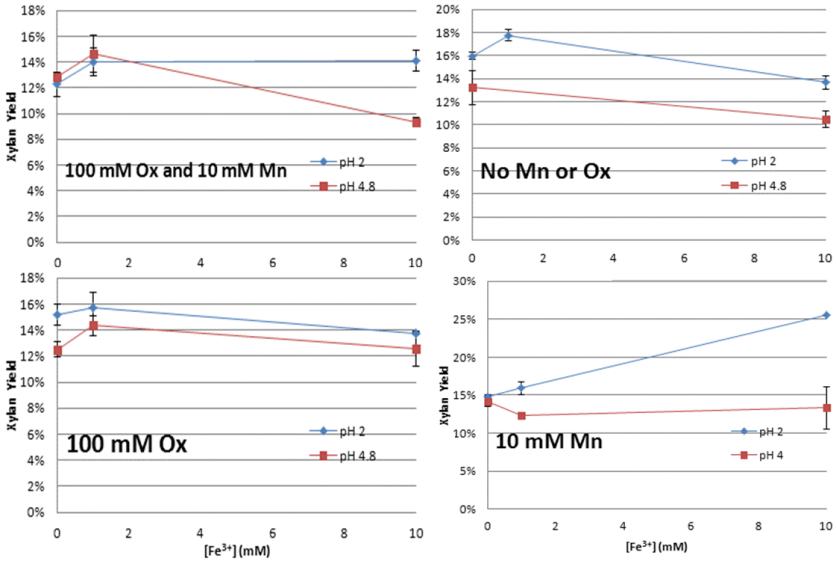

Figure 6.5 Xylan yield with varying ferric cation concentration at pH = 2 and 4.8 in the presence of 10 mM manganese(II) and 100 mM oxalate (upper left), the absence of oxalate or manganese(II) (upper right), the presence of 100 mM oxalate (lower left), or the presence of 10 mM manganese(II) (lower right). Error bars represent standard error (n = 3).

The absence of an effect of manganese, in combination with oxalate, on saccharification potential corroborates the findings of the kinetic model that manganese does not contribute to the redox chemistry of brown rot decay. This, however, needs to be placed in context as our efforts with Fenton's reagent were not particularly effective either in improving yields.

6.3.6 Effect of DMHQ and Fe Alone

DMHQ absorbed light at 575 nm in the absence of avicel. This interference was greatest at a pH of 4. Treatment with DMHQ generally increased the concentration of reducing end groups in crystalline cellulose beyond this interference, suggesting cellulose chain cleavage occurred (**Figure 6.6**). This was particularly true when ferric ammonium sulfate was the iron source at a pH of 5, with an absorption value that was 2.5 times greater than the sum of the avicel baseline absorption and the DMHQ interference level at

pH 5. Apart from the difference at pH 5, there was no noticeable difference in results between the two ferric iron sources.

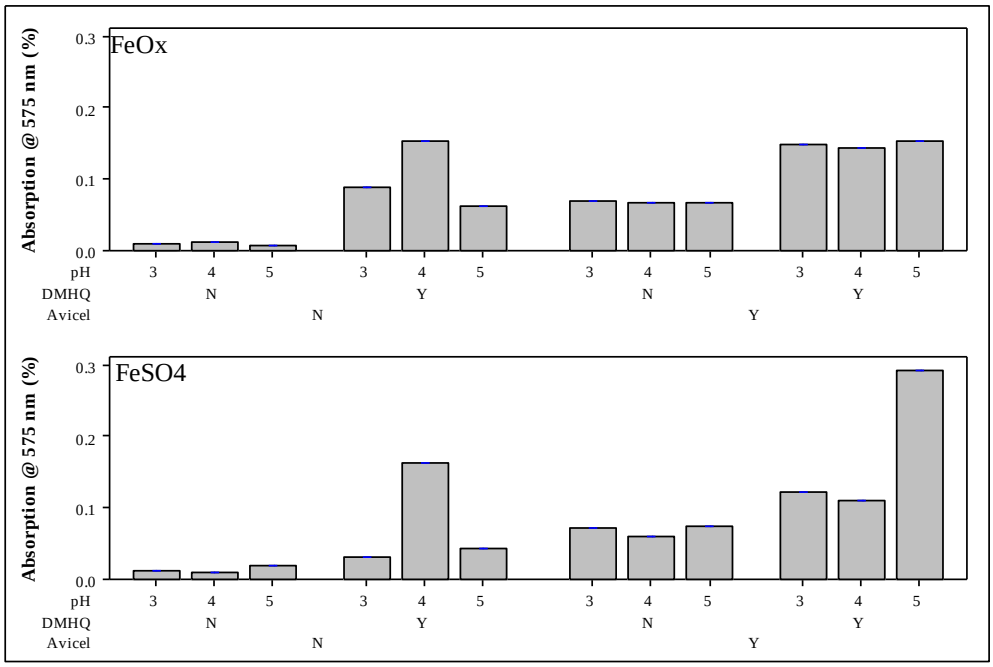

Figure 6.6 Absorption of 575 nm light by DNS assay samples of pretreated crystalline cellulose. FeOx = ferric ammonium oxalate and FeSO4 = Ferric ammonium sulfate (0.5 mM) and DMHQ (10 mM). Higher absorption is indicative of a greater reducing end concentration.

Despite little improvement in yields after Fenton treatment of section 6.3.2, these results, as well as the results of the study of section 6.3.3 indicate that the presence of DMHQ improves cellulose accessibility and contributes to cellulose degradation. Most notably, DMHQ and ferric iron alone (i.e. in the absence of externally supplied hydrogen peroxide) improve cellulose accessbility. When combined with evidence that measurable quantities of extracellular DMHQ have been found in fungi from several different clades (Korripally et al., 2013; Wei et al., 2010; Machuca et al., 2001; Suzuki et al., 2006), these results support the proposed mechanism of hydroquinone-driven Fenton oxidation as a contributing factor in brown rot decay.

6.4 Conclusions

A kinetic model was developed to explore the variable space of the proposed mechanism for hydroxyl radical generation during brown rot decay. Due to rate constant variation with pH and the possible exclusion of some critical fundamental reaction equations that were not readily available, there were some limitations to the accuracy of this model. Despite these limitations, this model generally agreed with several trends previously illustrated experimentally, including reduced hydroxyl radical generation with increased oxalate concentration, decreased DMHQ concentration, and a concentration optimum for ferric iron. As additional rate constant information becomes available, this model can be further enhanced and more fully developed.

Experimental studies demonstrated that Fenton oxidation can not be ruled out as a contributing means of brown rot decay, though questions remain regarding the compatibility of the oxidative portion of the mechanism with the enzymatic portion. Both experimental and modeling studies showed that the availability of iron is of critical importance to this mechanism, as other transition metals like manganese were significantly less effective reducing agents and did not readily produce hydroxyl radicals. Mimicry of Fenton-based oxidation did improve cellulose accessibility in wood samples and reduced the degree of polymerization of cellulose as seen with brown rot decay, but the extent of these changes was not as significant as those observed in previous Fenton pretreatment studies (e.g. Ratto et al., 1997). In addition to traditional Fenton's reagent (i.e. ferrous iron and hydrogen peroxide), it was shown that a combination of DMHQ / ferric was also effective for cellulose depolymerization. Though previous studies have

shown this effect on polyethylene glycol (Kerem et al., 1999), this is the first illustration of the effectiveness of this combination on cellulose in the absence of directly added hydrogen peroxide.

6.5 Supplemental Information

Table S6.1 Kinetic model reaction equations. k: rate constant. AVG: rate constant value is average from listed multiple sources.

k (M^{-1} s^{-1})	Reaction	Source
3.15E+07	$^1O2^*$ + HQ ==> products	AVG (Tratnyek & Hoigne, 1991; Martire et al., 1991)
4.17E+01	Fe(II) + H2O2 ==> Fe(III) + ·OH + OH-	Duesterberg et al., 2005
2.00E-03	Fe(II) + H2O2 ==> Fe(III) + HO2· + H+	Kwan & Voelker, 2002
2.00E-03	Fe(II) + H2O2 ==> Fe(III) + O2·- + 2H+	Kwan & Voelker, 2002
7.82E+05	Fe(III) + O2·- ==> Fe(II) + O2	Kwan & Voelker, 2002
7.82E+05	Fe(III) + HO2· ==> Fe(II) + O2 + H+	Kwan & Voelker, 2002
1.34E+06	Fe(II) + O2·- + 2H+ ==> Fe(III) + H2O2	Kwan & Voelker, 2002
1.34E+06	Fe(II) + HO2· + H+ ==> Fe(III) + H2O2	Kwan & Voelker, 2002
2.33E+06	HO2· + HO2· ==> H2O2 + O2	Kwan & Voelker, 2002
2.33E+06	O2·- + O2·- + 2H+ ==> H2O2 + O2	Kwan & Voelker, 2002
2.33E+06	HO2· + O2·- + H+ ==> H2O2 + O2	Kwan & Voelker, 2002
1.65E+07	O2·- + HQ + H+ ==> H2O2 + Q·-	Rao & Hayon 1973
1.65E+07	HO2· + HQ ==> H2O2 + Q·-	Rao & Hayon 1973
2.25E+05	C2O4-2 + H· ==> HC2O4·-2	Neta & Schuler 1972
2.00E-01	C2O4-2 + O2·- ==> products	Bielski & Richter 1977
2.60E+07	eaq- + C2O4-2 ==> C2O4·-3	AVG (Schwarz, 1992; Prasad et al., 1986; Mulazzani et al., 1986; Getoff et al., 1971)
1.00E+05	FeC2O4 + Fe(III) ==> C2O4-2 + Fe(III) + Fe(II)	Cooper & DeGraff, 1972
2.00E+06	Fe(III) + H· ==> Fe(II) + H+	Baxendale et al., 1968
2.50E+10	eaq- + H2C2O4 ==> H2C2O4·-	Micic & Draganic, 1969
1.60E+08	eaq- + Fe(II) ==> products	Baxendale et al., 1965
1.50E+08	Fe(III)OH + O2·- ==> O2 + FeOH+	Rush & Bielski, 1985
1.00E+07	Fe(II) + O2·- + 2H+ ==> Fe(III) + H2O2	Rush & Bielski, 1985
2.50E+06	FeC2O4plus + FeC2O4 ==> FeC2O4plus + C2O4-2 + Fe(II)	Cooper & DeGraff, 1972
1.20E+09	H· + Fe(III)OH ==> Fe(II) + H+	Baxendale et al., 1968
3.40E+05	H2C2O4 + H· ==> H3C2O4·	Neta et al., 1971
7.50E+06	Fe(II) + H· ==> Fe(III)H	Jayson et al., 1969
1.20E+06	HO2· + Fe(II) + H+ ==> H2O2 + Fe(III)	Rush & Bielski, 1985
6.00E+08	O·- + O2·- + H2O ==> O2 + OH- + OH-	Sehested et al., 1982

k (M^{-1} s^{-1})	Reaction	Source
1.00E+05	Mn(III) + O2·- ==> O2 + Mn(II)	Baral et al., 1985
9.70E+07	H2O + HO2· + O2·- ==> O2 + H2O2 + OH-	Bielski et al., 1985
1.30E+10	eaq- + O2·- ==> O2-2	Gruenbein et al., 1971
6.10E+10	H+ + O2·- ==> HO2·	AVG (Ilan & Rabani, 1976; Field et al., 1976)
1.00E+10	HO2· ==> O2·- + H+	Bielski et al., 1985
1.15E+00	H2O2 + O2·- ==> O2 + ·OH + OH-	AVG (Rigo et al., 1977; Ferrandi et al., 1978)
4.40E+03	MnO2plus ==> Mn(II) + O2·-	Pick-Kaplan & Rabani, 1976
1.10E+08	Mn(II) + O2·- ==> MnO2plus	Pick-Kaplan & Rabani, 1976
1.10E+08	HO2· + Mn(II) ==> MnO2plus + H+	Pick-Kaplan & Rabani, 1976
5.00E-01	H2O2 + HO2· ==> O2 + H2O + ·OH	Weinstein & Bielski, 1979
2.90E+07	eaq- + Mn(II) ==> Mn(I)	AVG (Baxendale et al., 1965; Rabani et al., 1977)
2.00E+10	HO2· + H· ==> H2O2	Feng et al., 1970
5.57E+05	HO2· + Fe(III) ==> O2 + Fe(II) + H+	AVG (Sehested et al., 1969; Allen et al., 1957)
9.17E+06	HO2· + HO2· ==> O2 + H2O2	AVG (Bielski et al., 1985; Christensen & Sehested, 1988)
5.87E+07	H2O2 + H· ==> H2O + ·OH	AVG (Sweet & Thomas, 1964; Mezyk & Bartels, 1995; Elliot, 1989)
1.14E+10	eaq- + H2O2 ==> ·OH + OH-	AVG (Gordon et al., 1963; Christensen et al., 1994; Elliot et al., 1990; Greenstock & Wiebe, 1981; Milsavljevic & Micic, 1978; Cercek, 1969)
2.40E+00	HO2· + H2O2 ==> O2 + H2O + ·OH	Dainton & Rowbottom, 1953
2.40E+00	O2·- + H+ + H2O2 ==> O2 + H2O + ·OH	Dainton & Rowbottom, 1953
7.10E+08	Glucose· + HQ- ==> products	Steenken, 1979
6.00E+07	Glucose + H· ==> Glucose· + H2	AVG (Rabani, 1962; Buxton et al., 1988; Neta & Schuler, 1971; Rabani & Stein, 1962)
1.00E+00	HO2· + H2 ==> H2O2 + H·	Field et al., 1976
1.00E+00	O2·- + H+ + H2 ==> H2O2 + H·	Field et al., 1976
1.00E+07	eaq- + H2 ==> products	Hart et al., 1964
9.67E+07	O·- + H2 ==> eaq- + H2O	AVG (Hicket & Sehested, 1991; Matheson & Rabani, 1965)
7.70E+09	eaq- + CO2 ==> CO2·-	Gordon et al., 1963
1.00E+06	CO2 + H· ==> ·CO2H	Keene et al., 1965
5.00E+07	CO3·- + CO2·- ==> CO3-2 + CO2	Draganic et al., 1991
2.00E+05	Mn(II) + CO2·- ==> Mn(I) + CO2	Pick-Kaplan & Rabani, 1976
3.90E+05	eaq- + CO3-2 ==> products	Nash et al., 1981
5.27E+08	CO2·- + CO2·- ==> C2O4-2	AVG (Buxton & Sellers, 1973; Fojtik et al., 1970; Neta et al., 1969)
5.25E+08	CO3·- + O2·- ==> O2 + CO3-2	AVG (Behar et al., 1970; Eriksen et al., 1985)
6.77E+05	H2O2 + CO2·- ==> ·OH + OH- + CO2	AVG (Buxton & Wilmarth, 1963; Schwarz, 1992; Kishore et al., 1987)
2.87E+09	O2 + CO2·- ==> CO2 + O2·-	AVG (Adams & Willson, 1976; Ilan & Rabani, 1976; Buxton et al., 1976)
7.00E+04	Glucose + CO3·- ==> products	Chen & Hoffman, 1973

k (M^{-1} s^{-1})	Reaction	Source
1.00E+06	H2CO3 + HO2· ==> CO3·- + HO2- + 2H+	Schmidt, 1972
1.00E+06	H2CO3 + O2·- ==> CO2·- + HO2- + H+	Schmidt, 1972
1.00E+06	HCO3- + HO2· ==> CO3·- + HO2- + H+	Schmidt, 1972
1.00E+06	HCO3- + O2·- ==> CO3·- + HO2-	Schmidt, 1972
1.00E+06	CO3-2 + HO2· ==> CO3·- + HO2-	Schmidt, 1972
1.00E+06	CO3-2 + H+ + O2·- ==> CO3·- + HO2-	Schmidt, 1972
4.40E+04	HCO3- + H· ==> products	Nehari & Rabani, 1963
2.00E+03	CO2·- + HCO3- ==> HCO2- + CO3·-	Draganic et al., 1991
1.40E+05	HCO2- + CO3·- ==> HCO3- + CO2·-	AVG (Chen et al., 1973; Draganic et al., 1991; Lilie et al., 1978)
5.77E+05	H2O2 + CO3·- ==> HCO3- + HO2·	AVG (Eriksen et al., 1983; Draganic et al., 1991; Behar et al., 1970)
3.10E+05	HO2· + Fe(III) ==> H+ + Fe(II) + O2	Bielski et al., 1985
1.95E+10	eaq- + O2 ==> O2-	AVG (Elliot, 1989; Bielski et al., 1985)
2.20E+10	eaq- + H+ ==> H·	Bielski et al., 1985
2.00E+10	H· + O2 ==> HO2·	Bielski et al., 1985
1.30E+08	HCO2- + H· ==> CO2·- + H2	Bielski et al., 1985
2.40E+09	CO2·- + O2 ==> CO2 + O2·-	Bielski et al., 1985
2.15E+07	CO3·- + Mn(II) ==> MnCO3+	AVG (Cope et al., 1978; Ferraudi & Perkovic, 1993)
2.00E+06	C2O4·- ==> CO2 + CO2·-	Mulazzani et al., 1986
1.50E+08	Fe(III) + O2·- ==> O2+ Fe(II)	Balmer & Sulzberger, 1999
3.30E+05	Fe(III) + HO2· ==> O2 + Fe(II) + H+	Graedel & Mandich, 1986
1.00E+06	FeC2O4plus + O2·- ==> O2 + FeC2O4	Sedlack & Hoigne, 1993
1.00E+06	Fe(C2O4)2- + O2·- ==> O2 + Fe(C2O4)2-2	Sedlack & Hoigne, 1993
1.00E+06	Fe(C2O4)3-3 + O2·- ==> O2 + Fe(C2O4)3-4	Sedlack & Hoigne, 1993
1.20E+05	FeC2O4plus + HO2· ==> O2 + FeC2O4	Sedlack & Hoigne, 1993
1.20E+05	Fe(C2O4)2- + HO2· ==> O2 + Fe(C2O4)2-2	Sedlack & Hoigne, 1993
1.20E+05	Fe(C2O4)3-3 + HO2· ==> O2 + Fe(C2O4)3-4	Sedlack & Hoigne, 1993
8.00E+09	FeC2O4plus + CO2·- ==> CO2 + FeC2O4	Joeng & Yoon, 2004
8.00E+09	Fe(C2O4)2- + CO2·- ==> CO2 + Fe(C2O4)2-2	Joeng & Yoon, 2004
8.00E+09	Fe(C2O4)3-3 + CO2·- ==> CO2 + Fe(C2O4)3-4	Joeng & Yoon, 2004
7.20E+08	Fe(II) + O2·- + H+ ==> Fe(III) + H2O2 + OH-	Matthews, 1983
7.20E+05	Fe(II) + HO2· ==> Fe(III) + H2O2 + OH-	Graedel & Mandich, 1986
6.30E+01	Fe(II) + H2O2 ==> Fe(III) + ·OH + OH-	Hartwick, 1957
3.10E+04	FeC2O4 + H2O2 ==> FeC2O4plus + ·OH + OH-	Sedlack & Hoigne, 1993
9.70E+07	HO2· + O2·- ==> HO2- + O2	Bielski et al., 1985
1.00E+10	Fe(III) + C2O4-2 ==> FeC2O4plus	Faust and Zepp, 1993
3.98E+00	FeC2O4plus ==> Fe(III) + C2O4-2	Faust and Zepp, 1993
1.00E+10	FeC2O4plus + C2O4-2 ==> Fe(C2O4)2-	Faust and Zepp, 1993
1.59E+03	Fe(C2O4)2- ==> C2O4-2 + FeC2O4plus	Faust and Zepp, 1993

k (M^{-1} s^{-1})	Reaction	Source
1.00E+10	Fe(C2O4)2- + C2O4-2 ==> Fe(C2O4)3-3	Faust and Zepp, 1993
2.63E+05	Fe(C2O4)3-3 ==> Fe(C2O4)2- + C2O4-2	Faust and Zepp, 1993
1.00E+10	Fe(II) + C2O4-2 ==> FeC2O4	Faust and Zepp, 1993
5.00E+04	FeC2O4 ==> Fe(II) + C2O4-2	Faust and Zepp, 1993
1.00E+10	FeC2O4 + C2O4-2 ==> Fe(C2O4)2-2	Faust and Zepp, 1993
7.94E+07	Fe(C2O4)2-2 ==> FeC2O4 + C2O4-2	Faust and Zepp, 1993
1.00E+10	HC2O4+ ==> C2O4-2 + H+	Zuo & Hoigne, 1992
1.62E+14	C2O4-2 + H+ ==> HC2O4+	Zuo & Hoigne, 1992
4.30E+05	H2CO2 + H· ==> ·CO2H + H2	AVG (Hart & Boag, 1962; Buxton et al., 1988; Neta et al., 1971)
5.50E+02	H2O + H· ==> ·OH + H2	Hartig & Getoff, 1982
2.40E+10	eaq- + H· ==> OH- + H2	Christensen et al., 1994
5.75E+09	eaq- + eaq- ==> OH- + H2	AVG (Gordon et al., 1963; Schmidt & Bartels, 1995; Telser & Schindewolf, 1986; Hickel & Sehested, 1985)
7.80E+09	H· + H· ==> H2	Pagsberg et al., 1969
4.30E+01	2,5-DMHQ + FeC2O4plus ==> 2,5-DMHQ· + Fe(II) + H+ + C2O4-2	Suzuki et al., 2006
4.30E+01	2,5-DMHQ + Fe(C2O4)2- ==> 2,5-DMHQ· + Fe(II) + H+ + 2C2O4-2	Suzuki et al., 2006
4.30E+01	2,5-DMHQ + Fe(C2O4)3-3 ==> 2,5-DMHQ· + Fe(II) + H+ + 3C2O4-2	Suzuki et al., 2006
4.50E+03	2,5-DMHQ + Fe(III) ==> Fe(II) + H+ + 2,5-DMHQ·	Varela & Tien, 2003
1.00E+00	Q·- + H+ ==> Q·	Adams & Michael, 1967
8.33E+05	Q· ==> Q·- + H+	Adams & Michael, 1967
7.81E-01	2Q·- ==> Q + HQ-2	Adams & Michael, 1967
1.00E+00	Q + HQ-2 ==> 2Q·-	Adams & Michael, 1967
1.64E-01	2,5-DMHQ ==> 2,5-DMBQ + 2H+	Huang et al., 1984
1.12E-03	2,5-DMBQ + 2H+ ==> 2,5-DMHQ	Huang et al., 1984
1.30E+03	Q + HQ ==> 2Q·- + 2H+	Roginsky et al., 1999
1.60E-08	2Q·- + 2H+ ==> Q + HQ	Roginsky et al., 1999
2.30E+10	eaq- + Q ==> Q·-	Milosavljevic & Micic, 1978
8.30E+09	H· + Q ==> Q·	Willson, 1971
9.35E+08	O2·- + Q ==> O2 + Q·-	AVG (Willson, 1971; Greenstock & Ruddock, 1976; Simic & Hayon, 1973; Rao & Hayon, 1973)
4.60E+04	HQ ==> Q·	Adams & Michael, 1967
5.00E+05	eaq- + K+ ==> products	Baxendale et al., 1964
5.00E+09	Cu+ + H· ==> CuH+	Mulac & Meyerstein, 1982
9.40E+09	Cu+ + 2H+ + O2·- ==> H2O2 + Cu(II)	von Piechowski et al., 1993
1.00E+10	Cu+ + CO2·- ==> CuCO2	Ershov et al., 1991
1.30E+07	Fe(III) + Cu+ ==> Fe(II) + Cu(II)	Bjergbakke et al., 1976

k (M^{-1} s^{-1})	Reaction	Source
4.70E+03	H2O2 + Cu+ ==> HCuO2	Kozlov & Berdnikov, 1973
2.30E+09	H2O + HO2· + Cu+ ==> H2O2 + Cu(II) + OH-	Kozlov & Berdnikov, 1973
1.00E+10	2H2O + Cu+ + O2·- ==> H2O2 + Cu(II) + 2OH-	Rabani et al., 1973
4.60E+05	O2 + Cu+ ==> Cu(II) + O2·-	Bjergbakke et al., 1976
2.70E+10	eaq- + Cu+ ==> Cu	Sukhov et al., 1986
1.50E+08	Cu(II) + Cl2·- ==> products	Storer et al., 1975
2.50E+08	Zn+ + Cu(II) ==> Cu+ + Zn(II)	Meyerstein & Mulac, 1968
1.00E+04	CO3·- + Cu(II) ==> products	Cope et al., 1978
1.20E+09	HO2· + Cu(II) ==> O2 + Cu+ + H+	Cabelli et al., 1987
5.00E+08	CuCO2 + Cu(II) ==> 2Cu+ + CO2	Ershov et al., 1991
1.00E+08	CuCO2 + Cu+ ==> Cu2+ + CO2	Ershov et al., 1991
3.00E+07	CuCO2 + O2 ==> products	Das & Johnson, 1980
1.08E+09	Cu(II) + CO2·- ==> Cu+ + CO2	AVG (Ilan et al., 1978; Ershov et al., 1991)
8.00E+09	Cu(II) + O2·- ==> O2 + Cu+	Rabani et al., 1973
7.30E+07	Cu(II) + H· ==> Cu+ + H+	AVG (Baxendale & Hughes, 1988; Buxton et al., 1988; Johnson & Nazhat, 1984; Freiberg & Meyerstein, 1968; Baxendale et al., 1968)
4.50E+10	eaq- + Cu(II) ==> Cu+	Peled & Czapski, 1970
1.00E+04	Zn(II) + CO3·- ==> products	Cope et al., 1978
3.00E+05	Zn(II) + H· ==> products	Hayon & Moreau, 1965
3.50E+08	2Zn+ ==> Zn + Zn(II)	Rabani et al., 1977
4.00E+09	Zn+ + CO2·- ==> HCO2- + Zn(II)	Rabani et al., 1977
1.00E+06	Zn+ + H+ ==> products	Meyerstein & Mulac, 1968
1.90E+09	Zn+ + H· ==> ZnH+	Rabani et al., 1977
3.00E+09	Zn+ + Q ==> Q·- + Zn(II)	Sellers & Simic, 1976
2.17E+09	H2O2 + Zn+ ==> ·OH + Zn(II) + OH-	AVG (Meyerstein & Mulac, 1968; Rabani et al., 1977; Buxton et al., 1976)
2.85E+09	O2 + Zn+ ==> Zn(II) + O2·-	AVG (Baxendale et al., 1966; Meyerstein & Mulac, 1968)
1.01E+04	Zn(II) + CO2·- ==> products	AVG (Rabani et al., 1977; Buxton & Sellers, 1975)
8.44E+08	eaq- + Zn(II) ==> Zn+	AVG (Anbar & Hart, 1965; Rabani et al., 1977; Blum & Grossweiner, 1982)
1.50E+10	Cr(IV) + H· ==> products	Sharpe & Sehested, 1989
1.10E+09	Cr(II) + CO2·- ==> Cr(III)CO2-	Ellis et al., 1973
1.50E+09	Cr(II) + H· ==> Cr(III)H	Cohen & Meyerstein, 1974
7.06E+04	H2O2 + Cr(II) ==> Cr(III)OH + ·OH	Bakac & Espenson, 1983
1.50E+10	eaq- + Cr(II) ==> Cr+	Cohen & Meyerstein, 1974
4.87E+10	eaq- + Cr(III) ==> products	AVG (Anbar & Hart, 1965; Baxendale et al., 1965)
4.17E+05	Cr(IV) + HO2· ==> products	AVG (Sharpe & Sehested, 1989; Al-Sheikhly & McLaughlin, 1991)
1.70E+08	O2 + Cr(II) ==> Cr(III)O2	AVG (Sellers & Simic, 1976; Ilan et al. 1975)
3.20E+08	Cr(II) + Q ==> Q·- + Cr(III)	Sellers & Simic, 1976

k (M^{-1} s^{-1})	Reaction	Source
1.57E+04	Cr(III)H + H+ ==> Cr(III) + H2	AVG (Cohen & Meyerstein, 1974; Ryan & Espenson, 1981; Mulac et al., 1982)
1.30E+03	H2O + Cl2·- ==> H2ClO + Cl-	McElroy, 1990
1.90E+06	HCO2- + Cl2·- ==> Cl- + Cl- + CO2·- + H+	Hasegawa & Neta, 1978
6.70E+03	H2CO2 + Cl2·- ==> products	Hasegawa & Neta, 1978
2.40E+09	Cr(II) + Cl2·- ==> Cl- + Cl- + Cr(III)	Laurence & Thornton, 1974
8.50E+06	Mn(II) + Cl2·- ==> Mn(III)Cl + Cl-	Ferraudi, 1993
8.50E+06	Mn(II) + Cl2·- ==> Mn(III) + 2Cl-	Laurence & Thornton, 1973
1.00E+07	Fe(II) + Cl2·- ==> Fe(III) + 2Cl-	Thornton & Laurence, 1973
4.50E+07	OH- + Cl2·- ==> HOCl- + Cl-	Grigor'ev et al., 1987
1.50E+09	Cl2·- + HQ ==> Q·- + 2Cl- + H+	Hasegawa & Neta, 1978
2.00E+09	Cl2·- + O2·- ==> O2 + 2Cl-	Zhestkova & Pikaev, 1974
3.00E+09	HOCl + Cl· ==> Cl- + ClO· + H+	Klaning & Wolff, 1985
7.50E+06	HOCl + O2·- ==> O2 + ·OH + Cl-	Long & Bielski, 1980
1.00E+04	HOCl- + Cl- ==> OH- + Cl2·-	Grigor'ev et al., 1987
1.00E+06	HCO2- + ClO· ==> products	Alfassi et al., 1988
6.00E+02	CO3-2 + ClO· ==> CO3·- + ClO-	Huie et al., 1991
1.00E+06	eaq- + Cl- ==> products	Thomas et al., 1964
1.00E+05	Cl- + H· ==> products	Draganic & Draganic, 1972
1.40E+05	H2O2 + Cl2·- ==> products	Hasegawa & Neta, 1978
2.83E+09	HO2· + Cl2·- ==> O2 + 2Cl- + H+	AVG (Gilbert et al., 1977; Gogolev et al., 1984; Navaratnam et al., 1980)
1.87E+07	Fe(II) + Cl2·- ==> Cl- + Fe(III)Cl	AVG (Ward & Kuo, 1968; Thorton & Laurence, 1973; Jayson et al., 1973)
8.00E+09	Cl2·- + H· ==> 2Cl- + H+	Lierse et al., 1987
1.00E+09	Cl2·- + HQ ==> Q· + 2Cl- + H+	Willson, 1973
2.35E+09	Fe(III)Cl + H· ==> Cl- + Fe(II) + H+	AVG (Schwarz, 1957; Navon & Stein, 1966)
5.00E+09	ClO· + ClO· ==> products	AVG (Buxton & Subhani, 1972; Klaning & Wolff, 1985)
1.45E+10	Cl· + Cl- ==> Cl2·-	AVG (Jayson et al., 1973; Nagarajan & Fessenden, 1985)
1.11E+05	Cl2·- ==> Cl· + Cl-	Jayson et al., 1973
3.78E+09	Cl2·- + Cl2·- ==> Cl3- + Cl-	AVG (Langmuir & Hayon, 1967; Ferraudi, 1993; McElroy, 1990; Lierse et al., 1987; Ward & Kuo, 1968)
1.00E+10	HSO4- ==> SO4-2 + H+	CRC Handbook, 2008
9.77E+11	SO4-2 + H+ ==> HSO4-	CRC Handbook, 2008
1.30E+09	Zn+ + S2O8-2 ==> Zn(II) + SO4-2 + SO4·-	Buxton et al., 1976
1.00E+05	S2O8-2 + CO2·- ==> SO4-2 + CO2 + SO4·-	Buxton et al., 1990
1.40E+07	S2O8-2 + H· ==> HSO4 + SO4-2	Matthews et al., 1970
1.20E+07	H2O2 + SO4·- ==> HO2· + HSO4-	Wine et al., 1989
1.20E+07	H2O2 + SO4·- ==> HO2· + SO4-2 + H+	Maruthamuthu & Neta, 1978
3.50E+09	HO2· + SO4·- ==> O2 + HSO4-	Jiang et al., 1992

k (M^{-1} s^{-1})	Reaction	Source
1.00E+10	H· + SO4·- ==> HSO4-	Jiang et al., 1992
8.40E+09	eaq- + HSO5- ==> ·OH + SO4-2	Roebke et al., 1969
1.00E+05	HSO5- + SO4·- ==> HSO4- + SO5·-	Maruthamuthu & Neta, 1977
3.00E+00	H2O + Fe(II) + SO5·- ==> Fe(III)OH + HSO5-	Warneck & Ziajka, 1995
5.00E+07	HO2· + SO5·- ==> O2 + HSO5-	Yermakov et al., 1995
2.70E+06	SO5·- + HQ ==> Q·- + H+ + HSO5-	Huie & Neta, 1985
3.50E+08	SO4·- + Q ==> Q(OH)·	Al-Suhybani & Hughes, 1986
2.10E+09	eaq- + SO3·- ==> OH- + SO3-2	Hornak, 1982
5.50E+08	CO3·- + SO3·- ==> SO4-2 + CO2	Lilie et al., 1978
1.80E+08	SO3·- + SO3·- ==> S2O6-2	Waygood & McElroy, 1992
3.90E+08	SO3·- + SO3·- ==> SO3 + SO3-2	AVG (Hayon et al., 1972; Waygood & McElroy, 1992; Buxton et al., 1990)
2.50E+08	Cl· + SO4-2 ==> Cl- + SO4·-	Huie et al. 1991
1.23E+10	eaq- + S2O8-2 ==> SO4-2 + SO4·-	AVG (Roebke et al., 196; Hentz et al., 1972; Buxton et al., 1988)
6.33E+05	S2O8-2 + SO4·- ==> S2O8- + SO4-2	AVG (McElroy & Waygood, 1990; Herrmann et al., 1995; Jiang et al., 1992)
1.25E+09	HSO3- + SO4·- ==> SO4-2 + H+ + SO3·-	AVG (Hayon et al., 1972; Neta & Huie, 1986)
8.60E+08	SO3-2 + SO4·- ==> SO4-2 + SO3·-	AVG (Hayon et al., 1972; Deister & Warneck, 1990; Neta & Huie, 1986)
2.00E+07	Mn(II) + SO4·- ==> Mn(III) + SO4-2	AVG (Gogolev et al., 1986; Neta & Huie, 1986)
6.45E+08	Fe(II) + SO4·- ==> Fe(III)SO4	AVG (Heckel et al., 1966; McElroy & Waygood, 1990)
9.10E+08	SO5·- + SO5·- ==> O2 + SO4·- + SO4·-	Yermakov et al., 1993
1.40E+08	HCO2- + SO4·- ==> SO4-2 + CO2·- + H+	AVG (Redpath & Willson, 1975; Wine et al., 1989)
9.30E+05	H2CO2 + SO4·- ==> ·CO2H + SO4-2 + H+	AVG (Dogliotti & Hayon, 1967; Wine et al., 1989)
1.00E+06	eaq- + SO4-2 ==> products	AVG (Baxendale et al., 1964; Thomas et al., 1964)
7.65E+02	H2O + SO4·- ==> ·OH + SO4-2 + H+	AVG (Hayon et al., 1972; Herrmann et al., 1995; McElroy & Waygood, 1990; Tang et al., 1988)
1.30E+08	SO5·- + SO5·- ==> O2 + S2O8-2	Herrmann et al., 1995
2.30E+08	Cl- + SO4·- ==> Cl· + SO4-2	AVG (Chawla & Fesssenden, 1975; Padmaja et al., 1993; Huie et al., 1991; McElroy, 1990; Huie & Clifton, 1990; Wine et al., 1989; Slama-Schwok & Rabani, 1986; Kim & Hamill, 1976)
4.77E+07	OH- + SO4·- ==> ·OH + SO4-2	AVG (Roebke et al., 1969; Herrmann et al., 1995; Redpath & Willson, 1975)
1.48E+09	O2 + SO3·- ==> SO5·-	AVG (Hayon et al., 1972; Buxton et al., 1990; Huie et al., 1989; Huie & Neta, 1984)
4.71E+08	SO4·- + SO4·- ==> S2O8-2	AVG (Herrmann et al., 1995; Huie & Clifton, 1993; Jiang et al., 1992; McElry & Waygood, 1990; Huie et al., 1989; Tang et al., 1988; Subhani & Kauser, 1978; Hayon & McGarvey, 1967; Dogliotti & Hayon, 1967)
1.40E+07	CO3·- + CO3·- ==> products	AVG (Chen et al., 1973; Weeks & Rabani, 1966; Czapski et al., 1994; Mandal et al., 1991; Huie & Clifton, 1990; Saini & Bhattacharyya, 1986; Simic & Hunter, 1984; Mulac et al., 1984; Klaning & Sehested, 1978; McGinniss & Kah, 1977; Zhestkova & Pikaev, 1976)
3.00E+07	C-2 + SO3·- ==> C·- + SO3-2	Huie & Neta, 1985
2.70E+06	SO5·- + C ==> C·- + H+ + HSO5-	Huie & Neta, 1985

k (M^{-1} s^{-1})	Reaction	Source
4.70E+04	HO2· + C ==> products	Bielski, 1983
1.75E+05	C + O2·- ==> products	AVG (Bielski, 1983; Deeble et al., 1988)
1.00E+10	H2C2O4 ==> HC2O4- + H+	CRC Handbook, 2008
1.78E+11	HC2O4- + H+ ==> H2C2O4	CRC Handbook, 2008
1.00E+10	HC2O4- ==> C2O4-2 + H+	CRC Handbook, 2008
6.46E+13	C2O4-2 + H+ ==> HC2O4-	CRC Handbook, 2008
1.00E+10	H2SO3 ==> HSO3- + H+	CRC Handbook, 2008
7.08E+11	HSO3- + H+ ==> H2SO3	CRC Handbook, 2008
1.00E+10	HSO3- ==> SO3-2 + H+	CRC Handbook, 2008
1.58E+17	SO3-2 + H+ ==> HSO3-	CRC Handbook, 2008
2.10E+07	CO3·- + SO3-2 ==> CO3-2 + SO3·-	AVG (Lilie et al., 1978; Huie et al., 1991)
3.00E+08	O·- + SO3-2 ==> OH- + SO3·-	Zagorski et al., 1971
8.20E+01	HO2· + SO3-2 ==> H2O2 + OH- + SO3·-	Sadat-Shafai et al., 1981
8.20E+01	O2·- + SO3-2 ==> H2O2 + OH- + SO3·-	Sadat-Shafai et al., 1981
1.30E+06	eaq- + SO3-2 ==> products	Anbar & Hart, 1968
1.26E+08	HQ- + SO3·- ==> Q·- + SO3-2	Huie & Neta, 1985
1.00E+10	H3PO4 ==> H2PO4- + H+	CRC Handbook, 2008
1.45E+12	H2PO4- + H+ ==> H3PO4	CRC Handbook, 2008
1.00E+10	H2PO4- ==> HPO4-2 + H+	CRC Handbook, 2008
1.62E+17	HPO4-2 + H+ ==> H2PO4-	CRC Handbook, 2008
1.00E+10	HPO4-2 ==> PO4-3 + H+	CRC Handbook, 2008
2.09E+22	PO4-3 + H+ ==> HPO4-2	CRC Handbook, 2008
8.00E+07	Glucose + HPO4·- ==> Glucose· + HPO4-2 + H+	Nakashima & Hayon, 1970
2.70E+07	H2O2 + HPO4·- ==> HPO4-2 + H+ + H+ + O2·-	Nakashima & Hayon, 1970
1.00E+04	HPO4·- + Cl- ==> products	Maruthamuthu & Neta, 1978
1.00E+04	HPO4·- + SO4-2 ==> products	Maruthamuthu & Neta, 1978
2.20E+07	HCO2- + PO4·-2 ==> CO2·- + HPO4-2	Maruthamuthu & Neta, 1977
1.50E+08	H2PO4· + HCO2- ==> CO2·- + H2PO4- + H+	Maruthamuthu & Neta, 1977
5.30E+09	eaq- + H2P2O8-2 ==> H2PO4· + H2PO4-	Levey & Hart, 1975
5.00E+05	H2PO4- + H· ==> HPO4·- + H2	Grabner et al., 1973
2.70E+07	HCO2- + HPO4·- ==> CO2·- + H2PO4-	AVG (Nakashima & Hayon, 1970; Maruthamuthu & Neta, 1977)
3.00E+08	HPO4·- + HPO4·- ==> P2O8-4 + H+ + H+	AVG (Black & Hayon, 1970; Grabner et al., 1973)
1.20E+08	PO4·-2 + PO4·-2 ==> P2O8-4	AVG (Black & Hayon, 1970; Grabner et al., 1973)
3.50E+05	PO4·-2 + OH- ==> ·OH + PO4-3	AVG (Grabner et al., 1973; Maruthamuthu & Neta, 1978)
7.00E+04	H2PO4- + SO4·- ==> products	Maruthamuthu & Neta, 1978
1.00E+09	eaq- + H3PO4 ==> H2PO4- + H·	Ye & Schuler, 1986
5.00E+05	H3PO4 + H· ==> H2PO4· + H2	Grabner et al., 1973
1.10E+08	Glucose + H2PO4· ==> Glucose· + H2PO4- + H+	Nakashima & Hayon, 1970

k (M^{-1} s^{-1})	Reaction	Source
	H2PO4· + H2O2 ==>	
5.50E+07	H2PO4- + H+ + H+ + O2·-	Nakashima & Hayon, 1970
2.20E+06	H2PO4· + Cl- ==> Cl· + H2PO4-	Maruthamuthu & Neta, 1978
1.90E+09	H2PO4· + Cl- + H+ ==> H3PO4 + Cl·	Jiang et al., 1992
1.40E+05	eaq- + HPO4-2 ==> products	Grabner et al., 1973
1.20E+06	HPO4-2 + SO4·- ==> HPO4·- + SO4-2	Maruthamuthu & Neta, 1978
3.50E+06	O·- + HPO4-2 ==> products	Grabner et al., 1973
5.00E+04	HPO4-2 + H· ==> PO4·-2 + H2	Grabner et al., 1973
1.20E+07	eaq- + H2PO4- ==> HPO4-2 + H·	Grabner et al., 1973
1.50E+09	H2PO4· + H2PO4· ==> H2P2O8-2 + 2H+	AVG (Black & Hayon, 1970; Grabner et al., 1973)
1.30E+05	H2PO4· + H2O ==> H3PO4 + ·OH	Jiang et al., 1992
1.00E-02	HCO2- + O2·- ==> products	Bielski & Richter, 1977
2.20E+10	eaq- + O·- ==> OH-	Matheson & Rabani, 1965
1.40E+09	HCO2- + O·- ==> products	Buxton, 1969
4.00E+08	HO2- + O·- ==> OH- + O2·-	Buxton et al., 1988
9.00E+08	O3·- + O3·- ==> products	Subhani & Kauser, 1978
9.00E+10	O3·- + H+ ==> O2 + ·OH	Sehested et al., 1984
5.20E+10	O3·- + H+ ==> HO3·	Buehler et al., 1984
7.00E+08	O·- + O3·- ==> O4-2	Gall & Dorfman, 1969
7.00E+08	O·- + O3·- ==> O2·- + O2·-	Sehested et al., 1982
8.00E+03	eaq- + HCO2- ==> products	Schwarz, 1992
9.30E+07	H2O + O·- ==> ·OH + OH-	Buxton, 1970
4.65E+09	O·- + O·- ==> O2-2	AVG (Adams et al., 1966; Rabani & Matheson, 1966)
3.40E+09	O2 + O·- ==> O3·-	AVG (Adams et al., 1966; Elliot & McCracken, 1989; Buxton et al., 1988; Klaning et al., 1981; Buxton et al., 1969)
4.28E+03	O3·- ==> O2 + O·-	AVG (Behar & Czapski, 1968; Elliot & McCracken, 1989)
3.50E+09	eaq- + HO2- ==> products	Felix et al., 1967
1.20E+09	HO2- + H· ==> ·OH + OH-	Mezyk & Bartels, 1995

Table S6.2 Material balance diagrams for pretreated and saccharified spruce wood powder.

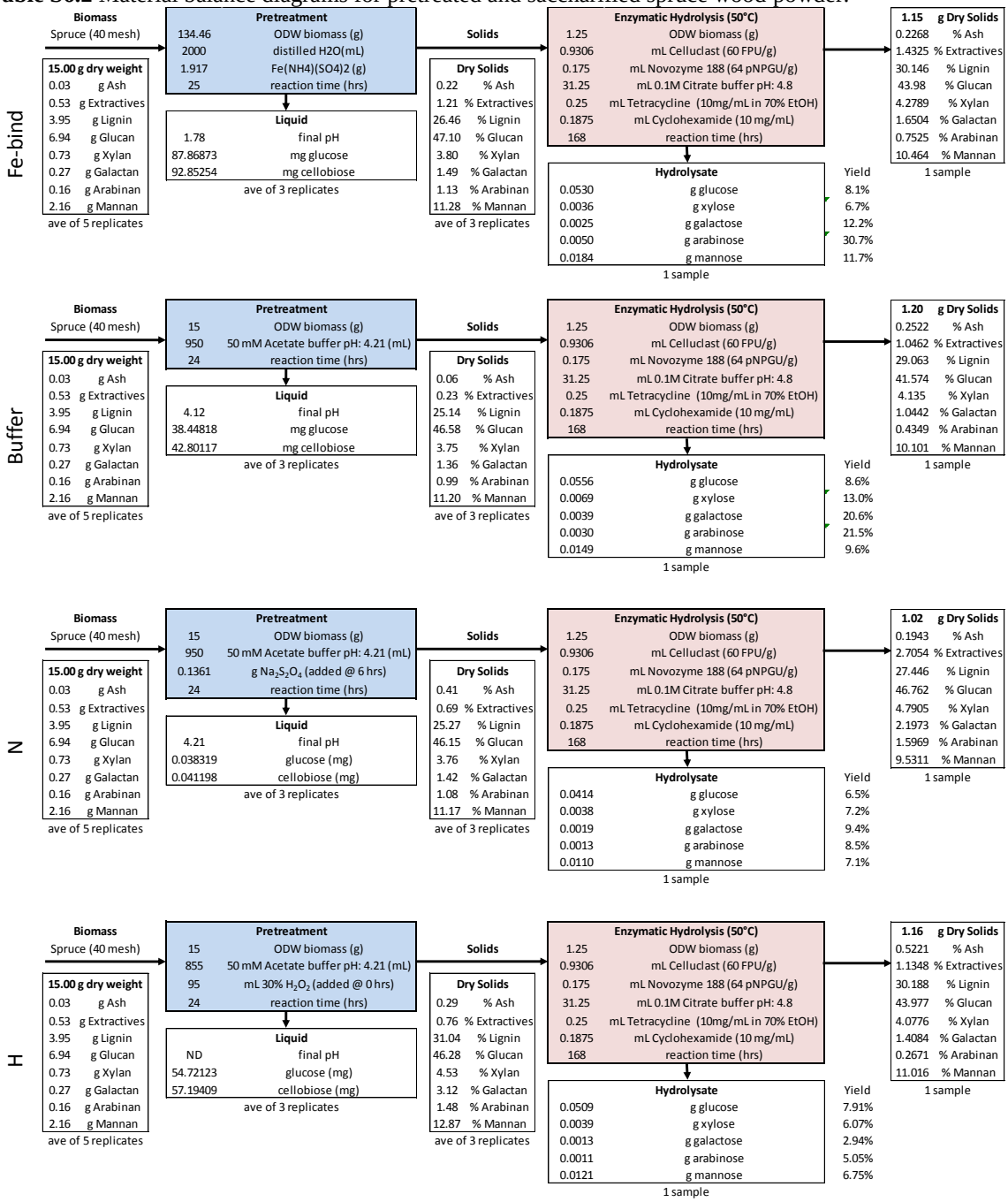

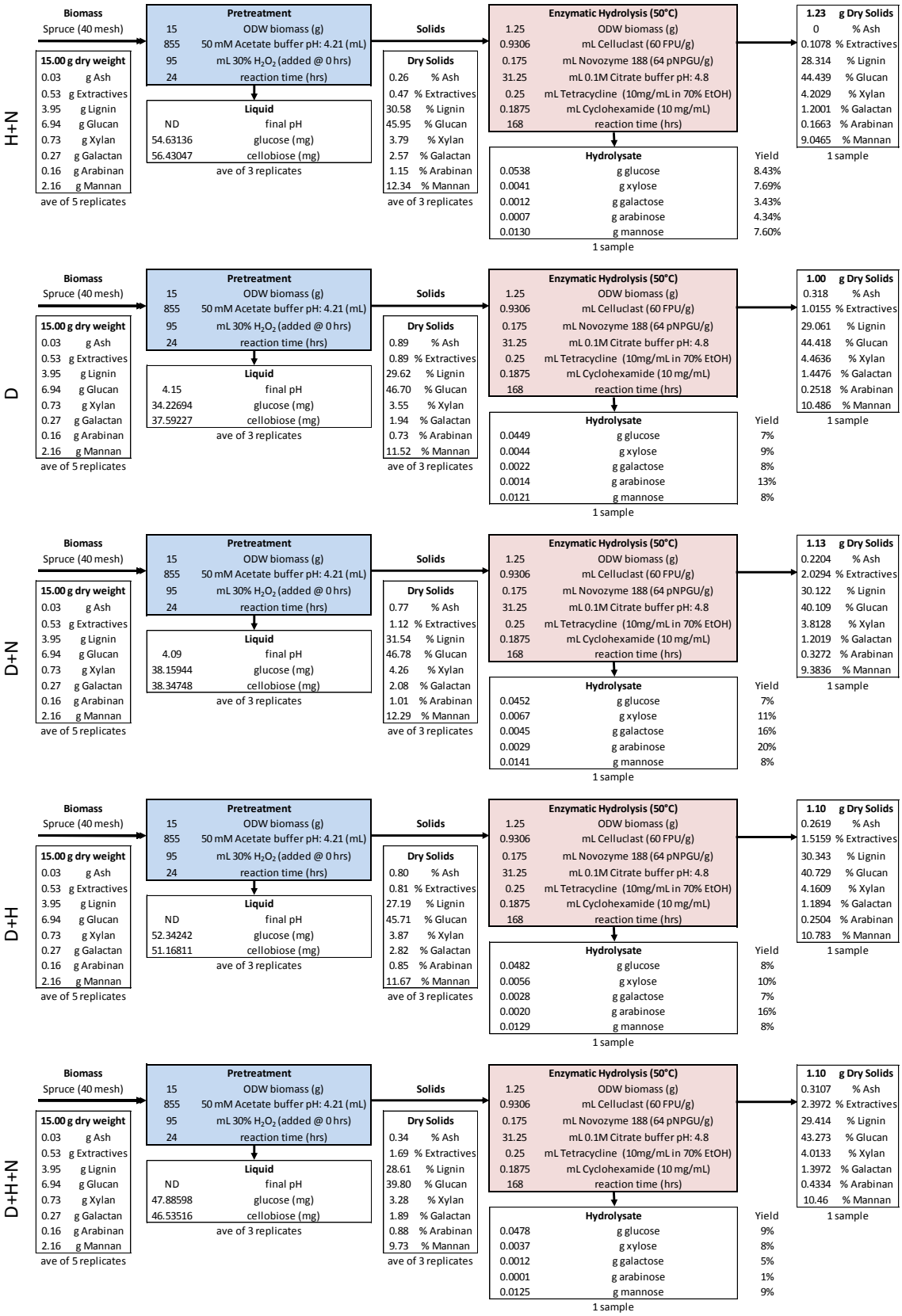
H+N
Biomass
Spruce (40 mesh)
15.00 g dry weight
0.03 g Ash
0.53 g Extractives
3.95 g Lignin
6.94 g Glucan
0.73 g Xylan
0.27 g Galactan
0.16 g Arabinan
2.16 g Mannan
ave of 5 replicates
Pretreatment
15 ODW biomass (g)
855 50 mM Acetate buffer pH: 4.21 (mL)
95 mL 30% H2O2 (added @ 0 hrs)
24 reaction time (hrs)
Liquid
ND final pH
54.63136 glucose (mg)
56.43047 cellobiose (mg)
ave of 3 replicates
Solids
Dry Solids
0.26 % Ash
0.47 % Extractives
30.58 % Lignin
45.95 % Glucan
3.79 % Xylan
2.57 % Galactan
1.15 % Arabinan
12.34 % Mannan
ave of 3 replicates
Enzymatic Hydrolysis (50°C)
1.25 ODW biomass (g)
0.9306 mL Celluclast (60 FPU/g)
0.175 mL Novozyme 188 (64 pNPGU/g)
31.25 mL 0.1M Citrate buffer pH: 4.8
0.25 mL Tetracycline (10mg/mL in 70% EtOH)
0.1875 mL Cyclohexamide (10 mg/mL)
168 reaction time (hrs)
Hydrolysate
0.0538 g glucose
0.0041 g xylose
0.0012 g galactose
0.0007 g arabinose
0.0130 g mannose
1 sample
Yield
8.43%
7.69%
3.43%
4.34%
7.60%
1.23 g Dry Solids
0 % Ash
0.1078 % Extractives
28.314 % Lignin
44.439 % Glucan
4.2029 % Xylan
1.2001 % Galactan
0.1663 % Arabinan
9.0465 % Mannan
1 sample
D
Biomass
Spruce (40 mesh)
15.00 g dry weight
0.03 g Ash
0.53 g Extractives
3.95 g Lignin
6.94 g Glucan
0.73 g Xylan
0.27 g Galactan
0.16 g Arabinan
2.16 g Mannan
ave of 5 replicates
Pretreatment
15 ODW biomass (g)
855 50 mM Acetate buffer pH: 4.21 (mL)
95 mL 30% H2O2 (added @ 0 hrs)
24 reaction time (hrs)
Liquid
4.15 final pH
34.22694 glucose (mg)
37.59227 cellobiose (mg)
ave of 3 replicates
Solids
Dry Solids
0.89 % Ash
0.89 % Extractives
29.62 % Lignin
46.70 % Glucan
3.55 % Xylan
1.94 % Galactan
0.73 % Arabinan
11.52 % Mannan
ave of 3 replicates
Enzymatic Hydrolysis (50°C)
1.25 ODW biomass (g)
0.9306 mL Celluclast (60 FPU/g)
0.175 mL Novozyme 188 (64 pNPGU/g)
31.25 mL 0.1M Citrate buffer pH: 4.8
0.25 mL Tetracycline (10mg/mL in 70% EtOH)
0.1875 mL Cyclohexamide (10 mg/mL)
168 reaction time (hrs)
Hydrolysate
0.0449 g glucose
0.0044 g xylose
0.0022 g galactose
0.0014 g arabinose
0.0121 g mannose
1 sample
Yield
7%
9%
8%
13%
8%
1.00 g Dry Solids
0.318 % Ash
1.0155 % Extractives
29.061 % Lignin
44.418 % Glucan
4.4636 % Xylan
1.4476 % Galactan
0.2518 % Arabinan
10.486 % Mannan
1 sample
D+N
Biomass
Spruce (40 mesh)
15.00 g dry weight
0.03 g Ash
0.53 g Extractives
3.95 g Lignin
6.94 g Glucan
0.73 g Xylan
0.27 g Galactan
0.16 g Arabinan
2.16 g Mannan
ave of 5 replicates
Pretreatment
15 ODW biomass (g)
855 50 mM Acetate buffer pH: 4.21 (mL)
95 mL 30% H2O2 (added @ 0 hrs)
24 reaction time (hrs)
Liquid
4.09 final pH
38.15944 glucose (mg)
38.34748 cellobiose (mg)
ave of 3 replicates
Solids
Dry Solids
0.77 % Ash
1.12 % Extractives
31.54 % Lignin
46.78 % Glucan
4.26 % Xylan
2.08 % Galactan
1.01 % Arabinan
12.29 % Mannan
ave of 3 replicates
Enzymatic Hydrolysis (50°C)
1.25 ODW biomass (g)
0.9306 mL Celluclast (60 FPU/g)
0.175 mL Novozyme 188 (64 pNPGU/g)
31.25 mL 0.1M Citrate buffer pH: 4.8
0.25 mL Tetracycline (10mg/mL in 70% EtOH)
0.1875 mL Cyclohexamide (10 mg/mL)
168 reaction time (hrs)
Hydrolysate
0.0452 g glucose
0.0067 g xylose
0.0045 g galactose
0.0029 g arabinose
0.0141 g mannose
1 sample
Yield
7%
11%
16%
20%
8%
1.13 g Dry Solids
0.2204 % Ash
2.0294 % Extractives
30.122 % Lignin
40.109 % Glucan
3.8128 % Xylan
1.2019 % Galactan
0.3272 % Arabinan
9.3836 % Mannan
1 sample
D+H
Biomass
Spruce (40 mesh)
15.00 g dry weight
0.03 g Ash
0.53 g Extractives
3.95 g Lignin
6.94 g Glucan
0.73 g Xylan
0.27 g Galactan
0.16 g Arabinan
2.16 g Mannan
ave of 5 replicates
Pretreatment
15 ODW biomass (g)
855 50 mM Acetate buffer pH: 4.21 (mL)
95 mL 30% H2O2 (added @ 0 hrs)
24 reaction time (hrs)
Liquid
ND final pH
52.34242 glucose (mg)
51.16811 cellobiose (mg)
ave of 3 replicates
Solids
Dry Solids
0.80 % Ash
0.81 % Extractives
27.19 % Lignin
45.71 % Glucan
3.87 % Xylan
2.82 % Galactan
0.85 % Arabinan
11.67 % Mannan
ave of 3 replicates
Enzymatic Hydrolysis (50°C)
1.25 ODW biomass (g)
0.9306 mL Celluclast (60 FPU/g)
0.175 mL Novozyme 188 (64 pNPGU/g)
31.25 mL 0.1M Citrate buffer pH: 4.8
0.25 mL Tetracycline (10mg/mL in 70% EtOH)
0.1875 mL Cyclohexamide (10 mg/mL)
168 reaction time (hrs)
Hydrolysate
0.0482 g glucose
0.0056 g xylose
0.0028 g galactose
0.0020 g arabinose
0.0129 g mannose
1 sample
Yield
8%
10%
7%
16%
8%
1.10 g Dry Solids
0.2619 % Ash
1.5159 % Extractives
30.343 % Lignin
40.729 % Glucan
4.1609 % Xylan
1.1894 % Galactan
0.2504 % Arabinan
10.783 % Mannan
1 sample
D+H+N
Biomass
Spruce (40 mesh)
15.00 g dry weight
0.03 g Ash
0.53 g Extractives
3.95 g Lignin
6.94 g Glucan
0.73 g Xylan
0.27 g Galactan
0.16 g Arabinan
2.16 g Mannan
ave of 5 replicates
Pretreatment
15 ODW biomass (g)
855 50 mM Acetate buffer pH: 4.21 (mL)
95 mL 30% H2O2 (added @ 0 hrs)
24 reaction time (hrs)
Liquid
ND final pH
47.88598 glucose (mg)
46.53516 cellobiose (mg)
ave of 3 replicates
Solids
Dry Solids
0.34 % Ash
1.69 % Extractives
28.61 % Lignin
39.80 % Glucan
3.28 % Xylan
1.89 % Galactan
0.88 % Arabinan
9.73 % Mannan
ave of 3 replicates
Enzymatic Hydrolysis (50°C)
1.25 ODW biomass (g)
0.9306 mL Celluclast (60 FPU/g)
0.175 mL Novozyme 188 (64 pNPGU/g)
31.25 mL 0.1M Citrate buffer pH: 4.8
0.25 mL Tetracycline (10mg/mL in 70% EtOH)
0.1875 mL Cyclohexamide (10 mg/mL)
168 reaction time (hrs)
Hydrolysate
0.0478 g glucose
0.0037 g xylose
0.0012 g galactose
0.0001 g arabinose
0.0125 g mannose
1 sample
Yield
9%
8%
5%
1%
9%
1.10 g Dry Solids
0.3107 % Ash
2.3972 % Extractives
29.414 % Lignin
43.273 % Glucan
4.0133 % Xylan
1.3972 % Galactan
0.4334 % Arabinan
10.46 % Mannan
1 sample

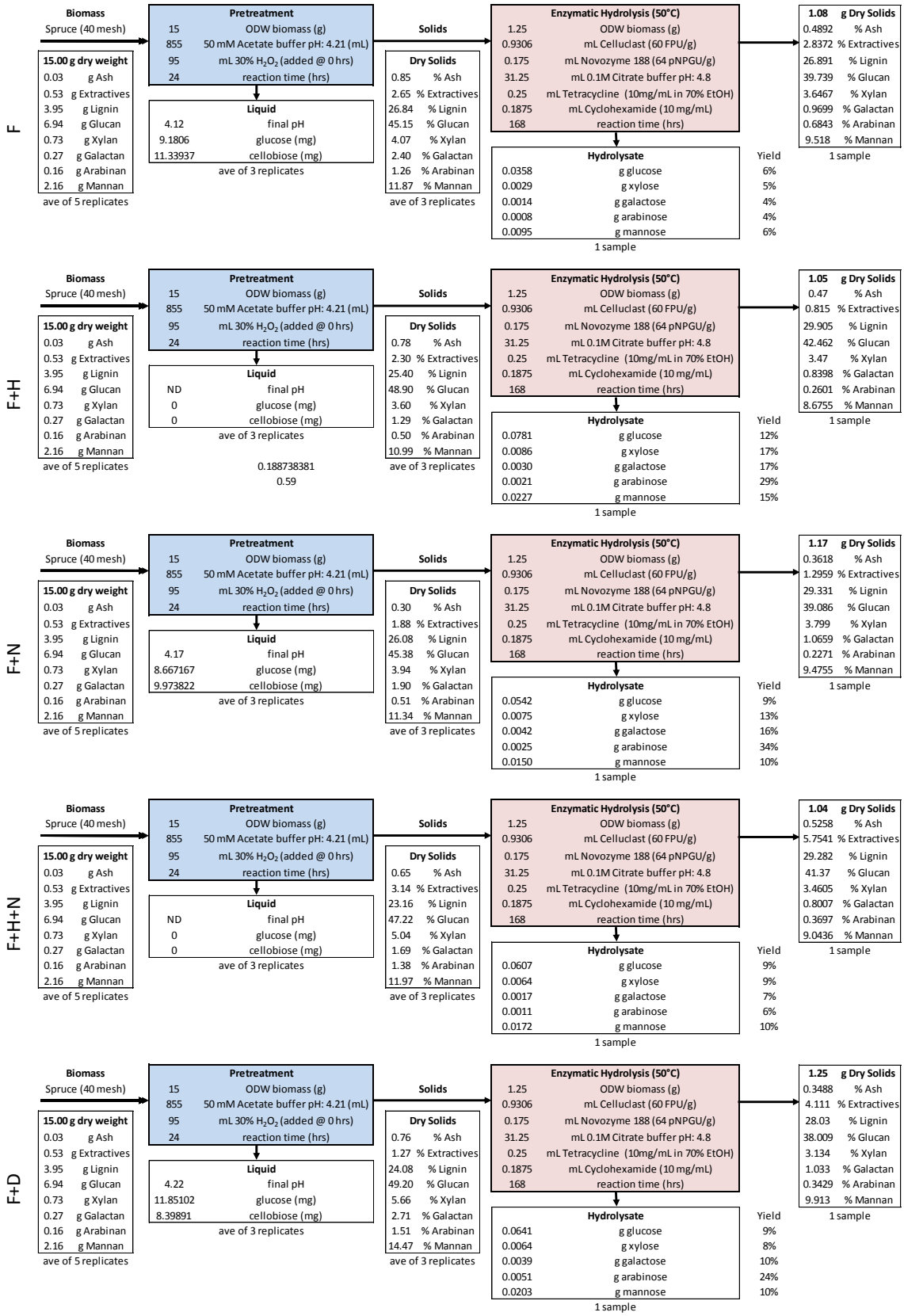
F
Biomass
Spruce (40 mesh)
15.00 g dry weight
0.03 g Ash
0.53 g Extractives
3.95 g Lignin
6.94 g Glucan
0.73 g Xylan
0.27 g Galactan
0.16 g Arabinan
2.16 g Mannan
ave of 5 replicates
Pretreatment
15 ODW biomass (g)
855 50 mM Acetate buffer pH: 4.21 (mL)
95 mL 30% H2O2 (added @ 0 hrs)
24 reaction time (hrs)
Liquid
4.12 final pH
9.1806 glucose (mg)
11.33937 cellobiose (mg)
ave of 3 replicates
Solids
Dry Solids
0.85 % Ash
2.65 % Extractives
26.84 % Lignin
45.15 % Glucan
4.07 % Xylan
2.40 % Galactan
1.26 % Arabinan
11.87 % Mannan
ave of 3 replicates
Enzymatic Hydrolysis (50°C)
1.25 ODW biomass (g)
0.9306 mL Celluclast (60 FPU/g)
0.175 mL Novozyme 188 (64 pNPGU/g)
31.25 mL 0.1M Citrate buffer pH: 4.8
0.25 mL Tetracycline (10mg/mL in 70% EtOH)
0.1875 mL Cyclohexamide (10 mg/mL)
168 reaction time (hrs)
Hydrolysate
0.0358 g glucose
0.0029 g xylose
0.0014 g galactose
0.0008 g arabinose
0.0095 g mannose
1 sample
Yield
6%
5%
4%
4%
6%
1.08 g Dry Solids
0.4892 % Ash
2.8372 % Extractives
26.891 % Lignin
39.739 % Glucan
3.6467 % Xylan
0.9699 % Galactan
0.6843 % Arabinan
9.518 % Mannan
1 sample
F+H
Biomass
Spruce (40 mesh)
15.00 g dry weight
0.03 g Ash
0.53 g Extractives
3.95 g Lignin
6.94 g Glucan
0.73 g Xylan
0.27 g Galactan
0.16 g Arabinan
2.16 g Mannan
ave of 5 replicates
Pretreatment
15 ODW biomass (g)
855 50 mM Acetate buffer pH: 4.21 (mL)
95 mL 30% H2O2 (added @ 0 hrs)
24 reaction time (hrs)
Liquid
ND final pH
0 glucose (mg)
0 cellobiose (mg)
ave of 3 replicates
0.188738381
0.59
Solids
Dry Solids
0.78 % Ash
2.30 % Extractives
25.40 % Lignin
48.90 % Glucan
3.60 % Xylan
1.29 % Galactan
0.50 % Arabinan
10.99 % Mannan
ave of 3 replicates
Enzymatic Hydrolysis (50°C)
1.25 ODW biomass (g)
0.9306 mL Celluclast (60 FPU/g)
0.175 mL Novozyme 188 (64 pNPGU/g)
31.25 mL 0.1M Citrate buffer pH: 4.8
0.25 mL Tetracycline (10mg/mL in 70% EtOH)
0.1875 mL Cyclohexamide (10 mg/mL)
168 reaction time (hrs)
Hydrolysate
0.0781 g glucose
0.0086 g xylose
0.0030 g galactose
0.0021 g arabinose
0.0227 g mannose
1 sample
Yield
12%
17%
17%
29%
15%
1.05 g Dry Solids
0.47 % Ash
0.815 % Extractives
29.905 % Lignin
42.462 % Glucan
3.47 % Xylan
0.8398 % Galactan
0.2601 % Arabinan
8.6755 % Mannan
1 sample
F+N
Biomass
Spruce (40 mesh)
15.00 g dry weight
0.03 g Ash
0.53 g Extractives
3.95 g Lignin
6.94 g Glucan
0.73 g Xylan
0.27 g Galactan
0.16 g Arabinan
2.16 g Mannan
ave of 5 replicates
Pretreatment
15 ODW biomass (g)
855 50 mM Acetate buffer pH: 4.21 (mL)
95 mL 30% H2O2 (added @ 0 hrs)
24 reaction time (hrs)
Liquid
4.17 final pH
8.667167 glucose (mg)
9.973822 cellobiose (mg)
ave of 3 replicates
Solids
Dry Solids
0.30 % Ash
1.88 % Extractives
26.08 % Lignin
45.38 % Glucan
3.94 % Xylan
1.90 % Galactan
0.51 % Arabinan
11.34 % Mannan
ave of 3 replicates
Enzymatic Hydrolysis (50°C)
1.25 ODW biomass (g)
0.9306 mL Celluclast (60 FPU/g)
0.175 mL Novozyme 188 (64 pNPGU/g)
31.25 mL 0.1M Citrate buffer pH: 4.8
0.25 mL Tetracycline (10mg/mL in 70% EtOH)
0.1875 mL Cyclohexamide (10 mg/mL)
168 reaction time (hrs)
Hydrolysate
0.0542 g glucose
0.0075 g xylose
0.0042 g galactose
0.0025 g arabinose
0.0150 g mannose
1 sample
Yield
9%
13%
16%
34%
10%
1.17 g Dry Solids
0.3618 % Ash
1.2959 % Extractives
29.331 % Lignin
39.086 % Glucan
3.799 % Xylan
1.0659 % Galactan
0.2271 % Arabinan
9.4755 % Mannan
1 sample
F+H+N
Biomass
Spruce (40 mesh)
15.00 g dry weight
0.03 g Ash
0.53 g Extractives
3.95 g Lignin
6.94 g Glucan
0.73 g Xylan
0.27 g Galactan
0.16 g Arabinan
2.16 g Mannan
ave of 5 replicates
Pretreatment
15 ODW biomass (g)
855 50 mM Acetate buffer pH: 4.21 (mL)
95 mL 30% H2O2 (added @ 0 hrs)
24 reaction time (hrs)
Liquid
ND final pH
0 glucose (mg)
0 cellobiose (mg)
ave of 3 replicates
Solids
Dry Solids
0.65 % Ash
3.14 % Extractives
23.16 % Lignin
47.22 % Glucan
5.04 % Xylan
1.69 % Galactan
1.38 % Arabinan
11.97 % Mannan
ave of 3 replicates
Enzymatic Hydrolysis (50°C)
1.25 ODW biomass (g)
0.9306 mL Celluclast (60 FPU/g)
0.175 mL Novozyme 188 (64 pNPGU/g)
31.25 mL 0.1M Citrate buffer pH: 4.8
0.25 mL Tetracycline (10mg/mL in 70% EtOH)
0.1875 mL Cyclohexamide (10 mg/mL)
168 reaction time (hrs)
Hydrolysate
0.0607 g glucose
0.0064 g xylose
0.0017 g galactose
0.0011 g arabinose
0.0172 g mannose
1 sample
Yield
9%
9%
7%
6%
10%
1.04 g Dry Solids
0.5258 % Ash
5.7541 % Extractives
29.282 % Lignin
41.37 % Glucan
3.4605 % Xylan
0.8007 % Galactan
0.3697 % Arabinan
9.0436 % Mannan
1 sample
F+D
Biomass
Spruce (40 mesh)
15.00 g dry weight
0.03 g Ash
0.53 g Extractives
3.95 g Lignin
6.94 g Glucan
0.73 g Xylan
0.27 g Galactan
0.16 g Arabinan
2.16 g Mannan
ave of 5 replicates
Pretreatment
15 ODW biomass (g)
855 50 mM Acetate buffer pH: 4.21 (mL)
95 mL 30% H2O2 (added @ 0 hrs)
24 reaction time (hrs)
Liquid
4.22 final pH
11.85102 glucose (mg)
8.39891 cellobiose (mg)
ave of 3 replicates
Solids
Dry Solids
0.76 % Ash
1.27 % Extractives
24.08 % Lignin
49.20 % Glucan
5.66 % Xylan
2.71 % Galactan
1.51 % Arabinan
14.47 % Mannan
ave of 3 replicates
Enzymatic Hydrolysis (50°C)
1.25 ODW biomass (g)
0.9306 mL Celluclast (60 FPU/g)
0.175 mL Novozyme 188 (64 pNPGU/g)
31.25 mL 0.1M Citrate buffer pH: 4.8
0.25 mL Tetracycline (10mg/mL in 70% EtOH)
0.1875 mL Cyclohexamide (10 mg/mL)
168 reaction time (hrs)
Hydrolysate
0.0641 g glucose
0.0064 g xylose
0.0039 g galactose
0.0051 g arabinose
0.0203 g mannose
1 sample
Yield
9%
8%
10%
24%
10%
1.25 g Dry Solids
0.3488 % Ash
4.111 % Extractives
28.03 % Lignin
38.009 % Glucan
3.134 % Xylan
1.033 % Galactan
0.3429 % Arabinan
9.913 % Mannan
1 sample

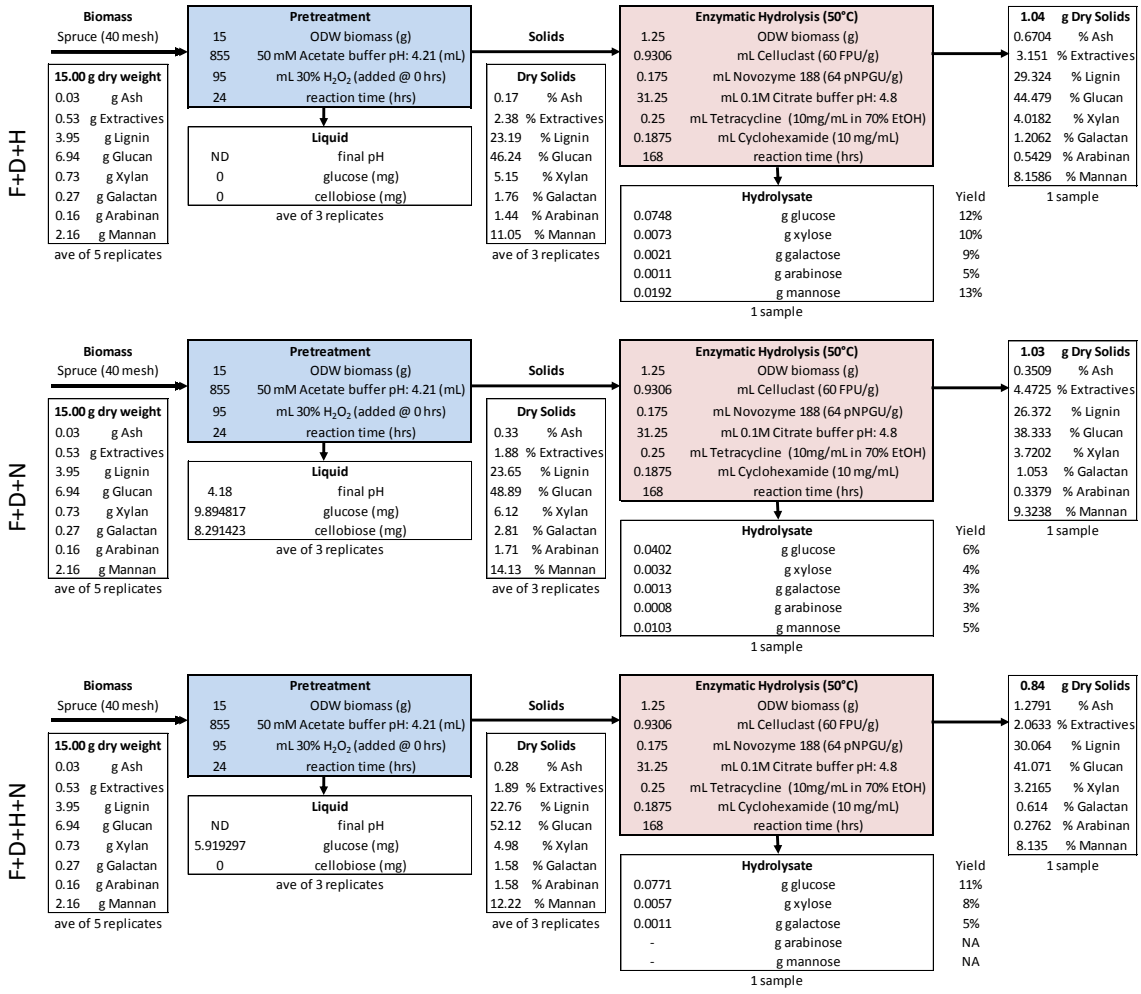
F+D+H
Biomass
Spruce (40 mesh)
15.00 g dry weight
0.03 g Ash
0.53 g Extractives
3.95 g Lignin
6.94 g Glucan
0.73 g Xylan
0.27 g Galactan
0.16 g Arabinan
2.16 g Mannan
ave of 5 replicates
Pretreatment
15 ODW biomass (g)
855 50 mM Acetate buffer pH: 4.21 (mL)
95 mL 30% H2O2 (added @ 0 hrs)
24 reaction time (hrs)
Liquid
ND final pH
0 glucose (mg)
0 cellobiose (mg)
ave of 3 replicates
Solids
Dry Solids
0.17 % Ash
2.38 % Extractives
23.19 % Lignin
46.24 % Glucan
5.15 % Xylan
1.76 % Galactan
1.44 % Arabinan
11.05 % Mannan
ave of 3 replicates
Enzymatic Hydrolysis (50°C)
1.25 ODW biomass (g)
0.9306 mL Celluclast (60 FPU/g)
0.175 mL Novozyme 188 (64 pNPGU/g)
31.25 mL 0.1M Citrate buffer pH: 4.8
0.25 mL Tetracycline (10mg/mL in 70% EtOH)
0.1875 mL Cyclohexamide (10 mg/mL)
168 reaction time (hrs)
Hydrolysate
Yield
0.0748 g glucose 12%
0.0073 g xylose 10%
0.0021 g galactose 9%
0.0011 g arabinose 5%
0.0192 g mannose 13%
1 sample
1.04 g Dry Solids
0.6704 % Ash
3.151 % Extractives
29.324 % Lignin
44.479 % Glucan
4.0182 % Xylan
1.2062 % Galactan
0.5429 % Arabinan
8.1586 % Mannan
1 sample
F+D+N
Biomass
Spruce (40 mesh)
15.00 g dry weight
0.03 g Ash
0.53 g Extractives
3.95 g Lignin
6.94 g Glucan
0.73 g Xylan
0.27 g Galactan
0.16 g Arabinan
2.16 g Mannan
ave of 5 replicates
Pretreatment
15 ODW biomass (g)
855 50 mM Acetate buffer pH: 4.21 (mL)
95 mL 30% H2O2 (added @ 0 hrs)
24 reaction time (hrs)
Liquid
4.18 final pH
9.894817 glucose (mg)
8.291423 cellobiose (mg)
ave of 3 replicates
Solids
Dry Solids
0.33 % Ash
1.88 % Extractives
23.65 % Lignin
48.89 % Glucan
6.12 % Xylan
2.81 % Galactan
1.71 % Arabinan
14.13 % Mannan
ave of 3 replicates
Enzymatic Hydrolysis (50°C)
1.25 ODW biomass (g)
0.9306 mL Celluclast (60 FPU/g)
0.175 mL Novozyme 188 (64 pNPGU/g)
31.25 mL 0.1M Citrate buffer pH: 4.8
0.25 mL Tetracycline (10mg/mL in 70% EtOH)
0.1875 mL Cyclohexamide (10 mg/mL)
168 reaction time (hrs)
Hydrolysate
Yield
0.0402 g glucose 6%
0.0032 g xylose 4%
0.0013 g galactose 3%
0.0008 g arabinose 3%
0.0103 g mannose 5%
1 sample
1.03 g Dry Solids
0.3509 % Ash
4.4725 % Extractives
26.372 % Lignin
38.333 % Glucan
3.7202 % Xylan
1.053 % Galactan
0.3379 % Arabinan
9.3238 % Mannan
1 sample
F+D+H+N
Biomass
Spruce (40 mesh)
15.00 g dry weight
0.03 g Ash
0.53 g Extractives
3.95 g Lignin
6.94 g Glucan
0.73 g Xylan
0.27 g Galactan
0.16 g Arabinan
2.16 g Mannan
ave of 5 replicates
Pretreatment
15 ODW biomass (g)
855 50 mM Acetate buffer pH: 4.21 (mL)
95 mL 30% H2O2 (added @ 0 hrs)
24 reaction time (hrs)
Liquid
ND final pH
5.919297 glucose (mg)
0 cellobiose (mg)
ave of 3 replicates
Solids
Dry Solids
0.28 % Ash
1.89 % Extractives
22.76 % Lignin
52.12 % Glucan
4.98 % Xylan
1.58 % Galactan
1.58 % Arabinan
12.22 % Mannan
ave of 3 replicates
Enzymatic Hydrolysate (50°C)
1.25 ODW biomass (g)
0.9306 mL Celluclast (60 FPU/g)
0.175 mL Novozyme 188 (64 pNPGU/g)
31.25 mL 0.1M Citrate buffer pH: 4.8
0.25 mL Tetracycline (10mg/mL in 70% EtOH)
0.1875 mL Cyclohexamide (10 mg/mL)
168 reaction time (hrs)
Hydrolysate
Yield
0.0771 g glucose 11%
0.0057 g xylose 8%
0.0011 g galactose 5%
- g arabinose NA
- g mannose NA
1 sample
0.84 g Dry Solids
1.2791 % Ash
2.0633 % Extractives
30.064 % Lignin
41.071 % Glucan
3.2165 % Xylan
0.614 % Galactan
0.2762 % Arabinan
8.135 % Mannan
1 sample

BIBLIOGRAPHY

Adams, G.E. and Michael, B.D. (1967). Pulse radiolysis of benzoquinone and hydroquinone. Semiquinone formation by water elimination from trihydroxy-cyclohexadienyl radicals. *Transactions of the Faraday Society*. 63: 1171-1180.

Adaskaveg, J.E., Blanchette, R.A., and Gilbertson, R.L. (1991) Decay of date palm wood by white rot and brown rot fungi. Can J Bot 69: 615–629.

Adney, B., and Baker, J. (1996) Measurement of cellulose activities (NREL/TP-510-42628). National Renewable Energy Laboratory, Golden, CO.

Akamatsu, Y., Takahashi, M., & Shimada, M. (1994). Production of oxalic acid by wood-rotting basidiomycetes grown on low and high nitrogen culture media. *Material und Organismen, 28*, 251-264.

Alvira, P., Tomás-Pejó, E., Ballesteros, M., & Negro, M. J. (2010). Pretreatment technologies for an efficient bioethanol production process based on enzymatic hydrolysis: a review. *Bioresource Technology, 101*(13), 4851-4861.

Anagnost, S. E. (1998). Light microscopic diagnosis of wood decay. *IAWA Journal.* 19: 141-167.

Ander, P. & Eriksson, K.E. (1977). Selective degradation of wood components by white rot fungi. *Physiologia Plantarum, 41*(4), 239-248.

Antai SP, Crawford DL (1982) Degradation of extract-free lignocelluloses by Coriolus versicolor and Poria placenta. Eur J Appl Microbiol Biotechnol 14:165–168.

Arantes, V. & Milagres, A.M.F. (2006). Degradation of cellulosic and hemicellulosic substrates using a chelator-mediated Fenton reaction. *Journal of Chemical Technology and Biotechnology*, *81*, 413-419.

Arantes, V., Qian, Y., Kelley, S.S., Milagres, A.M.F., Filley, T.R., Jellison, J., & Goodell, B. (2009). Biomimetic oxidative treatment of spruce wood studied by pyrolysis-molecular beam mass spectrometry coupled with multivariate analysis and ^{13}C-labeled tetramethylammonium hydroxide thermochemolysis: implications for fungal degradation of wood. *Journal of Biological Inorganic Chemistry*, *14*, 1253-1263.

Arantes V, Jellison J, Goodell B (2012) Peculiarities of brown rot fungi and biochemical Fenton reaction with regard to their potential as a model for bioprocessing biomass. Appl Microbiol Biotechnol 94(2):323–338.

Arenz, B.E., Held, B.E., Jurgens, J.A., Farrell, R.L., and Blanchette, R.A. (2006) Fungal diversity in soils and historic wood from the Ross Sea Region of Antarctica. *Soil Biology & Biochemistry* 38: 3057-3064.

Arora DS (1995) Biodelignification of wheat straw by different fungal associations. Biodegradation 6:57–60

ASTM (1994) Standard method of accelerated laboratory test of natural decay resistance of woods (D 1413-76). In: 1994 annual book of standards. Sect. 4 Vol. 04.10. American Society for Testing and Materials, Philadelphia, pp 218–224.

ASTM (2007) Standard Test Method for Wood Preservatives by Laboratory Soil-Block Cultures (ASTM D1413-07). West Conshohocken, PA, USA: American Society for Testing and Materials International. doi: 10.1520/D1413-07.

Baldock, J. A., Oades, J. M., Nelson, P. N., Skene, T. M., Golchin, A., & Clarke, P. (1997). Assessing the extent of decomposition of natural organic materials using solid-state 13C NMR spectroscopy. *Australian Journal of Soil Research*, *35*, 1061-1083.

Baldrian, P. (2006). Fungal laccases–occurrence and properties. *FEMS microbiology reviews*, *30*(2), 215-242.

Baucher, M., Monties, B., Montagu, M.V., and Boerjan, W. (1998) Biosynthesis and genetic engineering of lignin. CRC Crit Rev Plant Sci 17: 125–197.

Bielski, B.H.J. and Richter, H.W. (1977). A study of the superoxide radical chemistry by stopped-flow radiolysis and radiation induced oxygen consumption. *Journal of the American Chemical Society*. 99: 3019-3023.

Bielski, B.H.J., Cabelli, D.E., Arudi, R.L., and Ross, A.B. (1985). Reactivity of HO_2/O^-_2 radicals in aqueous solution. *Journal of Physical and Chemical Reference Data*. 14(4): 1041-1100.

Blanchette, R.A. (1980). Wood decomposition by *Phellinus* (*Fomes*) *pini*: a scanning electron microscopy study. *Canadian Journal of Botany*. 58(13): 1496-1503.

Blanchette, R.A. (1984a). Screening wood decayed by white rot fungi for preferential lignin degradation. *Applied and Environmental Microbiology*. 48(3): 647-653.

Blanchette, R. A. (1984b). Manganese accumulation in wood decayed by white rot fungi. *Phytopathology*, *74*(6), 725-730.

Blanchette, R. A., Burnes, T. A., Leatham, G. F., & Effland, M. J. (1988). Selection of white rot fungi for biopulping. *Biomass*, *15*(2), 93-101.

Blanchette, R. A., W Krueger, E., Haight, J. E., Akhtar, M., & Akin, D. E. (1997). Cell wall alterations in loblolly pine wood decayed by the white rot fungus, *Ceriporiopsis subvermispora*. *Journal of Biotechnology*, *53*(2), 203-213.

Boerjan, W., Ralph, J., & Baucher, M. (2003). Lignin biosynthesis. *Annual review of plant biology*, *54*(1), 519-546.

Bonnarme, P., & Jeffries, T. W. (1990). Mn (II) regulation of lignin peroxidases and manganese-dependent peroxidases from lignin-degrading white rot fungi.*Applied and Environmental Microbiology*, *56*(1), 210-217.

Börjesson, P. (1999). Environmental effects of energy crop cultivation in Sweden – I: identification and quantification. *Biomass and Bioenergy*, *16*(2), 137-154.

Boudet, A.M., Kajita, S., Grima-Pettenati, J., & Goffner, D. (2003). Lignins and lignocellulosics: a better control of synthesis for new and improved uses. *Trends in Plant Science*, *8*(12), 576-581.

Brancato, A. and Banerjee, S. (2010). Effect of recycling on the surface and pore structure of wood fibre. *Appita Journal*. 63(1): 42-44.

BuckeridgeMS, Rayon C, Urbanowicz B, TinéMAS, Carpita NC (2004) Mixed linkage (1→3), (1→4) –β-D-glucans of grasses. Cereal Chem 81(1):115–127

Bu'Lock, J. D. (1955). Constituents of the higher fungi. Part IV. A quinone from Polyporus fumosus. *J Chem Soc*, 575-6.

Buxton, G.V., Greenstock, C.L., Helman, W.P., and Ross, A.B. (1988) Critical review of rate constants for reactions of hydrated electrons, hydrogen atoms, and hydroxyl radicals ($\cdot OH/\cdot O^-$) in aqueous solution. *Journal of Physical and Chemical Reference Data* 17: 513-886.

Campbell, W.G. & Booth, J. (1929). The effect of partial wood decay on the alkali solubility of wood. *Biochemical Journal*, *23*(3), 566-572.

Cartwright, K.S.G. (1937) A re-investigation into the cause of Brown Oak Fistulina hepatica (Huds.) Fr. Trans Br Mycol Soc 21: 68–83.

Chen B, Gui F, Xie B, Deng Y, Sun X, Lin M, Tao Y, Li S (2013) Composition and expression of genes encoding carbohydrate enzymes in the straw-degrading mushroom Volvariella volvacea. PLoS One 8(3):e58780

Chen, F., and Dixon, R.A. (2007) Lignin modification improves fermentable sugar yields for biofuel production. Nat Biotechnol 25: 759–761.

Chen, J., Huijun, X., Xuliang, Z., Guoqiang, Z., Zhihui, B., Hongxun, Z. (2008). Substrate-induced changes in microbial community-level physiological profiles and their application to discriminate microbial communities. *Journal of Environmental Sciences*. 20: 725-731.

Chen SF,Mowery RA, Scarlata CJ, Chambliss CK (2007) Compositional analysis of water-soluble materials in corn stover. J Agric Food Chem 55(15):5912–5918.

Chiaramonti, D., Prussi, M., Ferrero, S., Oriani, L., Ottonello, P., Torre, P., & Cherchi, F. (2012). Review of pretreatment processes for lignocellulosic ethanol production, and development of an innovative method. *Biomass and Bioenergy*.

Clausen CA, Green F III,WoodwardBM, Evans JW, DeGroot RC (2000) Correlation between oxalic acid production and copper tolerance in Wolfiporia cocos. Int Biodeterior Biodegrad 46:69–76

Clifford, D. J., Carson, D. M., McKinney, D. E., Bortiatynski, J. M., & Hatcher, P. G. (1995). A new rapid technique for the characterization of lignin in vascular plants: thermochemolysis with tetramethylammonium hydroxide (TMAH).*Organic Geochemistry*, *23*(2), 169-175.

Cohen, R., Jensen, K. A., Houtman, C. J., & Hammel, K. E. (2002). Significant levels of extracellular reactive oxygen species produced by brown rot basidiomycetes on cellulose. *FEBS letters*, *531*(3), 483-488.

Connolly, J. H., & Jellison, J. (1997). Two-way translocation of cations by the brown rot fungus *Gloeophyllum trabeum*. *International biodeterioration & biodegradation*, *39*(2), 181-188.

Cooper, G.D. and DeGraff, B.A. (1972). The photochemistry of the monoxalatoiron(III) ion. *Journal of Physical Chemistry*. 76: 2618-2625.

Cornwell, W.K., Cornelissen, J.H.C, Amatangelo, K., Dorrepaal, E., Eviner, V.T., Godoy, O., Hobbie, S.E., Hoorens, B., Kurokawa, H., Pérez-Harguindeguy, N., Quested, H.M., Santiago, L.S., Wardle, D.A., Wright, I.J., Aerts, R., Allison, S.D., Van Bodegom, P., Brovkin, V., Chatain, A., Callaghan, T.V., Diaz, S., Garnier, E., Gurvich, D.E., Kazakou, E., Klein, J.A., Read, J., Reich, P.B.,

Soudzilovskaia, N.A., Vaieretti, M., and Westoby, M. (2008). Plant species traits are the predominant control on litter decomposition rates within biomes worldwide. *Ecology Letters*. 11(10): 1065-1071.

Cowling, E.B. (1961) Comparative biochemistry of the decay of sweetgum sapwood by white rot and brown rot fungi. US Dept Agric Tech Bull 1258: 1–79.

Cowling, E.B. & Brown, W. (1969). Structural features of cellulosic materials in relation to enzymatic hydrolysis. *Cellulases and their applications, 95*, 152-187.

Cowling, E.B. & Kirk, T.K. (1976). Properties of cellulose and lignocellulosic materials as substrates for enzymatic conversion processes. *Biotechnology and Bioengineering Symposium, 6*, 95-123.

CRC Handbook of Chemistry and Physics, 89th ed. (2008). Lide, D.R. (Ed.). Boca Raton, FL: CRC Press.

Crestini, C., Crucianelli, M., Orlandi, M., & Saladino, R. (2010). Oxidative strategies in lignin chemistry: a new environmental friendly approach for the functionalisation of lignin and lignocellulosic fibers. *Catalysis Today, 156*(1-2), 8-22.

Curling, S., and Winandy, J.E. (2008) Comparison of the effects of gamma irradiation and steam sterilization on southern pine sapwood. For Prod J 58: 87–90.

Curling, S., Clausen, C.A., and Winandy, J.E. (2002) Relationships between mechanical properties, weight loss and chemical composition of wood during incipient brown rot decay. For Prod J 52: 34–39.

Daniel, G. (1994). Use of electron microscopy for aiding our understanding of wood biodegradation. *FEMS microbiology reviews, 13*(2), 199-233.

Daniel G, Volc J, Filonova L, Plíhal O, Kubátová E, Halada P (2007) Characteristics of Gloeophyllum trabeum alcohol oxidase, an extracellular source of H2O2 in brown rot decay of wood. Appl Environ Microbiol 73(19):6241–6253

Dean, J.F.D. (1997) Lignin analysis. In Methods in Plant Biochemistry and Molecular Biology. Dashek, W.V. (ed.). Boca Raton, FL, USA: CRC Press, pp. 199–215.

De Groot RC, Evans JW, Forsyth CM, Morrell JJ (1998) Soil-contact decay tests using small blocks - a procedural analysis (FPL-RP-113). USDA Forest Service, Forest Prod Lab, Madison, WI

DeJong, E. & Field, J.A. (1997). Sulfur tuft and turkey tail: biosynthesis and biodegradation of organohalogens by basidiomycetes. *Annual Reviews in Microbiology, 51*, 375-414.

De Laat, J. and Gallard, H. (1999). Catalytic decomposition of hydrogen peroxide by Fe (III) in homogeneous aqueous solution: mechanism and kinetic modeling. *Environmental Science and Technology*. 33(16): 2726-2732.

Dinwoodie, J. M. (1989). *Wood: Nature's Cellular, Polymeric, Fibre-composite*. Brookfield, VT: Institute of Metals.

Doherty, W. O., Mousavioun, P., & Fellows, C. M. (2011). Value-adding to cellulosic ethanol: lignin polymers. *Industrial Crops and Products*, *33*(2), 259-276.

Dominguez-Faus, R., Powers, S.E., Burken, J.G., & Alvarez, P.J. (2009). The water footprint of biofuels: a drink or drive issue? *Environmental Science and Technology, 43*, 3005-3010.

Donner, S.D. & Kucharik, C.J. (2008). Corn-based ethanol production compromises goal of reducing nitrogen export by the Mississippi River. *Proceedings of the National Academy of Sciences, 105*(11), 4513-4518.

Duesterberg, C.K., Cooper, W.J., and Waite, T.D. (2005). Fenton-mediated oxidation in the presence and absence of oxygen. *Environmental Science and Technology*. 39(13): 5052-5058.

Duesterberg, C. K., & Waite, T. D. (2006). Process optimization of Fenton oxidation using kinetic modeling. *Environmental science & technology*, *40*(13), 4189-4195.

Eastwood DC, Floudas D, Binder M, Majcherczyk A, Schneider P, Aerts A, Asiegbu FO, Baker SE, Barry K, Bendiksby M, Blumentritt M, Coutinho PM, Cullen D, de Vries RP, Gathman A, Goodell B, Henrissat B, Ihrmark K, Kauserud H, Kohler A, LaButti K, Lapidus A, Lavin JL, Lee Y-H, Lindquist E, Lilly W, Lucas S, Morin E, Murat C, Oguiza JA, Park J, Pisabarro AG, Riley R, Rosling A, Salamov A, Schmidt O, Schmutz J, Skrede I, Stenlid J,Wiebenga A, Xie X, Kües U, Hibbett DS, Hoffmeister D, Högberg N, Martin F, Grigoriev IV, Watkinson SC (2011) The plant cell wall decomposing machinery underlies the functional diversity of forest fungi. Science 333:762–765

Eggeman, T., & Elander, R. T. (2005). Process and economic analysis of pretreatment technologies. *Bioresource technology*, *96*(18), 2019-2025.

Elhabiri, M., Carrër, C., Marmolle, F., & Traboulsi, H. (2007). Complexation of iron (III) by catecholate-type polyphenols. *Inorganica chimica acta*, *360*(1), 353-359.

Energy Independence and Security Act of 2007 § 153 U.S.C. § 202 (2007).

Enoki, A., Tanaka, H., & Itakura, S. (2003). Physical and chemical characteristics of glycopeptide from wood decay fungi. In *ACS Symposium Series* (Vol. 845, pp. 140-153). Washington, DC; American Chemical Society; 1999.

Eriksson, K.E., Blanchette, R.A., and Ander, P. (1990) Microbial and Enzymatic Degradation of Wood and Wood Components. Berlin, Germany: Springer-Verlag.

Eslyn WE, Highley TL (1976) Decay resistance and susceptibility of sapwood of fifteen tree species. Phytopathology 66:1010–1017

European Standard EN-113 (1996) Wood preservatives—method of tes for determining the protective effectiveness againstwood destroying basidiomycetes—determination of the toxic values. European Committee for Standardization, Brussels

Fackler, K., Schwanninger, M., Gradinger, C., Hinterstoisser, B., & Messner, K. (2007). Qualitative and quantitative changes of beech wood degraded by wood-rotting basidiomycetes monitored by Fourier transform infrared spectroscopic methods and multivariate data analysis. *FEMS microbiology letters*, *271*(2), 162-169.

Fackler, K., Stevanic, J. S., Ters, T., Hinterstoisser, B., Schwanninger, M., & Salmén, L. (2010). Localisation and characterisation of incipient brown rot decay within spruce wood cell walls using FT-IR imaging microscopy. *Enzyme and microbial technology*, *47*(6), 257-267.

Faust, B.C. and Zepp, R.G. (1993). Photochemistry of aqueous iron(III)-polycarboxylate complexes: roles in the chemistry of atmospheric and surface waters. *Environmental Science and Technology*. 27(12): 2517-2522.

Fekete, F. A., Chandhoke, V., & Jellison, J. (1989). Iron-binding compounds produced by wood-decaying basidiomycetes. *Applied and environmental microbiology*, *55*(10), 2720-2722.

Fengel D, Wegener G (1984) Wood: chemistry, ultrastructure, reactions. Walter de Gruyter, New York

Fenton, H.J.H. (1894). Oxidation of tartaric acid in the presence of iron. *Journal of the Chemical Society*, *65*, 899-910.

Filley, T. R., Minard, R. D., & Hatcher, P. G. (1999). Tetramethylammonium hydroxide (TMAH) thermochemolysis: proposed mechanisms based upon the application of

^{13}C-labeled TMAH to a synthetic model lignin dimer. *Organic Geochemistry*, *30*(7), 607-621

Filley, T.R., Cody, G.D., Goodell, B., Jellison, J., Noser, C., and Ostrofsky, A. (2002) Lignin demethylation and polysaccharide decomposition in spruce sapwood degraded by brown rot fungi. Org Geochem 33: 111–124.

Floudas D, Binder M, Riley R, Barry K, Blanchette RA, Henrissat B, Martinez AT, Otillar R, Spatafora JW, Yadav JS, Aerts A, Benoit I, Boyd A, Carlson A, Copeland A, Coutinho PM, de Vries RP, Ferreira P, Findley K, Foster B, Gaskell J, Glotzer D, Górecki P, Heitman J, Hesse C, Hori C, Igarashi K, Jurgens JA, Kallen N, Kersten P, Kohler A, Kües U, Kumar TKA, Kuo A, LaButti K, Larrondo LF, Lindquist E, Ling A, Lombard V, Lucas S, Lundell T, Martin R, McLaughlin DJ,Morgenstern I, Morin E,Murat C, Nagy LG, Nolan M, Ohm RA, Patyshakuliyeva A, Rokas A, Ruiz-Dueñas FJ, Sabat G, Salamov A, SamejimaM, Schmutz J, Slot JC, St. John F, Stenlid J, Sun H, Sun S, Syed K, TsangA,WiebengaA, YoungD, Pisabarro A, Eastwood DC, Martin F, Cullen D, Grigoriev IV, Hibbett DS (2012) The Paleozoic origin of enzymatic lignin decomposition reconstructed from 31 fungal genomes. Science 336(6089):1715–1719

Flournoy, D.S., Kirk, T.K., & Highley, T.L. (1991). Wood decay by brown rot fungi: changes in pore structure and cell wall volume. *Holzforschung*, *45*(5), 383-388.

Foston, M. & Ragauskas, A.J. (2012). Biomass characterization: recent progress in understanding biomass recalcitrance. *Industrial Biotechnology*, *8*(4), 191-208.

Foti, M.C., Daquino, C., Mackie, I.D., DiLabio, G.A., and Ingold, K.U. (2008). Reaction of phenols with the 2,2-diphenyl-1-picrylhydrazyl radical. Kinetics and DFT calculations applied to determine ArO-H bond dissociation enthalpies and reaction mechanism. *Journal of Organic Chemistry*. 73: 9270-9282.

Fry SC (1989) The structure and function of xyloglucan. J Exp Bot 40(1):1–11

Gao, Z., Mori, T., and Kondo, R. (2012) The pretreatment of corn stover with Gloeophyllum trabeum KU-41 for enzymatic hydrolysis. Biotechnol Biofuels 5: 28.

Getoff, N., Schwoerer, F., Markovic, V.M., Sehested, K., and Nielsen, S.O. (1971). Pulse radiolysis of oxalic acid and oxalates. *Journal of Physical Chemistry*. 75: 749-755.

Gilbertson, R.L., and Ryvarden, L. (1986) North American Polypores. Oslo, Norway: Fungiflora.

Giles, R.L., Galloway, E.R., Elliott, G.D., & Parrow, M.W. (2011). Two-stage fungal biopulping for improved enzymatic hydrolysis of wood. *Bioresource Technology, 102*, 8011-8016.

Glaze, W. H., Kang, J. W., & Chapin, D. H. (1987). The chemistry of water treatment processes involving ozone, hydrogen peroxide and ultraviolet radiation. *Ozone: Science and Engineering*. 9(4): 335-352.

Goodell, B., Jellison, J., Liu, J., Daniel, G., Paszczynski, A., Fekete, F., Krishnamurthy, S., Jun, L., and Xu, G. (1997) Low molecular weight chelators and phenolic compounds isolated from wood decay fungi and their role in the fungal biodegradation of wood. J Biotechnol 53: 133–162.

Grabber, J.H., Hatfield, R.D., Ralph, J., Zon´, J., and Amrhein, N. (1995) Ferulate cross-linking in cell walls isolated from maize cell suspensions. Phytochemistry 40: 1077–1082.

Grabber, J. H., Hatfield, R. D., Lu, F., & Ralph, J. (2008). Coniferyl ferulate incorporation into lignin enhances the alkaline delignification and enzymatic degradation of cell walls. *Biomacromolecules*, *9*(9), 2510-2516.

Green III, F., Larsen, M.J., Winandy, J.E., & Highley, T.L. (1991). Role of oxalic acid in incipient brown rot decay. *Material und Organismen, 26*(3), 191-213.

Green III, F. & Highley, T.L. (1997). Mechanism of brown rot decay: paradigm or paradox. *International Biodeterioration & Biodegradation, 39*(2-3), 113-124.

Green, F., III, and Clausen, C.A. (2003) Copper tolerance of brown rot fungi: time course of oxalic acid production. Int Biodeterior Biodegradation 51: 145–149.

Grethlein, H.E., Allen, D.C., & Converse, A.O. (1984). A comparative study of the enzymatic hydrolysis of acid-pretreated white pine and mixed hardwood. *Biotechnology and Bioengineering, 26*(12), 1498-1505.

Grigoriev, I.V., Cullen, D., Hibbett, D., Goodwin, S.B., Jeffries, T.W., Kubicek, C.P., Kuske, C., Magnuson, J.K., Martin, F., Spatafora, J., Tsang, A., & Baker, S.E. (2011). Fueling the future with fungal genomics. *Mycology*, *2*(3), 192-209.

Haber, F., & Weiss, J. (1932). Über die katalyse des hydroperoxydes. *Naturwissenschaften, 20*(51), 948-950.

Halliwell, G. (1965). Catalytic decomposition of cellulose under biological conditions. *Biochemical Journal, 95*(1), 35.

Hames, B. R., Thomas, S. R., Sluiter, A. D., Roth, C. J., & Templeton, D. W. (2003). Rapid biomass analysis. In *Biotechnology for Fuels and Chemicals* (pp. 5-16). Humana Press.

Hames, B., Scarlata, C., & Sluiter, A. (2005). Determination of protein content in biomass. *National Renewable Energy Laboratory, Golden, Colorado*.

Hames, B. R. (2009). Biomass compositional analysis for energy applications. In *Biofuels* (pp. 145-167). Humana Press.

Hammel, K. E., Kapich, A. N., Jensen, K. A., & Ryan, Z. C. (2002). Reactive oxygen species as agents of wood decay by fungi. *Enzyme and microbial technology*, *30*(4), 445-453.

Han G, ChengW,ManningM, Eloy P (2012) Performance of zinc boratetreated oriented structural straw board againstmold fungi, decay fungi, and termites—a preliminary trial. BioResources 7(3):2986–2995

Harmon, M.E., Franklin, J.F., Swanson, F.J., Sollins, P. Gregory, S.V., Lattin, J.D., et al. (1986) Ecology of coarse woody debris in temperate ecosystems. In Advances in Ecological Research. MacFadyen, A., and Ford, E.D. (eds). London, UK: Academic Press, pp. 133–302.

Hastrup, A.C.S., Howell, C., Jensen, B., & Green III, F. (2011). Non-enzymatic depolymerization of cotton cellulose by fungal mimicking metabolites. *International Biodeterioration & Biodegradation, 65*, 553-559.

Hastrup, A.C.S., Green III, F., Lebow, P.K., & Jensen, B. (2012a). Enzymatic oxalic acid regulation correlated with wood degradation in four brown rot fungi. *International Biodeterioration and Biodegradation, 75*, 109-114.

Hastrup, A. C. S., Howell, C., Larsen, F. H., Sathitsuksanoh, N., Goodell, B., & Jellison, J. (2012b). Differences in crystalline cellulose modification due to degradation by brown and white rot fungi. *Fungal biology*.

Hatakka AI (1983) Pretreatment of wheat straw by white rot fungi for enzymic saccharification of cellulose. Eur J Appl Microbiol Biotechnol 18(6):350–357

Hatakka, A. I., Mohammadi, O. K., & Lundell, T. K. (1989). The potential of white-rot fungi and their enzymes in the treatment of lignocellulosic feed. *Food Biotechnology*, *3*(1), 45-58.

Hedges, J.I., Blanchette, R.A., Weliky, K., and Devol, A.H. (1988) Effects of fungal degradation on the CuO oxidation products of lignin: a controlled laboratory study. Geochim Cosmochim Acta 52: 2717–2726.

Hibbett, D.S., and Donoghue, M.J. (2001) Analysis of character correlations among wood decay mechanisms, mating systems, and substrate ranges in homobasidiomycetes. Syst Biol 50: 215–242.

Highley, T.L. (1975) Can wood-rot fungi degrade cellulose without other wood constituents? For Prod J 25: 38–39.

Highley, T.L. (1977) Requirements for cellulose degradation by a brown rot fungus. Mater Organismen 12: 25–36.

Highley TL (1978) How moisture and pit aspiration affect decay of wood by white rot and brown rot fungi. Mater Org 13:197–206

Highley, T., Murmanis, L., & Palmer, J. G. (1983). Electron microscopy of cellulose decomposition by brown rot fungi. *Holzforschung-International Journal of the Biology, Chemistry, Physics and Technology of Wood*, *37*(6), 271-277.

Highley, T.L. (1987) Changes in chemical components of hardwood and softwood by brown rot fungi. Mater Organismen 22: 39–45.

Hill, J., Polasky, S., Nelson, E., Tilman, D., Huo, H., Ludwig, L., Neumann, J., Zheng, H., & Bonta, D. (2009). Climate change and health costs of air emissions from biofuels and gasoline. *Proceedings of the National Academy of Sciences*, *106*(6), 2077-2082.

Himmel, M.E., Ding, S.Y., Johnson, D.K., Adney, W.S., Nimlos, M.R., Brady, J.W., & Foust, T.D. (2007). Biomass recalcitrance: engineering plants and enzymes for biofuels production. *Science, 315*, 804-807.

Hirsch RL, Bezdek R, & Wendling.R. (2005). Peaking of world oil production: impacts, mitigation, & risk management. Department of Energy, National Energy Technology Laboratory. DOE/NETL-IR-2005-093.

Hodson, M.J., White, P.J., Mead, A., & Broadley, M.R. (2005). Phylogenetic variation in the silicon composition of plants. *Annals of Botany, 96*, 1027-1046.

Holtzapple, M., Cognata, M., Shu, Y., and Hendrickson, C. (1990). Inhibition of *Trichoderma reesei* cellulase by sugars and solvents. *Biotechnology and Bioengineering*. 36(3): 275-287.

Hoskinson RL, Karlen DL, Birrell SJ, Radtke CW, Wilhelm WW (2007) Engineering, nutrient removal, and feedstock conversion evaluations of four corn stover harvest scenarios. Biomass Bioenergy 31(2):126–136

Hunt, C., Kenealy, W., Horn, E., & Houtman, C. (2004). A biopulping mechanism: creation of acid groups on fiber. *Holzforschung, 58*, 434-439.

Hyde, S.M., and Wood, P.M. (1997) A mechanism for production of hydroxyl radicals by the brown rot fungus Coniophora puteana: Fe(III) reduction by cellobiose dehydrogenase and Fe(II) oxidation at a distance from the hyphae. Microbiology 143: 259–266.

Ianni, J.C. (2003). A comparison of the Bader-Deuflhard and the Cash-Karp Runge-Kutta integrators for the GRI-MECH 3.0 model based on the chemical kinetics code Kintecus. *Computational Fluid and Solid Mechanics*, 1368-1372.

Illman, B., Meinholtz, D.C., & Highley, T.L. (1989). Manganese as a probe of fungal degradation of wood. In: O'Rear, Llewellyn (eds) *Biodeterioration Research.* Plenum Press, New York, pp. 485–496.

Ilmén, M., Saloheimo, A., Onnela, M.L., and Penttilä, M.E. (1997). Regulation of cellulase gene expression in the filamentous fungus Trichoderma reesei. *Applied and Environmental Microbiology*. 63(4): 1298-1306.

Irwin D, Leathers TD, Greene RV, Wilson DB (2003) Corn fiber hydrolysis by Thermobifida fusca extracellular enzymes. Appl Microbiol Biotechnol 61(4):352–358

Irwin, D.C., Cheng, M., Xiang, B., Rose, J.K.C., & Wilson, D.B. (2003). Cloning, expression, and characterization of a family-74 xyloglucanase from Thermobifida fusca. *European Journal of Biochemistry, 270*(14), 3083-3091.

Itoh, H., Wada, M., Honda, Y., Kuwahara, M., & Watanabe, T. (2003). Bioorganosolve pretreatments for simultaneous saccharification and fermentation of beech wood by ethanolysis and white rot fungi. *Journal of Biotechnology, 103*, 273-280.

Jain, P. & Vigneshwaran, N. (2011). Effect of Fenton's pretreatment on cotton cellulosic substrates to enhance its enzymatic hydrolysis response. *Bioresource Technology, 103*(1), 219-226.

Jellison, J., Connolly, J., Smith, K., & Shortle, W. (1993). A comparison of inductively coupled plasma spectroscopy and netron activation analysis for the determination of cation concentrations in wood. *Document-the International Research Group on Wood Preservation*.

Jellison, J., Connolly, J., Goodell, B., Doyle, B., Illman, B., Fekete, F., & Ostrofsky, A. (1997). The role of cations in the biodegradation of wood by the brown rot fungi. *International Biodeterioration & Biodegradation* 39(2): 165-179.

Jensen Jr, K.A., Ryan, Z.C., Wymelenberg, A.V., Cullen, D., and Hammel, K.E. (2002). An NADH: quinone oxidoreductase active during biodegradation by the brown rot basidiomycete Gloeophyllum trabeum. *Applied and Environmental Microbiology* 68(6): 2699-2703.

Jeoh, T., Ishizawa, C.I., Davis, M.F., Himmel, M.E., Adney, W.S., & Johnson, D.K. (2007). Cellulase digestibility of pretreated biomass is limited by cellulose accessibility. *Biotechnology and Bioengineering, 98*(1), 112-122.

JGI (2013) Genome project list [WWW document]. URL www.genome.jgi.doe.gov/pages/fungi-1000-projects.jsf.

Jung, H. J. G. & Shalita-Jones, S. C. (1990). Variation in the extractability of esterified p-coumaric and ferulic acids from forage cell walls. *Journal of Agricultural and Food Chemistry*, *38*(2), 397-402.

Jung, Y. H., Kim, H. K., Park, H. M., Park, Y. C., Park, K., Seo, J. H., and Kim, K. H. (2015). Mimicking the Fenton reaction-induced wood decay by fungi for pretreatment of lignocellulose. *Bioresource technology* 179: 467-472.

Jurgensen, M.F., Larsen, M.J., Wolosiewicz, M., and Harvey, A.E. (1989). A comparison of dinitrogen fixation rates in wood litter decayed by white rot and brow-rot fungi. *Plant and Soil*. 115: 117-122.

Kaffenberger, J.T., and Schilling, J.S. (2013) Using a grass substrate to compare decay among two clades of brown rot fungi. Appl Microbiol Biotechnol 97: 8831–8840.

Kaffenberger, J.T. and Schilling, J.S. (2014). Comparing lignocellulose physiochemistry after decomposition by brown rot fungi with distinct evolutionary origins. *Environmental Microbiology*. DOI: 10.1111/1462-2920.12615.

Kamdem DP, Pizzi A, Jermannaud A (2002) Durability of heat-treated wood. Holz Roh Werkst 60(1):1–6

Kelley SS, Jellison J,Goodell B (2002) Use ofNIR and pyrolysis-MBMS coupled with multivariate analysis for detecting the chemical changes associated with brown rot biodegradation of spruce wood. FEMS Microbiol Lett 209:107–111

Kerem, Z., Jensen, K.A., and Hammel, K.E. (1999) Biodegradative mechanism of the brown rot basidiomycete Gloeophyllum trabeum: evidence for an extracellular hydroquinone-driven Fenton reaction. FEBS Lett 446: 49–54.

Khudyakov, J.I., D'haeseleer, P., Borglin, S.E., DeAngelis, K.M., Woo, H., Lindquist, E.A., Hazen, T.C., Simmons, B.A., & Thelen, M.P. (2012). Global transcriptome response to ionic liquid by a tropical rain forest soil bacterium, *Enterobacter lignolyticus*. *Proceedings of the National Academy of Sciences, 109*(32), E2173-E2182.

Kirk, T.K., and Adler, E. (1970) Methoxyl-deficient structural elements in lignin of sweetgum decayed by a brown rot fungus. Acta Chem Scand 24: 3379–3390.

Kirk, T.K., and Highley, T.L. (1973) Quantitative changes in structural components of conifer woods during decay by white-and brown rot fungi. Phytopathology 63: 1338–1342.

Kirk, T.K., Ibach, R., Mozuch, M.D., Conner, A.H., & Highley, T.L. (1991). Characteristics of cotton cellulose depolymerized by a brown rot fungus, by acid, or by chemical oxidants. *Holzforschung, 45*(4), 239-244.

Koenigs, J.W. (1974a). Production of hydrogen peroxide by wood-rotting fungi in wood and its correlation with weight loss, depolymerization, and pH changes. *Archives of Mcirobiology, 99*(1), 129-145.

Koenigs, J.W. (1974b). Hydrogen peroxide and iron: a proposed system for decomposition of wood by brown rot basidiomycetes. *Wood and Fiber Science, 6*(1), 66-80.

Kolthoff, I.M., Meehan, E.J., & Kimura, M. (1972). Formation of hydrogen peroxide upon oxidation of oxalic acid in presence and absence of oxygen – II: oxygen as oxidant. *Talanta, 19*, 1179-1186.

Korripally, P., Timokhin, V.I., Houtman, C.J., Mozuch, M.D., and Hammel, K.E. (2013) Evidence from Serpula lacrymans that 2,5-dimethoxyhydroquinone is a lignocellulolytic agent of divergent brown rot basidiomycetes. Appl Environ Microbiol 79: 2377–2383.

Kumar, P., Barrett, D.M., Delwiche, M.J., & Stroeve, P. (2009). Methods for pretreatment of lignocellulosic biomass for efficient hydrolysis and biofuel production. *Industrial and Engineering Chemistry Research, 48*, 3713-3729.

Kurakake, M., Ide, N., & Komaki, T. (2007). Biological pretreatment with two bacterial strains for enzymatic hydrolysis of office paper. *Current Microbiology, 54*, 424-428.

Kwan, W.P. and Voelker, B.M. (2002). Decomposition of hydrogen peroxide and organic compounds in the presence of dissolved iron and ferrihydrite. *Environmental Science and Technology*. 36(7): 1467-1476.

Ladisch, M.R., Lin, K.W., Voloch, M., and Tsao, G.T. (1983) Process considerations in the enzymatic hydrolysis of biomass. Enzyme Microb Technol 5: 81–102.

Lam, T.B.T., Iiyama, K., & Stone, B.A. (2003). Hot alkali-labile linkages in the walls of the forage grass Phalaris aquatica and Lolium perenne and their relation to in vitro wall digestibility. *Phytochemistry*, 64, 603-607.

Lanzalunga, O., & Bietti, M. (2000). Photo-and radiation chemical induced degradation of lignin model compounds. *Journal of Photochemistry and Photobiology B: Biology*, *56*(2), 85-108.

Lee, J.W., Gwak, K.S., Park, J.Y., Park, M.J., Choi, D.H., Kwon, M., & Choi, I.G. (2007). Biological pretreatment of softwood Pinus densiflora by three white rot fungi. *Journal of Microbiology, 45*(6), 485-491.

Li, C., Wang, Q., & Zhao, Z.K. (2008). Acid in ionic liquid: an efficient system for hydrolysis of lignocellulose. *Green Chemistry*, *10*, 177-182.

Li, M. (2007). Peak oil, the rise of China and India, and the global energy crisis. *Journal of Contemporary Asia, 37*(4), 449-471.

Liang Y, Sun W, Zhu YG, Christie P (2007) Mechanisms of siliconmediated alleviation of abiotic stresses in higher plants: a review. Environ Pollut 147:422–428.

Liu, H., Li, X.Z., Leng, Y.J., and Wang, C. (2006) Kinetic modeling of electro-Fenton reaction in aqueous solution. *Water Research* 41(5): 1161-1167.

Long, C.A. & Bielski, B.H.J. (1980). Rate of reaction of superoxide radical with chloride-containing species. *Journal of Physical Chemistry, 84*, 555-557.

Luo, W., D'Angelo, E.M., Coyne, M.S. (2008). Organic carbon effects on aerobic polychlorinated biphenyl removal and bacterial community composition in soils and sediments. *Chemosphere*. 70(3): 364-373.

Ma JF (2004) Role of silicon in enhancing the resistance of plants to biotic and abiotic stresses. Soil Sci Plant Nutr 50(1):11–18

Machuca, A., Napoleão, D., & Milagres, A.M.F. (2001). Detection of metal-chelating compounds from wood-rotting fungi *Trametes versicolor* and *Wolfiporia cocos*. *World Journal of Microbiology & Biotechnology, 17*, 687-690.

Malherbe, S. & Cloete, T.E. (2002). Lignocellulose biodegradation: fundamentals and applications. *Reviews in Environmental Science & Biotechnology, 1*, 105-114.

Manion, J.A., Huie, R.E., Levin, R.D., Burgess Jr., D.R., Orkin, V.L., Tsang, W., McGivern, W.S., Hudgens, J.W., Knyazev, V.D., Atkinson, D.B., Chai, E., Tereza, A.M., Lin, C.-Y., Allison, T.C., Mallard, W.G., Westley, F., Herron, J.T., Hampson, R.F., and Frizzell, D.H. (2013). NIST Chemical Kinetics Database, NIST Standard Reference Database 17, Version 7.0 (Web Version), Release 1.6.8, Data version 2013.03, National Institute of Standards and Technology, Gaithersburg, Maryland, 20899-8320. Web address: http://kinetics.nist.gov/

Mansfield, S.D., Kim, H., Lu, F., & Ralph, J. (2012). Whole plant cell wall characterization using solution-state 2D NMR. *Nature Protocols, 7*(9), 1579-1589.

Marles, M.A.S., Coulman, B.E., and Bett, K.E. (2008) Interference of condensed tannin in lignin analyses of dry bean and forage crops. J Agric Food Chem 56: 9797–9802.

Martin SB, Dale JL (1980) Biodegradation of turf thatch with wooddecay fungi. Phytopathology 70:297–301

Martinez D, Challacombe J, Morgenstern I, Hibbett D, Schmoll M, Kubicek CP, Ferreira P, Ruiz-Duenas FJ, Martinez AT, Kersten P, Hammel KE,VandenWymelenberg A, Gaskell J, Lindquist E, Sabat G, BonDurant SS, Larrondo LF, Canessa P, Vicuna R, Yadav J, Doddapaneni H, Subramanian V, Pisabarro AG, Lavin JL, Oguiza JA, Master E, Henrissat B, Coutinho PM, Harris P, Magnuson JK, Baker SE, Bruno K, Kenealy W, Hoegger PJ, Kües U, Ramaiya P, Lucas S, Salamov A, Shapiro H, Tu H, Chee CL, Misra M, Xie G, Teter S, Yaver D, James T, Mokrejs M, Pospisek M, Grigoriev IV, Brettin T, Rokhsar D, Berka R, Cullen D (2009) Genome, transcriptome, and secretome analysis of wood decay fungus Postia placenta supports unique mechanisms of lignocellulose conversion. Proc Natl Acad Sci U S A 106(6):1954–1959

Mártire, D.O., Braslavsky, S.E., and García, N.A. (1991) Sensitized photo-oxidation of dihydroxybenzenes and chlorinated derivatives. A kinetic study. *Journal of Photochemistry and Photobiology A: Chemistry*. 61(1): 113-124.

Maurice, S., Coroller, L., Debaets, S., Vasseur, V., Le Floch, G., and Barbier, G. (2011) Modelling the effect of temperature, water activity, and pH on the growth of Serpula lacrymans. J Appl Microbiol 111: 1436–1446.

Meadows, D.H., Meadows, D.L., Randers, J., & Behrens III, W.W. (1972). *The limits to growth: A report for the club of rome's project on the predicament of mankind*. New York: Universe Books.

Miller, G.L. (1959) Use of dinitrosalicylic acid reagent for determination of reducing sugar. *Analytical Chemistry*. 31: 426-428.

Mitchell, D. (2008). A note on rising food prices (Working Paper No. 4682). World Bank Policy Research Working Paper Series. Website: http://ssrn.com/abstract=1233058.

Monrroy M, Ortega I, Ramírez M, Baeza J, Freer J (2011) Structural change in wood by brown rot fungi and effect on enzymatic hydrolysis. Enzyme Microb Tech 49:472–477

Morrison, I.M. (2001). Polysaccharides: Plant Noncellulosic. *eLS*. DOI:10.1038/npg.els.0000696

Mosier, N., Wyman, C., Dale, B., Elander, R., Lee, Y.Y., Holtzapple, M., & Ladisch, M. (2005). Features of promising technologies for pretreatment of lignocellulosic biomass. *Bioresource Technology, 96*, 673-686.

Motulsky, H.J., and Ransnas, L.A. (1987) Fitting curves to data using nonlinear regression: a practical and nonmathematical review. FASEB J 1: 365–374.

Mulazzani, Q.G., D'Angelantonio, M., Venturi, M., Hoffman, M.Z., and Rodgers, M.A.J. (1986). Interaction of formate and oxalate ions with radiation-generated radicals in aqueous solution. Methylviologen as a mechanistic probe. *Journal of Physical Chemistry.* 90: 5347-5352.

Munir, E., Yoon, J.J., Tokimatsu, T., Hattori, T., and Shimada, M. (2001) A physiological role for oxalic acid biosynthesis in the wood-rotting basidiomycete Fomitopsis palustris. Proc Natl Acad Sci USA 98: 11126–11130.

Nash, J., and Sutcliffe, J.V. (1970) River flow forecasting through conceptual models part I–a discussion of principles. J Hydrol 10: 282–290.

Neta, P. and Schuler, R.H. (1972). Effect of ionic dissociation of organic compounds on their rate of reaction with hydrogen atoms. *Journal of Physical Chemistry*. 76: 2673-2679.

Nilsson, T. (1974). *The degradation of cellulose and the production of cellulase, xylanase, mannanase and amylase by woodattacking microfungi* (No. 114).

Öhgren, K., Bura, R., Saddler, J., and Zacchi, G. (2007) Effect of hemicellulose and lignin removal on enzymatic hydrolysis of steam pretreated corn stover. Bioresour Technol 98: 2503–2510.

Olofsson, K., Bertilsson, M., & Lidén, G. (2008). A short review on SSF-an interesting process option for ethanol production from lignocellulosic feedstocks. *Biotechnol Biofuels*, *1*(7), 1-14.

Osono, T. (2007) Ecology of ligninolytic fungi associated with leaf litter decomposition. Ecol Res 22: 955–974.

Otjen, L., Blanchette, R.A., Effland, M., and Leatham, G. (1987). Assessment of 30 white rot basidiomycetes for selective lignin degradation. *Holzforschung*. 41(6): 343-349.

Owens, E.M., Reddy, C.A., and Grethlein, H.E. (1994) Outcome of interspecific interactions among brown rot and white rot wood decay fungi. FEMS Microbiol Ecol 14: 19–24.

Pandey, K.K. & Pitman, A.J. (2003). FTIR studies of the changes in wood chemistry following decay by brown rot and white rot fungi. *International biodeterioration & biodegradation*, *52*(3), 151-160.

Perlack, R.D. & Stokes, B.J. (Leads), U.S. Department of Energy. (2011). U.S. Billion-Ton Update: Biomass Supply for a Bioenergy and Bioproducts Industry., ORNL/TM-2011/224. Oak Ridge National Laboratory, Oak Ridge, TN.

Pettersen, R. C. (1984). The chemical composition of wood. *The chemistry of solid wood*, *575*, 57-126.

Prasad, D.R., Hoffman, M.Z., Mulazzani, Q.G., and Rodgers, M.A.J. (1986). Pulsed-laser flash and continuous photolysis aof aqueous solutions of methyl viologen, oxalate, and their ion-pair complexes. *Journal of the American Chemical Society*. 108: 5135-5142.

Prousek, J. (2007). Fenton chemistry in biology and medicine. *Pure Applied Chemistry, 79*(12), 2325-2338.

Puri, V.P. (1984). Effect of crystallinity and degree of polymerization of cellulose on enzymatic saccharification. *Biotechnology and Bioengineering, 26*(10), 1219-1222.

Qian, Y. (2008). Study of basic wood decay mechanisms and their biotechnological applications. (Doctoral Dissertation). University of Maine: Orono, ME.

Qing, Q., Yang, B., and Wyman, C.E. (2010). Xylooligomers are strong inhibitors of cellulose hydrolysis by enzymes. *Bioresource Technology*. 101(24): 9624-9630.

Rao, P.S. and Hayon, E. (1973). Ionization constants and spectral characteristics of some semiquinone radicals in aqueous solution. *Journal of Physical Chemistry*. 77(19): 2274-2276.

Rättö, M., Ritschkoff, A.C., & Viikari, L. (1997). The effect of oxidative pretreatment on cellulose degradation by *Poria placenta* and *Trichoderma reesei* cellulases. *Applied Microbiology and Biotechnology*, *48*, 53-57.

Ray MJ, Leak DJ, Spanu PD, Murphy RJ (2010) Brown rot fungal early stage decay mechanism as a biological pretreatment for softwood biomass in biofuel production. Biomass Bioenerg 34(8):1257–1262

Reddy, C. A. (1995). The potential for white rot fungi in the treatment of pollutants. *Current Opinion in Biotechnology*, *6*(3), 320-328.

Riley, R., Salamov, A.A., Brown, D.W., Nagy, L.G., Floudas, D., Held, B.W., et al. (2014) Extensive sampling of basidiomycete genomes demonstrates inadequacy of the white rot/brown rot paradigm for wood decay fungi. Proc Natl Acad Sci USA 111: 9923–9928.

Ritschkoff AC,Viikari L (1991) The production of extracellular hydrogen peroxide by brown rot fungi. Mater Org 26:157–167.

Rowell, R., ed. (1984). *The Chemistry of Solid Wood*. Washington DC: American Chemical Society. Print.

Ruiz-Duenas, F.J., Lundell, T., Floudas, D., Nagy, L.G., Barrasa, J.M., Hibbett, D.S., and Martínez, A.T. (2013) Lignin-degrading peroxidases in polyporales: an evolutionary survey based on 10 sequenced genomes. Mycologia 105: 1428–1444.

Saddler, J.N. and Mackie, K. (1990). Bioconversion of lignocellulosics. *Biomass*. 22: 293-305.

Saha BC, Woodward J (eds) (1997) Fuels and chemicals from biomass. ACS Symp Ser 666. American Chemical Society, Washington, DC

Salvachúa, D., Prieto, A., López-Abelairas, M., Lu-Chau, T., Martínez, A.T., and Martínez, M.J. (2011) Fungal pretreatment: an alternative in second-generation ethanol from wheat straw. Bioresour Technol 102: 7500–7506.

Sanderson, M. A., Agblevor, F., Collins, M., & Johnson, D. K. (1996). Compositional analysis of biomass feedstocks by near infrared reflectance spectroscopy. *Biomass and bioenergy*, *11*(5), 365-370.

Sarkanen, K. V., & Ludwig, C. H. (1971). Lignins: occurrence, formation, structure and reactions. *Lignins: occurrence, formation, structure and reactions.*

Sarker P, Bosneaga E, Auer M (2009) Plant cell walls throughout evolution: towards a molecular understanding of their design principles. J Exp Bot 60(13):3615–3635

Schädel, C. Blöchl, A., Richter, A., & Hoch, G. (2010). Quantification and monosaccharide composition of hemicelluloses from different plant functional types. *Plant Physiology and Biochemistry*, *48*, 1-8.

Scheu, S., and Schaefer, M. (1998). Bottom-up control of the soil macrofauna community in a beechwood on limestone: manipulation of food resources. *Ecology*. 79(5): 1573-1585.

Schilling, J.S., and Jellison, J. (2005) Oxalate regulation by two brown rot fungi decaying oxalate-amended and nonamended wood. Holzforschung 59: 681–688.

Schilling, J.S., Tewalt, J.P., and Duncan, S.M. (2009) Synergy between pretreatment lignocellulose modifications and saccharification efficiency in two brown rot fungal systems. Appl Microbiol Biotechnol 84: 465–475.

Schilling, J.S. (2010) Effects of calcium-based materials and iron impurities on wood degradation by the brown rot fungus Serpula lacrymans. Holzforschung 64: 93–99.

Schilling JS, Norcutt A (2010) Effects of wood mixtures on deterioration by a filamentous brown rot fungus. Wood Fiber Sci 42(2):150–157

Schilling, J.S., Ai, J., Blanchette, R.A., Duncan, S.M., Filley, T.R., and Tschirner, U.W. (2012) Lignocellulose modifications by brown rot fungi and their effects, as pretreatments, on cellulolysis. Bioresour Technol 116: 147–154.

Schilling, J. S., Duncan, S. M., Presley, G. N., Filley, T. R., Jurgens, J. A., & Blanchette, R. A. (2013). Colocalizing incipient reactions in wood degraded by the brown rot fungus *Postia placenta*. *International Biodeterioration & Biodegradation*, *83*, 56-62.

Schilling, J.S., Kaffenberger, J.T., Liew, F.J., Song, Z. (2015). Signature Modifications Reveal Decomposer Community History. PlosOne, PONE-D-14-42686R1.

Schmidt, C.J., Whitten, B.K., & Nicholas, D.D. (1981). A proposed role for oxalic acid in non-enzymatic wood decay by brown rot fungi. *Proceedings of the Annual Meeting- AWPA*. Vol. 77.

Schmidt, K.H. (1972). Electrical conductivity techniques for studying the kinetics of radiation-induced chemical reactions in aqueous solutions. *International Journal for Radiation Physics and Chemistry.* 4(4): 439-468.

Schmidt, O.,Wei, D.S., Liese,W.,and Wollenberg, E. (2011) Fungal degradation of bamboo samples. Holzforschung 65:883–888

Schwartz, P. & Randall, D. (2003). *An abrupt climate change scenario and its implications for United States national security*. Jet Propulsion Laboratory. Pasadena, CA.

Schwarz, H.A. (1992). Reaction of the hydrated electron with water. *Journal of Physical Chemistry*. 96: 8937-8941.

Schwarze, F.W.M.R., Baum, S., and Fink, S. (2000) Dual modes of degradation by Fistulina hepatica in xylem cell walls of Quercus robur. Mycol Res 104: 846–852.

Seifert, K.A. (1983) Decay of wood by the Dacrymycytales. Mycologia 75: 1011–1018.

Selig, M., Weiss, N., and Ji, Y. (2008) Enzymatic saccharification of lignocellulosic biomass (NREL/TP-510-42629). National Renewable Energy Laboratory, Golden, CO.

Shimada, M., Akamatsu, Y., Ohta, A., & Takahashi, M. (1991). Biochemical relationships between biodegradation of cellulose and formation of oxalic acid in brown rot wood decay. *Intern. Res. Group. On Wood Preserv. Doc. No. IRG/WP*, *1427*, 1-12.

Shortle WC, Dudzik KR, Smith KT (2010) Development of wood decay in wound-initiated discolored wood of eastern red cedar. Holzforschung 64:529–536

Sjöstrom, E. (1993) Wood Chemistry: Fundamentals and Applications, 2nd edn. London, UK: Academic Press.

Sluiter, J., and Sluiter, A. (2010) Summative mass closure (NREL/TP-510-48087). National Renewable Energy Laboratory, Golden, CO.

Sluiter A, Ruiz R, Scarlata C, Sluiter J, Templeton D (2008a) Determination of extractives in biomass (NREL/TP-510-42619). National Renewable Energy Laboratory, Golden

Sluiter A, Hames B, Ruiz R, Scarlata C, Sluiter J, Templeton D, Crocker D (2008b) Determination of structural carbohydrates and lignin in biomass (NREL/TP-510-42618). National Renewable Energy Laboratory, Golden

Sluiter, J. B., Ruiz, R. O., Scarlata, C. J., Sluiter, A. D., & Templeton, D. W. (2010). Compositional analysis of lignocellulosic feedstocks. 1. Review and description of methods. *Journal of agricultural and food chemistry*, *58*(16), 9043.

Song, Z., Vail, A., Sadowsky, M.J., and Schilling, J.S. (2012) Competition between two wood-degrading fungi with distinct influences on residues. FEMS Microbiol Ecol 79: 109– 117.

Sonnenberg, E.D., Zheng, H., Joglekar, P., Higginbottom, S.K., Firbank, S.J., Bolam, D.N., and Sonnenberg, J.L. (2010). Specificity of polysaccharide use in intestinal bacteroides species determines diet-induced microbiota alterations. *Cell*. 141(7): 1241-1252.

Stangerlin DM, de Melo RR, Garlet A, Gatto DA (2011) Natural durability of Eucalyptus grandis and Bambusa vugaris particleboards under accelerated fungi decay test. Cienc Rural 41(8):1369–1374

Sticklen, M. B. (2008). Plant genetic engineering for biofuel production: towards affordable cellulosic ethanol. *Nature Reviews Genetics*, *9*(6), 433-443.

Stirling, R., Trung, T., Breuil, C., & Bicho, P. (2007). Predicting wood decay and density using NIR spectroscopy. *Wood and Fiber Science*, *39*(3), 414-423.

Sun, F., Li, J., Yuan, Y., Yan, Z., and Liu, X. (2011). Effect of biological pretreatment with *Trametes hirsute* yj9 on enzymatic hydrolysis of corn stover. *International Biodeterioration and Biodegradation*. 65: 931-938.

Sun, Y. and Cheng, J. (2002). Hydrolysis of lignocellulosic materials for ethanol production: a review. 83: 1-11.

Suprapti S (2010) Decay resistance of five Indonesian bamboo species against fungi. J Trop For Sci 22(3):287–294

Suzuki, M.R., Hunt, C.G., Houtman, C.J., Dalebroux, Z.D., & Hammel, K.E. (2006). Fungal hydroquinones contribute to brown rot of wood. *Environmental Microbiology*, *8*(12), 2214-2223.

Talbot, J.M., Martin, F., Kohler, A., Henrissat, B., and Peay, K. (2015). Functional guild classification predicts the enzymatic role of fungi in litter and soil biogeochemistry. *Soil Biology and Biochemistry*. doi:10.1016/j.soilbio.2015.05.006.

Tejirian, A., and Xu, F. (2010). Inhibition of cellulase-catalyzed lignocellulosic hydrolysis by iron and oxidative metal ions and complexes. *Applied and Environmental Microbiology* 76(23): 7673-7682.

Tewalt J, Schilling J (2010) Assessment of saccharification efficacy in the cellulose system of the brown rot fungus Gloeophyllum trabeum. Appl Microbiol Biotechnol 86:1785–1793

Thompson, D.N., Chen, H.C., & Grethlein, H.E. (1992). Comparison of pretreatment methods on the basis of available surface area. *Bioresource Technology, 39*(2), 155-163.

Tian, X., Fang, Z., & Guo, F. (2012). Impact and prospective of fungal pre-treatment of lignocellulosic biomass for enzymatic hydrolysis. *Biofuels, Bioproducts and Biorefining*, *6*(3), 335-350.

Tokgoz, S., Elobeid, A., Fabiosa, J., Hayes, D.J., Babock, B.A., Yu, T.H., Dong, F., & Hart, C.E. (2008). Bottlenecks, drought, and oil price spikes: impact on U.S. ethanol and agricultural sectors. *Applied Economic Perspectives and Policy, 30*(4): 604-622.

Torget R, Werdene P, Himmel M, Grohmann K (1990) Dilute acid pretreatment of short rotation woody and herbaceous crops. Appl Biochem Biotechnol 24(25):115–126

Tratnyek, P.G. and Hoigne, J. (1991) Oxidation of substituted phenols in the environment: a QSAR analysis of rate constants for reaction with singlet oxygen. *Environmental Science and Technology*. 25(9): 1596-1604.

Troya MT, Rubio F, Prieto MJ, Lorenzo D, Fernández-Cabo JL, Schöftner R (2009) Natural durability of reed (Phragmites australis) against wood decay organisms: relation to other forest species. Invest Agrar-Sist R 18(3):289–295

Turner, G.M. (2008). A comparison of *the limits to growth* with 30 years of reality. *Global Environmental Change, 18*, 397-411.

US DOE, Perlack RB, Stokes BJ (Leads) (2011) U.S. billion-ton update: biomass supply for a bioenergy and bioproducts industry (ORNL/TM-2011/224). Oak Ridge National Laboratory, Oak Ridge, TN

U.S. Department of Energy, Energy Information Administration. (2013). Monthly Energy Review, DOE Publ. No. EIA-0035(2013/03). Washington, DC: Dept. of Energy.

Vaidya, A., and Singh, T. (2012) Pre-treatment of Pinus radiata substrates by basidiomycetes fungi to enhance enzymatic hydrolysis. Biotechnol Lett 34: 1263–1267.

Vanden Wymelenberg A, Gaskell J, Mozuch M, BonDurant SS, Sabat G, Ralph J, Skyba O, Mansfield SD, Blanchette RA, Grigoriev IV, Kersten PJ, Cullen D (2011) Significant alteration of gene expression in wood decay fungi Postia placenta and Phanerochaete chrysosporium by plant species. Appl Environ Microbiol 77(13):4499–4507

Varela, E. and Tien, M. (2003). Effect of pH and oxalate on hydroquinone-derived hydroxyl radical formation during brown rot wood degradation. *Applied and Environmental Microbiology, 69*(10), 6025-6031

Vogel J (2008) Unique aspects of the grass cell wall. Curr Opin Plant Biol 11:301–307

Von Sonntag, C. (1980). Free-radical reactions of carbohydrates as studied by radiation techniques. *Advances in Carbohydrate Chemistry and Biochemistry, 37*, 7-77.

Waid, J.S. (1999) Does soil biodiversity depend upon metabiotic activity and influences? Appl Soil Ecol 13: 151– 158.

Wan, C. and Li, Y. (2011). Effectiveness of microbial pretreatment by *Ceriporiopsis subvermispora* on different biomass feedstocks. *Bioresource Technology*. 102(16): 7507-7512.

Wang, Z.J., Zhu, J.Y., Zalesny Jr., R.S., Chen, K.F. (2012). Ethanol production from poplar wood through enzymatic saccharification and fermentation by dilute acid and SPORL pretreatments. *Fuel*. 95: 606-614.

Wardman, P. (1989). *Reduction potentials of one-electron couples involving free radicals in aqueous solution* (pp. 1637-1755). American Chemical Society and the American Institute of Physics for the National Institute of Standards and Technology.

Wardman, P. & Candeias, L.P. (1996). Fenton chemistry: an introduction. *Radiation Research, 145*, 523-531.

Waring, R. H., McDonald, A. J. S., Larsson, S., Ericsson, T., Wiren, A., Arwidsson, E., ... & Lohammar, T. (1985). Differences in chemical composition of plants grown at constant relative growth rates with stable mineral nutrition.*Oecologia*, *66*(2), 157-160.

Watts, R.J., Udell, M.D., Rauch, P.A., and Leung, S.W. (1990). Treatment of pentachlorophenol-contaminated soils using Fenton's reagent. *Hazardous Waste and Hazardous Materials* 7(4): 335-345.

Wei, D., Houtman, C.J., Kapich, A.N., Hunt, C.G., Cullen, D., and Hammel, K.E. (2010) Laccase and its role in production of extracellular reactive oxygen species during wood decay by the brown rot basidiomycete Postia placenta. Appl Environ Microbiol 76: 2091–2097.

Wesenberg, D., Kyriakides, I., & Agathos, S. N. (2003). White rot fungi and their enzymes for the treatment of industrial dye effluents. *Biotechnology Advances*, *22*(1), 161-187.

Willmott, C.J. (1982) Some comments on the evaluation of model performance. Bull Am Meteorol Soc 63: 1309–1313.

Winandy, J.E., and Morrell, J.J. (1993) Relationship between incipient decay, strength, and chemical composition of Douglas-fir heartwood. Wood Fiber Sci 25: 278–288.

Wolfrum, E. J., & Sluiter, A. D. (2009). Improved multivariate calibration models for corn stover feedstock and dilute-acid pretreated corn stover. *Cellulose*, *16*(4), 567-576.

Wong, D. W. (2009). Structure and action mechanism of ligninolytic enzymes.*Applied biochemistry and biotechnology*, *157*(2), 174-209.

Worrall, J.J., Anagnost, S.E., and Zabel, R.A. (1997) Comparison of wood decay among diverse lignicolous fungi. Mycologia 89: 199–219.

Wyman, C. (2007). What is (and is not) vital to advancing cellulosic ethanol. *Trends in Biotechnology*, *25*(4), 153-157.

Xie, Y., Xiao, Z., Goodell, B., Jellison, J., Militz, H., & Mai, C. (2010). Degradation of wood veneers by Fenton's reagents: Effects of wood constituents and low

molecular weight phenolic compounds on hydrogen peroxide decomposition and wood tensile strength loss. *Holzforschung, 64*, 375-383.

Xu, C., Ma, F., Zhang, X., and Chen, S. (2010). Biological pretreatment of corn stover by *Irpex lacteus* for enzymatic hydrolysis. *Journal of Agricultural and Food Chemistry*. 58(20): 10893-10898.

Xu, G. & Goodell, B. (2001). Mechanisms of wood degradation by brown rot fungi: chelator-mediated cellulose degradation and binding of iron by cellulose. *Journal of Biotechnology, 87*, 43-57.

Yelle, D. J., Ralph, J., & Frihart, C. R. (2008a). Characterization of nonderivatized plant cell walls using high-resolution solution-state NMR spectroscopy. *Magnetic Resonance in Chemistry*, *46*(6), 508-517.

Yelle, D. J., Ralph, J., Lu, F., & Hammel, K. E. (2008b). Evidence for cleavage of lignin by a brown rot basidiomycete. *Environmental Microbiology*, *10*(7), 1844-1849.

Yelle, D.J., Wei, D., Ralph, J., and Hammel, K.E. (2011 Multidimensional NMR analysis reveals truncated lignin structures in wood decayed by the brown rot basidiomycete Postia placenta. Environ Microbiol 13: 1091–1100.

Yu, H., Guo, G., Zhang, X., Yan, K., & Xu, C. (2009). The effect of biological pretreatment with the selective white rot fungus *Echinodontium taxodii* on enzymatic hydrolysis of softwoods and hardwoods. *Bioresource Technology, 100*, 5170-5175.

Zabel RA, Morrell JJ (1992) Wood microbiology: decay and its prevention. Academic, San Diego

Zeikus, J.G. (1981). Lignin metabolism and the carbon cycle. In *Advances in Microbial Ecology*. Alexander, M. (ed.) Plenum Press, Springer, New York, pp. 211-243.

Zhang, X., Yu, H., Huang, H., & Liu, Y. (2007). Evaluation of biological pretreatment with white rot fungi for the enzymatic hydrolysis of bamoboo culms. *International Biodeterioration & Biodegradation, 60*(3), 159-164.

Zhang, Y.H.P., Berson, E., Sarkanen, S., and Dale, B.E. (2009). Sessions 3 and 8: pretreatment and biomass recalcitrance: fundamentals and progress. *Applied Biochemistry and Biotechnology* 153: 80–83.